ISSN: 1305-9319 e-ISSN: 1305-9327 Number: 1 Volume: 21 Year: 2025

MEDICAL JOURNAL OF BAKIRKÖY

www.bakirkoytip.org

ISSN: 1305-9319 e-ISSN: 1305-9327 Number: 1 Volume: 21 Year: 2025

MEDICAL JOURNAL OF BAKIRKÖY

Medical Journal of Bakırköy of is an official scientific Journal of University of Health Sciences Türkiye, Bakırköy Dr. Sadi Konuk Training and Research Hospital (BMJ)

It is published quarterly as 4 issues every year (March, June, September, December).

Please refer to the journal's webpage **(https://bakirkoymedj.org/)** for "Ethical Policy" and "Instructions to Authors".

The editorial and publication processes of the journal are shaped in accordance with the guidelines of the ICMJE, WAME, CSE, COPE, EASE, and NISO. The journal conforms with the Principles of Transparency and Best Practice in Scholarly Publishing (doaj.org/bestpractice). The Medical Journal of Bakırköy is indexed in **Web of Science; Emerging Sources Citation Index (ESCI), TUBITAK ULAKBIM TR Index, Scopus, EBSCO – Academic Search Complete, J-Gate, Embase, CINAHL Complete, ScopeMed, WorldCat, Infobase, Ulrich's Database, Ideal Online, Türkiye Atıf Dizini, Türk Medline** and **CNKI**.

The journal is published online.

Owner: University of Health Sciences Türkiye, Bakırköy Dr. Sadi Konuk Training and Research Hospital

Responsible Manager: Musa Çırak

Publisher Contact
Address: Molla Gürani Mah. Kaçamak Sk. No: 21/1 34093 İstanbul, Türkiye
GSM: +90 530 177 30 97
E-mail: info@galenos.com.tr/yayin@galenos.com.tr
Web: www.galenos.com.tr **Publisher Certificate Number:** 14521

Printing Date: March 2025
ISSN: 1305-9319 **E-ISSN:** 1305-9327
International scientific journal published quarterly.

Advisory Board

Advisory Board

Advisory Board

Advisory Board

Advisory Board

Contents

Researches

1 **Determining Hydrocephalus and V-P Shunt Requirements After Repair of Myelomeningocele Defects in Infants**
İnfantlarda Miyelomeningosel Defektlerinin Onarımı Sonrası Hidrosefali ve V-P Şant Gereksinimlerinin Belirlenmesi
Luay Şerifoğlu, Semra Işık, Mustafa Umut Etli, Murat Sait Seçkin, Gonca Gül Öndüç; İstanbul, Türkiye

7 **Evaluation of the Relationship Between 1st Trimester HbA1C, Fasting Blood Glucose, Thyroid Function Tests and Gestational Diabetes Mellitus**
1. Trimester HbA1C, Açlık Kan Şekeri ve Tiroid Fonksiyon Testlerinin Gestasyonel Diabetes Mellitus ile İlişkisinin Değerlendirilmesi
Özlem Dülger, Hatice Şeyma Akça, Sülbiye Karaburgu; Karaman, Türkiye

14 **Frequencies and Lines of Pediatric Distal Humerus Fractures: Where and How are the Fractures?**
Pediatrik Distal Humerus Kırıklarının Sıklığı ve Çizgileri: Kırıklar Nerede ve Nasıldır?
Malik Çelik, Ahmet Çanlıoğlu, Murat Tıngır, Vedat Öztürk, Cemal Kural; İstanbul, Trabzon, Türkiye

19 **Clinicopathological Reflections of Hashimoto's Thyroiditis and Papillary Thyroid Carcinoma Coexistence**
Hashimoto Tiroiditi - Papiller Tiroid Karsinomu Birlikteliğinin Klinikopatolojik Yansımaları
Can Akcura, Samet Alkana, Sedat Can Güney, Gamze Gelir Çavdar, Emel Şenol, Ayça Tan, Nilüfer Özdemir, Hasan Aydede, Zeliha Hekimsoy; Manisa, İzmir, Mersin, Türkiye

24 **Analysis of Molecular Differences in Metastatic Colorectal Cancers and Their Impact on Prognosis**
Metastatik Kolorektal Kanserlerde Moleküler Farklılıkların Analizi ve Prognostik Sonuçları
Ömer Faruk Özkan, Muhammed Kadir Yıldırak, Hanife Şeyda Ülgür, Emre Furkan Kırkan, Nurhilal Kızıltoprak, Haluk Kerim Karakullukçu, Melike Özçelik, Sevgi Kalkanlı Taş; İstanbul, Türkiye

31 **Evaluating the Efficacy and Associated Factors of Vagus Nerve Stimulation in Medically Refractory Epilepsy Patients**
Medikal Tedaviye Dirençli Epilepsi Hastalarında Vagus Sinir Stimülasyonunun Etkinliğinin ve İlişkili Faktörlerin Değerlendirilmesi
Ozan Haşimoğlu, Ozan Barut, Tuba Özge Karaçoban, Taha Hanoğlu, Nur Bahar Geylan, Buruç Erkan, Bekir Tuğcu; İstanbul, Bingöl, Türkiye

39 **Nail-fold Capillaroscopic Changes in Children with Juvenile Dermatomyositis and Specific Autoantibodies**
Jüvenil Dermatomiyozit Hastalarında Kapilleroskopik Değişiklikler ve Spesifik Otoantikorlarla İlişkisi
Şeyda Doğantan, Sema Nur Taşkın, Ayşenur Paç Kısaarslan, Muammer Hakan Poyrazoğlu; Kayseri, Türkiye

48 **Can Systemic Inflammation Response Index (SIRI) and Neutrophil-to-lymphocyte Ratio (NLR) Predict the Presence of Placenta Accreta Spectrum in Pregnant Women with Placenta Previa?**
Sistemik Enflamasyon Yanıt İndeksi (SIRI) ve Nötrofil-lenfosit Oranı (NLR), Plasenta Previalı Gebe Kadınlarda Plasenta Akreta Spektrumunun Varlığını Öngörebilir mi?
Nihal Çallıoğlu, Emre Kar, İlke Özer Arslan, Selvi Aydın Şenel, İbrahim Polat, Işıl Turan Bakırcı, Tuğçe Tunç Arslanoğlu; İstanbul, Tekirdağ, Türkiye

55 **Comparison of Post-Operative Long-Term Surgical Fibrosis in the Multifidus Muscle Between Microdiscectomy and Microendoscopic Discectomy**
Mikrodiskektomi ve Mikroendoskopik Diskektomi Sonrası Multifidus Kasındaki Uzun Dönem Cerrahi Fibrozisin Karşılaştırılması
Bülent Bozyiğit, Hakan Kına; İzmir, İstanbul, Türkiye

Contents

62 **The Impact of TRIMANO Adjustable Arm Holder on Proximal Humerus Fracture Management: Enhancing Surgery Duration, Surgical Efficiency, and Patient Outcomes**
TRIMANO Ayarlanabilir Kol Tutucusunun Proksimal Humerus Kırığı Yönetimindeki Etkisi: Cerrahi Süre, Cerrahi Verimlilik ve Hasta Sonuçlarının İyileştirilmesi
Cumhur Deniz Davulcu, Muhammed Yusuf Afacan; İstanbul, Türkiye

70 **Comprehensive Analysis of Factors Affecting Surgical Outcomes in Intracranial Aneurysm Patients with Poor Prognosis**
Kötü Prognozlu İntrakraniyal Anevrizma Hastalarında Cerrahi Sonuçları Etkileyen Faktörlerin Kapsamlı Analizi
Murat Baloğlu, Hakan Millet, Serdar Ercan; Eskişehir, Türkiye

76 **Effects of Scalp Block on Postoperative Analgesia in Craniotomy Surgery: A Prospective, Randomized Controlled, Double-Blind Study**
Kraniyotomi Cerrahisinde Scalp Bloğunun Postoperatif Analjezi Üzerindeki Etkileri: Prospektif, Randomize Kontrollü, Çift Kör Bir Çalışma
Muhammed Halit Satıcı, Mahmut Sami Tutar, Betül Kozanhan, Yasin Tire, İlker Çöven, Nuray Altay; Konya, Şanlıurfa, Türkiye

83 **Anatomical Study of Bile Ducts by Magnetic Resonance Cholangiopancreatography**
Safra Kanallarının Manyetik Rezonans Kolanjiyopankreatografi ile Anatomik Değerlendirmesi
Tahir Fatih Dikici, Zeliha Fazlıoğulları, Ayşe Gamze Özcan, Mustafa Koplay, Ahmet Kağan Karabulut, İsmihan İlknur Uysal, Nadire Ünver Doğan; Antalya, Konya, Türkiye

90 **Beyond Motor Symptoms: A Comprehensive Analysis of Sexual Dysfunction in Cervical Dystonia**
Servikal Distonide Cinsel İşlev Bozukluğu Üzerine Kapsamlı Bir Değerlendirme
Özge Gönül Öner, Gözde Baran; İstanbul, Türkiye

97 **Etiological and Clinical Characteristics of Cases with Pancreatitis**
Pankreatit Tanılı Olguların Etiyolojik ve Klinik Özellikleri
Pınar Bilen, Nafiye Urgancı, Merve Usta, Dilek Güller; İstanbul, Türkiye

104 **Comparison of the Efficacy of Different Local Anesthetic Volumes on the Success of Combined Interscalene-Supraclavicular Nerve Block**
Farklı Lokal Anestetik Hacimlerinin Kombine İnterskalen-Supraklavikular Sinir Bloğunun Başarısına Olan Etkinliklerinin Karşılaştırılması
Özlem Melike Ekşi, Gökhan Sertcakacılar, Yaser Pektaş, Güneş Özlem Yıldız, Zafer Çukurova, Gülsüm Oya Hergünsel; İstanbul, Türkiye; Texas, USA

112 **Association of Different Doses of Curcumin with Preadipocyte to Adipocyte Differentiation**
Farklı Kurkumin Dozları ile Preadiposit-Adiposit Farklılaşması Arasındaki İlişki
Pınar Çetinalp, Sevgin Değirmencioğlu, Sevda Tanrıkulu Küçük, Muhammed Seyithanoğlu, Yıldız Öner İyidoğan, Hikmet Koçak; İstanbul, Kırklareli, Kahramanmaraş, Türkiye

Case Report

121 **A Novel Approach in Cerebellar Cystic Pilocytic Astrocytoma Surgery: Spherical Coordinate System**
Serebellar Kistik Pilositik Astrositom Cerrahisinde Yeni Bir Yaklaşım: Küresel Koordinat
Abdullah Emre Taçyıldız, Özden Erhan Sofuoğlu, Rabia Burçin Girgin; Malatya, Karabük İstanbul, Türkiye

Editorial

Bakırköy Medical Journal is proud to be a general medical journal that has been published regularly, periodically and continuously since 2005. I would like to express my endless gratitude and appreciation to everyone who has contributed to its regular publication for such a long time. I have full faith that our journal, which has come from the past to the present, will achieve greater successes in the future with your valuable contributions.

Bakırköy Medical Journal is currently included in many important national and international indexes as well as ESCI. Our goal is to meet the SCI and/or SCI-expanded criteria and be included in these databases. As the editorial board, we are working with all our might to achieve this goal. We believe that we will achieve this goal with your valuable contributions and extraordinary publications. We will need your ideas more than ever on this journey.

We are excited to present you with many interesting and high-quality articles in the first issue of this year. We believe that you will read it with pleasure and enjoyment. We hope to be together with high-quality and qualified studies in the upcoming issues.

Musa ÇIRAK, MD., PhD.
Chief Editor

Medical Journal of Bakırköy

Med J Bakirkoy 2025;21:1-6
DOI: 10.4274/BMJ.galenos.2024.2024.4-11

Research

Determining Hydrocephalus and V-P Shunt Requirements After Repair of Myelomeningocele Defects in Infants

İnfantlarda Miyelomeningosel Defektlerinin Onarımı Sonrası Hidrosefali ve V-P Şant Gereksinimlerinin Belirlenmesi

Luay Şerifoğlu, Semra Işık, Mustafa Umut Etli, Murat Sait Seçkin, Gonca Gül Öndüç

University of Health Sciences Türkiye, Ümraniye Training and Research Hospital, Clinic of Neurosurgery, İstanbul, Türkiye

ABSTRACT

Objective: Myelomeningocele (MM) is an important developmental defect that requires surgical treatment, and hydrocephalus is an important complication that may develop after surgical closure of the defect. To analyze the factors that may determine the need for shunting in patients with MM defects and hydrocephalus.

Methods: A retrospective analysis of 103 patients (63 females and 40 males) who were treated for MM between 2016 and 2023 at our institution was conducted. The infants were divided into two groups: Group 1; those who underwent V-P shunt surgery following MM repair surgeries (n=81) and Group 2; those who did not receive V-P shunt surgery following MM repair (n=22). Parameters such as head circumference, MM sac integrity, MM sac location, and birth weight were examined. The results were analyzed to identify any potential differences between the two groups.

Results: The study included 103 patients with MM abnormalities. The rate of V-P shunt insertion was significantly higher in infants with preoperative hydrocephalus, those with an open MM sac structure, and those with abnormalities in the thoracic/thoracolumbar region.

Conclusion: Development of hydrocephalus and the need for V-P shunt placement after defect repair are crucial in infants born with MM. This evaluation helps in planning the management of these patients with the aim of minimizing complications and improving the overall prognosis.

Keywords: Myelomeningocele, hydrocephalus, frontal and occipital horn ratio

ÖZ

Amaç: Miyelomeningosel (MM) cerrahi tedavi gerektiren önemli bir gelişimsel defekt olup, defektin cerrahi olarak kapatılmasından sonra gelişebilecek komplikasyonlar arasında hidrosefali önemli bir yer tutmaktadır. Hidrosefali ile birlikte MM defekti olan hastalarda postoperatif dönemde şant ihtiyacını belirleyebilecek faktörlerin analiz edilmesidir.

Gereç ve Yöntem: Kliniğimizde 2016-2023 yılları arasında MM nedeniyle tedavi gören 103 hastanın (63 kadın, 40 erkek) retrospektif analizi yapıldı. Bebekler iki gruba ayrıldı: Grup 1; MM onarımı ameliyatı sonrası V-P şant ameliyatı geçirenler (n=81) ve Grup 2; MM onarımı sonrası V-P şant ameliyatı geçirmeyenler (n=22). Baş çevresi, MM kesesi bütünlüğü, MM kesesinin yeri, doğum ağırlığı gibi parametreler incelendi. Sonuçlar, iki grup arasındaki potansiyel farklılıkları belirlemek için analiz edildi.

Bulgular: Bu çalışmaya MM anormallikleri olan 103 hastayı dahil ettik. Preoperatif hidrosefalisi olan, MM kesesi yapısı açık olan ve torasik/torakolomber bölgede anormalliği olan bebeklerde V-P şant takılma oranı anlamlı olarak daha yüksekti.

Sonuç: MM ile doğan bebeklerde hidrosefali gelişimi ve defektin onarımı sonrası V-P şant yerleştirilmesi ihtiyacı önemlidir. Bu değerlendirme, komplikasyonları en aza indirmeyi ve genel prognozu iyileştirmeyi hedefleyerek bu hastaların yönetiminin planlanmasına yardımcı olur.

Anahtar Kelimeler: Miyelomeningosel, hidrosefali, frontal ve oksipital boynuz oranı

Address for Correspondence: Luay Şerifoğlu MD, University of Health Sciences Türkiye, Ümraniye Training and Research Hospital, Clinic of Neurosurgery, İstanbul, Türkiye
E-mail: luaybeyin@gmail.com **ORCID ID:** orcid.org/0000-0003-0253-9950

Cite as: Şerifoğlu L, Işık S, Etli MU, Seçkin MS, Öndüç GG. Determining hydrocephalus and V-P shunt requirements after repair of myelomeningocele defects in infants. Med J Bakirkoy. 2025;21:1-6

Received: 05.07.2024
Accepted: 12.07.2024
Publication Date: 25.03.2025

INTRODUCTION

Myelomeningocele (MM) is the most common and severe form of open neural tube defects (ONTDs) and may cause significant morbidity and mortality due to hydrocephalus, lower extremity paralysis, and neurogenic bowel and bladder dysfunction. These conditions require multidisciplinary management, such as neurosurgical, orthopedic, and nephrourological treatments (1).

One of the most important hypotheses regarding the formation of neurological deficits in infants with ONTD is the "double hit hypothesis" proposed by Heffez et al. (1), which suggests a two-stage effect. A neural tube defect initially occurs during neurulation, followed by further damage due to continuous exposure to amniotic fluid. Additionally, the skin defect leaves neural tissue vulnerable to mechanical trauma from the uterine wall and the neurotoxic effects of amniotic fluid, resulting in additional neurological injury. The interruption of simultaneous normal neural tube development can lead to lifelong disabilities, including paralysis, incontinence, and cognitive impairments (1,2).

The incidence of hydrocephalus in patients with ONTD varies from 60% to 90%, and 80% of those who develop hydrocephalus require surgical diversion of Cerebrospinal Fluid (CSF) (3). Ultrasonography (USG) and magnetic resonance imaging (MRI) are widely used for the anatomical assessment of intracranial structures, especially ventricular sizes, in the follow-up and treatment of hydrocephalus. There are many techniques to assess hydrocephalus; however, the frontal occipital horn ratio (FOHR) has been shown to be a reliable index for clinical diagnosis and follow-up of infantile ventriculomegaly (4).

The aim of our study was to identify risk factors for determining the need for CSF diversion surgery in the postoperative period through preoperative evaluation of patients with MM.

METHODS

A retrospective analysis of 103 patients (63 females and 40 males) who were treated for MM and MS between 2013 and 2023 at our institution was conducted. The goal of this study was to identify factors influencing the decision to perform CSF diversion surgeries, which are ventriculo-peritoneal shunt (V-PS) surgeries, at our clinic. The infants were divided into two groups: Group 1; those who underwent V-P shunt surgery following MM repair surgeries (n=81) and Group 2; those who did not receive V-P shunt surgery following MM repair (n=22). Parameters such as head circumference (HC), MM sac integrity, MM sac location, and birth weight were examined. Additionally, preoperative ventricular volumes were measured using transfontanel USGs (TFUSG) and cranial MRIs to calculate the FOHR. The results were analyzed to identify any potential differences between the two groups.

Human subjects: All participants in this study provided consent or waived consent. This study University of Health Sciences Türkiye, Ümraniye Training and Research Hospital Clinical Research Ethics Committee (decision no: 557, date: 21.12.2023).

Animal subjects: All authors have confirmed that this study did not involve animal subjects or tissue.

Imaging Technique

For USG, a radiology specialist used a 5-8 MHz curved array EPIC system probe (Philips Healthcare) through the open anterior fontanel. This method was used to measure the sizes of the frontal, occipital, and temporal horns, as well as the biparietal diameters, across the coronal, sagittal, and oblique planes.

MRI was performed using a 1.5- Tesla system (Magnetom Avanto, Siemens Healthcare). The routine MRI protocol included spin-echo T2- weighted images (slice thickness, 2 mm; interslice gap, 2.2 mm), 3D T1-weighted magnetization-prepared rapid gradient-echo imaging (MP-RAGE, Siemens Healthcare), axial 2D T2-weighted fluid-attenuated inversion recovery (FLAIR) imaging, axial susceptibility-weighted imaging, and axial echo-planar DWI. The fast protocol comprised axial, coronal, and sagittal plane T2-weighted imaging with a slice thickness of 4 mm and an interslice gap of 5 mm, axial echo-planar FLAIR imaging, axial echo-planar DWI, and axial T2* and sagittal T1* volumetric interpolated breath-hold examination (VIBE) imaging techniques. In particular, ventricular volumes were measured using coronal and axial T2-weighted images.

Evaluation of Images

The USG were reviewed by two neurosurgeons and one pediatric neuroradiologist, each with a minimum of 10 years of experience in their field. Coronal USG images were examined to determine the bifrontal horn size, maximum bitemporal horn size, maximum bioccipital horn size, and maximum biparietal calvarial size. The same team analyzed the MRI ventricular volumes using analyze software (version 12.0, Analyze Direct). In MRI, T2-weighted image signal intensities were normalized within a range of 0 to 1 and segmented using a region-growing technique, as described in previously published studies (5,6). For the FOHR, measurements were made of the bifrontal horn diameter at approximately the largest frontal horn size at the level

of the foramen of Monro, bilateral occipital horn diameter at the largest occipital horn size at the level of the atria of the lateral ventricles, and the biparietal size at the largest transverse calvarial dimension; all measurements were conducted on axial (Figure 1) and coronal (Figure 2) images.

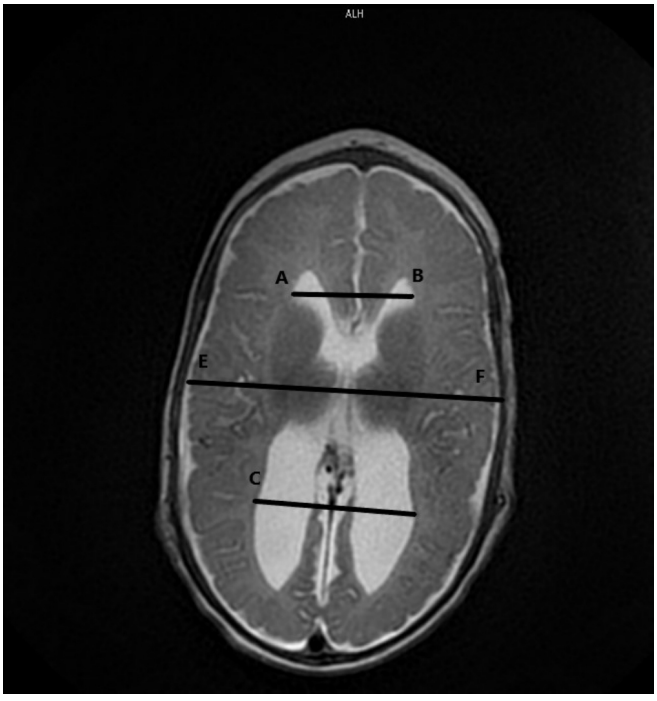

Figure 1. Axial MRI image showing linear measurements used to calculate the frontal occipital horn ratio: Bifrontal horn dimension (arrow AB), bioccipital horn dimension (arrow CD), and biparietal dimension (arrow EF)
MRI: Magnetic resonance imaging

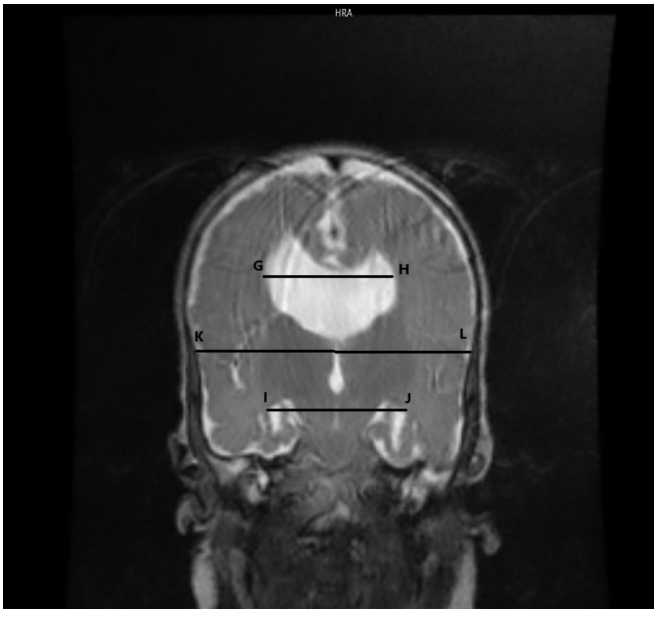

Figure 2. Coronal MRI image showing linear measurements used to calculate the frontal temporal horn ratio: Bifrontal horn dimension (arrow GH), bitemporal horn dimension (arrow IJ), and biparietal dimension (arrow KL)
MRI: Magnetic resonance imaging

The FOHR was calculated as follows: (bifrontal horn size+bioccipital horn size) / (2×biparietal calvarial size).

Statistical Analysis

The assumption of normality for continuous variables was tested using the Kolmogorov-Smirnov test. Categorical variables are presented as frequencies (n, %), whereas continuous variables are presented as mean and standard deviation. Comparisons between two groups for continuous variables were conducted using the Independent sample t-test. The relationship between two continuous variables was examined using the pearson correlation test. For qualitative comparisons between groups, chi-square tests (pearson chi-square test and Fisher's exact test) were used. Results were considered statistically significant at a confidence interval of 95% if $p<0.05$. All statistical analyses were performed using SPSS software version 26 (IBM Corp., Armonk, NY, USA).

RESULTS

We included 103 patients with MM abnormalities. The average weight of infants by the time of MM/MS surgery was 3163.60±624.99 grams. According to routinely performed preoperative TFUSGs and MRIs on newborns with MM, 81 were diagnosed with hydrocephalus and 22 were found to be normal. During the postoperative follow-up of 81 infants with hydrocephalus, 74 required V-P shunt placement and 7 did not. Conversely, among the 22 infants without evident hydrocephalus, 9 required a V-P shunt insertion in the postoperative period.

When considering the location of the MM; 22 infants had the lumbar region, 10 had the sacral region, 8 had the thoracic region, 23 had the lumbosacral level, and 40 had the thoracolumbar level. Other characteristics of the infants were as follows: average HC was 36.56±4.95 cm, lesion diameter was 5.68±1.90 cm, and the FOHR was 0.52±0.13. We determined that 77 infants had an open MM sac structure and 26 had an unruptured sac structure. Additionally, 67 infants were found to have complete paralysis, whereas 28 had partial neurological deficits (Table 1).

The lesion diameter ($t=2.606$; $p=0.011$) and the FOHR ($t=10.007$; $p<0.001$) were significantly higher in 81 infants undergoing V-P shunt procedure. There was no statistically significant difference in the weight of the infants based on whether or not they required a V-P shunt surgery ($p>0.05$). The rate of V-P shunt insertion was significantly higher in infants with preoperative hydrocephalus (91% vs. 37%;

p<0.001), those with an open MM sac structure (95% vs. 35%; p<0.001), and those with abnormalities in the thoracic/thoracolumbar region (92% vs. 71%; p=0.009). Among the infants who underwent V-P shunt surgery, 75% showed complete motor and sensory loss, whereas 21% had partial deficits (p<0.001) (Table 2).

DISCUSSION

MM is known as the most common neural tube defect (NTD); however, a study by Schindelmann et al. (7) showed that myeloschisis (MS) is not as rare as it is believed, but rather a common NTD. Contrary to the literature, their results showed that MS (31%) occurred more frequently than MM (23%) (7). Therefore, the distribution and classification of NTDs differ significantly between studies. The reported incidence of MS is often lower than the actual incidence, likely due to the need for a more detailed neuropathological examination to ascertain the presence of a neural placode (7). Although the presence of a membrane (MM sac) and cyst surrounding the defect is generally considered a distinguishing feature between MM and MS, the clinical presentation of these two forms of ONTDs remains the same (8). Our findings indicate that the presence of a MM sac covering the lesion or evidence of CSF leakage can be determinant factors for postoperative hydrocephalus development.

Table 1. Characteristics of babies with myelomeningocele

Variables (n=100)	**n (%)**
Baby weight (gr), mean±SD	3163.60±624.99
Hydrocephalus	
Yes	81
No	22
Myelomeningocele pouch structure	
Open	77
Closed	26
Ventriculoperitoneal (VP) shunt requirement	
Yes	81
No	22
Lesion diameter (cm), mean±SD	5.68±1.90
Baby head circumference (HC) (cm), mean±SD	36.56±4.95
Fronto-occipital horn ratio (FOHR), mean±SD	0.52±0.13
Lesion location	
Lumbar region	22
Sacrum region	10
Thoracic area	8
Lumbosacral region	23
Thoracolumbar area	40
Deficit existence	
Yes	67
Partial	25
No	8
Transfontanel ultrasonography (TFUSG)	
Yes	94
No	9

SD: Standard deviation

Numerous studies have acknowledged that the absence of a MM sac significantly increases the risk of developing postoperative hydrocephalus requiring a V-P shunt (9). In our study, the need for a V-P shunt placement was found in 34% of cases where the sac was notably intact, compared with 94% in cases where it was open, which was statistically significant.

Another important issue in infants with MM is the diagnosis of hydrocephalus and the timing of treatment. In historical reports published until 1990, many opted for V-P shunt implantation at birth even if the HC was within normal limits (10). Consequently, numerous studies reported high rates of V-P shunt placement, such as Januschek et al. (11) reported an 85% V-P shunt rate, Laskay et al. (12) 84.6%, and Marreiros et al. (13) 70%. However, by tolerating larger ventricles and applying better postoperative wound care, few experienced centers have managed to reduce the V-P shunt rates to 55-65% (14).

Although V-P shunt surgeries are the most effective and widely used treatment method for hydrocephalus, alternative treatments have also come to the fore as a result of recent technological advances. Warf (15) summarized in their study that techniques such as endoscopic third ventriculostomy and choroid plexus cauterization can be an alternative for hydrocephalus in non-developing countries that cannot support shunt equipments.

The primary concern in the management of infants with detected preoperative ventriculomegaly is the progression, regression, or stability of ventriculomegaly. The long-term neurocognitive impact of allowing larger ventricles is unknown, but it appears to be insignificant in short-term evaluations. On the other hand, these patients may be spared the morbidity associated with repeated operations and complications due to V-P shunt insertion (14).

To monitor the hydrocephalus and evaluate the timing of V-P shunt placement, knowing the volume of the ventricles (VV) is crucial. Data obtained from routine neonatal TFUSGs for identifying intracranial pathologies or from MRIs for a more detailed understanding can be used to create VV indices. In their study, Radhakrishnan et al. (4) found that the FOHR,

Table 2. Ventriculoperitoneal (V-P) shunt-related variables in infants with myelomeningocele

		V-P Shunt requirement		
		Yes (n=81)	No (n=22)	
Variables	**Total, n**	**n (%)**	**n (%)**	**p-value**
Baby waight (gr), mean±SD	100	3181.51±638.35	3088.16±575.18	0.561[a]
Hydrocephalus[#]				< 0.001[c]*
Yes	81	74 (91.4)	7 (8.6)	
No	22	9 (36.8)	13 (63.2)	
Myelomeningocele pouch structure[#]				< 0.001[c]*
Open	77	73 (94.8)	4 (5.2)	
Closed	26	9 (34.8)	17 (65.2)	
Lesion diameter (cm), mean±SD		5.93±1.88	4.67±1.68	**0.011[a]***
Baby head circumference (cm), mean±SD		37.01±5.06	34.56±3.98	0.057
FOHR, mean±SD		0.55±0.12	0.37±0.05	< 0.001[a]*
Lesion localion[#]				**0.009[b]***
Sacrum/lumbar/lumbosacral region	52	37 (71.2)	15 (28.8)	
Thoracic / tracolumbar area	51	46 (91.7)	5 (8.3)	
Deficit existence**				< 0.001[c] *
Yes	67	61 (75.3)	6 (31.6)	
Partial	25	17 (21)	8 (42.1)	
No	11	4 (3.7)	7 (26.3)	

*p<0.05, **Column percentage given, [a]Independent sample t-test, [b]Pearson chi-square test, [c]Fisher's exact test, [#]Line percentage was given, SD: Standard deviation

a VV index derived from TFUSG and MRI, showed a strong correlation between both imaging methods, and a clinical FOHR threshold of 0.55 demonstrated high sensitivity in identifying infantile hydrocephalus (4). Particularly, FOHR can be used to measure the severity of ventriculomegaly (16,17). We obtained similar results from preoperative TFUSG and MRI examinations concerning FOHR results. A close relationship was found between values exceeding 0.55 and the likelihood of requiring a V-P shunt insertion.

Another significant factor in determining the need for hydrocephalus treatment and V-P shunt placement is the routine measurement of HC. The study conducted by Vonzun et al. (18) showed that preoperative and/or postoperative HC and ventricular measurements were determinants of the need for a V-P shunt in the first year of life. They found that a HC above the 95th percentile predicted an 80% likelihood of needing a V-P shunt due to late hydrocephalus (18). We found this rate to be approximately 81% in infants with a HC of 37 cm or more, which is similar to the findings of Protzenko et al. (19), who showed that a birth HC of 38 cm or more was a significant factor for V-P shunt requirement.

We observed that regardless of the morphology of the defect, there is a greater need for V-P shunt placement in patients with lesions located in the thoracic level, larger than 5 cm in diameter, and those with more severe deficits in our study. Some studies have indicated that the development of hydrocephalus is generally not related to the anatomical level or size of the lesion but rather to MS (1-20). Another study showed that hydrocephalus and the need for a V-P shunt placement were more common in higher spinal-level lesions (19). We believe that a possible reason for these differing results might be not fully understanding the distinctions between MM and MS. Additionally, similar to our findings, no significant impact of birth weight and gender has been identified on the need for a V-P shunt (18).

Considering all results, it was observed that knowing parameters such as the size and level of the lesion, the integrity of the sac, HC, and FOHR can play a role in determining the risk and the need for a V-P shunt due to hydrocephalus that may develop after MM repair.

Study Limitations

This study is limited by its single-center nature and relatively small number of patients. The findings could be more definitive when considered by larger groups and various centers, leading to the development of guidelines or scales.

CONCLUSION

In infants born with MM, determining the development of hydrocephalus and the need for V-P shunt placement

after defect repair is crucial. The shunt procedure, while life saving, is associated with numerous complications. Therefore, evaluating the lesion and ventricular condition in the preoperative period is essential to understand which cases carry a higher risk and to make certain predictions regarding the outcome. This evaluation helps in planning the management of these patients with the aim of minimizing complications and improving the overall prognosis.

ETHICS

Ethics Committee Approval: This study University of Health Sciences Türkiye, Ümraniye Training and Research Hospital Clinical Research Ethics Committee (decision no: 557, date: 21.12.2023).

Informed Consent: Animal subjects: All authors have confirmed that this study did not involve animal subjects or tissue.

FOOTNOTES

Authorship Contributions

Surgical and Medical Practices: L.Ş., S.I., M.U.E., M.S.S., Design: L.Ş., M.U.E., Data Collection or Processing: L.Ş., G.G.Ö., Analysis or Interpretation: L.Ş., S.I., Literature Search: L.Ş., S.I., G.G.Ö., Writing: L.Ş., S.I., M.U.E.

Conflict of Interest: No conflict of interest was declared by the authors.

Financial Disclosure: The authors declare that this study received no financial support.

REFERENCES

1. Heffez DS, Aryanpur J, Hutchins GM, Freeman JM. The paralysis associated with myelomeningocele: clinical and experimental data implicating a preventable spinal cord injury. Neurosurgery. 1990;26:987-92.
2. Copp AJ, Adzick NS, Chitty LS, Fletcher JM, Holmbeck GN, Shaw GM. Spina bifida. Nat Rev Dis Primers. 2015;1:15007.
3. Blount JP, Maleknia P, Hopson BD, Rocque BG, Oakes WJ. Hydrocephalus in spina bifida. Neurol India. 2021;69(Supplement):S367-71.
4. Radhakrishnan R, Brown BP, Kralik SF, Bain D, Persohn S, Territo PR, et al. Frontal occipital and frontal temporal horn ratios: comparison and validation of head ultrasound-derived indexes with mri and ventricular volumes in infantile ventriculomegaly. AJR Am J Roentgenol. 2019;213:925-31.
5. Tirkes T, Lin C, Cui E, Deng Y, Territo PR, Sandrasegaran K, et al. Quantitative MR evaluation of chronic pancreatitis: extracellular volume fraction and MR relaxometry. AJR Am J Roentgenol. 2018;210:533-542.
6. Handa RK, Territo PR, Blomgren PM, Persohn SA, Lin C, Johnson CD, et al. Development of a novel magnetic resonance imaging acquisition and analysis workflow for the quantification of shock wave lithotripsy-induced renal hemorrhagic injury. Urolithiasis. 2017;45:507-13.
7. Schindelmann KH, Paschereit F, Steege A, Stoltenburg-Didinger G, Kaindl AM. Systematic classification of spina bifida. J Neuropathol Exp Neurol. 2021;80:294-305.
8. Jeelani Y, McComb JG. Congenital hydrocephalus associated with myeloschisis. Childs Nerv Syst. 2011;27:1585-8.
9. Pastuszka A, Koszutski T, Horzelska E, Marciniak S, Zamłyński M, Olejek A. Absence of a hernia sack in patients undergoing prenatal repair of spina bifida increases the risk of developing shunt-dependent hydrocephalus. Diagnostics (Basel). 2023;13:343.
10. Hagemann C, Krajewski K, Henne T, Stücker R, Kunkel P. Postnatal repair of open neural tube defects: a single center with 90-month interdisciplinary follow-up. J Clin Med. 2021;10:4510.
11. Januschek E, Röhrig A, Kunze S, Fremerey C, Wiebe B, Messing-Jünger M. Myelomeningocele - a single institute analysis of the years 2007 to 2015. Childs Nerv Syst. 2016;32:1281-7.
12. Laskay NMB, Arynchyna AA, McClugage SG 3rd, Hopson B, Shannon C, et al. A comparison of the MOMS trial results to a contemporaneous, single-institution, postnatal closure cohort. Childs Nerv Syst. 2017;33:639-46.
13. Marreiros H, Loff C, Calado E. Who needs surgery for pediatric myelomeningocele? A retrospective study and literature review. J Spinal Cord Med. 2015;38:626-40.
14. Thompson DN. Postnatal management and outcome for neural tube defects including spina bifida and encephalocoeles. Prenat Diagn. 2009;29:412-9.
15. Warf BC. The impact of combined endoscopic third ventriculostomy and choroid plexus cauterization on the management of pediatric hydrocephalus in developing countries. World Neurosurg. 2013;79(Suppl 2):S23.e13-5.
16. Antes S, Welsch M, Kiefer M, Gläser M, Körner H, Eymann R. The frontal and temporal horn ratio to assess dimension of paediatric hydrocephalus: a comparative volumetric study. Acta Neurochir Suppl. 2013;118:211-4.
17. Antes S, Kiefer M, Schmitt M, Lechtenfeld M, Geipel M, Eymann R. Frontal and temporal horn ratio: a valid and reliable index to determine ventricular size in paediatric hydrocephalus patients? Acta Neurochir Suppl. 2012;114:227-30.
18. Vonzun L, Winder FM, Meuli M, Moerlen U, Mazzone L, Kraehenmann F, et al. Prenatal sonographic head circumference and cerebral ventricle width measurements before and after open fetal myelomeningocele repair - prediction of shunting during the first year of life. Ultraschall Med. 2020;41:544-9.
19. Protzenko T, Bellas A, Pousa MS, Protzenko M, Fontes JM, de Lima Silveira AM, et al. Reviewing the prognostic factors in myelomeningocele. Neurosurg Focus. 2019;47:E2.
20. Hagemann C, Krajewski K, Henne T, Stücker R, Kunkel P. Postnatal Repair of Open Neural Tube Defects: A Single Center with 90-Month Interdisciplinary Follow-Up. J Clin Med. 2021;10:4510.

Medical Journal of Bakırköy

Med J Bakirkoy 2025;21:7-13
DOI: 10.4274/BMJ.galenos.2024.2024.6-3

Research

Evaluation of the Relationship Between 1st Trimester HbA1C, Fasting Blood Glucose, Thyroid Function Tests and Gestational Diabetes Mellitus

1. Trimester HbA1C, Açlık Kan Şekeri ve Tiroid Fonksiyon Testlerinin Gestasyonel Diabetes Mellitus ile İlişkisinin Değerlendirilmesi

Özlem Dülger[1], Hatice Şeyma Akça[2], Sülbiye Karaburgu[3]

[1]Karamanoğlu Mehmetbey University Faculty of Medicine, Department of Obstetrics and Gynecology, Karaman, Türkiye
[2]Karamanoğlu Mehmetbey University, Karaman Training and Research Hospital, Clinic of Emergency Medicine, Karaman, Türkiye
[3]Karaman Training and Research Hospital, Clinic of Endocrinology, Karaman, Türkiye

ABSTRACT

Objective: This study aimed to examine the relationship between gestational diabetes mellitus (GDM) and fasting blood glucose (FBG), thyroid function tests, and HbA1C values in the first trimester of healthy pregnant women who do not have DM and visit our gynecology and obstetrics polyclinic for regular checkups.

Methods: This retrospective study included pregnant patients who applied to the Karaman Training and Research Hospital, Clinic of Obstetrics and Gynecology between 01.08.2023 and 01.05.2024. The department applied statistical analyses using the Statistical Package for the Social Sciences (SPSS Inc., version 20.0; Chicago, IL). Statistical significance was set as $p<0.05$.

Results: Our study included 78 patients: 59 (75.6%) were in the non-GDM group and 19 (24.4%) were in the GDM group. We calculated the under the curve as 0.912 (0.60-0.96) for 2nd trimester FBG at a cut-off value of 88 and 0.786 (0.37-0.93) for 2nd trimester HbA1C at a cut-off value of 5. We observed that both 2nd trimester FBG and 2nd trimester HbA1C significantly outperformed 1st-trimester FBG in predicting GDM (p=0.00, p=0.04). It was observed that 2nd-trimester FBG predicted GDM significantly better than 2nd-trimester HbA1C (p=0.028). Although no statistically significant difference was detected between 1st trimester HbA1C and 2nd trimester HbA1C in predicting GDM (p=0.481), it was observed that 2nd trimester FBG predicted GDM statistically significantly better than first trimester HbA1c (p=0.004).

Conclusion: First- and second-trimester HbA1c and FBG and oral glucose tolerance test (OGTT) values can predict gestational diabetes. HbA1C cannot be used instead of OGTT, but it is an important predictor.

Keywords: Gestational diabetes mellitus, fasting blood glucose, HbA1c, thyroid function test

ÖZ

Amaç: Çalışmamızın amacı, kadın hastalıkları ve doğum polikliniğimize düzenli kontrollerine gelen sağlıklı ve bilinen diabetes mellitus (DM) tanısı olmayan gebelerin birinci trimesterdeki açlık kan şekeri (AKŞ), tiroid fonksiyon testleri ve HbA1C değerlerinin gestasyonel DM (GDM) ile ilişkisini değerlendirmektir.

Gereç ve Yöntem: Çalışmamız retrospektif olarak planlanmış olup, Karaman Eğitim ve Araştırma Hastanesi, Kadın Hastalıkları ve Doğum Kliniği'ne 01.08.2023-01.05.2024 tarihleri arasında başvuran gebe hastalar çalışmaya dahil edildi. İstatistiksel analizlerde SPSS Inc., versiyon 20.0; Chicago, IL kullanıldı. İstatistiksel anlamlılık $p<0,05$ olarak kabul edildi.

Bulgular: Çalışmamızda toplam hasta sayısı 78 olup hastalarımızın 59'u (%75,6) GDM olmayan, 19'u (%24,4) ise GDM olan gruba dahildi. Hesaplanan eğri altında kalan alan değeri 2. trimester AKŞ için 88 kesim değerinde 0,912 (0,60-0,96), 2. trimester HbA1C için 5 kesim değerinde 0,786 (0,37-0,93) olarak hesaplandı. İkinci trimester AKŞ'nin ve 2. trimester HbA1C'nin 1. trimester AKŞ'ye göre GDM'si, istatistiksel anlamlı olarak daha iyi öngördüğü gözlemlendi (p=0,00, p=0,04). İkinci trimester AKŞ'nin 2. trimester HbA1C'ye göre ise GDM'si istatistiksel anlamlı olarak daha iyi öngördüğü gözlemlendi (p=0,028). İkinci trimester AKŞ'nin 1. trimester HbA1C'ye göre GDM'si istatistiksel anlamlı olarak daha iyi öngördüğü gözlemlendi (p=0,004).

Address for Correspondence: Özlem Dülger MD, Karamanoğlu Mehmetbey University Faculty of Medicine, Department of Obstetrics and Gynecology, Karaman, Türkiye
E-mail: ozlem_dulger@yahoo.com.tr **ORCID ID:** orcid.org/0000-0003-0400-1513

Cite as: Dülger Ö, Akça HŞ, Karaburgu S. Evaluation of the relationship between 1st trimester HbA1C, fasting blood glucose, thyroid function tests and gestational diabetes mellitus. Med J Bakirkoy. 2025;21:7-13

Received: 28.06.2024
Accepted: 07.08.2024
Publication Date: 25.03.2025

Sonuç: Birinci ve ikinci trimester HbA1C ile ikinci trimester FBG ve OGTT değerleri, gestasyonel diyabeti öngörebilmektedir. HbA1C, OGTT yerine kullanılamaz ama önemli bir prediktördür.

Anahtar Kelimeler: Gestasyonel diabetes mellitus, açlık kan şekeri, HbA1c, tiroid fonksiyon testleri

INTRODUCTION

Gestational diabetes mellitus (GDM) is a metabolic disease diagnosed during pregnancy (1,2). Although its prevalence has been gradually increasing, the average is 17.8% (9.3%-25.5%) (3). Mothers diagnosed with GDM have a higher risk of adverse birth outcomes, and their risk of being diagnosed with type 2 DM in later life increases by sevenfold (4-6). Important risk factors for GDM: body mass index >38.6 kg/m^2, fasting blood glucose (FBG) (rapid blood sugar)> 81 mg/dL, presence of polycystic ovary syndrome, and abdominal circumference >91.5 cm. The multiple coexistence of these risk factors significantly increases the incidence of GDM (7). Thyroid hormones are a group of hormones that are very important for both the mother and the fetus in maintaining current and long-term health (4). Thyroid stimulating hormone (TSH), free thyroxine (FT4), thyroglobulin, and thyroid peroxidase antibody (anti-TPO) are the most commonly used tests to measure thyroid functions (4). Thyroid dysfunction is closely related to DM; While the prevalence of thyroid dysfunction increases in patients diagnosed with type 1 and 2 DM, the risk of type 2 DM also increases in people with thyroid dysfunction (4-7). Physiological changes are observed in thyroid function during pregnancy, and inadequate adaptation to these changes leads to thyroid dysfunction (8).

Glycosylated hemoglobin (HbA1C) is a test used for the diagnosis and follow-up of Type 2 diabetes. The HbA1C test reflects the average glucose concentration over the last two to three months. FBG and oral glucose tolerance test (OGTT) are instantaneous values. Fasting is not necessary for HbA1C analysis (7,9). The ADA has accepted an HbA1C level of ≥6.5 among the diagnostic criterion for diabetes (10). There are many studies in the literature that evaluate the relationship between thyroid function tests (TFT) (4-6) and HbA1C and GDM (11,12). However, there are a limited number of studies in which TFT, fast blood glucose (FBG), and HbA1C were evaluated together (13), and the first trimester (14), and comparisons of the first and second trimesters were investigated (15).

Aim

The primary aim of our study was to evaluate the relationship between GDM and TFT, FBG, and HbA1C values in the first trimester of pregnant women who are healthy and have no known diagnosis of DM and come to our gynecology and obstetrics polyclinic for regular checkups. Our secondary aim was to compare the relationship between FBG, TFT and HbA1C values in the first and second trimesters with GDM.

METHODS

Study Design

Our study was planned retrospectively, and pregnant patients who applied to Karaman Training and Research Hospital, Clinic of Obstetrics and Gynecology between 01.08.2023 and 01.05.2024 were included in the study. This hospital is a high-volume regional hospital with intensive referrals.The instant study was carried out with the permission of Local Ethics Committee of the Karamanoğlu Mehmetbey University Faculty of Medicine (number: 06-2024/19, date: 30.05.2024).

Patient Population

Pregnant women with live singletons, over the age of 18, who regularly came for pregnancy follow-up, and whose last menstrual date was known were included in our study. Pregnant women with known type 1 and type 2 DM, multiple pregnancies, pregnancies with anomalies, pregnant women who did not accept OGTT screening or could not tolerate OGTT, pregnant women with comorbidities, and pregnancies that ended with abortion and baby death in the womb during their follow-up were not included in the study.

Data Collection

Obstetric information of pregnant women (gravide, parity, abortion), age, height, weight, examination findings, 1st and 2nd Trimester FBG, HbA1C, TFT, 75 gr. OGTT results were recorded by scanning the hospital database. In our study population, those diagnosed with gestational diabetes and those not diagnosed with gestational diabetes were recorded. The 1st trimester test results were obtained with data between the 6th and 13th weeks of pregnancy, and the 2nd trimester test results were obtained with data from the 24th and 28th weeks of pregnancy of the same pregnant women.

Diagnosis of GDM: GDM was diagnosed with routine examination and OGTT scan results. GDM was diagnosed with 75-g oral OGTT according to American Diabetes Association (ADA) criteria (10). Gestational diabetes was diagnosed when one of the following criteria was positive:

FBG: 92 mg/dL, 180 mg/dL in the 1st hour after OGTT, and 153 mg/dL in the 2nd hour after OGTT.

Statistical Analysis

The Statistical Package for the Social Sciences (SPSS Inc., version 20.0; Chicago, IL) was used for statistical analyses applied to the department. Normal analysis of continuous data was performed using the Shapiro-Wilk test. Those with normal distribution were determined using Student's t-test. Those that did not conform to the normal distribution were evaluated using the Mann-Whitney test and Brunner Munzel test. The HbA1c, fasting blood sugar, and other hormonal parameters of pregnant women diagnosed with and without GDM were compared using the Mann-Whitney U test and Brunner Munzel test. A receiver operating characteristic (ROC) curve was created for gestational diabetes, and the area under the curve (AUC) values for individual variables were obtained. The AUC values of the parameters were calculated and tested mutually for significance using the DeLong quality test. Statistical significance was set as $p<0.05$.

RESULTS

In our study, the total number of patients was 78, 59 (75.6%) of our patients were in the non-GDM group and 19 (24.4%) were in the GDM group. Considering the first trimester values, FBG was an average of 85.0±6.3 mg/dL in the non-GDM group and 87.0±6.6 mg/dL in the GDM group, and there was no statistically significant difference (p=0.245). HbA1C was an average of 5.2±0.3% in the non-GDM group and 5.4±0.3% in the GDM group, and there was a statistically significant difference (p=0.002). Free T3 (FT3) was 2.9±0.4 ng/dL, and there was no statistically significant difference (p=0.458). The average free T4 (FT4) level was 1.2 (1.1 to 1.2) ng/dL in both groups, and there was no statistically significant difference (p=0.514). There was no significant difference between the two groups in terms of TPO and TG antibody status (p=0.813, p=0.982 respectively).

When the second trimester values were examined, the average FBG was 82.2±5.8 mg/dL in the non-GDM group and 93.6±6.2 mg/dL in the GDM group, and a statistically significant difference was found (p<0.001). HbA1C was an average of 4.9±0.3% in the non-GDM group and an average of 5.3±0.3% in the GDM group. A statistically significant difference was also found for this parameter (p<0.001). The average 2nd trimester FT3 was 3.0±0.3 ng/dL in both groups, and there was no statistically significant difference (p=0.826). The 2nd trimester FT4 was 1.0±0.1 ng/dL on average in both groups, and there was no statistically significant difference (p=0.599).

When the OGTT parameters were examined, the OGTT-FBG, 75 g OGTT 1st hour and 2nd hour values were statistically significantly higher in GDM patients (<0.001, <0.001, <0.001 respectively). There were no statistically significant differences in terms of TSH values both in the low and high categories and between the alternative categories (p=0.135, p=0.572 in the 1st and 2nd Trimester, respectively).

The demographic data of our patients, the values of FBG, HbA1c, and TFT in the 1st and 2nd trimester, and the OGTT data are presented in Table 1.

Table 2 presents the AUC values of FBG and HbA1c in the first trimester. The cut-off value of 1st trimester HbA1C was statistically significant for the diagnosis of GDM, and the AUC was calculated as 0.740 (0.94-0.38) for HbA1C at a cut-off value of 5.2. AUC = 0.591 (0.33-0.81) for 1st trimester FBG at a cut-off value of 89.

Table 3 presents the AUC values of 2nd trimester FBG and 2nd trimester HbA1C. The cut-off value of 2nd trimester FBG and 2nd trimester HbA1C were statistically significant in the diagnosis of GDM, and the AUC values were 0.912 (0.60-0.96) for 2nd trimester FBG at a cut-off value of 88 and 0.786 (0.37-0.93) for 2nd trimester HbA1C at a cut-off value of 5.

AUC values were compared in Table 4, and the DeLong test was performed. Accordingly, it was observed that 2nd trimester FBG and 2nd trimester HbA1C predicted GDM statistically significantly better than 1st trimester fasting blood sugar (p=0.00, p=0.04). It was observed that 2nd trimester FBG predicted GDM significantly better than 2nd trimester HbA1C (p=0.028). Although no statistically significant difference was detected between 1st trimester HbA1C and 2nd trimester HbA1C in terms of predicting GDM (p=0.481); It was observed that 2nd trimester FBG predicted GDM statistically significantly better than the first trimester HbA1c (p=0.004).

According to the ROC curve analysis, 1st and 2nd trimester HbA1C and 2nd trimester FBG and OGTT values showed strong performance in predicting gestational diabetes. Some parameters, such as age, showed lower predictive performance (Figure 1).

DISCUSSION

In our study, HbA1c was significantly higher in the GDM group in the first trimester. The cut-off value with the highest Youden index was 5.2, showing 89.47% sensitivity and 54.24% specificity in predicting gestational diabetes. The model demonstrated high prediction performance with an AUC value of 0.740. First trimester FBG showed 52.63% sensitivity and 66.1% specificity for predicting gestational

Table 1. Relationship between demographic characteristics, FBG, HbA1C, TFT, and gestational diabetes

	GDM (-)	GDM (+)	Total	p-value
Age (mean SD)	27.3 (5.4)	29.6 (5.0)	27.9 (5.4)	0.113
Size (mean SD)	1.6 (0.1)	1.6 (0.1)	1.6 (0.1)	0.839
Weight (median IQR)	67.0 (57.5 to 74.0)	72.0 (60.0 to 81.0)	67.5 (58.2 to 76.0)	0.111
Gravida (mean SD)				
1	30 (50.8)	5 (26.3)	35 (44.9)	0.171
2	11 (18.6)	4 (21.1)	15 (19.2)	
3	10 (16.9)	6 (31.6)	16 (20.5)	
4	5 (8.5)	4 (21.1)	9 (11.5)	
5	3 (5.1)	0 (0.0)	3 (3.8)	
Chemical pregnancy (mean SD)	1 (1.7)	0 (0.0)	1 (1.3)	1.000
Abortion story (mean SD)				
0	45 (76.3)	15 (78.9)	60 (76.9)	0.481
1	8 (13.6)	4 (21.1)	12 (15.4)	
2	5 (8.5)	0 (0.0)	5 (6.4)	
3	1 (1.7)	0 (0.0)	1 (1.3)	
Curettage (mean SD)	1 (1.7)	0 (0.0)	1 (1.3)	1.000
Thyroglobulin (mean SD)	9 (15.3)	2 (10.5)	11 (14.1)	0.982
Thioperoxidase (mean SD)	9 (15.3)	4 (21.1)	13 (16.7)	0.813
1st trimester				
FBG (mg/dL) (mean SD)	85.0 (6.3)	87.0 (6.6)	85.5 (6.4)	0.245
HbA1C (%) (mean SD)	5.2 (0.3)	5.4 (0.3)	5.2 (0.3)	0.002
FT3 (ng/dL) (mean SD)	2.9 (0.4)	2.9 (0.4)	2.9 (0.4)	0.458
FT4 (ng/dL) (median IQR)	1.2 (1.1 to 1.3)	1.2 (1.2 to 1.2)	1.2 (1.1 to 1.2)	0.514
TSH (mIU/L) (median IQR)	1.3 (1.0 to 2.2)	1.0 (0.5 to 1.6)	1.2 (0.9 to 2.1)	0.135
2nd trimester				
FBG (mg/dL) (mean SD)	82.2 (5.8)	93.6 (6.2)	85.0 (7.7)	<0.001
HbA1C (%) (mean SD)	4.9 (0.3)	5.3 (0.3)	5.0 (0.3)	<0.001
FT3 (ng/dL) (mean SD)	3.0 (0.3)	3.0 (0.3)	3.0 (0.3)	0.826
FT4 (ng/dL) (mean SD)	1.0 (0.1)	1.0 (0.1)	1.0 (0.1)	0.599
TSH level (mIU/L) (median IQR)	1.9 (1.5 to 2.7)	1.6 (1.2 to 3.1)	1.9 (1.4 to 2.8)	0.572
2.TR-75 OGTT-FBG (mean SD)	82.5 (5.9)	94.2 (5.8)	85.3 (7.7)	<0.001
75 OGTT, 1st hour (mean SD)	125.4 (24.0)	159.8 (27.7)	133.8 (28.9)	<0.001
75 OGTT-2nd hour (mean SD)	101.4 (17.2)	128.4 (29.1)	108.0 (23.6)	<0.001

GDM: Gestational diabetes mellitus, FBG: Fast blood glucose, FT4: Free thyroxine, TSH: Thyroid stimulating hormone, OGTT: Oral glucose tolerance test

Table 2. Receiver operating characteristic analysis of 1st trimester FBG and HbA1C for the prediction of diagnosis

	Cut-off value	Sensitivity	Specificity	NPV%	PPV %	95% CI	Youden's index	AUC	p-value
1st trimester FBG (mg/dL)	89	52.63%	66.1%	81.25%	33.3 %	33-81.25%	0.187	0.591	0.121
1st trimester HbA1C (%)	5.2	89.47%	54.24%	94.12%	38.64%	38.64-94.12%	0.437	0.740	0.000

FBG: Fast blood glucose, NPV: Negative predictive value, PPV: Positive predictive value, AUC: Area under the curve, CI: Confidence interval

Table 3. Receiver operating characteristic analysis of 2nd trimester FBG and 2nd trimester HbA1C for the prediction of diagnosis

	Cut-off value	Sensitivity	Specificity	NPV%	PPV %	95% CI	Youden's index	AUC	p value
2nd trimester FBG (mg/dL)	88	89.47%	81.36%	96%	60.71%	60.71-96%	0.708	0.912	0.000
2nd trimester HbA1C (%)	5	89.47%	52.54%	93.94%	37.78%	37.78-93.94%	0.420	0.786	0.000

FBG: Fast blood glucose, NPV: Negative predictive value, PPV: Positive predictive value, AUC: Area under the curve, CI: Confidence interval

Table 4. AUC differences in 1st trimester FBG, 1st trimester HbA1C, 2nd trimester FBG, 2nd trimester HbA1C

	AUC 1	AUC 2	AUC difference	CI lower	CI upper	p (delong test)
1st tr FBG vs. 1st tr HbA1C	0.591	0.740	0.149	0.34	0.041	0.124
1st tr FBG vs. 2nd tr FBG	0.591	0.912	0.322	0.474	0.169	0.00
1st tr FBG vs. 2nd tr HbA1C	0.591	0.786	0.196	0.382	0.009	0.04
1st tr FBG vs. age	0.591	0.635	0.045	0.257	0.168	0.680
1st tr HbA1C vs. 2nd tr FBG	0.740	0.912	0.172	0.289	0.055	0.004
1st tr HbA1C vs. 2nd tr HbA1c	0.740	0.786	0.046	0.175	0.083	0.481
1st tr HbA1C vs. age	0.740	0.635	0.105	0.074	0.284	0.251
2nd tr FBG vs. 2nd tr HbA1C	0.912	0.786	0.126	0.014	0.238	0.028
2nd tr FBG vs. age	0.912	0.635	0.277	0.117	0.437	0.001
2nd tr HbA1C vs. age	0.786	0.635	0.151	0.017	0.319	0.077

tr: Trimester, FBG: Fast blood glucose, AUC: Area under the curve, CI: Confidence Interval, p<0.05, statistically significant

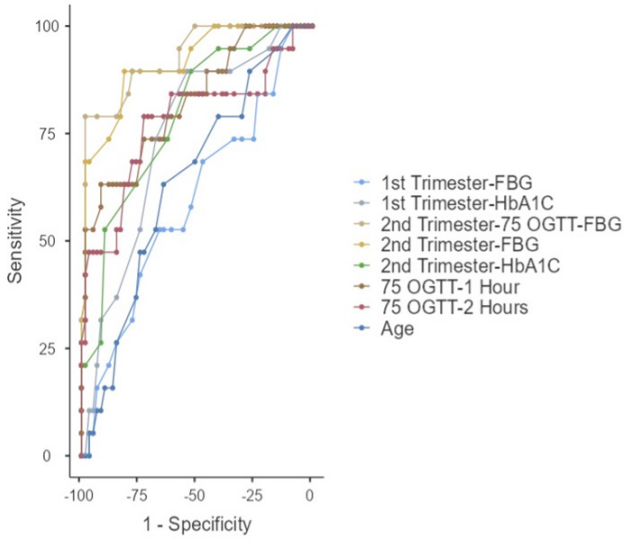

Figure 1. Receiver operating characteristic curves for the FBG, HbA1c, OGTT, and age for the prediction of GDM
FBG: Fasting blood glucose, OGTT: Glucose tolerance test, GDM: Gestational diabetes mellitus

diabetes. FBG demonstrated moderate predictive performance with an AUC of 0.591. Although the AUC difference between HbA1C and FBG was not significant, 1st trimester HbA1c was a strong parameter in predicting GDM based on the Youden index and AUC values. When 2nd trimester HbA1C and 2nd trimester FBG were examined, the AUC value of HbA1C was 0.786, which was highly predictive of GDM. It is clear that FBG is a more powerful parameter for predicting GDM than HbA1C, with an AUC value of 0.912. The AUC difference was statistically significant.

As a result, especially 1st and 2nd trimester HbA1C and 2nd trimester FBG and OGTT values showed strong performance in predicting gestational diabetes. Although there are studies showing that age increases the incidence of GDM, no statistically significant relationship was found between age and GDM in our study (2). No statistically significant relationship was detected between TFT (TSH, FT3, FT4, TPO, thyroglobulin) and GDM in the first and second trimesters. Studies investigating the relationship between TFT and GDM and obtaining different results have taken place in the literature. In a retrospective study including more than 2,000 pregnant women, high FT4 was not observed in pregnant women who developed GDM; No significant relationship could be detected between TSH and GDM (4). In a study by Zhang et al. (5), the relationship between TSH concentrations and GDM was similar to that in our study. In another study evaluating the relationship between FT4 levels and GDM, high F4 levels were shown to predict GDM (6).

According to our study, although we found a clear superiority of FBG in the 2nd trimester, HbA1C level proved that it can strongly predict GDM in both the first and second

trimesters. HbA1c is expected to fall below normal values during pregnancy. This condition should also be taken into consideration in the relationship between GDM diagnosis and HbA1C level (7). Several studies have evaluated the relationship between HbA1C and FBG levels and GDM (8,9). In a retrospective study including 107 pregnant women, it was concluded that HbA1C and FBG could predict GDM, but TFT such as FT4 and TSH could not be used in the diagnosis of GDM, similar to our study (8). In a prospectively planned study, it was concluded that HbA1c in the first trimester could not be used instead of OGTT, and a statistically significant relationship was found between HbA1C and the risk of GDM development (9). In a meta-analysis evaluating OGTT and HbA1C tests performed in the second or third trimester of pregnancy, it was found that HbA1C could predict GDM with an AUC value >0.800 (11). In our study, OGTT FBG and OGTT 1st hour AUC values were higher than HbA1C. Therefore, according to our study, we cannot say that we can use HbA1C instead of OGTT. In a study investigating the relationship between HbA1C levels in the third trimester and GDM, it was determined that there was a statistically significant relationship between HbA1C and GDM, but since the AUC was less than 0.80, it was determined that HbA1C was not sufficient to predict GDM (12). In another study examining HbA1C and FBG values taken in the first trimester, the ability of HbA1C and FBG values to predict GDM was similar to that of our study (13). Again, a prospective observational study conducted in the first trimester determined that HbA1C could predict GDM (14).

The studies mostly consisted of data from specific trimesters. The comparison of data obtained in different trimesters, as in our study, has also begun to take place in the literature. In a study evaluating 45 patients diagnosed with GDM, HbA1C levels in both the first and second trimesters were statistically significantly higher in pregnant women diagnosed with GDM than in the control group, similar to our study (15). We also think that many pregnancy-related complications can be prevented using pre-pregnancy data. In a prospective study by Alwash et al. (16), pre-pregnancy FBG levels were associated with GDM. Pre-pregnancy HbA1C and TFT values will also contribute to the literature.

Study Limitations

Because our study was retrospective, data were obtained from the hospital data system. Our number of patients was limited to obtain detailed examinations and both trimester values of the patients.

CONCLUSION

First- and second-trimester HbA1c and FBG and OGTT values can predict gestational diabetes. HbA1C cannot be used instead of OGTT, but it is an important predictor. Second-trimester FBG is more powerful in predicting GDM than first- and second-trimester HbA1c and first-trimester FBG.

ETHICS

Ethics Committee Approval: The instant study was carried out with the permission of Local Ethics Committee of the Karamanoğlu Mehmetbey University Faculty of Medicine (number: 06-2024/19, date: 30.05.2024).

Informed Consent: Retrospective study.

FOOTNOTES

Authorship Contributions

Surgical and Medical Practices: Ö.D., Concept: Ö.D., H.Ş.A., Design: Ö.D., H.Ş.A., S.K., Data Collection or Processing: Ö.D., Analysis or Interpretation: Ö.D., H.Ş.A., Literature Search: Ö.D., H.Ş.A., S.K., Writing: H.Ş.A.

Conflict of Interest: No conflict of interest was declared by the authors.

Financial Disclosure: The authors declare that this study received no financial support.

REFERENCES

1. Hod M, Kapur A, Sacks DA, Hadar E, Agarwal M, Di Renzo GC, et al. The International Federation of Gynecology and Obstetrics (FIGO) initiative on gestational diabetes mellitus: a pragmatic guide for diagnosis, management, and care. Int J Gynaecol Obstet. 2015;131:173-211.
2. Yuen L, Saeedi P, Riaz M, Karuranga S, Divakar H, Levitt N, et al. Projections of the prevalence of hyperglycaemia in pregnancy in 2019 and beyond: Results from the International Diabetes Federation Diabetes Atlas, 9th edition. Diabetes Res Clin Pract. 2019;157:107841.
3. Sacks DA, Hadden DR, Maresh M, Deerochanawong C, Dyer AR, Metzger BE, et al. HAPO study cooperative research group. Frequency of gestational diabetes mellitus at collaborating centers based on IADPSG consensus panel-recommended criteria: the hyperglycemia and adverse pregnancy outcome (HAPO) study. Diabetes Care. 2012;35:526-8.
4. Chen G, Gou X-Y, Pang T, Li P, Zhou Z, Lin D, et al. Associations between thyroid function and gestational diabetes mellitus in Chinese pregnant women: a retrospective cohort study. BMC Endocr Disord. 2022;22:44
5. Zhang Y, Sun W, Zhu S, Huang Y, Huang Y, Gao Y, et al. The Impact of Thyroid Function and TPOAb in the First Trimester on Pregnancy Outcomes: A Retrospective Study in Peking. J Clin Endocrinol Metab. 2020;105:167.
6. Yang S, Shi FT, Leung PC, Huang HF, Fan J. Low Thyroid Hormone in Early Pregnancy Is Associated With an Increased Risk of Gestational Diabetes Mellitus. J Clin Endocrinol Metab. 2016;101:4237-43.

7. Nielsen LR, Ekbom P, Damm P, Glümer C, Frandsen MM, Jensen DM, Mathiesen ER. HbA1c levels are significantly lower in early and late pregnancy. Diabetes Care. 2004;27:1200-01.
8. Özışık H, Çetinkalp Ş, Suner A, Hortu İ, Ergenoğlu AM, Erdoğan M. Comparison of thyroid function tests in pregnant women with and without gestational diabetes. Turk J Diab Obes. 2021;3:285-90.
9. Valadan M, Bahramnezhad Z, Golshahi F, Feizabad E. The role of first-trimester HbA1c in the early detection of gestational diabetes. BMC Pregnancy Childbirth. 2022;22:71.
10. American Diabetes Association. Standards of medical care in diabetes--2010. Diabetes Care. 2010;33(Suppl 1):11-61.
11. Renz PB, Chume FC, Timm JRT, Pimentel AL, Camargo JL. Diagnostic accuracy of glycated hemoglobin for gestational diabetes mellitus: a systematic review and meta-analysis. Clin Chem Lab Med. 2019;57:1435-49.
12. Rayis DA, Ahmed ABA, Sharif ME, ElSouli A, Adam I. Reliability of glycosylated hemoglobin in the diagnosis of gestational diabetes mellitus. J Clin Lab Anal. 2020;34:23435.
13. Kırlangıc MM, Arıcı Halıcı BN. Evaluation of first trimester fasting blood glucose, HOMA-IR and HbA1c in prediction of gestational diabetes mellitus in nonobese pregnant women: A retrospective study. Turk J Diab Obes. 2022;3:267-73.
14. Sahoo G, Das S, Panda P, Pravalina R. Role of serum hba1c level for prediction of gestational diabetes mellitus in first trimester. IRJMS. 2024;5:421-7.
15. Abbas S, Khattak M, Hameed S, Saeed S, Shabir R. HbA1c as an early diagnostic marker in gestational diabetes mellitus. The Professional Medical Journal, 2024;31:750-6.
16. Alwash S, McIntyre D, Mamun A. The pre-pregnancy fasting blood glucose, glycated hemoglobin and lipid profiles as blood biomarkers for gestational diabetes mellitus: evidence from a multigenerational cohort study. J Matern Fetal Neonatal Med. 2023;36:2195524.

Medical Journal of Bakırköy

Med J Bakirkoy 2025;21:14-18
DOI: 10.4274/BMJ.galenos.2024.2024.8-6

Research

Frequencies and Lines of Pediatric Distal Humerus Fractures: Where and How are the Fractures?

Pediatrik Distal Humerus Kırıklarının Sıklığı ve Çizgileri: Kırıklar Nerede ve Nasıldır?

Malik Çelik[1], Ahmet Çanlıoğlu[2], Murat Tıngır[3], Vedat Öztürk[1], Cemal Kural[1]

[1]University of Health Sciences Türkiye, Bakırköy Dr. Sadi Konuk Training and Research Hospital, Clinic of Orthopaedics and Traumatology, İstanbul, Türkiye

[2]University of Health Sciences Türkiye, Kartal Dr. Lütfi Kırdar Training and Research Hospital, Clinic of Orthopaedics and Traumatology, İstanbul, Türkiye

[3]State Hospital, Clinic of Orthopedics and Traumatology, Trabzon, Türkiye

ABSTRACT

Objective: The type, lines, and location of the fracture play an important role in the complications and clinical course of distal humerus fractures in children. This study aims to demonstrate the fracture lines of pediatric distal humerus fractures on a 2D model, determine where the fractures are concentrated, and investigate the relationship between these findings and age range.

Methods: A total of 194 pediatric distal humerus fractures were retrospectively reviewed and analyzed. For each fracture, a map of the fracture lines was drawn and graphically overlaid on the 2D model (anterior, lateral) with this method, fracture lines were determined according to age ranges. Fracture models and density maps were created.

Results: Our analysis was based on 194 X-ray images of pediatric distal humerus fractures, including 131 male and 63 female patients. It included 14 epiphyses, 83 physes and 97 metaphyses fractures. In the mapping, it was seen that the fracture lines between the ages of 2-6 were mostly concentrated on the physis. In addition, it was mostly seen in the metaphysis in patients aged 6-12 years.

Conclusion: Pediatric distal humeral fracture lines follow characteristic patterns that are closely related to bone structure and age. Understanding the characteristics of these fractures can assist surgeons during diagnosis, preoperative planning, and implementation of surgical strategies.

Keywords: Pediatric, elbow, distal humerus, fracture frequency, fracture lines

ÖZ

Amaç: Çocuklarda distal humerus kırıklarının komplikasyonları ve klinik seyrinde kırığın tipi, hatları ve yeri önemli rol oynar. Bu çalışmanın amacı, pediatrik distal humerus kırıklarının kırık hatlarını 2 boyutlu bir modelde göstermek, kırıkların nerede yoğunlaştığını belirlemek ve bu bulgular ile yaş aralığı arasındaki ilişkiyi araştırmaktır.

Gereç ve Yöntem: Toplam 194 pediatrik distal humerus kırığı retrospektif olarak incelendi ve analiz edildi. Her kırık için, kırık hatlarının haritası 2 boyutlu modele (ön, yan) çizildi ve grafiksel olarak üst üste bindirildi. Bu yöntemle, kırık hatları yaş aralıklarına göre belirlendi. Kırık modelleri ve yoğunluk haritaları oluşturuldu.

Bulgular: Analizimiz, 131 erkek ve 63 kadın hastayı içeren 194 pediatrik distal humerus kırığı röntgen görüntüsüne dayanmaktadır. On dört epifiz, 83 fiziz ve 97 metafiz kırığı içeriyordu. Haritalamada, 2-6 yaş arasındaki kırık hatlarının çoğunlukla fizizde yoğunlaştığı görüldü. Ayrıca, 6-12 yaş aralığındaki hastalarda çoğunlukla metafizde görüldü.

Sonuç: Pediatrik distal humerus kırık hatları, kemik yapısı ve yaşla yakından ilişkili karakteristik desenleri takip eder. Bu kırıkların özelliklerini anlamak, cerrahlara tanı, ameliyat öncesi planlama ve cerrahi stratejilerin uygulanması sırasında yardımcı olabilir.

Anahtar Kelimeler: Pediatrik, dirsek, distal humerus, kırık sıklığı, kırık hatları

Address for Correspondence: Malik Çelik, University of Health Sciences Türkiye, Bakırköy Dr. Sadi Konuk Training and Research Hospital, Clinic of Orthopaedics and Traumatology, İstanbul, Türkiye
E-mail: drmalikcelik@hotmail.com **ORCID ID:** orcid.org/0000-0002-3696-9644

Cite as: Çelik M, Çanlıoğlu A, Tıngır M, Öztürk V, Kural C. Frequencies and lines of pediatric distal humerus fractures: where and how are the fractures? Med J Bakirkoy. 2025;21:14-18

Received: 22.08.2024
Accepted: 04.10.2024
Publication Date: 25.03.2025

INTRODUCTION

Distal humerus fractures are a significant concern among pediatric orthopaedic injuries, accounting for approximately 60% of all elbow fractures. These fractures occur at the distal end of the humerus, just above the elbow joint, and are often encountered in children due to their active lifestyles and vulnerability to traumatic incidents (1). It is essential for healthcare providers to comprehend the epidemiology, clinical presentation, classification, and management of distal humerus fractures, as these fractures can significantly impact a child's functional recovery and limb development (2-4).

Distal humerus fractures in children can vary in severity from mild to moderate to severe and can be managed through a range of treatment options, including non-surgical methods such as casting and surgical procedures such as closed reduction or open reduction (5). The choice of treatment depends on various factors, including the fracture type, degree of displacement, age of the patients, and associated neurovascular compromise. These fractures demand specialized care, as complications such as neurovascular injury and malunion can have lasting effects on a child's quality of life (6,7).

The advancement of medical imaging software has led to the popularization of "fracture mapping", a novel technique used to describe the distribution of fracture lines. Fracture mapping can record the size, shape, number, and orientation of fracture fragments, and help surgeons determine the most appropriate treatment (8). In the literature, many different anatomical regions in adult patients, such as patella fracture (9), tibia plateau fracture (10), femur intertrochanteric fracture (11), and distal humerus fracture (12), have been investigated based on Tri-dimensional (3D) images, and the results have been published. These studies have shown that fracture mapping can provide valuable information for preoperative planning and postoperative evaluation, ultimately improving patient outcomes. Additionally, the use of 3D imaging in fracture mapping has the potential to revolutionize the field of orthopaedic surgery by allowing for more precise and personalized treatment strategies (10). However, concerns about created using tomography (CT) imaging in pediatric patients have led to a paucity of similar studies for the pediatric population.

The study aimed to map the most common fracture lines and locations using X-ray (2D) imaging. We hypothesized that we would find differences in fracture pattern and location as the physis closes and bone maturity occurs in different age ranges.

METHODS

Study design

After approval from the local ethics committee, the study was conducted retrospectively. Patients admitted to our tertiary hospital with elbow fractures between October 1, 2019, and October 1, 2023, were evaluated. The inclusion criteria were as follows: (1) distal humeral fractures; (2) under 18 years of age; (3) patients who were followed up in our hospital for at least 6 months. The exclusion criteria were as follows: • >18 years; • complex fracture (with radius, ulna, dislocation); • insufficient medical record (Figure 1). The patients were divided into four groups according to age: Ages 0-2, ages 2-6, ages 6-12, and ages 12-18 (13). The etiology of the patients' injuries, whether surgery was performed, and the presence of post-fracture complications were noted. The distal humerus was anatomically noted as having three regions: Metaphysis, physis, and epiphysis.

Distal Humerus Templates

2D images were imported into Adobe Illustrator (Adobe Inc., Mountain View, CA, USA) and used as the fracture mapping templates.

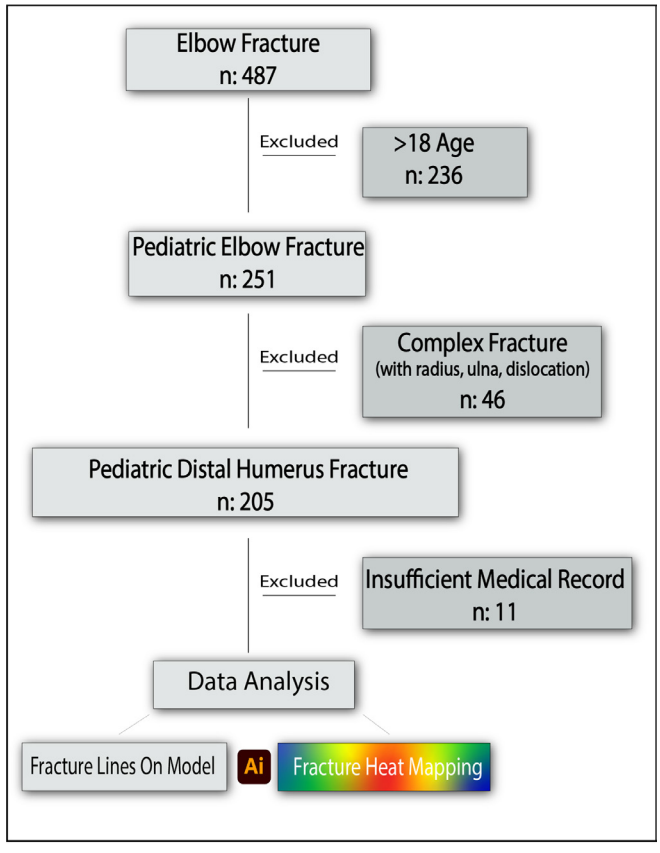

Figure 1. Study flowchart

Fracture Lines Heat Map

The original Digital Imaging and Communications in Medicine files were collected and analyzed with Synapse Vincente (Fujifilm Co., Ltd., Tokyo, Japan). The fracture lines were clearly observed. These reductive fracture models were then modified to generate 2D images that were presented in the same anatomical plane as the templates. In Adobe Illustrator, the fracture lines were manually drawn onto the template layer and then graphically overlapped to compile a fracture map. The superimposition of all layers resulted in maps showing density variations in correlation with the frequency and location of fractures.

Statistical Analysis

The IBM SPSS 26 (Chicago, IL, USA) program was used for statistical analysis. Descriptive statistical methods (minimum, maximum, median) were used when evaluating the study data. The chi-square test was used in the analysis of qualitative independent data. Statistical significance was accepted as $p<0.05$.

RESULTS

The patients' demographic features are presented in Table 1. Among the 194 X-ray images, there are 131 male and 63 female patients, including 32 (16.5%) aged 0-2; 100 (51.5%) aged 2-6; 53 (27.3%) aged 6-12; and 9 (4.6%) aged 12-18 (Figure 2). According to the fracture area, the epiphysis 14 (7.2%), the physis 83 (42.8%), and the metaphysis 97 (50%) (Figure 3).

Table 1. Demographic features of the patients

		Frequency (n)	Percent (%)
Age range	0-2 year	32	16.5
	2-6 year	100	51.5
	6-12 year	53	27.3
	12-18 year	9	4.6
Gender	Male	131	67.5
	Female	63	32.5
Etiology	Low energy	177	91.2
	High energy	17	8.8
Surgery	(+)	168	86.6
	(-)	26	13.4
Complication	(+)	180	92.8
	(-)	14	7.2
Fracture location	Epiphysis	14	7.2
	Physis	83	42.8
	Metaphysis	97	50.0

The descriptive features of pediatric distal humerus fracture patients in age groups are presented in Table 2. The etiology of fracture and complication rates did not differ significantly between groups ($p>0.05$). However, low-energy falls and fractures without complications were more common in both groups. A statistical difference was detected between age groups and fracture regions. Fracture lines were seen more frequently in the physis in the "0-2 age" group and in the metaphysis in the "6-12 age" group ($p<0.05$).

DISCUSSION

The histological structure of the bone, which changes with age, the anatomy of the distal humerus, and the activity levels of children at different ages make these fractures

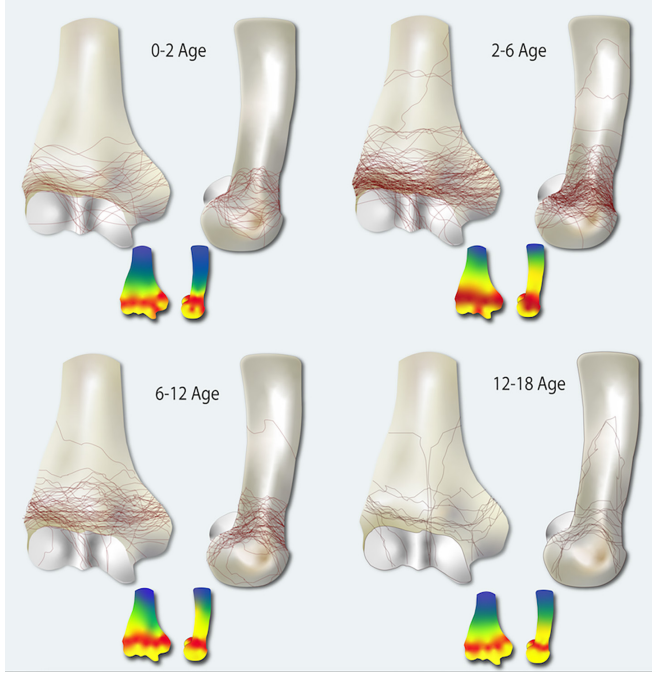

Figure 2. Fracture lines and heat map of pediatric supracondylar fracture by age range

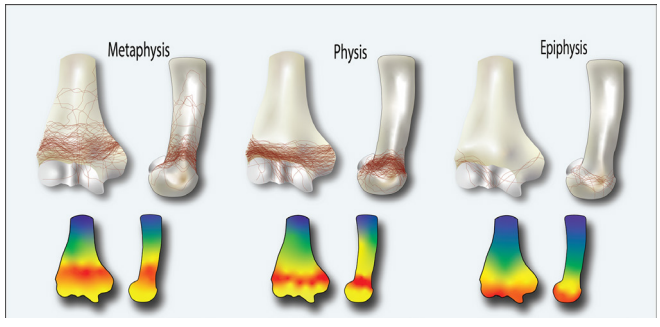

Figure 3. Fracture lines and heat map of pediatric supracondylar fracture by fracture region

Table 2. Relationship between age range and demographic features

		Age (year)				p[c]
		0-2	2-6	6-12	12-18	
Gender	Male	13	68	41	9	0.001
	Female	19	32	12	0	
Surgery	(+)	20	90	50	8	0.001
	(-)	12	10	3	1	
Etiology	Low energy	32	91	47	7	0.233
	High energy	0	9	6	2	
Complication	(-)	32	90	49	9	0.226
	(+)	0	10	4	0	
Fracture region	Epiphysis	7	5	2	0	0.001
	Physis	24	49	7	3	
	Metaphysis	1	46	44	6	

[c]Chi-square test

inevitable. I continues to be a challenge for families and healthcare professionals. This study is valuable because it investigates the fracture lines, their localization, and their relationship with age in pediatric patients presenting with a diagnosis of distal humerus fracture. The most important finding of our study was that physeal fractures were more common in younger age groups, and metaphyseal fractures were more common in older age groups.

Omid et al. (14) and Cheng et al. (2) found that pediatric distal humerus fractures are commonly observed in school-age children. This age group had a higher fracture rate in our study, which is consistent with previously published studies. An elevated risk of fracture is a well-known result of high activity levels, less parental control, and an active role in public play events. All of this can increase as children reach school age (15). Distractions that occur during play, along with the experimentation accompanying the learning of new informational skills, may also contribute to an increased risk of fractures. So, we believe that the pattern of increased injury frequency and severity that we observed between ages 2-6 and 6-12 could be related to social development at school age. On the other hand, although some current publications in the literature (16,17) suggest that the number of patients is the same for both genders, in our study we observed that distal humerus fractures are more common in males, in line with traditional knowledge.

The distal humerus includes several ossification processes that develop at various ages. The fracture structure changes when the ossification centres transition from cartilage to bone. Knowing the general ossification sequence gives the surgeon important information that helps characterize the anatomy on radiographs and guide treatment (18). At one year of age, the capitellum initially appears. Around ages 4-5, the medial epicondyle starts to ossify; this is followed by the trochlea's epiphysis around ages 8 or 9. Around age 10, the lateral condyle often develops last (19,20). The varying ages at which ossification occurs also explain the frequency of distal humerus fractures at different ages.

With the development of artificial intelligence, technological innovations, and medical imaging software, intelligent medicine has become popular as a research topic in orthopaedic literature (21,22). Large amounts of data can be collected from models CT, X-ray, and magnetic resonance images of patients, and more objective data can be obtained about the anatomical region. Due to the increasing interest in big data analysis to serve orthopaedic diagnosis, implant design, preoperative preparation, patient/medical education and treatment using CT images, Armitage et al. (8) examined scapula fractures and Cole et al. (23) examined pilon fractures. Over the years, many anatomical regions, such as the proximal femur (11), tibial plateau (10), distal radius (24), and calcaneus (25), have been examined with this hypothesis, and the results have been published. In their study investigating adult distal humerus fractures, Wang et al. (12) published the fracture lines and density map. However, they did not provide data regarding pediatric patients. High radiation is one of the biggest obstacles to performing tomography on pediatric patients. Therefore, we only have X-ray images as data. Using two-dimensional mapping technology, we characterized the fracture lines and location characteristics of pediatric distal humerus fractures in our study.

Study Limitations

It should be noted that there are certain limitations to this study. First, this study's sample size is small. Secondly, since patients referred to our tertiary hospital were included in the study, we found that there was a discrepancy between the surgical rate and the literature. Thirdly, since only AP and lateral X-ray imaging were evaluated in the study, the three-dimensional fracture line could not be evaluated. In addition, drawing the fracture line manually may have caused subjective results. Finally, there hasn't been any analysis done on the injury mechanism of pediatric distal humeral fractures and how it relates to fracture maps. Further studies could increase the sample size and investigate the difference. However, our study also had important aspects. To our knowledge, our study is the first to examine the fracture mapping method in pediatric distal humerus fractures.

CONCLUSION

In conclusion, pediatric distal humerus fractures are common and cause serious disabilities when inadequately treated. This continues to be a challenge for treatment practitioners. Fracture mapping offers numerous advantages, including precision in assessment, optimized treatment planning, improved surgical guidance, complication prediction, long-term monitoring, research potential, and enhanced patient education.

ETHICS

Ethics Committee Approval: This study was approved by the Clinical Research Ethics Committee of the University of Health Sciences Türkiye, Bakırköy Dr. Sadi Konuk Training and Research Hospital, (decision no: 2022-20-04, date: 17.10.2022).

Informed Consent: Since this study was retrospective, patient consent was not required.

FOOTNOTES

Authorship Contributions

Surgical and Medical Practices: M.Ç., V.Ö., C.K., Concept: M.Ç., Design: M.Ç., V.Ö., C.K., Data Collection or Processing: M.Ç., A.Ç., M.T., Analysis or Interpretation: M.Ç., A.Ç., M.T., C.K., Literature Search: M.Ç., A.Ç., M.T., V.Ö., Writing: M.Ç., V.Ö.

Conflict of Interest: No conflict of interest was declared by the authors.

Financial Disclosure: The authors declared that this study received no financial support.

References

1. Otsuka NY, Kasser JR. Supracondylar fractures of the humerus in children. J Am Acad Orthop Surg. 1997;5:19-26.
2. Cheng JC, Lam TP, Maffulli N. Epidemiological features of supracondylar fractures of the humerus in Chinese children. J Pediatr Orthop B. 2001;10:63-7.
3. Schuller A, Hahn S, Pichler L, Hohensteiner A, Sator T, Jaindl M, et al. Correlation of fall height, fracture severity and clinical outcome in pediatric supracondylar fractures-a retrospective analysis with an observation period of 20 years. Children. 2023;10:510.
4. Çelik M, Kantarci M, Sapmaz İ.E, Baca E, Duramaz A. Characterization and mapping of upper extremity fractures in children by a tertiary hospital quarantine and post-quarantine period. Jt Dis Relat Surg. 2024;35:692-8.
5. Vaquero-Picado A, Gonzalez-Moran G, Moraleda L. Management of supracondylar fractures of the humerus in children. EFORT Open Rev. 2018;3:526-40.
6. White L, Mehlman CT, Crawford AH. Perfused, pulseless, and puzzling: a systematic review of vascular injuries in pediatric supracondylar humerus fractures and results of a POSNA questionnaire. J Pediatr Orthop. 2010;30:328-35.
7. Wu J, Perron AD, Miller MD, Powell SM, Brady WJ. Orthopedic pitfalls in the ED: pediatric supracondylar humerus fractures. Am J Emerg Med. 2002;20:544-50.
8. Armitage BM, Wijdicks CA, Tarkin IS, Schroder LK, Marek DJ, Zlowodzki M, et al. Mapping of scapular fractures with three-dimensional computed tomography. J Bone Joint Surg Am. 2009;91:2222-8.
9. Cho JW, Yang Z, Lim EJ, Sakong S, Choi W, Son WS, et al. Multifragmentary patellar fracture has a distinct fracture pattern which makes coronal split, inferior pole, or satellite fragments. Sci Rep. 2021;11:22836.
10. Molenaars RJ, Mellema JJ, Doornberg JN, Kloen P. Tibial plateau fracture characteristics: computed tomography mapping of lateral, medial, and bicondylar fractures. J Bone Joint Surg Am. 2015;97:1512-20.
11. Li M, Li ZR, Li JT, Lei MX, Su XY, Wang GQ, et al. Three-dimensional mapping of intertrochanteric fracture lines. Chin Med J (Engl). 2019;132:2524-33.
12. Wang C, Zhu Y, Long H, Lin Z, Zhao R, Sun B, et al. Three-dimensional mapping of distal humerus fracture. J Orthop Surg Res. 2021;16:545.
13. Williams K, Thomson D, Seto I, Contopoulos-Ioannidis DG, Ioannidis JP, Curtis S, et al. Standard 6: age groups for pediatric trials. Pediatrics. 2012;129(Suppl 3):153-60.
14. Omid R, Choi PD, Skaggs DL. Supracondylar humeral fractures in children. J Bone Joint Surg Am. 2008;90:1121-32.
15. Petridou E, Sibert J, Dedoukou X, Skalkidis I, Trichopoulos D. Injuries in public and private playgrounds: the relative contribution of structural, equipment and human factors. Acta Paediatr. 2002;91:691-7.
16. Farnsworth CL, Silva PD, Mubarak SJ. Etiology of supracondylar humerus fractures. J Pediatr Orthop. 1998;18:38-42.
17. Mitchelson AJ, Illingworth KD, Robinson BS, Elnimeiry KA, Wilson CJ, Markwell SJ, et al. Patient demographics and risk factors in pediatric distal humeral supracondylar fractures. Orthopedics. 2013;36:700-6.
18. Yigitbay A, Celik M. A rare case: transphyseal distal humerus fracture in a newborn. Acta Chir Orthop Traumatol Cech. 2024;9:120-2.
19. Gartland JJ. Management of supracondylar fractures of the humerus in children. Surg Gynecol Obstet. 1959;109:145-54.
20. Skaggs DL. Elbow fractures in children: diagnosis and management. J Am Acad Orthop Surg. 1997;5:303-12.
21. Bini SA. Artificial intelligence, machine learning, deep learning, and cognitive computing: what do these terms mean and how will they impact health care? J Arthroplasty. 2018;33:2358-61.
22. Langerhuizen DWG, Janssen SJ, Mallee WH, van den Bekerom MPJ, Ring D, Kerkhoffs G, et al. What are the applications and limitations of artificial intelligence for fracture detection and classification in orthopaedic trauma imaging? A systematic review. Clin Orthop Relat Res. 2019;477:2482-91.
23. Cole PA, Mehrle RK, Bhandari M, Zlowodzki M. The pilon map: fracture lines and comminution zones in OTA/AO type 43C3 pilon fractures. J Orthop Trauma. 2013;27:152-6.
24. Li S, Zhang YQ, Wang GH, Li K, Wang J, Ni M. Melone's concept revisited in comminuted distal radius fractures: the three-dimensional CT mapping. J Orthop Surg Res. 2020;15:222.
25. Zhang B, Lu H, Quan Y, Wang Y, Xu H. Fracture mapping of intra-articular calcaneal fractures. Int Orthop. 2023;47:241-9.

Medical Journal of Bakırköy

Med J Bakirkoy 2025;21:19-23
DOI: 10.4274/BMJ.galenos.2024.2023.10-9

Research

Clinicopathological Reflections of Hashimoto's Thyroiditis and Papillary Thyroid Carcinoma Coexistence

Hashimoto Tiroiditi - Papiller Tiroid Karsinomu Birlikteliğinin Klinikopatolojik Yansımaları

Can Akcura[1], Samet Alkan[1], Sedat Can Güney[1], Gamze Gelir Çavdar[2], Emel Şenol[3], Ayça Tan[4], Nilüfer Özdemir[1], Hasan Aydede[5], Zeliha Hekimsoy[1]

[1]Manisa Celal Bayar University Faculty of Medicine, Department of Endocrinology and Metabolism, Manisa, Türkiye

[2]University of Health Sciences Türkiye, İzmir Bozyaka Training and Research Hospital, Department of Endocrinology and Metabolism, İzmir, Türkiye

[3]University of Health Sciences Türkiye, Mersin State Hospital, Department of Endocrinology and Metabolism, Mersin, Türkiye

[4]Manisa Celal Bayar University Faculty of Medicine, Department of Pathology, Manisa, Türkiye

[5]Manisa Celal Bayar University Faculty of Medicine, Department of General Surgery, Manisa, Türkiye

ABSTRACT

Objective: Papillary thyroid carcinoma (PTC) is the most common subtype of thyroid cancer. Hashimoto's thyroiditis (HT), a chronic inflammation of the thyroid gland, is one of the most common autoimmune diseases worldwide. In this study, we aimed to determine the relationship between PTC and HT and the clinicopathological effects of the combination of HT and PTC on the course of PTC.

Methods: In this cross-sectional retrospective study, PTC cases who underwent surgery and were followed up at our institution's endocrinology outpatient clinic between 2014 and 2022 were divided into two groups according to the presence of HT. Demographic data of both groups, pathological features of the tumor, and preoperative laboratory findings were examined.

Results: A total of 42.4% (n=118) of 278 cases were accompanied by HT. The mean age of the patients was 46.44±12.2 years. The majority of patients were female (80.6%, n=224). Multifocality was significantly less common in the HT group (p=0.037).

Conclusion: Although multifocality was significantly less common in the HT group, no other statistically significant parameter was discovered in other clinicopathological findings. In light of these findings, the effect of HT on the course of PTC cannot be clearly determined. Considering the conflicting results regarding the effect of HT-PTC coexistence on the course of PTC in the literature, a comprehensive prospective study on this subject is necessary.

Keywords: Clinicopathology, Hashimoto's thyroiditis, multifocality, papillary thyroid carcinoma

ÖZ

Amaç: Papiller tiroid karsinomu (PTC), tiroid kanserinin en sık görülen alt tipidir. Tiroid bezinin kronik enflamasyonu ile karakterize Hashimoto tiroiditi (HT), dünya çapında en yaygın otoimmün hastalıklardan biridir. Bu çalışmada PTC ile HT arasındaki ilişkiyi ve HT ile PTC birlikteliğinin PTC seyri üzerindeki klinikopatolojik etkilerini belirlemeyi amaçladık.

Gereç ve Yöntem: Bu kesitsel retrospektif çalışmada 2014-2022 yılları arasında kurumumuzda opere olup sonrasında endokrinoloji kliniğimizce takip edilen PTC olguları HT varlığına göre iki gruba ayrıldı. Her iki grubun demografik verileri, tümörün patolojik özellikleri ve hastaların ameliyat öncesi laboratuvar bulguları incelendi.

Bulgular: Toplam 278 olgunun %42,4'üne (n=118) HT'nin eşlik ettiği görüldü. Hastaların yaş ortalaması 46,44±12,2 yıldı. Hastaların çoğunluğu kadındı (%80,6 n=224). Multifokalitenin HT grubunda anlamlı derecede daha az olduğu görüldü (p=0,037).

Sonuç: Multifokalite HT grubunda anlamlı olarak daha az görülmesine rağmen diğer klinikopatolojik bulgularda istatistiksel olarak anlamlı başka bir parametre saptanmadı. Bu bulgular ışığında HT'nin PTK'nin seyrine etkisini net olarak ortaya koymak mümkün değildir. Literatürde HT-PTC birlikteliğinin PTC seyrine etkisine ilişkin çelişkili sonuçların olduğu göz önüne alındığında bu konuda kapsamlı prospektif çalışmalara ihtiyaç olduğu açıktır.

Anahtar Kelimeler: Klinikopatoloji, Hashimoto tiroiditi, multifokalite, papiller tiroid karsinomu

Address for Correspondence: Can Akcura MD, Manisa Celal Bayar University Faculty of Medicine, Department of Endocrinology and Metabolism, Manisa, Türkiye
E-mail: can.akcura@hotmail.com **ORCID ID:** orcid.org/0000-0003-4182-9002

Cite as: Akcura C, Alkana S, Güney SC, Gelir Çavdar G, Şenol E, Tan A, et al. Clinicopathological reflections of hashimoto's thyroiditis and papillary thyroid carcinoma coexistence. Med J Bakirkoy. 2025;21:19-23

Received: 02.11.2023
Accepted: 23.07.2024
Publication Date: 25.03.2025

INTRODUCTION

Thyroid carcinoma is the most common cancer of the endocrine system, accounting for 3.4% of all cancer types diagnosed annually (1). Papillary thyroid carcinoma (PTC), a differentiated thyroid cancer, is the most common subtype.

Hashimoto's thyroiditis (HT), a chronic inflammation of the thyroid gland, is one of the most common autoimmune diseases worldwide. It has a prevalence rate of 5-10% and is characterized by hypothyroidism, positivity of serum anti-thyroid peroxidase and/or anti-thyroglobulin antibodies, and lymphocyte infiltration with destruction of thyroid follicle cells (2).The relationship between PTC and HT is a long-standing issue. This subject has biomolecular and clinicopathological aspects, and many related studies have been carried out. As a result of these studies, many biomolecular properties in common were found. These findings include *RET/PTC* oncogene rearrangement, BRAF (V600E) mutation partnership, phosphatidylinositol 3-kinase/Akt pathway, *CD98* and *P63* gene expression, and *human 8-oxoguanine DNA glycosylase* gene mutations (3).

From a clinicopathological point of view, HT was investigated to determine if it increased the risk of PTC development. In addition, the pathological features and clinical course of PTC based on HT were also studied. The results of the studies conducted in these areas do not fully overlap with each other, and there are serious contradictions at some points. In this study, we aimed to reveal the clinicopathological effect of HT-PTC coexistence on the course of PTC by screening patients diagnosed with PTC who were followed up in our clinic. We categorized the patients into groups according to HT association and examined the clinical, pathological, and laboratory findings of the patients in each group.

METHODS

In this study, we included patients with a diagnosis of PTC who were followed up in the endocrinology outpatient clinic of our institution between 2014 and 2022 and whose surgical pathology results were available in the hospital data processing system. The patients were divided into two groups according to the diagnosis of HT in addition to the diagnosis of PTC based on the surgical pathology results and were categorized as the PTC and HT group (group 1) and the PTC-only group (group 2). Demographic data (age, gender) of the patients in both groups, tumor size in the pathology result, number of tumor foci, presence of lymphovascular invasion, presence of extrathyroidal invasion, surgical margin positivity, serum free triiodothyronine (fT3), free thyroxine (fT4), thyroid stimulating hormone (TSH) levels, and thyroid autoantibody (anti-TPO, anti-TG) levels were studied. The study was approved by the Ethics Committee of Manisa Celal Bayar University Faculty of Medicine on 21.06.2023 (approval number: 20.478.486).

Statistical Analysis

The analysis of the obtained data was performed using statistical package for the social sciences 22.0 software. The concordance of quantitative data with normal distribution was examined using the Kolmogorov-Smirnov test. In the comparison of normally distributed variables between groups, an independent samples t-test was used, and descriptive statistics were presented as mean ± standard deviation. Intergroup comparisons of non-normally distributed variables were made using the Mann-Whitney U test, and descriptive statistics were presented as median (minimum-maximum). In the qualitative variables analysis, chi-square tests were used according to the groups, and the results were presented as frequencies (%). A p-value of <0.05 were considered statistically significant.

RESULTS

As a result of our study, data from 278 patients with PTC were obtained. It was observed that in 42.4% (n=118) of these 278 cases, PTC was accompanied by HT. The mean age of the patients was 46.4412.2± years. The majority of patients were female (80.6%, n=224). In the subgroup analyses, the incidence of HT was significantly higher in female patients, and the patients with PTC coexisting with HT were significantly younger. The demographic information about the patients is presented in Table 1.

Regarding clinicopathological findings, multifocality was significantly less common in group 1 (p=0.037). Extrathyroidal extension (2.5% in group 1 vs. 0.6% in group 2) and surgical margin positivity (9.3% in group 1 vs. 6.9% in group 2) were proportionally higher in group 1. However, lymphovascular invasion was proportionally lower in group 1 (1.7% in group 1 vs. 3.1% in group 2). None of these three findings were statistically significant (Table 2).

The mean tumor size was found to be smaller (13.13 mm in group 2 compared to 11.99 mm in group 1) in group 1, but this difference was not statistically significant. The majority of tumor subtypes in both groups were classical and follicular subtypes. Although the prevalence of the classical subtype was proportionally higher in group 1 (32.2% in group 1 vs. 22.5% in group 2), this rate was not statistically significant (Table 3).

When the preoperative laboratory findings of both groups (fT3, fT4, TSH, anti-TPO, and anti-TG) were examined,

thyroid autoantibody levels were significantly higher in group 1. In terms of thyroid function tests, although the mean TSH level was higher in group 1 (1.72 uU/mL in group 1 compared to 1.37 uU/mL in group 2), this correlation was not statistically significant (p=0.076). fT3 and fT4 levels were similar in both groups. The laboratory findings are detailed in Table 4.

DISCUSSION

The relationship between PTC and HT has long been a popular topic. The presence of common biomolecular pathways in both clinical settings requires further research to reveal the effect of HT on the development and prognosis of PTC. The literature on this subject has conflicting results. Age, gender, tumor size, tumor subtype, tumor foci number (multifocality), lymphovascular invasion, and extrathyroidal extension, which we analyzed in this study, are all prognostic factors of PTC (4). In addition, thyroid function tests and thyroid autoantibody levels, which are among the laboratory findings, have also been shown to play a role in the prognosis of PTC (5). In our study, we aimed to reveal the clinicopathological effects of HT on the course of PTC by dividing the PTC cases in our clinic

Table 1. Demographic data of the patients

	Group 1 (n=118)	Group 2 (n=160)	p-value*
Female	103 (87.3%)	121 (75.6%)	**0.015**
Male	15 (12.7%)	39 (24.4%)	**0.015**
Mean age (years)	44.64±11.46	47.68±12.62	**0.037**

Group 1: Hashimoto's thyroiditis+papillary thyroid carcinoma, group 2: Papillary thyroid carcinoma only,
*Independent sample t-test

Table 2. Clinicopathological properties of the patients

	Group 1 (n=118)	Group 2 (n=160)	p-value*
Multifocality	50 (42.4%)	88 (55%)	**0.037**
Lymphovascular invasion	2 (1.7%)	5 (3.1%)	0.452
Surgical margin positivity	11 (9.3%)	11 (6.9%)	0.455
Extrathyroidal extension	3 (2.5%)	1 (0.6%)	0.185
Mean tumor size (mm)	11.99±11.66	13.13±14.91	0.473

Group 1: Hashimoto's thyroiditis + papillary thyroid carcinoma, Group 2: Papillary thyroid carcinoma only,
*Chi-square analysis

Table 3. Pathological subtyping of the patients

Tumor subtype	Group 1 (n=118)	Group 2 (n=160)	Total (n=278)
Classic	38 (32.2%)	36 (22.5%)	74 (26.6%)
Follicular	47 (39.8%)	68 (42.5%)	115 (41.4%)
Classic+follicular	13 (11.0%)	25 (15.6%)	38 (13.7%)
Oncocytic	16 (13.6%)	24 (15.0%)	40 (14.4%)
Solid	4 (3.4%)	7 (4.4%)	11 (3.9%)

Group 1: Hashimoto's thyroiditis+papillary thyroid carcinoma, group 2: Papillary thyroid carcinoma only

Table 4. Preoperative laboratory findings

	Group 1 (n=118)	Group 2 (n=160)	p-value
TSH	1.72±1.44	1.37±1.08	0.076*
fT4	0.876±0.199	0.881±0.146	0.876*
fT3	3.74±0.65	3.68±0.55	0.422**
Anti-TPO	8.5 (0.2-1300)	0.5 (0.1-55.5)	**0.0001****
Anti-TG	3.94 (0.01-800.13)	0.30 (0.02-101.36)	**0.0001****

Group 1: Hashimoto's thyroiditis+papillary thyroid carcinoma, group 2: Papillary thyroid carcinoma only,
*Independent sample t-test, **Mann-Whitney U test, TSH: Thyroid stimulating hormone, fT4: Free thyroxine, fT3: Free triiodothyronine, anti-TPO and anti-TG: Thyroid autoantibody

into two groups according to the coexistence of HT and by examining the clinical and pathological features of these two groups.

The demographic analysis revealed that the patients in group 1 were significantly younger (p=0.037). Moreover, the incidence of HT with PTC was significantly higher in women than in men (p=0.015). Both findings are similar to those of previous studies in the literature.

When the HT-PTC coexistence was examined in terms of tumor size, we found that the tumor size was smaller in group 1 (mean 11.99 mm in group 1 vs. mean 13.13 mm in group 2). Although not statistically significant, this result is in line with the literature. In the study of Cappellacci et al. (6), the mean tumor size was found to be 13.711.9± mm in patients with PTC and 17.616.5± mm in patients without Hashimoto's thyroiditis, and this difference was found to be statistically significant (p=0.007). In our study, the evaluation of the histopathological data of the cases revealed contradictory results, consistent with the literature. When both groups were analyzed in terms of the number of tumor foci (multifocality), multifocality was found to be less common in group 1 compared with the other group, and this result was statistically significant (p=0.037). When methodologically similar studies were examined, findings contradicting our results regarding multifocality were found. Tang et al. (2), Molnár et al. (7), and Hanege et al. (8) found a higher rate of multifocality in patients with HT-PTC coexistence. When the two groups were evaluated in terms of lymphovascular invasion, no statistically significant difference was found, but lymphovascular invasion was found to be proportionally lower in group 1 (1.7% in group 1 compared to 3.1% in group 2). When the literature was examined, some studies, similar to ours, revealed that vascular invasion and lymph node metastasis were at a lower rate in patients with HT-PTC coexistence (2,7). However, Konturek et al. (9) found a fourfold increase in the risk factor of level VI lymph nodes in patients with PTC accompanied by HT.In our study, the surgical margin positivity was slightly higher in group 1 (6.9% group 2 vs. 9.3% group 1). However, this rate was not statistically significant. According to the 2015 guidelines of the American Thyroid Society, microscopic tumor invasion is categorized as an intermediate-risk group. However, a more recent study reported that microscopic surgical margin in patients with PTC was not an independent prognostic factor for recurrence-free survival (10,11).

In a meta-analysis by Tang et al. (2), extrathyroidal extension was found at a lower rate in patients with HT-PTC coexistence. In our study, a higher rate of extrathyroidal extension was observed in group 1 (2.5% in group 1 vs. 0.6% in group 2), but this result was not statistically significant.

When both groups were analyzed in terms of tumor subtypes, no statistically significant difference was found in terms of subtype distribution. The most common subtypes in both groups were classical and follicular subtypes. The rates of the oncocytic variant, a less common form, were similar in both groups (13.6% in group 1, 15% in group 2).

There are many studies in the literature on how the coexistence of HT with PTC affects the course of PTC; unfortunately, they do not conclude whether these effects are good or bad prognostic factors. In our study, multifocality was found to be statistically significantly low in group 1, but the absence of a significant correlation in other parameters prevented us from making a definite assumption about the effect of HT-PTC coexistence on the course of PTC.

Limitation

Because our study was a retrospective cross-sectional study, the patients analyzed were already diagnosed with PTC. For this reason, no information could be obtained regarding the effect of the presence of HT on the development of PTC. This is a major limitation of our study.

CONCLUSION

It is clear that the association between HT-PTC and HT-PTC has been a matter of curiosity for a long time, and many studies have been conducted on this topic. Our study, like most of the studies in the literature, could not clearly identify this association as an indicator of good or poor prognosis, and some contradictory results were obtained for some of the histological parameters. As a result, more comprehensive, multicenter prospective studies on this subject are needed.

ETHICS

Ethics Committee Approval: The study was approved by the Ethics Committee of Manisa Celal Bayar University Faculty of Medicine on 21.06.2023 (approval number 20.478.486).

Informed Consent: Retrospective study.

FOOTNOTES

Authorship Contributions

Surgical and Medical Practices: A.T., H.A., Concept: C.A., N.Ö., H.A., Z.H., Design: C.A., N.Ö., Z.H., Data Collection or Processing: C.A., S.A., G.G.Ç., E.Ş., Analysis or Interpretation: S.C.G., A.T., N.Ö., Literature Search: C.A., S.A., S.C.G., G.G.Ç., Writing: C.A., S.A.

Conflict of Interest: No conflict of interest was declared by the authors.

Financial Disclosure: The authors declared that this study received no financial support.

REFERENCES

1. Prete A, Borges de Souza P, Censi S, Muzza M, Nucci N, Sponziello M. Update on Fundamental Mechanisms of Thyroid Cancer. Front Endocrinol (Lausanne). 2020;11:102.
2. Tang Q, Pan W, Peng L. Association between Hashimoto thyroiditis and clinical outcomes of papillary thyroid carcinoma: A meta-analysis. PLoS One. 2022;17:e0269995.
3. Noureldine SI, Tufano RP. Association of Hashimoto's thyroiditis and thyroid cancer. Curr Opin Oncol. 2015;27:21-5.
4. Ito Y, Miyauchi A. Prognostic factors of papillary and follicular carcinomas in Japan based on data of kuma hospital. J Thyroid Res. 2012;2012:973497.
5. Lee IS, Hsieh AT, Lee TW, Lee TI, Chien YM. The association of thyrotropin and autoimmune thyroid disease in developing papillary thyroid cancer. Int J Endocrinol. 2017;2017:5940367.
6. Cappellacci F, Canu GL, Lai ML, Lori E, Biancu M, Boi F, et al. Association between hashimoto thyroiditis and differentiated thyroid cancer: A single-center experience. Front Oncol. 2022;12:959595.
7. Molnár C, Molnár S, Bedekovics J, Mokánszki A, Győry F, Nagy E, et al. Thyroid carcinoma coexisting with Hashimoto's thyreoiditis: clinicopathological and molecular characteristics clue up pathogenesis. Pathol Oncol Res. 2019;25:1191-7.
8. Hanege FM, Tuysuz O, Celik S, Sakallıoglu O, Arslan Solmaz O. Hashimoto's thyroiditis in papillary thyroid carcinoma: a 22-year study. Acta Otorhinolaryngol Ital. 2021;41:142-5.
9. Konturek A, Barczyński M, Wierzchowski W, Stopa M, Nowak W. Coexistence of papillary thyroid cancer with Hashimoto thyroiditis. Langenbecks Arch Surg. 2013;398:389-94.
10. Back K, Kim SK, Chai YJ, Kim JH, Choe JH, Kim JS. Does microscopic positive tumor margin in papillary thyroid cancer really matter? Surgery. 2019;166:1160-7.
11. Haugen BR, Alexander EK, Bible KC, Doherty GM, Mandel SJ, Nikiforov YE, et al. 2015 Americanthyroid association management guidelines for adult patients with thyroid nodules and differentiated thyroid cancer: The American Thyroid Association Guidelines task force on thyroid nodules and differentiated thyroid cancer. Thyroid. 2016;26:1-133.

Medical Journal of Bakırköy

Med J Bakirkoy 2025;21:24-30
DOI: 10.4274/BMJ.galenos.2024.2023.3-8

Research

Analysis of Molecular Differences in Metastatic Colorectal Cancers and Their Impact on Prognosis

Metastatik Kolorektal Kanserlerde Moleküler Farklılıkların Analizi ve Prognostik Sonuçları

Ömer Faruk Özkan[1], Muhammed Kadir Yıldırak[2], Hanife Şeyda Ülgür[2], Emre Furkan Kırkan[2], Nurhilal Kızıltoprak[1], Haluk Kerim Karakullukçu[2], Melike Özçelik[3], Sevgi Kalkanlı Taş[4]

[1]University of Health Sciences Türkiye, Hamidiye Faculty of Medicine; İstanbul Sultan 2. Abdülhamid Han Training and Research Hospital, Clinic of General Surgery, İstanbul, Türkiye

[2]University of Health Sciences Türkiye, Ümraniye Training and Research Hospital, Clinic of General Surgery, İstanbul, Türkiye

[3]University of Health Sciences Türkiye, Ümraniye Training and Research Hospital, Clinic of Oncology, İstanbul, Türkiye

[4]University of Health Sciences Türkiye, İstanbul Training and Research Hospital, Clinic of Immunology, İstanbul, Türkiye

ABSTRACT

Objective: Colorectal malignancies are the third most common cancer types according to the World Health Organization and the second leading cause of cancer-related deaths. It is the most common type of cancer that results in mortality in lung and prostate cancer and after lung and breast cancer. Improvements in screening programs, an increase in their availability, and new developments in treatment strategies have resulted in better survival outcomes in the modern era. In terms of treatment; surgery, chemotherapy, targeted therapies, and immunotherapy can be used for colon cancer management. Combination regimens of fluoropyrimidine provide a survival advantage over the best supportive care in the treatment of metastatic colorectal cancer. In addition, adding targeted therapies to standard chemotherapy provided better survival than chemotherapy alone. As with many other malignancies, better survival outcomes are achieved in colorectal cancers with treatments tailored according to the molecular characteristics of the tumor. In this study, we aimed to analyze the effects of selected treatments on survival that are tailored according to molecular differences in metastatic colorectal cancers.

Methods: Patients aged 18 years or older, with pathologically confirmed metastatic colorectal cancer diagnosis, and who are suitable for intensive combination chemotherapy [Eastern Cooperative Oncology Group 0-2 (ECOG 0-2)], are enrolled in the study. Demographic findings (age, gender, ECOG performance status), clinical status (metastatic site, systemic treatments administered initially or in further steps, progression-free survival and overall survival), molecular findings [presence of Kirsten rat sarcoma viral oncogene homolog (KRAS), NRSAS, and BRAF mutations] and pathology-related data (histological type, differentiation, tumor location, microsatellite instability status, T and N stage, lymphovascular invasion, perineural invasion for early stage cancers at diagnosis which became metastatic later) were extracted from patients' files and evaluated retrospectively. The prognostic status was estimated using the Kaplan-Meier curve.

Results: The median survival time was 33.80±4.83 and the 5-year survival rate was 38%. The median survival time was observed as 29.32±5.33 in patients with KRAS mutant and 134.17±68.66 in patients with wild KRAS (p=0.005). While the median survival time in patients with neuroblastoma rat sarcoma (NRAS) mutant is 19.02±0.00, it is 33.80±4.83 in patients with Nras wild (p=0.62). While the median survival time was 26.28±12.14 in patients with BRAF mutant, it was 33.80±8.39 in patients with BRAF wild (p=0.055).

Conclusion: Survival without treatment is extremely low in patients with metastatic colorectal cancer, and new treatment strategies can be applied according to the molecular behavior of the tumor. Monoclonal antibodies are the most preferred targeted therapies. Examples of these antibodies are bevacizumab and aflibercept, which target vascular endothelial growth factor (VEGF), and cetuximab and panitumumab, which target epidermal growth factor receptor (EGFR). Among these treatments, anti-VEGF molecules are effective regardless of the presence of molecular biomarkers, whereas anti-EGFR treatments are only effective in the absence of mutations in the EGFR-RAS-RAF-MEK pathway.

Keywords: Colorectal cancer, metastasis, KRAS, NRSAS, BRAF, monoclonal antibodies, prognosis

Address for Correspondence: Nurhilal Kızıltoprak, University of Health Sciences Türkiye, Hamidiye Faculty of Medicine; İstanbul Sultan 2. Abdülhamid Han Training and Research Hospital, Clinic of General Surgery, İstanbul Türkiye
E-mail: drnurhilalkiziltoprak@gmail.com **ORCID ID:** orcid.org/0000-0003-4241-5872

Received: 26.03.2023
Accepted: 14.06.2024
Publication Date: 25.03.2025

Cite as: Özkan F, Yıldırak MK, Ülgür HŞ, Kırkan EF, Kızıltoprak N, Karakullukçu HK, et al. Analysis of molecular differences in metastatic colorectal cancers and their impact on prognosis. Med J Bakirkoy. 2025;21:24-30

ÖZ

Amaç: Kolorektal kanserler Dünya Sağlık Örgütü verilerine göre en sık görülen 3. kanser türü olup kansere bağlı ölüm nedenlerinde ise tüm popülasyonda 2. sırada yer almaktadır. Erkeklerde akciğer ve prostat kanserinden, kadınlarda ise akciğer ve meme kanseriden sonra ölüme neden olan kanser tipidir. Bu noktada bakıldığında gerek tarama programlarının oluşturulması, gerekse tedavi stratejilerinde sağlanan gelişmeler günümüzde sağkalım üzerine olumlu gelişmelerin olduğunu göstermektedir. Tedavi stratejisi açısından bakıldığında kolon kanserinin yönetiminde cerrahi tedavi, kemoterapatikler, hedefe yönelik tedaviler ve immünoterapi uygulanabilmektedir. Metastatik kolorektal kanser tedavisinde fluoropirimidin kombinasyon rejimlerinin en iyi destek tedaviye kıyasla sağkalım avantajı sağladığı gösterilmiştir. Kemoterapiye eklenen hedefe yönelik tedaviler ile de sadece kemoterapiye kıyasla genel sağkalımda iyileşme sağlanmıştır. Monoklonal antikorlar en sık uygulanan hedefe yönelik tedavilerdir. Vasküler endotelyal büyüme faktörünü (VEGF) hedefleyen bevacizumab, aflibercept ve epidermal büyüme faktörü reseptörünü (EGFR) hedefleyen cetuximab, panitimumab bunlara örnektir. Bu tedaviler arasından anti-VEGF tedaviler, moleküler biyobelirteçden bağımsız olarak etkinlik gösterirken, anti-EGFR tedaviler EGFR-RAS-RAF-MEK yolağında mutasyon olmadığı durumlarda etki gösterirler. Pek çok kanser türünde olduğu gibi, kolorektal kanserlerde de tümörün moleküler özelliklerine göre seçilen tedaviler ile sağkalım sonuçları daha iyi elde edilmiştir. Bu çalışmada metastatik kolorektal kanserlerde moleküler farklılıkların analizi ve sonucuna göre seçilen tedavilerin sağkalım sonuçları araştırılacaktır.

Gereç ve Yöntem: Çalışmaya 18 yaş ve üzeri, metastatik kolorektal kanser tanısı patolojik olarak doğrulanmış, performans statüsü intensif kemoterapi kombinasyonuna uygun hastalar [(Doğu Kooperatif Onkoloji Grubu 0-2 (ECOG 0-2)] dahil edilecektir. Hastalara ait demografik (yaş, cinsiyet, ECOG performans statüsü), klinik (metastaz yeri, 1. basamak ve sonraki basmaklarda uygulanan sistemik tedaviler, progresyonsuz sağkalım ve genel sağkalım süreleri) moleküler [Kirsten sıçan sarkomu viral onkogen homologu (KRAS), NRSAS, BRAF mutasyon varlığı] ve patolojik datalar (tümör histolojik tip, diferansiasyon, tümör yerleşim yeri, mikrosatellit instabilite durumu, tanıda erken evre olup sonradan metastatik olanlar için T, N evresi, lenfovasküler invazyon, perinöral invazyon) retrospektif olarak hasta dosyalarından elde edilecektir. Prognostik durumu Kaplan-Meier ile hesaplanacaktır.

Bulgular: Median sağkalım süresi 33,80±4,83 ve 5 yıllık sağkalım oranı %38 olarak bulunmuştur. KRAS mutant olan hastalarda median sağkalım süresi 29,32±5,33 KRAS wild olan hastalarda 134,17±68,66 olarak gözlenmiştir (p=0,005). NRAS mutant olan hastalarda median sağkalım süresi 19,02±0,00 iken Nras wild olan hastalarda 33,80±4,83'tür (p=0,62). BRAF mutant olan hastalarda median sağkalım süresi 26,28±12,14 iken BRAF wild olan hastalarda 33,80±8,39 olarak bulunmuştur (p=0,055).

Sonuç: Metastatik kolorektal kanserlerde tedavisiz sağkalım son derece düşük olup, tümörün moleküler davranışına göre yeni tedavi stratejileri uygulanabilmektedir. Monoklonal antikorlar en sık uygulanan hedefe yönelik tedavilerdir. VEGF'yi hedefleyen bevacizumab, aflibercept ve EGFR'yi hedefleyen cetuximab, panitimumab bunlara örnektir. Bu tedaviler arasından anti-VEGF tedaviler, moleküler biyobelirteçden bağımsız olarak etkinlik gösterirken, anti-EGFR tedaviler EGFR-RAS-RAF-MEK yolağında mutasyon olmadığı durumlarda etki gösterirler.

Anahtar Kelimeler: Kolorektal kanser, metastaz, KRAS, NRSAS, BRAF, monoklonal antikorlar, prognoz

INTRODUCTION

Colon and rectum cancers are common malignancies with poor prognoses, especially in advanced stages (1). The prevalence of metastatic colorectal cancers (CRC) remains considerable despite significant advances in diagnostic methods and treatment, the implementation of screening programs, and the adoption of multidisciplinary approaches with particularly favorable benefits. New-generation chemotherapeutics and response-guided surgical strategies offer benefits to patients with metastatic CRC (2).

The therapeutic strategies for colon cancer include surgery, chemotherapy, targeted therapies, and immunotherapy. Fluoropyrimidine combination regimens provide a survival advantage in the treatment of metastatic CRC compared with the best supportive therapy (3). With the addition of targeted therapies to chemotherapy, overall survival (OS) has been improved compared with chemotherapy alone (4). Among targeted therapies, monoclonal antibodies are the most commonly used agents. Examples of such therapeutics include bevacizumab and aflibercept targeting vascular endothelial growth factor (VEGF), cetuximab, and panitumumab targeting epidermal growth factor receptor (EGFR). The efficacy of anti-VEGF treatment is independent of the molecular biomarker, but anti-EGFR treatment is effective only when there are no mutations in the EGFR-RAS-RAF-MEK pathway (5).

In this study, we aimed to evaluate the effects of the commonly used monoclonal antibodies VEGF- and EGFR-targeting therapeutics cetuximab and panitumumab on prognosis and survival in patients with metastatic CRC.

METHODS

We performed this study by using the data from a thesis study in the Hamidiye Institute of Health Sciences Molecular Oncology Ph.D. program. Upon University of Health Sciences Türkiye, Ümraniye Training and Research Hospital Clinical Research Ethics Committee (number: B.10.1.TKH.4.34.H.GP.0.01/157, date: 27.05.2021) approval, this study included patients, who were treated due to the diagnosis of metastatic CRC in the Medical Oncology Clinic of the University of Health Sciences Türkiye, Ümraniye Training and Research Hospital during the period between January 2016 and June 2021. Patients with missing data and severe comorbid diseases were excluded from the study. A total of 102 patients were included in the study. Patients' data were retrieved from the hospital's IT department.

Patients aged >18 years with a pathologically confirmed diagnosis of metastatic CRC and a suitable performance

status [Eastern Cooperative Oncology Group 0-2 (ECOG 0-2)] for intensive combination chemotherapy were included in the study.

Patients' demographic data (age, sex, and ECOG performance status), clinical features [metastatic site, first-line and second or higher lines of systemic treatment, progression-free survival (PS), and OS], molecular characteristics (KRAS, NRAS, and BRAF mutations), and pathologic diagnosis [histologic type, tumor differentiation, tumor location, microsatellite instability (MSI), T-N stages of metastatic patients with a diagnosis of early-stage disease, and lymphovascular and perineural invasion] were retrospectively retrieved from patients' files. Prognosis was estimated by the Kaplan-Meier analysis.

The primary aim of our study was to evaluate the outcomes of contemporary anti-VEGF and anti-EGF therapies in CRC and to analyze the molecular differences between right and left colon tumors along with their impact on prognosis using survival analyses on the data retrieved retrospectively. The secondary aims of the study were to evaluate the BRAF, KRAS, and NRAS mutation rates in patients with metastatic disease and to compare the age and sex of patients with lymphovascular and perineural invasion in surgical pathology specimens in light of the published information.

Statistical Analysis

Descriptive analysis (frequency distributions, percentage, mean, standard deviation (SD), 95% confidence intervals, median) were used as a statistical method to analyze the study data. We analyzed conformity to a normal distribution using graphical representations and the Kolmogorov-Smirnov test. For data without a normal distribution, the Kruskal-Wallis H test and Mann-Whitney U test were used to examine differences between groups. The chi-square test was used to examine discontinuous data. The results were examined using the 95% confidence interval at the $p<0.05$ significance level. The descriptive analysis in this study included frequency distributions, percentages, mean, SD (mean ± SD), 95% confidence intervals, and median.

The log-rank test was performed to examine the effects of chemotherapy regimens, molecular analysis findings, and disease stage on survival. Survival rates were calculated by the Kaplan-Meier survival analysis. The effects of chemotherapy regimens and genetic mutations on survival were also calculated in another log-rank analysis with correction for the stage at diagnosis. The SPSS and Microsoft Excel programs were used to analyze the data.

RESULTS

This study enrolled patients diagnosed with metastatic CRC in the Medical Oncology Clinic of the University of Health Sciences Türkiye, Ümraniye Training and Research Hospital between January 2016 and June 2021. A total of 102 patients were included in the study.

The mean age was 62.96±10.82 years (Figure 1). The mean ages of the male and female patients was 63.27±10.62 and 62.48±11.23 years, respectively (Table 1). There was not a statistically significant difference in age between the male and female patient groups (p=0.82). Among the subjects, 62 (60.8%) and 40 (39.2%) were male and female, respectively.

The genetic analyses of the patients revealed KRAS, NRAS, and BRAF mutations in 43 (42.2%), 3 (2.9%), and 8 patients (7.8%), respectively. Out of the 63 (61.8%) patients with MSI, 53 (52%) had MSI and 10 (9.8%) had MSI. The distribution of the TNM stages in accordance with the AJCC staging system was as follows: 2 (2.0%) patients in Stage 1, 14 (13.7%) patients in Stage 2, 24 (23.5%) patients in Stage 3, and 62 (60.8%) patients in Stage 4 (Figure 2).

Of the 40 patients who underwent surgery, lymphovascular invasion was negative in 15 patients (24.5%) had lymphovascular invasion and 25 (24.5%) had no lymphovascular invasion. The examination of the data for perineural invasion showed that it was negative in 21 (20.6%) but positive in 19 (18.6%) patients.

Of the 102 patients, peritoneal metastasis was detected in 19 patients (18.6%) and bone metastasis in 2 patients (2.0%). Figure 2 shows the distribution of metastatic patients. In the first-line treatment protocols, 3 patients (2.9%)

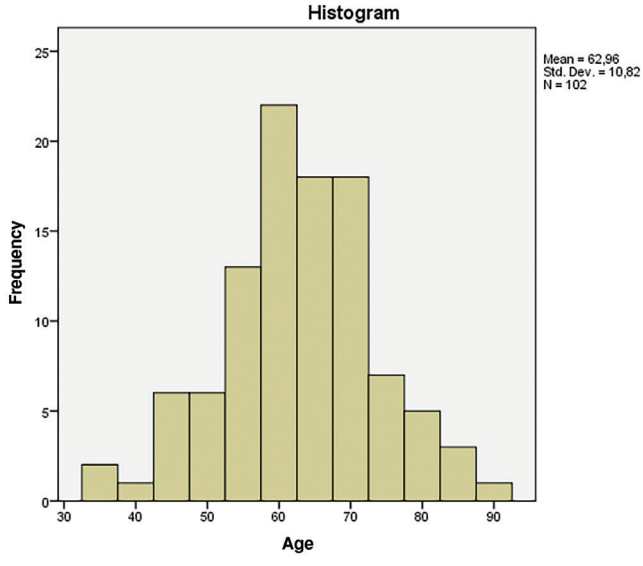

Figure 1. Graph of age distribution

received routine chemotherapy with FOLFOX [folinic acid (leucovorin), fluorouracil (5-FU), and oxaliplatin] or FOLFIRI [folinic acid (leucovorin), 5-FU, and irinotecan)], 57 patients (55.9%) received anti-VEGF therapy with bevacizumab, and 42 patients (41.3%) received anti-EGFR therapy with panitumumab or cetuximab, as third-generation chemotherapeutic agents in addition to the FOLFOX and FOLFIRI regimens. Of the 43 patients with progression, 6 received routine second-line chemotherapy protocols, and 28 and 9 started anti-VEGF and anti-EGFR therapy, respectively, as additional agents to second-line treatment. Seventeen of the 19 patients with progression for the third time started immunotherapy as indicated after molecular and genetic analysis (Table 2).

The median survival time of 33.80±4.83 months and a 5-year survival rate was 38%. The median survival times were as follows: 29.32±5.33 months in KRAS-mutant patients, 134.17±68.66 months in KRAS-wild patients (p=0.005); 19.02±0.00 months in NRAS-mutant patients and 33.80±4.83 months in NRAS-wild patients (p=0.62); and 26.28±12.14 in BRAF-mutant patients and 33.80±8.39 in BRAF-wild patients (p=0.055). Table 3 presents the 1- and 5-year survival rates and the comparison of survival with the results of KRAS, NRAS, and BRAF analyses. Figures 3-5 show Kaplan-Meier curves as a function of the genetic analysis results.

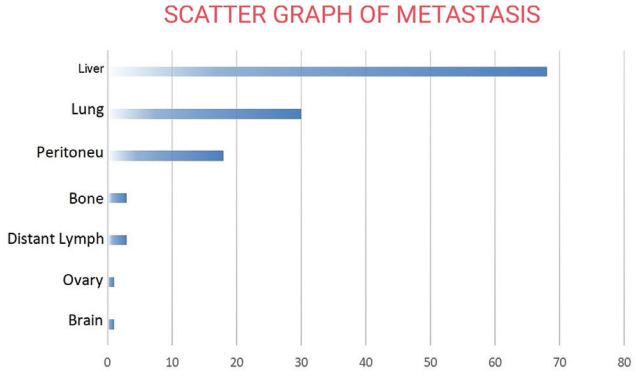

Figure 2. Metastasis distribution

Table 1. Age distribution by gender

		Gender	
		Male	**Female**
Mean		63.27	62.48
95% confidence interval	Lower limit	60.58	58.88
	Upper limit	65.97	66.07
Median		64	61
Standard deviation		10.62	11.23
Minimum		35	36
Maximum		84	91
Range		49	55
Interquartile range		13	15

DISCUSSION

Cancer remains a significant and preventable cause of death after heart disease. Several studies on the early diagnosis and prevention of cancer are available. Colon and rectum cancers are among the most common malignant tumors and the most important causes of cancer-related morbidity and mortality globally (6). The World Health Organization reports that, as of 2018, cancers of the colon and rectum were the third most common cancers worldwide (1.8 million cases) after those of the lung and breasts and the second most common cause of cancer-related mortality (862,000 deaths) after those of the lung (7).

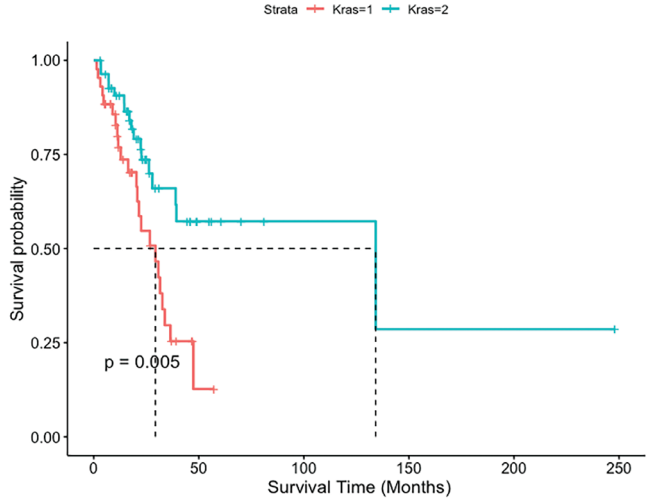

Figure 3. Survival curve obtained by KRAS analysis
KRAS: Kirsten rat sarcoma viral oncogene homolog

Table 2. Distribution of treatment protocols

	n (%)
First-line treatment	
Routine chemotherapy	3 (2.9%)
CT+anti-VEGF therapy	57 (55.9%)
CT+anti-EGF	42 (41.3%)
Second progression	
Routine chemotherapy	6 (14%)
CT+anti-VEGF therapy	28 (65.1%)
CT+anti-EGF	9 (20.9%)
Third progression	
Routine CT	1 (5.6%)
Immunotherapy	17 (94.4%)

VEGF: Endothelial growth factor, CT: Computed tomography, EGF: Epidermal growth factor receptor

The majority of colorectal tumors develop as a result of chromosomal instability and mutations in tumor suppressor genes and oncogenes (8). RAS oncogene mutations are found in approximately 50% of CRC cases. BRAF oncogene mutations are detected approximately in 5-10% of colorectal tumors. The *RAS* and *BRAF* genes encode intracellular proteins involved in the EGFR signaling pathway. Therefore, mutations in these genes can cause resistance to EGFR-targeting therapeutics. Therapeutic agents targeting VEGF, on the other hand, offer favorable survival benefits independent of any biomarker when combined with chemotherapy in metastatic colorectal cancer. The standard first-line systemic treatment for metastatic CRC is fluoropyrimidine-based chemotherapy with irinotecan or oxaliplatin, combined with targeted agents including anti-VEGF or anti-EGFR antibodies (9). In our study, 45% of the patients had RAS mutations and 7.8% had BRAF mutations, consistent with the published information. Besides molecular characteristics, the patients included in our study were clinically eligible candidates to receive an intensive chemotherapy. All patients received oxaliplatin or irinotecan combined with fluoropyrimidine as the first-line systemic treatment. All but 3 patients received targeted therapy with anti-EGFR (41.3%) and anti-VEGF (55.9%) agents in combination with this first-line chemotherapy regimen.

KRAS-mutant patients have a worse prognosis than wild-type patients (10). However, the absence of KRAS mutation predicts sensitivity to EGFR-targeting therapeutics (11). Similar to the reports by the majority of studies conducted to date, we found a significantly shorter OS in patients with RAS mutations than in patients with RAS-wild-type tumors. The median survival time was 29 months in KRAS-mutant patients and 134 months in KRAS-wild patients (p=0.005).

Recent studies have focused on conditions other than RAS mutations to identify patients who will benefit most from anti-EGFR-based therapies, which are first-line therapeutics in wild-type metastatic CRC. Subgroup analysis of data from randomized studies comparing "chemotherapy +anti-EGFR agents" vs. "chemotherapy +anti-VEGF agents" vs. "chemotherapy only" showed a correlation between anti-EGFR efficacy and the primary tumor site (6). Treatment with anti-EGFR agents confers a clinically significant survival benefit to RAS-wild tumors originating from the left colon. A pooled analysis of data from 5 randomized clinical trials (FIRE-3, CRYSTAL, PRIME, PEAK, and CALGB/SWOG 80405) revealed significant benefits in PS [hazard ratio (HR), 0.78; p=0.002] and OS (HR, 0.75; p<0.001) with cetuximab

Table 3. Comparison of genetic analysis and survival outcomes

		Survival% (year)			p-value
	Median Survival (months) (n±SD)	**1-year**	**3-year**	**5-year**	
Overall survival	33.80±4.83	85%	49%	38%	
Site					0.597
Right colon	32.65±3.01	79%	44%	29%	
Left colon	47.40±0.0	88%	55%	46%	
Rectum	33.80±7.31	82%	36%	36%	
KRAS					**0.005**
Mutant	29.37±5.33	76%	29%	12%	
Wild	134.17±68.66	90%	66%	57%	
NRAS					0.628
Mutant	19.02±0.0	NA	NA	NA	
Wild	33.80±4.83	84%	49%	39%	
BRAF					**0.055**
Mutant	26.28±12.14	72%	38%	NA	
Wild	33.80±8.39	86%	49%	43%	
MSI					**0.029**
Negative	26.71±4.48	78%	37%	24%	
Low	134.17±0.0	92%	74%	59%	
High	21.52±8.27	78%	31%	NA	high

MSI: Microsatellite instability BRAF: B-Raf proto-onkogen serin/threonin kinaz, NRAS: Neuroblastoma RAS viral oncogene homolog, KRAS: Kirsten rat sarcoma viral oncogene homolog, SD: Standard deviation

or panitumumab combined with chemotherapy only in tumors originating from the left colon (12). The FIRE-3 study (FOLFIRI plus Cetuximab Versus FOLFIRI plus Bevacizumab as First-Line Treatment for Patients with Metastatic Colorectal Cancer) showed OS benefit (38.3 vs. 28.0 months; HR, 0.63; p=0.002) with FOLFIRI/cetuximab compared with FOLFIRI/bevacizumab in tumors originating from the left colon. However, no significant differences were observed for tumors originating from the right colon (p=0.28). These results suggest that fluoropyrimidine-based chemotherapy combined with cetuximab or panitumumab has become the preferred first-line treatment option for patients with tumors originating from the left colon. On the contrary, anti-VEGF agents in combination with fluoropyrimidine-based chemotherapy have been recommended in the guidelines as the preferred first-line treatment regimen for patients with tumors originating from the right colon because of other molecular changes causing intrinsic resistance to anti-EGFR agents. In our study, the primary tumor site was another stratification factor.

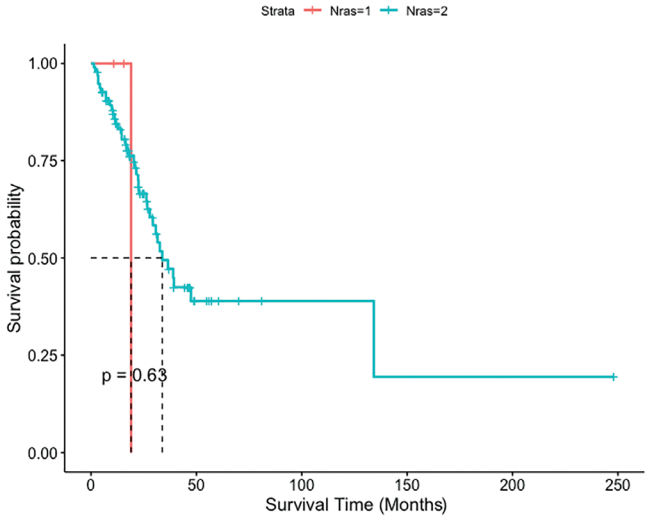

Figure 4. Survival curve obtained via NRAS analysis
NRAS: Neuroblastoma RAS viral oncogene homolog

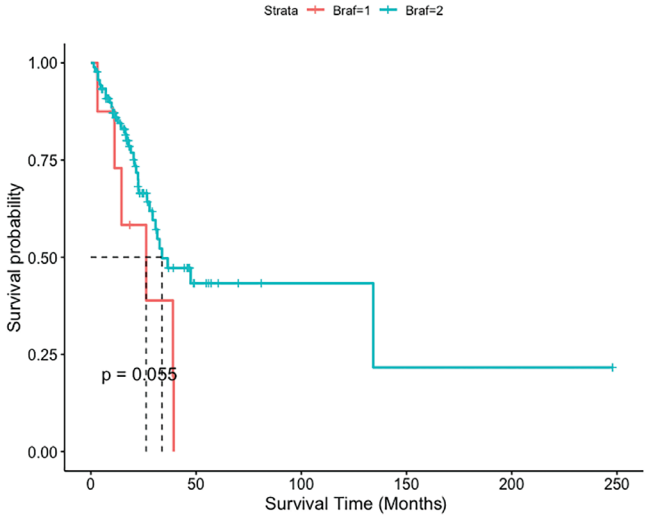

Figure 5. Survival curve determined by BRAF analysis
BRAF: B-Raf proto-onkogen serin/threonin kinaz

Tumors originating from the left colon were found in 52.9% of patients in our study. The survival analysis revealed a median OS of 33.80±4.83 months for all patients included in the study, consistent with the current literature. In our study, the median OS for patients with tumors originating from the left colon was longer but statistically insignificant compared with those originating from the right colon (32.65±3.01 months vs. 36.50±12.29 months, p=0.506). These figures are not consistent with the published information, and we believe that the small sample size of our study might have caused these results.

In the current era of personalized therapies, the discovery of novel prognostic and predictive biomarkers is extremely important for the management of CRC, as it is for the management of all solid tumors. One of these biomarkers is MSI. In most metastatic CRC cases, the MSI status is either MSI-stable (MSS) or mismatch repair-proficient (pMMR). The MSI-high (MSI-H)/mismatch repair-deficient (dMMR) feature occurs in 2-4% of all CRC. The benefit of this approach is limited, with a median OS of 13.6-21.5 months in patients with MSI-H/dMMR CRC treated using the standard first-line systemic therapy (13). Although MSS/pMMR tumors do not benefit from immunotherapy because of their immunosuppressive microenvironment, clinically significant benefits have been demonstrated with immunotherapy in MSI-H/dMMR tumors (14). A phase-III study reported fewer side effects with clinically and statistically significant survival benefits with the anti-PD1 monoclonal antibody pembrolizumab in MSI-H/dMMR tumors compared with standard fluoropyrimidine-based chemotherapy [median PS, respectively: Pembrolizumab vs. chemotherapy, 16.5 vs. 8.2 months; HR, 0.60 (95% CI, 0.45-0.80); p=0.0002] (14). MSI status could not be confirmed for all patients in our study. Of the patients with an established MSI status in our study, 15.9% had MSI-H tumors. This value was higher than that reported in the literature, suggesting that the small sample size of our study may have been the cause.

The most important limitation of this retrospective study is the selection bias resulting from the nature of the study. The MSI status was not established for all patients, and the expression of HER-2, another important biomarker, was not tested in this study, making it impossible for us to conduct further analyses. The small sample size is another limitation

of the study, as it might have affected reaching statistical significance. However, an important aspect of this study is testing for RAS and BRAF mutations and MSI in a single center to ensure homogeneity.

CONCLUSION

In this single-center retrospective study, we presented real-life data from clinical practice and analyzed molecular differences and associated prognostic outcomes in patients with metastatic colorectal cancer. The results of our study are consistent with those reported by previous randomized studies, from the aspect of the optimization of treatment efficacy, enabling the achievement of significant improvements in oncological endpoints through patient selection according to the primary tumor site and molecular characteristics.

ETHICS

Ethics Committee Approval: Approved by the Clinical Research Ethics Committee of University of Health Sciences Türkiye, Ümraniye Training and Research Hospital (number: B.10.1.TKH.4.34.H.GP.0.01/157, date: 27.05.2021).

Informed Consent: Retrospective study.

FOOTNOTES

Authorship Contributions

Surgical and Medical Practices: Ö.F.Ö., Concept: Ö.F.Ö., M.K.Y., Design: Ö.F.Ö., M.K.Y., M.Ö., S.K.T., Data Collection or Processing: Ö.F.Ö., H.Ş.Ü., M.Ö., S.K.T., Analysis or Interpretation: Ö.F.Ö., H.Ş.Ü., M.Ö., S.K.T., Literature Search: Ö.F.Ö., E.F.K., H.K.K., M.Ö., S.K.T., Writing: Ö.F.Ö., E.F.K., N.K.

Conflict of Interest: No conflict of interest was declared by the authors.

Financial Disclosure: The authors declared that this study received no financial support.

REFERENCES

1. Xi Y, Xu P. Global colorectal cancer burden in 2020 and projections to 2040. Transl Oncol. 2021;14:101174.
2. Das S, Ciombor KK, Haraldsdottir S, Goldberg RM. Promising new agents for colorectal cancer. Curr Treat Options Oncol. 2018;19:29.
3. Piedbois P, Buyse M, Rustum Y, Machover D, Erlichman C, Carlson RW, et al. Modulation of fluorouracil by leucovorin in patients with advanced colorectal cancer: Evidence in terms of response rate by the advanced colorectal cancer meta-analysis project. J Clin Oncol. 1992;10:896–903.
4. Piawah S, Venook AP. Targeted therapy for colorectal cancer metastases: A review of current methods of molecularly targeted therapy and the use of tumor biomarkers in the treatment of metastatic colorectal cancer. Cancer. 2019;125:4139-47.
5. Ohhara Y, Fukuda N, Takeuchi S, Honma R, Shimizu Y, Kinoshita I, Dosaka-Akita H. Role of targeted therapy in metastatic colorectal cancer. World J Gastrointest Oncol. 2016;8:642-55.
6. Van Cutsem E, Köhne CH, Láng I, Folprecht G, Nowacki MP, Cascinu S, et al. Cetuximab plus irinotecan, fluorouracil, and leucovorin as first-line treatment for metastatic colorectal cancer: updated analysis of overall survival according to tumor KRAS and BRAF mutation status. J Clin Oncol. 2011;29:2011-9.
7. De Roock W, Piessevaux H, De Schutter J, Janssens M, De Hertogh G, Personeni N, et al. KRAS wild-type state predicts survival and is associated to early radiological response in metastatic colorectal cancer treated with cetuximab. Ann Oncol. 2008;19:508-515.
8. Heinemann V, Kraemer N, Buchner H, Weikersthal LF, Decker T, Kiani A, et al. Somatic DNA mutations, tumor mutational burden (TMB), and MSI status: Association with efficacy in patients(pts) with metastatic colorectal cancer (mCRC) of FIRE-3 (AIO KRK-0306). J Clin Oncol. 2018;36:3591.
9. Bokemeyer C, Bondarenko I, Makhson A, Hartmann JT, Aparicio J, de Braud F, et al. Fluorouracil, leucovorin, and oxaliplatin with and without cetuximab in the first-line treatment of metastatic colorectal cancer. J Clin Oncol. 2009;27:663-71.
10. Cerottini JP, Caplin S, Saraga E, Givel JC, Benhattar J. The type of K-ras mutation determines prognosis in colorectal cancer. Am J Surg. 1998;175:198-202.
11. Amado RG, Wolf M, Peeters M, Van Cutsem E, Siena S, Freeman DJ, et al. Wild-type KRAS is required for panitumumab efficacy in patients with metastatic colorectal cancer. J Clin Oncol. 2008;26:1626-34.
12. Holch JW, Ricard I, Stintzing S, Modest DP, Heinemann V. The relevance of primary tumour location in patients with metastatic colorectal cancer: A meta-analysis of first-line clinical trials. Eur J Cancer. 2017;70:87-98.
13. Tougeron D, Sueur B, Zaanan A, de la Fouchardiére C, Sefrioui D, Lecomte T, et al. Prognosis and chemosensitivity of deficient MMR phenotype in patients with metastatic colorectal cancer: An AGEO retrospective multicenter study. Int J Cancer. 2020;147:285-96.
14. André T, Shiu KK, Kim TW, Jensen BV, Jensen LH, Punt C, Smith D, et al. Pembrolizumab in microsatellite-instability-high advanced colorectal cancer. N Engl J Med. 2020;383:2207-18.

Medical Journal of Bakırköy

Med J Bakirkoy 2025;21:31-38
DOI: 10.4274/BMJ.galenos.2025.2024.11-1

Research

Evaluating the Efficacy and Associated Factors of Vagus Nerve Stimulation in Medically Refractory Epilepsy Patients

Medikal Tedaviye Dirençli Epilepsi Hastalarında Vagus Sinir Stimülasyonunun Etkinliğinin ve İlişkili Faktörlerin Değerlendirilmesi

Ozan Haşimoğlu[1], Ozan Barut[2], Tuba Özge Karaçoban[1], Taha Hanoğlu[1], Nur Bahar Geylan[3], Buruç Erkan[1], Bekir Tuğcu[1]

[1]University of Health Sciences Türkiye, Başakşehir Çam and Sakura City Hospital, Clinic of Neurosurgery, İstanbul, Türkiye

[2]Bingöl State Hospital, Clinic of Neurosurgery, Bingöl, Türkiye

[3]University of Health Sciences Türkiye, Başakşehir Çam and Sakura City Hospital, Clinic of Neurosurgery Nursing, Neuropsychiatry, İstanbul, Türkiye

ABSTRACT

Objective: This study investigated seizure control rates and factors associated with treatment response in a series of patients with medically refractory epilepsy who underwent vagus nerve stimulation (VNS).

Methods: We conducted a retrospective observational study of 82 patients who received VNS implantation between 2007 and 2024. Demographic data, epilepsy characteristics, and preoperative and postoperative outcomes, including seizure frequency, were analyzed. Seizure outcomes were assessed using the International League Against Epilepsy and Engel classifications, and statistical analyses were performed to identify factors associated with seizure control.

Results: The average follow-up duration was 67.1 months. At 12 months post-VNS, 73.18% of patients achieved more than a 50% reduction in seizure frequency, with 36.59% experiencing a 75-100% reduction. Higher response rates were observed among patients with a history of epilepsy surgery. No significant associations were found between treatment response and age, gender, or epilepsy type.

Conclusion: VNS implantation is an effective treatment option for seizure control in patients with medically refractory epilepsy. This study highlights factors potentially associated with better outcomes, suggesting that VNS may be particularly beneficial in specific patient subgroups. Further research with larger, prospective studies is recommended to confirm these findings.

Keywords: Vagus nerve stimulation, seizure control, medically refractory epilepsy, neuromodulation, treatment response

ÖZ

Amaç: Bu çalışmada, vagus sinir stimülasyonu (VNS) uygulanan medikal tedaviye dirençli epilepsi tanılı hastaların nöbet kontrol oranları ve tedavi yanıtıyla ilişkili faktörler araştırıldı.

Gereç ve Yöntem: 2007 ile 2024 yılları arasında VNS implantasyonu uygulanan 82 hastada retrospektif bir gözlemsel çalışma yürüttük. Demografik veriler, epilepsi özellikleri ve nöbet sıklığı dahil olmak üzere ameliyat öncesi ve sonrası sonuçlar analiz edildi. Nöbet sonuçları Uluslararası Epilepsi ile Savaş Derneği ve Engel sınıflandırmaları kullanılarak değerlendirildi ve nöbet kontrolüyle ilişkili faktörleri belirlemek için istatistiksel analizler yapıldı.

Bulgular: Ortalama takip süresi 67,1 aydı. VNS'den 12 ay sonra hastaların %73,18'i nöbet sıklığında %50'den fazla azalma elde etti ve %36,59'u %75-100 azalma yaşadı. Epilepsi cerrahisi öyküsü olan hastalarda daha yüksek yanıt oranları gözlendi. Tedavi yanıtı ile yaş, cinsiyet veya epilepsi türü arasında önemli bir ilişki bulunamadı.

Sonuç: VNS implantasyonu, medikal tedaviye dirençli epilepsi hastalarında nöbet kontrolü için etkili bir tedavi seçeneğidir. Bu çalışma, daha iyi sonuçlarla ilişkili olabilecek faktörleri vurgulayarak, VNS'nin belirli hasta alt gruplarında özellikle yararlı olabileceğini öne sürmektedir. Bu bulguları doğrulamak için daha büyük, prospektif çalışmalarla daha fazla araştırma yapılması önerilmektedir.

Anahtar Kelimeler: Vagus siniri stimülasyonu, nöbet kontrolü, medikal tedaviye dirençli epilepsi, nöromodülasyon, tedavi yanıtı

Address for Correspondence: Ozan Haşimoğlu MD, University of Health Sciences Türkiye, Başakşehir Çam and Sakura City Hospital, Clinic of Neurosurgery, İstanbul, Türkiye
E-mail: ozanhasim@hotmail.com **ORCID ID:** orcid.org/0000-0003-1394-5188

Received: 08.11.2024
Accepted: 14.01.2025
Publication Date: 25.03.2025

Cite as: Haşimoğlu O, Barut O, Karaçoban TÖ, Hanoğlu T, Geylan NB, Erkan B, et al. Evaluating the efficacy and associated factors of vagus nerve stimulation in medically refractory epilepsy patients. Med J Bakirkoy. 2025;21:31-38

INTRODUCTION

Epilepsy, with a prevalence of approximately 0.5-1% according to the World Health Organization, is a neurological disorder affecting nearly 50 million people globally, with a bimodal incidence distribution showing higher rates in both young and elderly populations (1,2). According to the International League Against Epilepsy (ILAE), epilepsy that remains uncontrolled despite the appropriate dosage and combination of at least two well-tolerated antiepileptic drugs is classified as medically refractory epilepsy, comprising about 30-40% of all epilepsy cases (3,4). Although focal epilepsies arising from focal epileptogenic lesions may be amenable to surgical intervention, only 10-30% of these patients benefit from resective surgeries, posing a significant challenge in seizure management for epileptologists and epilepsy surgeons (5,6).

Neuromodulation surgery serves as a crucial alternative for patients with medically refractory epilepsy who are either unsuitable for resective surgery or do not achieve desired outcomes postoperatively (7-9). Vagus nerve stimulation (VNS) was one of the first three neuromodulation methods approved by the United States Food and Drug Administration in 1997 (8). VNS therapy can be applied in patients with medically refractory epilepsy who are not suitable for resective surgery, those with multiple or bilaterally independent symptomatic localization-related epilepsy syndromes, cryptogenic or symptomatic generalized epilepsy accompanied by diffuse epileptogenic anomalies, or those who have undergone unsuccessful intracranial epilepsy surgeries.

In this study, we aim to assess long-term outcomes, specifically the effects on seizure frequency, anti-epileptic drug use, and quality of life in patients who underwent VNS implantation between 2007 and 2024, and to discuss our findings in the context of the existing literature, thus underscoring the significance of VNS implantation in seizure control for patients with medically refractory epilepsy.

METHODS

Participant Analysis

This study was conducted retrospectively, following approval from University of Health Sciences Türkiye, Başakşehir Çam and Sakura City Hospital Ethics Committee (decision no: 162, date: 19.04.2023) and in compliance with the Helsinki Declaration. The study was designed as a retrospective observational study. We included 82 patients with medically refractory epilepsy who underwent VNS implantation between 2007 and 2024, as recommended by the local epilepsy surgery council, comprising adult, or pediatric epileptologists, neurosurgeons, psychiatrists, or child, psychiatrists, psychologists, and neuroradiologists. Only patients with at least 12 months of follow-up were included, while cases lacking regular follow-up were excluded.

Preoperative demographic data were recorded, including age, sex, handedness, age at seizure onset, seizure type, epilepsy etiology, magnetic resonance imaging (MRI) findings, video-electroencephalography (vEEG) findings, positron emission tomography (PET) findings, neuropsychological assessment results, the number of antiepileptic drugs used prior to VNS implantation, duration of epilepsy, seizure frequency, and the year of VNS implantation. Postoperatively, patients were followed by an adult or pediatric epileptologist. Data recorded during the postoperative follow-up included the number of anti-epileptic drugs, seizure frequency at the 3rd, 6th, and 12th months, recorded complications, time until battery replacement, and subjective assessments by the caregiver.

Seizure type and epilepsy etiology were categorized based on the 2017 ILAE classification (10). For all patients with a follow-up period longer than one year, seizure outcomes were evaluated by the epilepsy surgery council using both ILAE and Engel classifications, as both classifications offer unique categorical characteristics that contribute to the study (11).

Seizure reduction in the postoperative period was monitored using seizure diaries maintained by a single evaluator. Seizure reduction data were generated based on the change in seizure frequency at the end of the first year compared with the frequency prior to VNS implantation. Seizure reduction rates were categorized as 0-25%, 25-50%, 50-75%, and 75-100%, according to existing literature assessments (12-14). A reduction of more than 50% in seizure frequency was considered the target therapeutic response. This classification aimed to capture the degree of change in seizure frequency. It is not comprehensively represented in the ILAE and Engel classifications.

Surgical Procedure

The VNS implantation is a well-defined procedure (15). During the VNS implantation surgery, the patient is positioned supine with the head rotated 45 degrees to the right and slightly extended to minimize the risk of bradycardia. This positioning targeting the left vagus nerve. The first incision is planned horizontally at the midpoint between the clavicle and mastoid process, where it intersects the medial border of the sternocleidomastoid muscle. The second incision is made parallel to the left pectoral muscle, 3-5 cm inferior

to the clavicle. Following the standard anterior cervical exposure, the left vagus nerve is isolated for a minimum length of 3 cm, distal to the cardiac branches and proximal to the recurrent laryngeal nerve. Helical electrodes are then placed around the 3 cm exposed segment of the vagus nerve (Figure 1). The electrode cable is routed through a subcutaneous tunnel to the pectoral area. Subsequently, the VNS generator is positioned subcutaneously or subpectorally using the second incision and connected to the electrode cable. In all patients, the LivaNova Demipulse model device was used. The VNS generator is programmed externally with a handheld wand, and total impedance is measured to complete the surgery.

Statistical Analysis

Data analysis was performed using IBM SPSS Statistics for Windows, Version 25.0 (IBM Corp., Armonk, NY, USA). Appropriate tests were selected to evaluate the relationships between prognostic parameters and categorical and continuous variables. The associations between prognostic parameters (ILAE score, Engel score, postoperative medication changes, and postoperative seizure reduction) and categorical variables such as gender, epilepsy surgery, MRI lesion 1 (presence/absence), MRI lesion 2 (single/multiple foci), EEG focus status, and epilepsy type (focal/generalized) were analyzed using the chi-square test. This test was applied to assess the independence between categorical variables, with p-values below 0.05 considered statistically significant.

Pearson correlation analysis was applied to assess the relationships between prognostic parameters and continuous variables such as the duration of epilepsy (years), age at seizure onset, and epilepsy frequency (number of seizures per day). The Pearson correlation test examines the linear relationship between two continuous variables, with the strength and direction of the association evaluated using the correlation coefficient (r). In all analyses, a p-value of less than 0.05 was considered the threshold for statistical significance.

The chi-square test was also used to evaluate the association between epilepsy surgery and postoperative seizure reduction. The distribution of continuous variables was reported as mean±standard deviation, while categorical variables were presented as frequencies and percentages.

RESULTS

The mean age of patients included in our study was 25.94 years (range: 5-53 years). The average follow-up duration was 67.1 months (range: 12-199 months). The mean age at seizure onset was 6.39 years, and the mean duration of epilepsy was 19.46 years (range: 2-41 years). The average number of seizures per day was 3.68, and the mean number of anti-epileptic drugs used was 3.23 (Table 1).

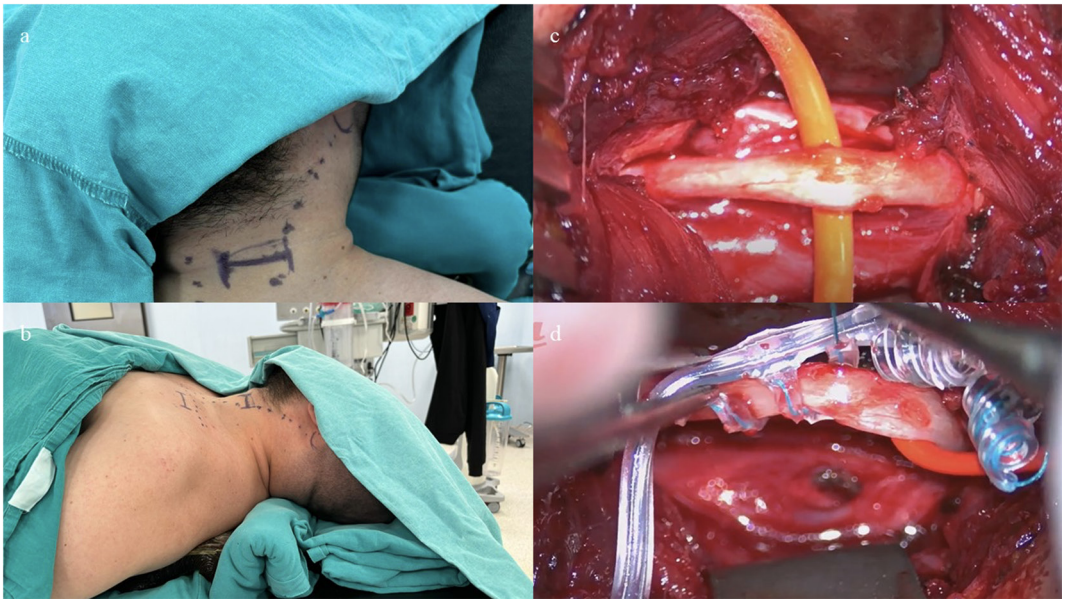

Figure 1. Vagus nerve stimulation (VNS) implantation procedure. This figure illustrates the standard procedure for VNS implantation. a: The patient is positioned supine, with the head rotated 45 degrees to the right and slightly extended to target the left vagus nerve. b: The first horizontal incision is planned at the midpoint between the clavicle and mastoid process, intersecting the medial border of the sternocleidomastoid muscle. The second incision is made parallel to the left pectoral muscle, approximately 5-8 cm below the clavicle. c: Following anterior cervical exposure, the left vagus nerve is isolated over a minimum length of 3 cm, distal to the cardiac branches and proximal to the recurrent laryngeal nerve. d: Helical electrodes are placed around the exposed vagus nerve segment

In terms of categorical data, 34.15% of patients were female, and 65.85% were male. The percentage of patients with a known epilepsy etiology was 54.88%, while 45.12% had an unknown etiology. Among the patients, 26.83% had focal epilepsy, and 73.17% had generalized epilepsy. The proportion of patients who underwent epilepsy surgery was 18.29%, and 81.71% had not undergone surgery. MRI revealed lesions in 54.88% of patients, with 45.12% showing no lesions (Table 1).

In the postoperative ILAE score distribution, 74.39% of patients were classified as ILAE 4, 20.73% as ILAE 5, 3.66% as ILAE 6, and 1.22% as ILAE 3. In terms of the Engel score distribution, 70.73% of patients were classified as Engel 3-A, 10.98% as Engel 4-B, 9.76% as Engel 2-B, 3.66% as Engel 4-A, 3.66% as Engel 4-C, and 1.22% as Engel 2-D (Figure 2).

Postoperative anti-epileptic drugs were reduced in 24.39% of patients, while remaining unchanged in 75.61%. The rates of seizure reduction were as follows: 75-100% reduction in 36.59% of patients, 50-75% reduction in 36.59%, 25-50% reduction in 8.54%, and 0-25% reduction or an increase in seizures in 18.28% of patients. Overall, 73.18% of patients were classified as responsive to treatment (Figure 2).

Statistical analyses showed no significant associations between gender and ILAE score, Engel score, postoperative medication changes, or postoperative seizure reduction ($p>0.05$). Similarly, there were no significant associations between epilepsy type (focal/generalized) and prognostic parameters ($p>0.05$). However, a significant association was found between epilepsy surgery and postoperative seizure reduction ($p=0.025$), with patients who had undergone surgery showing greater seizure reduction. MRI findings did not show a significant association with prognostic parameters. MRI findings of single versus multiple foci exhibited borderline significant associations with Engel score and postoperative seizure reduction but did not reach statistical significance ($p=0.079$ and $p=0.098$). No significant associations were observed between EEG focus status (single focus/multiple foci) and prognostic parameters ($p>0.05$). Additionally, no significant associations were found between age at seizure onset and duration of epilepsy and prognostic parameters ($p>0.05$). A borderline association was observed between the duration of epilepsy and Engel score, but it did not reach statistical significance ($p=0.080$). No significant association was found between seizure frequency per day and prognostic parameters ($p>0.05$).

Table 1. Clinical and demographic characteristics of patients before VNS implantation

Characteristic	Value
Age (mean, min-max)	25.94 (5-53)
Follow-up duration (mean, min-max, months)	67.1 (12-199)
Age at seizure onset (mean, min-max, years)	6.39 (0-23)
Duration of epilepsy (mean, min-max, years)	19.46 (2-41)
Number of antiepileptic drugs (mean, min-max)	3.23 (1-5)
Seizures per day (mean, min-max)	3.68 (0.1-10)
Gender (female/male, %)	34.15 / 65.85
Epilepsy etiology (known/unknown, %)	54.88 / 45.12
Type of epilepsy (focal/generalized, %)	26.83 / 73.17
History of epilepsy surgery (yes/no, %)	18.29 / 81.71
MRI findings (present/absent, %)	54.88 / 45.12

VNS: Vagus nerve stimulation, MRI: Magnetic resonance imaging

In terms of complications, a total of 5 patients (6.1%) developed wound site complications during the treatment period. Three of these occurred after the initial surgery, and two after generator replacement. All complications developed in the generator site. In one patient who developed a wound site complication after generator replacement, the abscess progressed, necessitating the removal of the entire system. Methicillin-resistant *Staphylococcus aureus* growth was identified in this case. The remaining patients recovered without sequelae following surgical revision and antibiotic therapy. Additionally, in one patient, the system was removed at the end of the third year due to unsuccessful seizure control (ILAE 6). Furthermore, 5 patients (6.1%) experienced hoarseness, and 3 patients (3.7%) developed coughing symptoms; all of these symptoms resolved with follow-up and medical treatment.

DISCUSSION

Since the introduction of VNS implantation as a novel treatment for drug-resistant epilepsy in the 1990's, numerous studies have been conducted. These studies generally consider a reduction of over 50% in seizure frequency in patients with drug-resistant epilepsy as a positive response to VNS therapy, with reported efficacy increasing over time Studies have demonstrated that VNS implantation provides significant seizure control in the treatment of refractory epilepsy. In a meta-analysis conducted by Wang et al. (14), which included 16 studies covering 1,080 patients, the treatment response rate varied between 38.89% and 73.21%. Another meta-analysis by Toffa et al. (16) reported a response rate ranging from 45% to 65%. More recent large single-center series reported by Boluk et al. (6) showed the highest reduction rate of 75.6% at the end of the 18th month, independent of seizure type; LoPresti et al. (17) documented a 52% seizure reduction, and Alexopoulos et al. (18) reported a reduction of 58.7%.

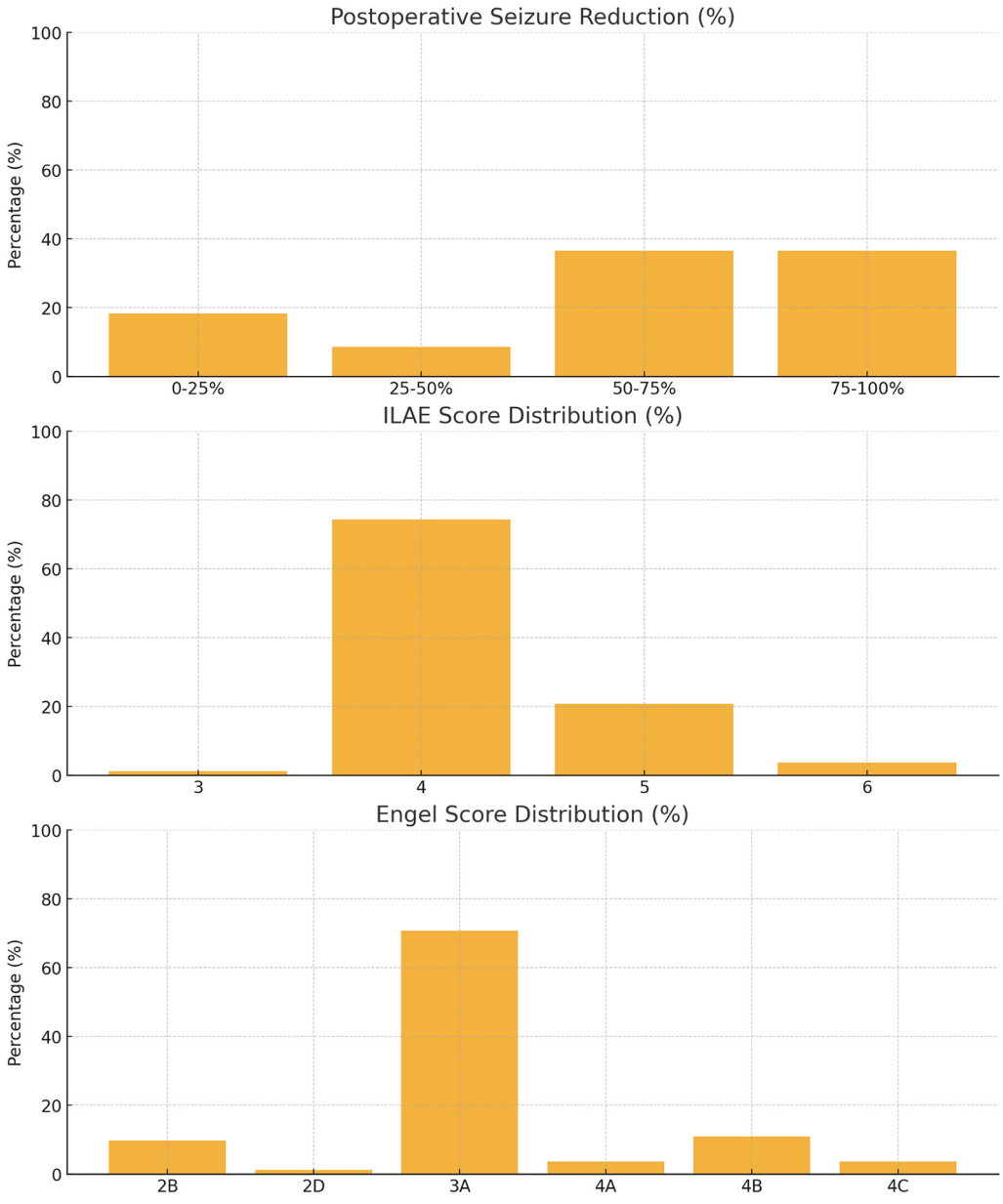

Figure 2. Distribution of postoperative outcomes following VNS implantation. This figure illustrates the distribution of postoperative outcomes in patients. The ILAE classification: • Grade 1: Completely seizure-free; no auras • Grade 2: Only auras; no other seizures • Grade 3: One to three seizure days per year; ±auras • Grade 4: Four seizure days per year to 50% reduction of baseline seizure days; ±auras • Grade 5: Less than 50% reduction of baseline seizure days to 100% increase of baseline seizure days; ±auras • Grade 6: More than 100% increase of baseline seizure days; ±auras. The Engel classification: • 1A: Completely seizure-free since surgery • 1B: Non-disabling simple partial seizures only • 1C: Some disabling seizures after surgery, but free of disabling seizures for at least 2 years • 1D: Generalized convulsions only with medication changes • 2A: Initially free of disabling seizures but rare disabling seizures now • 2B: Rare disabling seizures from the start • 3A: Worthwhile seizure reduction (≥50%) • 3B: <50% reduction in disabling seizures • 4A: No worthwhile improvement • 4B: No change • 4C: Worsening seizures

Consistent with the literature, our series demonstrated the efficacy of VNS implantation therapy, with a reduction in seizures of more than 50% in 73.18% of patients by the end of the 12th month. We selected the 12-month mark to allow the neuromodulation effect to develop fully, to observe the efficacy of VNS before potential long-term seizure-increasing factors could arise. Additionally, more than 75% seizure reduction was achieved in half of these patients, highlighting the significant improvement in quality of life provided by this therapy.

Some studies reporting on the efficacy and safety of VNS have indicated that initiating VNS implantation therapy within the first five years of epilepsy progression, and in the pediatric age group, results in higher effectiveness (16,19,20). In our study, we observed no significant differences in treatment response with respect to age and gender. We believe this may be due to the substantially higher number of adult patients compared to pediatric patients in our cohort. The alignment of our results with adult patient series in the literature supports this view. In a series of 45 pediatric patients who underwent VNS implantation, Soleman et al. (19) emphasized that early implantation at age five or younger, led to significantly greater improvements in quality of life and cognitive outcomes compared to VNS implantation performed after age five. In a meta-analysis by Englot et al. (20) involving 1,489 patients, the treatment response rate was reported as 49.2% in adults, while this rate increased to 55.3% in the pediatric age group and reached 62% in pediatric patients younger than six years. In contrast, some studies conducted in adult patient groups have reported that initiating VNS implantation therapy in the early stages following an epilepsy diagnosis enhances treatment response; however, patient age does not produce a significant difference in treatment efficacy (14,21,22).

Research have not established a clear relationship between epilepsy type and treatment response; however, various studies have reported significant differences in response periods between focal and generalized epilepsy. In our study, we did not observe a difference in treatment response between focal and generalized epilepsies, as reported in previous research. However, as our study was not specifically designed to assess the therapeutic effect between epilepsy types, statistical data on this topic were not included. Drees et al. (23) compared treatment response durations and early response rates between focal and generalized epilepsy patient groups, finding that the rate of super-responders was significantly higher in the generalized epilepsy group, although initially higher among patients with focal epilepsy (23).

Before initiating VNS implantation therapy, the resectability of lesions in all patients should be assessed (17,24). In our cohort, we utilized MRI, PET, and vEEG evaluations to assess epileptic foci to exclude candidates for resective epilepsy surgery prior to VNS implantation. However, 18.3% of our patients had a history of resective or ablative epilepsy surgery. The response to VNS in these patients was significantly better than in others within our study. As suggested in a similar study, this may be related to the reduction in epileptogenic load (25). Nonetheless, as demonstrated in our series, we emphasize that resective surgery should be the primary treatment choice in refractory epilepsy whenever feasible. Even if seizure control is not achieved due to insufficient resection, repeated resective surgery may yield better outcomes than VNS. Thorough patient selection evaluations can prevent the high number of unsuitable candidates noted in recent literature (17,26).

In our study, we were unable to determine the impact of etiological factors and vEEG findings on treatment response. However, consistent with the literature, we observed a near-significant improvement in treatment response among patients with multiple foci compared to those with a single focus on MRI. In the literature, LoPresti et al. (17) evaluated the relationship between seizure etiology and treatment response and found no significant association between seizure etiology and genetics. However, they reported a higher treatment response in patients with positive MRI findings. They identified brain atrophy as associated with poorer outcomes, whereas, unexpectedly, dysplastic hippocampus and periventricular leukomalacia were linked to better treatment responses. In light of our results, we believe that VNS implantation therapy may be more effective and should be considered earlier in patients with refractory epilepsy who have a history of epilepsy surgery or are not candidates for resective surgery, but present with multiple foci.

Complications of VNS are another factor influencing outcomes. Known complications of VNS include wound site complications, hoarseness, sore throat, coughing, dizziness, arrhythmias, vocal cord paralysis, sleep apnea syndrome, pneumothorax, muscle spasms, chronic diarrhea, and Horner syndrome (27). In the literature, wound site complications have been reported at rates of 2-7%, hoarseness at 37%, and coughing at 7%. Our case series aligns with the literature regarding the frequency of these complications (28-30).

Study Limitations

This study has several limitations that should be considered when interpreting the findings. First, as a retrospective study, it is susceptible to recall and selection biases, given its reliance on existing records rather than prospective data collection. Additionally, with a sample size of 82 patients, the results may not be generalizable to larger, more diverse populations.

Another limitation is the absence of a control group, which restricts our ability to attribute improvements solely to VNS therapy without accounting for potential placebo effects or the natural progression of epilepsy. Although we aimed to examine the effect of VNS on different types of epilepsy, the study was not specifically designed to assess differences

in efficacy across epilepsy types or etiologies, limiting our conclusions regarding which subtypes may benefit most from VNS. Moreover, other potential confounding factors, such as concurrent treatments, lifestyle influences, and adherence to antiepileptic medications, may have impacted seizure outcomes but were difficult to fully control in this retrospective setting.

Finally, as we exclusively used the LivaNova Demipulse model for VNS implantation, the findings may not be directly applicable to other VNS models or newer devices with potentially varying efficacy and safety profiles. Future studies with larger, prospective, and controlled designs could help address these limitations, enhancing the understanding of VNS's long-term impact across diverse patient populations.

CONCLUSION

In this retrospective study of VNS implantation therapy, we demonstrate its high efficacy in seizure control, which is consistent with the literature, and its positive impact on patients' quality of life. For seizures persisting after successful resective surgery, VNS remains highly effective in reducing seizure severity and frequency. For patients with refractory epilepsy, VNS implantation therapy should be considered the primary treatment option for patients who are not candidates for resective or ablative epilepsy surgery or whose seizures remain uncontrolled despite these surgical interventions.

ETHICS

Ethics Committee Approval: This study was conducted retrospectively, following approval from University of Health Sciences Türkiye, Başakşehir Çam ve Sakura City Hospital Ethics Committee (decision no: 162, date: 19.04.2023) and in compliance with the Helsinki Declaration.

Informed Consent: Since this research was retrospective, patient consent was not required in this research.

FOOTNOTES

Authorship Contributions

Surgical and Medical Practices: O.H., O.B., B.E., B.T., Concept: O.H., O.B., T.Ö.K., N.B.G., B.E., B.T., Design: O.H., O.B., T.H., B.E., B.T., Data Collection or Processing: O.B., T.Ö.K., T.H., N.B.G., Analysis or Interpretation: O.H., O.B., B.E., Literature Search: O.H., O.B., T.Ö.K., T.H., N.B.G., Writing: O.H., O.B., T.Ö.K., T.H., N.B.G., B.E., B.T.

Conflict of Interest: No conflict of interest was declared by the authors.

Financial Disclosure: The authors declare that this study received no financial support.

REFERENCES

1. Fiest KM, Sauro KM, Wiebe S, Patten SB, Kwon C-S, Dykeman J, et al. Prevalence and incidence of epilepsy: a systematic review and meta-analysis of international studies. Neurology. 2017;88:296-303.
2. Kotsopoulos IA, Van Merode T, Kessels FG, De Krom MC, Knottnerus JA. Systematic review and meta-analysis of incidence studies of epilepsy and unprovoked seizures. Epilepsia. 2002;43:1402-9.
3. Kwan P, Arzimanoglou A, Berg AT, Brodie MJ, Allen Hauser W, Mathern G, et al. Definition of drug resistant epilepsy: consensus proposal by the ad hoc task force of the ILAE Commission on Therapeutic Strategies. Epilepsia. 2010.
4. Amar AP, Heck CN, Levy ML, Smith T, DeGiorgio CM, Oviedo S, et al. An institutional experience with cervical vagus nerve trunk stimulation for medically refractory epilepsy: rationale, technique, and outcome. Neurosurgery. 1998;43:1265-76.
5. Schuele SU, Lüders HO. Intractable epilepsy: management and therapeutic alternatives. Lancet Neurol. 2008;7:514-24.
6. Boluk C, Ozkara C, Isler C, Uzan M. Vagus nerve stimulation in intractable epilepsy. Turk Neurosurg. 2022;32:97-102.
7. Téllez-Zenteno JF, Dhar R, Wiebe S. Long-term seizure outcomes following epilepsy surgery: a systematic review and meta-analysis. Brain. 2005;128:1188-98.
8. Handforth A, DeGiorgio C, Schachter S, Uthman B, Naritoku D, Tecoma E, et al. Vagus nerve stimulation therapy for partial-onset seizures: a randomized active-control trial. Neurology. 1998;51:48-55.
9. Labar D, Nikolov B, Tarver B, Fraser R. Vagus nerve stimulation for symptomatic generalized epilepsy: a pilot study. Epilepsia. 1998;39:201-5.
10. Scheffer IE, Berkovic S, Capovilla G, Connolly MB, French J, Guilhoto L, et al. ILAE classification of the epilepsies: Position paper of the ILAE Commission for Classification and Terminology. Epilepsia. 2017;58:512-21.
11. Rodgers WP, Durnford AJ, Kirkham FJ, Whitney A, Mullee MA, Gray WP. Interrater reliability of Engel, international league against epilepsy, and mchugh seizure outcome classifications following vagus nerve stimulator implantation. J Neurosurg Pediatr. 2012;10:226-9.
12. Chrastina J, Novák Z, Zeman T, Kočvarová J, Pail M, Doležalová I, et al. Single-center long-term results of vagus nerve stimulation for epilepsy: A 10–17 year follow-up study. Seizure. 2018;59:41-7.
13. Polkey CE, Nashef L, Queally C, Selway R, Valentin A. Long-term outcome of vagus nerve stimulation for drug-resistant epilepsy using continuous assessment, with a note on mortality. Seizure. 2022;96:74-8.
14. Wang HJ, Tan G, Zhu LN, Chen D, Xu D, Chu SS, et al. Predictors of seizure reduction outcome after vagus nerve stimulation in drug-resistant epilepsy. Seizure. 2019;66:53-60.
15. Schachter SC and Saper CB. Vagus nerve stimulation. Epilepsia. 1998;39:677-86.
16. Toffa DH, Touma L, El Meskine T, Bouthillier A, Nguyen DK. Learnings from 30 years of reported efficacy and safety of vagus nerve stimulation (VNS) for epilepsy treatment: a critical review. Seizure. 2020;83:104-23.
17. LoPresti MA, Huang J, Shlobin NA, Curry DJ, Weiner HL, Lam SK. Vagus nerve stimulator revision in pediatric epilepsy patients: a technical note and case series. Childs Nerv Syst. 2023;39:435-41.

18. Alexopoulos AV, Kotagal P, Loddenkemper T, Hammel J, Bingaman WE. Long-term results with vagus nerve stimulation in children with pharmacoresistant epilepsy. Seizure. 2006;15:491-503.
19. Soleman J, Stein M, Knorr C, Datta AN, Constantini S, Fried I, et al. Improved quality of life and cognition after early vagal nerve stimulator implantation in children. Epilepsy Behav. 2018;88:139-45.
20. Englot DJ, Rolston JD, Wright CW, Hassnain KH, Chang EF. Rates and predictors of seizure freedom with vagus nerve stimulation for intractable epilepsy. Neurosurgery. 2016;79:345-53.
21. Liu HY, Yang Z, Meng FG, Guan YG, Ma YS, Liang SL, et al. Preoperative heart rate variability as predictors of vagus nerve stimulation outcome in patients with drug-resistant epilepsy. Sci Rep. 2018;8:3856.
22. Chrastina J, Kocvarova J, Novak Z, Dolezalova I, Svoboda M, Brazdil M. Older age and longer epilepsy duration do not predict worse seizure reduction outcome after vagus nerve stimulation. J Neurol Surg A Cent Eur Neurosurg. 2018;79:152-8.
23. Drees C, Afra P, Verner R, Kaye L, Keith A, Jiang M, et al. Feasibility study of microburst VNS therapy in drug-resistant focal and generalized epilepsy. Brain Stimul. 2024;17:382-91.
24. Fisher RS and Handforth A. Reassessment: vagus nerve stimulation for epilepsy: a report of the therapeutics and technology assessment subcommittee of the American Academy of Neurology. Neurology. 1999;53:666-9.
25. Lesser RP. Unexpected places: How did vagus nerve stimulation become a treatment for epilepsy? Neurology. 1999;52:1117-8.
26. Solli E, Colwell NA, Markosian C, Johal AS, Houston R, Iqbal MO, et al. Underutilization of advanced presurgical studies and high rates of vagus nerve stimulation for drug-resistant epilepsy: a single-center experience and recommendations. Acta Neurochir (Wien). 2022;164:565-73.
27. Ohemeng KK and Parham K. Vagal nerve stimulation: indications, implantation, and outcomes. Otolaryngol Clin North Am. 2020;53:127-43.
28. Schachter SC, Sirven JI. Vagus nerve stimulation therapy for the treatment of epilepsy. UpToDate; 2018.
29. Liporace J, Hucko D, Morrow R, Barolat G, Nei M, Schnur J, et al. Vagal nerve stimulation: adjustments to reduce painful side effects. Neurology. 2001;57:885-6.
30. Elliott RE, Morsi A, Kalhorn SP, Marcus J, Sellin J, Kang M, et al. Vagus nerve stimulation in 436 consecutive patients with treatment-resistant epilepsy: long-term outcomes and predictors of response. Epilepsy Behav. 2011;20:57-63.

Medical Journal of Bakırköy

Med J Bakirkoy 2025;21:39-47
DOI: 10.4274/BMJ.galenos.2024.2024.3-11

Nail-fold Capillaroscopic Changes in Children with Juvenile Dermatomyositis and Specific Autoantibodies

Jüvenil Dermatomiyozit Hastalarında Kapilleroskopik Değişiklikler ve Spesifik Otoantikorlarla İlişkisi

Şeyda Doğantan, Sema Nur Taşkın, Ayşenur Paç Kısaarslan, Muammer Hakan Poyrazoğlu

Erciyes University Faculty of Medicine, Department of Pediatric Rheumatology, Kayseri, Türkiye

ABSTRACT

Objective: Microvascular changes observed during dermoscopy have been widely used for diagnosing and monitoring various connective tissue disorders, including juvenile dermatomyositis (JDM). This study investigated capillaroscopic changes in nail-folds, specifically, nail-fold capillary density (NFCD), in children with JDM.

Methods: A prospective study was conducted on children diagnosed with JDM between 2010 and 2021 who were examined via nail-fold capillaroscopy (n=14) during August and December 2021. Demographic and clinical data, myositis-specific autoantibodies for JDM, and capillaroscopic findings were prospectively collected. In addition to children with JDM (group JDM), we randomly selected 20 children with non-specific leg pain as the control group. Capillaroscopic findings were compared between the groups.

Results: The groups were similar in terms of age and sex characteristics (p=0.848 and p=0.635). Ten children had myositis-specific autoantibodies (71.4%). The median NFCD was significantly lower in the JDM group than in the controls (p=0.001). Children with JDM had a significantly higher frequency and amount of disorganized, tortuous, crossing, enlarged, and giant capillaries than healthy controls (p<0.05). There were significantly higher values of the neoangiogenesis score and MES in Group JDM than in Controls (p<0.001 and p<0.001). Children with positive autoantibodies had higher NFCD and lower interpapillary distance values (p<0.05).

Conclusion: Children with JDM exhibited remarkable morphological changes during nail-fold capillaroscopy. Higher neoangiogenesis scores, higher MES values, and decreased NFCD might play a role in diagnosing and differentiating childhood JDM.

Keywords: Juvenile dermatomyositis, dermoscopy, microscopic angioscopy, microvascular density, nails, capillaries

ÖZ

Amaç: Dermoskopi sırasında gözlenen mikrovasküler değişiklikler, juvenil dermatomiyozit (JDM) de dahil olmak üzere çeşitli bağ dokusu bozukluklarının tanı ve takibinde yaygın olarak kullanılmaktadır. Bu çalışma, JDM'li çocuklarda kapilleroskopik tırnak kıvrımı değişikliklerini, daha doğrusu tırnak kıvrımı kılcal yoğunluğunu (NFCD) araştırdı.

Gereç ve Yöntem: 2010-2021 yılları arasında JDM tanısı alan ve Ağustos ve Aralık 2021'de tırnak kıvrımı kapilleroskopisi (n=14) ile incelenen çocuklar üzerinde prospektif bir çalışma yapıldı. Demografik ve klinik özellikler, JDM için miyozite özgü otoantikorlar ve kapillaroskopik bulgular ileriye dönük olarak toplandı. JDM'li çocukların (grup JDM) yanı sıra, spesifik olmayan bacak ağrısı olan 20 çocuğu da kontrol grubu olarak rastgele seçtik. Gruplar arasında kapillaroskopik bulgular karşılaştırıldı.

Bulgular: Gruplar yaş ve cinsiyet özellikleri açısından benzerdi (p=0,848 ve p=0,635). Miyozite özgü otoantikorları pozitif olan 10 çocuk (%71,4) vardı. Medyan NFCD, Grup JDM'de control grubuna göre anlamlı derecede düşüktü (p=0,001). JDM'li çocuklarda düzensiz, kıvrımlı, çapraz, genişlemiş ve dev kapillerlerin sıklığı ve sayısı sağlıklı kontrollere göre anlamlı derecede yüksekti (p<0.05). Grup JDM'de neoanjiyogenez skoru ve mikroanjiyopati değerlendirme skoru (MES) değerleri, kontrol grubuna göre anlamlı derecede yüksekti (p<0,001 ve p<0,001). Otoantikorları pozitif olan çocuklarda NFCD daha yüksek ve papiller mesafe değerleri daha düşüktü (p<0,05).

Sonuç: JDM'li çocuklarda tırnak kıvrımı kapilleroskopisi sırasında dikkat çekici morfolojik değişiklikler görüldü. Daha yüksek neoanjiyogenez skorları, daha yüksek MES değerleri ve azalmış NFCD, çocukluk çağı JDM'nin tanı ve ayrımında rol oynayabilir.

Anahtar Kelimeler: Juvenil dermatomiyozit, dermoskopi, mikroskobik anjiyoskopi, mikrovasküler dansite, tırnaklar, kılcal damarlar

Address for Correspondence: Şeyda Doğantan, Erciyes University Faculty of Medicine, Department of Pediatric Rheumatology, Kayseri, Türkiye

E-mail: drseydacayan@gmail.com **ORCID ID:** orcid.org/0000-0002-9082-6804

Cite as: Doğantan Ş, Taşkın SN, Paç Kısaarslan A, Poyrazoğlu MH. Nail-fold capillaroscopic changes in children with juvenile dermatomyositis and specific autoantibodies.. Med J Bakirkoy. 2025;21:39-47

Received: 04.04.2024
Accepted: 03.06.2024
Publication Date: 25.03.2025

Introduction

Juvenile dermatomyositis (JDM) is a childhood autoimmune connective tissue disease associated with skin, skeletal system, and internal organ disturbances (1). It is categorized as a subgroup of idiopathic inflammatory myopathies according to the European League Against Rheumatism/American College of Rheumatology classification criteria (2,3). An immune response originating from the capillary endothelium of the endomysium is considered an early event causing skin involvement in JDM (3,4). Vascular skin changes play a diagnostic and prognostic role as they precede the development of subsequent myositis (5).

Dermoscopy has recently been used to observe the morphologic features of the skin using *in vivo* magnification (3,6). Standardized basic dermoscopic parameters of inflammatory, infiltrative, and infectious dermatoses have been described (3,7,8). Previous studies have reported that early microvascular changes in various rheumatic diseases can be assessed using nail-fold capillaroscopy (NFC) (3,6,9,10). In this way, NFC can differentiate the types of connective tissue disorders in patients with primary and secondary Raynaud's phenomenon and mixed connective tissue diseases, including polymyositis and dermatomyositis (2,11,12). Besides, it has been speculated that the findings of NFC are related to disease activity and the levels of myositis-specific and-associated autoantibodies for JDM (1,2,5,12,13).

We aimed to evaluate dermoscopic vascular changes via NFC in patients with JDM and to compare these findings with those of healthy children. We present the following case reports in accordance with the STROBE reporting checklist.

METHODS

Study

A prospective study including nail-fold capillaroscopic findings of children with JDM was performed in Erciyes University Faculty of Medicine, Department of Paediatric Rheumatology. This study was approved by the Erciyes University Clinical Research Ethics Committee (decision no: 2021/355, date: 05.05.2021). The analysis was performed in accordance with the principles of the Helsinki Declaration. Written informed consent was obtained from the parents of the children.

Patients

Between August and December 2021, we performed nail-fold capillaroscopic examinations in 14 children with JDM. The diagnosis of probable or definitive JDM was based on the Bohan and Peter criteria, including disease onset before the age of 18 years and ≥24 months from symptom onset to follow-up (14). A predefined treatment protocol was applied to all children with JDM (1). Children with overlap syndrome, juvenile-onset mixed connective tissue disease, and juvenile polymyositis were excluded.

Blood samples were obtained for the anti-nuclear antibody (ANA), the extractable nuclear antigen antibody titer measurements, and the myositis-specific autoantibodies for JDM were measured at the last follow-up examinations. Anti-transcriptional factor-1-γ/p155/140, anti-NXP-2/anti-MJ, anti-SRP, anti-pl-7, anti-pl-12, anti-pm-Scl-75, Mi-2 alpha, Mi-2 beta, MDA5, SAE1, Ku, pm-Scl-100, Jo-1, SEJ, OJ, Ro-52, and anti-SRP were the autoantibodies in the category of the myositis-specific autoantibodies (14). We tested the presence of autoantibodies using an Immunoblot assay (Myositis Profile Euroline Blot test kit, Euroimmun, Lübeck, Germany) at the Biochemistry Laboratory of Erciyes University, Faculty of Medicine.

Definitions

The first muscular or dermatological symptom was considered as the disease onset. The disease duration was calculated using the interval between the start and last follow-up examination. The Childhood Myositis Assessment Scale (CMAS) was used to assess proximal muscle strength, function, and endurance (15). The scale includes 14 physical maneuvers, with a maximum score of 52. Assessment of improvement or worsening between two quantitative evaluations of an individual patient is the primary function of the CMAS. A trained physical therapist applied the CMAS to all the children in the study (15).

The disease course was categorized as mono, polyphasic, or chronic (16). Remission within 36 months of diagnosis without relapse was defined as a monophasic course. Relapse of the disease at any time point after the previous remission was considered a polyphasic event. Chronic disease course was defined as persistent evidence of disease 36 months after diagnosis.

NFC

After resting for at least 20 min at room temperature (20-24 °C), a video microscope (MEDL4N Dino-Lite Pro Capillary Scope, Dino-Lite Europe, NN Almere, the Netherlands) was used to perform capillaroscopic measurements as described previously (1,17). A pediatric rheumatologist with an experience of 3 years on NFC examined all fingers except the thumb.

We also investigated the morphological changes related to capillary dropout, branching and dilatation, areas of hemorrhage, avascular area, neovascular changes with neoangiogenesis score, capillary disorganization, and the number of vessels per millimeter (1,18-20). The measurements of the internal capillary diameter between 25 and 50 μm and ≥50 μm were defined as dilated and giant capillaries (18). We considered criteria for determining morphological changes as described previously (19).

The parameters included the total number of capillaries over the nail-fold width, mean nail-fold capillary density (NFCD) per millimeter, capillary size, and numbers of dilated, giant, branching, and tortuous capillaries. Each patient's microangiopathy evaluation score (MES) was calculated as defined Sulli et al. (21). In this scale, the loss of capillaries, disorganization of the microvascular array, and capillary ramifications were semi-quantitatively evaluated with scores ranging from zero to three. The summation of the scores for each parameter revealed that the MES ranged from zero to nine.

Groups

The study group included children with JDM (group JDM). We randomly selected 20 children with nonspecific leg pain as the control group (the control).

Variables

Data on demographic characteristics (age, sex), clinical characteristics (age at diagnosis, CMAS scores at the admission and the last follow-up, disease duration, physical findings, and medications), and laboratory findings were collected and stored.

Statistical Analysis

For descriptive statistics, mean±standard deviation was used to present continuous data with normal distribution. The median with minimum-maximum values was applied for continuous variables without normal distribution. Numbers and percentages were used as categorical variables. The Shapiro-Wilk, Kolmogorov-Smirnov, and Anderson-Darling tests analyzed the normal distribution of the numerical variables.

The Pearson chi-square and Fisher's exact tests were used to compare differences between categorical variables in 2x2 tables. The Fisher-Freeman Halton test was used for the RxC tables.

The Mann-Whitney U test was used to compare two independent groups in which numerical variables had no normal distribution.

Spearman's correlation coefficients were calculated to analyze the relationships of NFCD and MES with demographic (age) and clinical variables (age at diagnosis, CMAS at diagnosis, disease duration, duration for steroid use, and the length of follow-up).

Jamovi (Version 2.2.5.0) and JASP (Version 0.16.1) were used for statistical analysis. The significance level (p-value) was set at 0.05 in all statistical analyses.

RESULTS

There were 14 and 20 children in the JDM and control. The mean age of children with JDM was 10.4±4.0 years. There were nine male and five female children in Group JDM. The groups were similar in terms of age and sex characteristics (p=0.848 and p=0.635). ANA positivity was more frequently detected in the JDM group than in the Controls (p<0.001).

The clinical characteristics of children with JDM are presented in Table 1. The median age at diagnosis was 11.5 years (range, 4-16 years). The median CMAS score at admission was 40, ranging from 30 to 50. The medication distribution in the JDM group is detailed in Table 1. The median follow-up time was 3 years (range, 0.1-11 years)

Table 1. Clinical characteristics of children with JDM (group JDM, n=14)

	Value
Age at diagnosis (year)§	11.5 (4-16)
CMAS score at diagnosis§	40 (30-50)
Disease duration (year)§	3 (0.1-11)
Disease course‡	
Monophasic	10 (71.4)
Polyphasic	3 (21.4)
Chronicity‡	1 (7.1)
Medications	
Steroid‡	9 (81.8)
Duration of steroid use (month)§	12 (9-24)
DMARD‡	11 (78.6)
Mycophenolic acid	3 (27.3)
Methotrexate	6 (54.5)
Hydroxychloroquine	2 (18.2)
Duration (month)§	2 (1-9)
bDMARD‡	2 (14.3)
Etanercept	1 (50)
Adalimumab	1 (50)
IVIG‡	6 (42.9)
Follow-up (year)	3 (1-11)
CMAS score at the last follow-up§	52 (50-52)

‡n (%), §median (minnimum-maximum)
JDM: Juvenile dermatomyositis, CMAS: Childhood Myositis Assessment Scale, DMARD: Disease-modifying anti-rheumatic drugs, bDMARD: Biologic disease-modifying anti-rheumatic drugs, IVIG: Intravenous immunoglobulin

in group JDM. Nevertheless, the median CMAS score increased to 52 during the last follow-up examination.

Table 2 presents the frequencies of the ENA antibody profiles observed in children with JDM. In four children (28.6%), we detected four ENA antibodies: SM/RNP (n=1), SS-B (n=1), and PCNA (n=2). Ten children (71.4%) were negative for ENA antibodies in group JDM.

Although in four children (28.6%), there were negative results for the myositis-specific autoantibodies, TIF-1 (n=3), NXP-2 (n=2), p1-12 (n=1), p1-7 (n=1), pm-75 (n=1), SRP (n=1), and Jo-1 (n=1) were detected in group JDM. Thus, we noticed positive results for myositis-specific autoantibodies in ten children (71.4%) (Table 3). Children with positive and negative myositis-specific autoantibodies had similar demographic and clinical characteristics (p>0.05) (Table 3).

The nail-fold capillaroscopic findings and their comparisons are presented in Table 4 and Figures 1-3. We detected significant differences between the groups (p<0.05). The median NFCD was significantly lower in the JDM group than in the Controls (p=0.001). The widths of the arteries, veins, and apical loop were substantially lower in children with JDM than in the Controls (p=0.001, p=0.001, and p=0.003). We found significantly higher values of the neoangiogenesis score and MES in the JDM group than in the controls (p<0.001 and p<0.001).

There were significant differences in the morphological capillary abnormalities via NFC between the groups (p<0.05) (Table 4). The children with JDM had significantly higher frequency and number of capillaries with disorganized, tortuous, crossing, enlarged, and giant features than the healthy controls (p<0.05).

We also compared the nail-fold capillaroscopic findings between children with and without myositis-specific

Table 2. Distribution of the extractable nuclear antigen antibody profile in children with JDM (group JDM, n=14)

	Value
Extractable nuclear antigen antibodies‡	
Anti-SM/RNP	1 (7.1)
Anti-SS-B (anti KU positive)	1 (7.1)
Anti-PCNA	2 (14.3)
Negative	10 (71.4)
Myositis-specific autoantibodies‡	
Negative	4 (28.6)
Anti-TIF1	3 (21.4)
Anti-NXP2	2 (14.2)
Anti-pl12	1 (7.1)
Anti-pl7	1 (7.1)
Anti-pm75	1 (7.1)
Anti-SRP	1 (7.1)
Anti-histidyl tRNA synthetase (anti-Jo-1)	1 (7.1)

‡n (%), JDM: juvenile dermatomyositis, Ds-DNA: Double-stranded DNA, CCP: Cyclic citrullinated peptide, PCNA: Proliferating cell nuclear antigen protein

Table 3. Demographic and clinical characteristics of children with and without myositis-specific autoantibodies

Children			
	With positive autoantibodies (n=10)	**Negative autoantibodies (n=4)**	**p-value**
Age (year)†	12.8 (5.0-16.0)	9.5 (4.0-11.0)	0.118**
Sex‡			
Male	6 (60.0)	3 (75.0)	0.999*
Female	4 (40.0)	1 (25.0)	
ANA titer‡			
Negative	0 (0.0)	2 (50.0)	0.066*
Positive	10 (100.0)	2 (50.0)	
Age at diagnosis (year)§	12.5 (5.0-16.0)	9.5 (4.0-11.0)	0.118**
CMAS score at diagnosis§	39.5 (30.0-49.0)	42.0 (38.0-50.0)	0.135**
Disease duration (year)§	3.0 (0.8-11.0)	3.2 (0.1-6.5)	0.618**
Physical findings‡			
Calcinosis	1 (10.0)	2 (50.0)	0.176*
Skin involvement			
Mild	5 (50.0)	3 (75.0)	0.999*
Moderate	2 (20.0)	0 (0.0)	
Severe	3 (30.0)	1 (25.0)	
Muscular involvement‡			
Mild	7 (70.0)	3 (75.0)	0.999*
Moderate	3 (30.0)	1 (25.0)	
Disease course‡			
Monophasic	7 (70.0)	3 (75.0)	0.999*
Polyphasic	3 (30.0)	0 (0.0)	0.505*
Chronicity‡	0 (0.0)	1 (25.0)	0.286*
Medications			
Steroid‡	7 (87.5)	2 (66.7)	0.491*
Duration of steroid use (month)§	12.0 (9.0-24.0)	12.0 (9.0-12.0)	0.592**
IVIG‡	4 (40.0)	2 (50.0)	**0.999***
Follow-up (year)§	3.0 (1.0-11.0)	3.2 (1.0-6.5)	0.669**
CMAS score at the last follow-up§	52.0 (50.0-52.0)	52.0 (52.0-52.0)	0.527**

†: mean standard deviation, ‡: n (%), §: median (min-max)
JDM: Juvenile dermatomyositis, ANA: Anti-nuclear antibody. CMAS: Childhood Myositis Assessment Scale, DMARD: Disease-modifying anti-rheumatic drugs, bDMARD: Biologic disease-modifying anti-rheumatic drugs, IVIG: Intravenous immunoglobulin, CMAS: Childhood Myositis Assessment Scale

autoantibodies. There were significant differences in the capillary density calculations and the length of the intercapillary distances between the groups (p<0.05). Capillary density was significantly higher in children with positive autoantibodies (p=0.021), contrary to the significantly lower values of intercapillary distance (p=0.023). The other findings were similar between the groups (p>0.05) (Table 5).

We found significantly higher values of the neoangiogenesis score and MES in the JDM group than in the controls (p<0.001 and p<0.001). The measurements of NFCD and MES were not significantly correlated with age, age at diagnosis, CMAS at diagnosis, disease duration, duration of steroid use, and length of follow-up (p>0.05) (Table 6).

DISCUSSION

This study demonstrated significant microvascular changes in the qualitative and semi-quantitative evaluation of nail-fold capillaroscopic findings in children with JDM compared with healthy children. Higher neoangiogenesis scores, MES values, and decreased NFCD were remarkable findings in JDM. Morphological capillary abnormalities were detected more frequently in children with JDM than in healthy controls. The NFCD and intercapillary distance

Table 4. Nail-fold capillaroscopy findings of the groups

	Group JDM (n=14)	Control (n=20)	p-value
Capillary density (capillary count/mm)§	8.0 (5.0-11.0)	10.0 (8.0-11.0)	**0.001****
Capillary length (µm)§	299.5 (221.0-628.0)	329.0 (232.0-470.0)	0.649**
Arterial width (µm)§	14.0 (10.0-71.0)	11.0 (9.0-15.0)	**0.001****
Venous width (µm)§	17.0 (13.0-82.0)	14.0 (10.0-17.0)	**0.001****
Apical loop width (µm)§	21.5 (14.0-79.0)	14.5 (12.0-33.0)	**0.003****
The intercapillary distance (µm)§	114.0 (92.0-251.0)	112.0 (98.0-225.0)	0.752**
Morphological changes			
Number of overall capillaries (per linear mm)§	0.812 (0.500-1.000)	0.0 (0.0-0.125)	**<0.001****
Capillary disorganization§	0.438 (0.250-0.625)	0.0 (0.0-0.250)	**<0.001****
Capillary tortuosity‡			
<%50	13 (92.9)	0 (0.0)	**<0.001***
None	1 (7.1)	20 (100.0)	
Number of tortuous capillaries (per linear mm)§	0.500 (0.0-0.750)	0.0 (0.0-0.0)	**<0.001****
Crossing capillaries‡			
>%50	1 (7.1)	0 (0.0)	**0.011***
<%50	10 (71.4)	6 (30.0)	
None	3 (21.4)	14 (70.0)	
Number of capillaries crossing (per linear mm)§	0.375 (0.0-0.750)	0.0 (0.0-0.0)	**<0.001****
Dilated (enlarged) capillaries‡	8 (57.1)	4 (20.0)	**0.036***
Number of enlarged capillaries (per linear mm)§	0.625 (0.0-0.750)	0.0 (0.0-0.0)	**<0.001****
Giant capillaries‡	3 (21.4)	0 (0.0)	0.061*
Number of giant capillaries (per linear mm)§	0.0 (0.0-0.625)	0.0 (0.0-0.0)	**0.005****
Avascular areas‡	3 (21.4)	0 (0.0)	0.061*
Microhemorrhage‡	5 (35.7)	0 (0.0)	**0.007***
Microhemorrhage area§	0.0 (0.0-0.375)	0.0 (0.0-0.0)	**0.004****
Pericapillary edema‡	2 (14.3)	0 (0.0)	0.162*
Neoangiogenesis‡	7 (50.0)	0 (0.0)	**0.001***
Neoangiogenesis score§	0.562 (0.250-0.750)	0.0 (0.0-0.125)	**<0.001****
MES§	1.875 (1.250-2.300)	0.0 (0.0-0.375)	**<0.001****

‡n (%), §median (min-max)
MES: Microangiopathy evolution score, JDM: Juvenile dermatomyositis

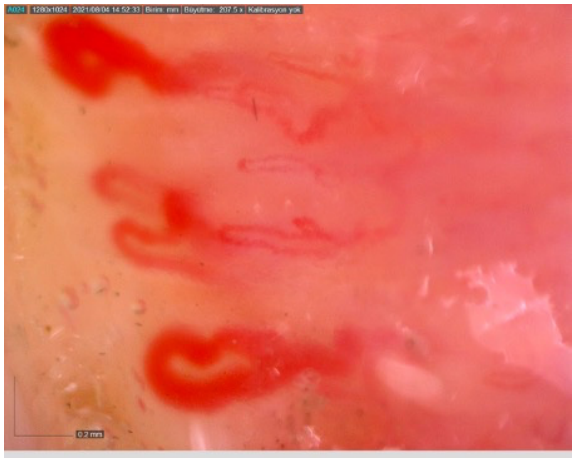

Figure 1. Examples of abnormal capillary shapes (morphology); Giant capillaries (homogeneous enlargement of all three limbs, normal shape, and apical diameter ≥50 µm)

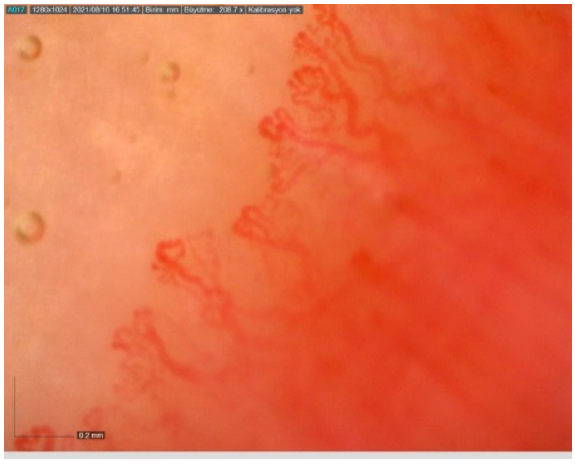

Figure 2. Examples of abnormal capillary shapes (morphology); Capillary "ramifications"

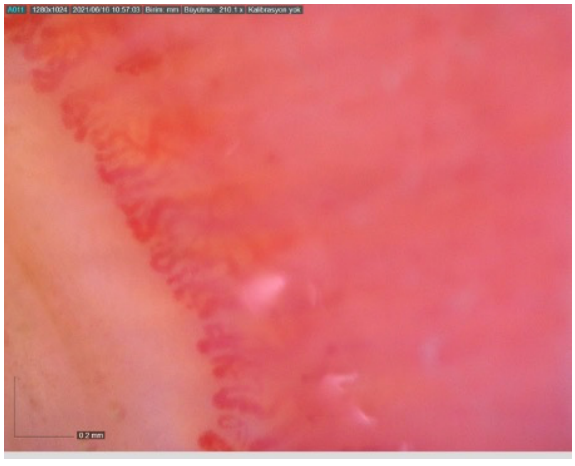

Figure 3. Examples of abnormal capillary shapes (morphology); "Meandering" capillaries

values differed significantly between children with and without myositis-specific autoantibodies. Although their clinical presentations were similar, higher NFCD values in children with positive autoantibodies might be explained by possible pathophysiological mechanisms.

Decrements in NFCD, increments in avascular areas of the relevant regions, minor (tortuous, crossed, and enlarged capillaries), and significant capillary morphological changes (mega, meandering, branching, bushy, bizarre, and disorganized polymorphic capillaries) were common findings observed in several chronic inflammatory and connective tissue diseases during childhood and adulthood, such as sclerosis, scleroderma, eczema, psoriasis, dermatomyositis, cutaneous lupus erythematosus, mixed connective tissue diseases, coronavirus (SARS-CoV-2) infection, and chronic hepatitis (2,11,17,19-25). We also detected these microangiopathic changes in children with JDM. Depending on the underlying diseases, various findings were recommended to diagnose or survey their evolution. Although authors are expected to specify each disease's most demonstrative pathological changes, they failed in these comparative studies (2,11,17,21). These microvascular abnormalities may be regarded as evidence of endothelial tissue damage due to microvascular involvement rather than pathognomonic signs. In addition to including several capillaroscopic parameters in this study, we detected significant differences in the capillaroscopic evaluations between the JDM and healthy control groups. Nevertheless, the lack of comparison between JDM and other pediatric rheumatological diseases led to the detection of specific capillaroscopic findings of JDM.

Schmeling et al. (1) investigated the association between NFCD and JDM. They showed that NFCD was a marker for skin and muscle disease activity and a reflection of activity changes depending on the clinical visits of children with JDM. NFCD was also proposed as a dynamic marker of global disease activity of adult dermatomyositis (5). Besides, the early occurrence of nail-fold abnormalities was considered a universal finding in JDM (1,26). This feature may be necessary for the diagnostic efficacy of NFCD in JDM. Barth et al. (18) showed that decreased NFCD and increased neovascularization were significantly associated with higher disease activity and impaired muscle function in adult patients with long-lasting JDM. The same research team reported that NFCD was a predictive marker of lung involvement in long-term JDM (14). It is believed that the grades or extensiveness of nail-fold microangiopathic changes in various rheumatological or connective tissue diseases reflect the severity of the underlying pathologies (22). These changes might be helpful during the onset of

Table 5. Nailfold capillaroscopy findings of children with and without myositis-specific autoantibodies

	Children		
	With positive autoantibodies (n=10)	**Negative autoantibodies (n=4)**	**p-value**
Capillary density (capillary count/mm)§	8.5 (5.0-11.0)	7.0 (6.0-7.0)	**0.021****
Capillary length (µm)§	299.5 (221.0-628.0)	327.5 (232.0-470.0)	0.999**
Arterial width (µm)§	13.0 (10.0-71.0)	26.0 (22.0-30.0)	0.089**
Venous width (µm)§	16.0 (13.0-82.0)	31.5 (28.0-38.0)	0.088**
Apical loop width (µm)§	16.5 (14.0-79.0)	30.0 (26.0-37.0)	0.088**
The intercapillary distance (µm)§	111.0 (92.0-251.0)	154.5 (135.0-188.0)	**0.023****
Morphological changes			
Number of overall capillaries (per linear mm)§	0.9 (0.5-1.0)	0.8 (0.8-1.0)	0.884**
Capillary disorganization§	0.4 (0.2-0.6)	0.5 (0.4-0.6)	0.462**
Capillary tortuosity‡			
<%50	9 (90.0)	4 (100.0)	0.999*
None	1 (10.0)	0 (0.0)	
Number of tortuous capillaries (per linear mm)§	0.5 (0.0-0.8)	0.6 (0.5-0.6)	0.271**
Crossing capillaries‡			
>%50	1 (10.0)	0 (0.0)	0.999*
<%50	7 (70.0)	3 (75.0)	
None	2 (20.0)	1 (25.0)	
Number of capillaries crossing (per linear mm)§	0.4 (0.0-0.6)	0.4 (0.4-0.8)	0.183**
Dilated (enlarged) capillaries‡	5 (50.0)	3 (75.0)	0.580*
Number of enlarged capillaries (per linear mm)§	0.6 (0.0-0.8)	0.6 (0.5-0.8)	0.770**
Giant capillaries‡	1 (10.0)	2 (50.0)	0.176*
Number of giant capillaries (per linear mm)§	0.0 (0.0-0.6)	0.1 (0.0-0.2)	0.620**
Avascular areas‡	1 (10.0)	2 (50.0)	0.176*
Microhemorrhage‡	3 (30.0)	2 (50.0)	0.580*
Microhemorrhage area§	0.0 (0.0-0.2)	0.1 (0.0-0.4)	0.320**
Pericapillary edema‡	1 (10.0)	1 (25.0)	0.505*
Neoangiogenesis‡	3 (30.0)	4 (100.0)	0.070*
Neoangiogenesis score§	0.5 (0.2-0.8)	0.8 (0.5-0.8)	0.103**
MES§	1.9 (1.2-2.3)	2.1 (1.6-2.1)	0.277**

‡n (%), §median (minimum-maximum)
MES: Microangiopathy evolution score

Table 6. Correlation analysis of NFCD and MES with numerical demographic and clinical parameters

		Capillary density	MES
Age	r	0.182	0.074
	p	0.532	0.803
Age at diagnosis	r	0.175	0.053
	p	0.550	0.857
CMAS upon diagnosis	r	-0.175	0.217
	p	0.550	0.457
Disease duration	r	-0.056	-0.149
	p	0.848	0.612
Duration of steroid use	r	0.216	-0.361
	p	0.458	0.205
Follow-up	r	-0.077	-0.140
	p	0.794	0.634

Spearman's rho correlation coefficient was used
NFCD: Nail-fold capillary density, MES: Microangiopathy evolution score, CMAS: Childhood Myositis Assessment Scale

the disease or during clinical follow-up examinations. In addition, several scores based on capillaroscopic changes in the nail-folds were considered sensitive tools for quantifying and monitoring microvascular damage (18).

Pizzorni et al. (22) reported a positive association between MES and skin telangiectasia in systemic sclerosis. They also thought that vascular damage might be a predictive factor for future organ involvement. Avcı et al. (23) found no relationship between capillaroscopic changes and nail involvement in psoriasis and eczema. The present study found significantly higher MES values in children with JDM than in healthy children. Nevertheless, no follow-up data showed changes in the nail-fold capillaroscopic changes according to treatment duration or duration in this study. In addition, there were no significant correlations between

NFCD and MES and other clinical parameters. Previous studies have shown a relationship between NFCD, age, and disease duration (14,27). We did not find any correlation between these parameters. Our study group included only children with a mean age of 10.4±4.0 years, contrary to Sanner's study in which older patients (24.9±12.7 years) were investigated (27). Heterogeneous demographic and clinical characteristics may be factors for such conflicting findings.

NFCD is one of the most common capillaroscopic findings in several connective tissue disorders. Many researchers have reported significant decreases, as in this study (1,5,14,18,23 24). Although the extent of the avascular area was significantly different between patients with psoriasis and eczema and healthy controls, the relatively low number of children with the avascular area might be the reason for not reaching statistical differences in the present study (23). Therefore, large-scale studies are needed to describe the pathognomonic microangiopathic findings of JDM.

This study found significant differences in the NFC findings between children with and without myositis-specific autoantibodies. Children with positive autoantibodies had higher NFCD and lower intercapillary distance values. Previous studies have investigated the possible association between NFCD measurements and the positivity of several myositis-specific autoantibodies. Sugimoto et al. (13) found that the scores during nail-fold video capillaroscopy were inversely correlated with anti-melanoma differentiation-associated gene 5 antibody titers in patients with dermatomyositis. Liu et al. (28) reported higher arteriolar densities in patients with dermatomyositis and positive anti-nuclear matrix protein-2 antibodies. They also showed thickened vascular walls, thrombosis, and lipid accumulation in these patients. Positive myositis-specific autoantibodies are associated with a higher degree of perivascular inflammation in children with juvenile overlap myositis (29). Another study evaluated the impact of anti-Jo-1 antibodies on the pathology of the perimysium and neighboring muscle fibers in patients with myopathy (30). They found that capillary density was normal, contrary to reduced capillary density in dermatomyositis. The case series design of the paper should be considered when evaluating the findings. Thus, the impact of positive myositis-specific autoantibodies on capillaroscopic changes in patients with JDM remains unclear. Future studies are needed to clarify these controversial issues.

Study Limitations

The relatively small number was the study's main limitation. The small number of children with positive myositis-specific autoantibodies prevented a more dynamic analysis. In addition, the variances between the duration of the disease and the time of NFC might be a limiting factor in obtaining more accurate findings. Prospective studies that control the disease characteristics, including duration, severity, and different phenotypic involvements, might be helpful in obtaining more powerful results.

CONCLUSION

In conclusion, children with JDM exhibited remarkable nail-fold capillaroscopic changes that might be useful in diagnosing and differentiating connective tissue disorders in children.

ETHICS

Ethics Committee Approval: This study was approved by the Erciyes University Clinical Research Ethics Committee (decision no: 2021/355, date: 05.05.2021).

Informed Consent: Written informed consent was obtained from the parents of the children.

FOOTNOTES

Authorship Contributions

Surgical and Medical Practices: Ş.D., S.N.T., Concept: Ş.D., Design: Ş.D., Data Collection or Processing: Ş.D., S.N.T., Analysis or Interpretation: Ş.D., Literature Search: Ş.D., Writing: Ş.D., S.N.T., A.P.K., M.H.P.

Conflict of Interest: No conflict of interest was declared by the authors.

Financial Disclosure: The authors declare that this study received no financial support.

REFERENCES

1. Schmeling H, Stephens S, Goia C, Manlhiot C, Schneider R, Luthra S, et al. Nailfold capillary density is importantly associated over time with muscle and skin disease activity in juvenile dermatomyositis. Rheumatology (Oxford). 2011;50:885-93.
2. Shenavandeh S, Rashidi F. Nailfold capillaroscopy changes with disease activity in patients with inflammatory myositis including overlap myositis, pure dermatomyositis, and pure polymyositis. Reumatologia. 2022;60:42-52.
3. Lundberg IE, Tjärnlund A, Bottai M, Werth VP, Pilkington C, de Visser M, et al. 2017 European League Against Rheumatism/American College of Rheumatology classification Criteria for adult and juvenile idiopathic inflammatory myopathies and their major subgroups. Arthritis Rheumatol. 2017;69:2271-82.
4. Pozharashka J, Miteva L, Dourmishev L. Cutaneous manifestations and their corresponding dermoscopic features in patients with dermatomyositis. Dermatol Pract Concept. 2022;12:e2022142.
5. Johnson D, van Eeden C, Moazab N, Redmond D, Phan C, Keeling S, et al. Nailfold capillaroscopy abnormalities correlate with disease activity in adult dermatomyositis. Front Med (Lausanne). 2021;8:708432.

6. Melsens K, Cutolo M, Schonenberg-Meinema D, Foeldvari I, Leone MC, Mostmans Y, et al. Standardized nailfold capillaroscopy in children with rheumatic diseases: a worldwide study. Rheumatology (Oxford). 2023;62:1605-15.
7. Roberts-Thomson PJ, Patterson KA, Walker JG. Clinical utility of nailfold capillaroscopy. Intern Med J. 2023;53:671-9.
8. Errichetti E, Zalaudek I, Kittler H, Apalla Z, Argenziano G, Bakos R, et al. Standardization of dermoscopic terminology and basic dermoscopic parameters to evaluate in general dermatology (non-neoplastic dermatoses): an expert consensus on behalf of the International Dermoscopy Society. Br J Dermatol. 2020;182:454-67.
9. Kayser C, Bredemeier M, Caleiro MT, Capobianco K, Fernandes TM, de Araújo Fontenele SM, et al. Position article and guidelines 2018 recommendations of the Brazilian Society of Rheumatology for the indication, interpretation and performance of nailfold capillaroscopy. Adv Rheumatol. 2019;59:5.
10. Shenavandeh S, TorabiJahromi M, Mohammadzadeh S. Glomerulopathy in patients with dermatomyositis in early active disease: clinical, pathological and capillaroscopic manifestations, and response to treatment. Reumatologia. 2022;60:200-8.
11. Monfort JB, Chasset F, Barbaud A, Frances C, Senet P. Nailfold capillaroscopy findings in cutaneous lupus erythematosus patients with or without digital lesions and comparison with dermatomyositis patients: A prospective study. Lupus. 2021;30:1207-13.
12. Piette Y, Reynaert V, Vanhaecke A, Bonroy C, Gutermuth J, Sulli A, et al. Standardised interpretation of capillaroscopy in autoimmune idiopathic inflammatory myopathies: a structured review on behalf of the EULAR study group on microcirculation in Rheumatic Diseases. Autoimmun Rev. 2022;21:103087.
13. Sugimoto T, Mokuda S, Kohno H, Ishitoku M, Araki K, Watanabe H, et al. Nailfold capillaries and myositis-specific antibodies in anti-melanoma differentiation-associated gene 5 antibody-positive dermatomyositis. Rheumatology (Oxford). 2022;61:2006-15.
14. Barth Z, Schwartz T, Flatø B, Aaløkken TM, Koller A, Lund MB, et al. Association between nailfold capillary density and pulmonary and cardiac involvement in medium to longstanding juvenile dermatomyositis. Arthritis Care Res (Hoboken). 2019;71:492-7.
15. Quiñones R, Morgan GA, Amoruso M, Field R, Huang CC, Pachman LM. Lack of achievement of a full score on the childhood myositis assessment scale by healthy four-year-olds and those recovering from juvenile dermatomyositis. Arthritis Care Res (Hoboken). 2013;65:1697-701.
16. Gowdie PJ, Allen RC, Kornberg AJ, Akikusa JD. Clinical features and disease course of patients with juvenile dermatomyositis. Int J Rheum Dis. 2013;16:561-7.
17. Soubrier C, Seguier J, Di Costanzo MP, Ebbo M, Bernit E, Jean E, et al. Nailfold videocapillaroscopy alterations in dermatomyositis, antisynthetase syndrome, overlap myositis, and immune-mediated necrotizing myopathy. Clin Rheumatol. 2019;38:3451-8.
18. Barth Z, Witczak BN, Flatø B, Koller A, Sjaastad I, Sanner H. Assessment of microvascular abnormalities by nailfold capillaroscopy in juvenile dermatomyositis after medium- to long-term followup. Arthritis Care Res (Hoboken). 2018;70:768-76.
19. Çakmak F, Demirbuga A, Demirkol D, Gümüş S, Torun SH, Kayaalp GK, et al. Nailfold capillaroscopy: A sensitive method for evaluating microvascular involvement in children with SARS-CoV-2 infection. Microvasc Res. 2021;138:104196.
20. Wakura R, Matsuda S, Kotani T, Shoda T, Takeuchi T. The comparison of nailfold videocapillaroscopy findings between anti-melanoma differentiation-associated gene 5 antibody and anti-aminoacyl tRNA synthetase antibody in patients with dermatomyositis complicated by interstitial lung disease. Sci Rep. 2020;10:15692.
21. Sulli A, Secchi ME, Pizzorni C, Cutolo M. Scoring the nailfold microvascular changes during the capillaroscopic analysis in systemic sclerosis patients. Ann Rheum Dis. 2008;67:885-7.
22. Pizzorni C, Giampetruzzi AR, Mondino C, Facchiano A, Abeni D, Paolino S, et al. Nailfold capillaroscopic parameters and skin telangiectasia patterns in patients with systemic sclerosis. Microvasc Res. 2017;111:20-4.
23. Avcı EB, Erdemir VA, Erdem O, Işık R, Aksu AEK. Evaluation of serum vascular endothelial growth factor level and findings of nailfold capillaroscopy by dermatoscope in the differential diagnosis of palmoplantar psoriasis and palmoplantar eczema. Microvasc Res. 2023;145:104441.
24. Pancar GS, Kaynar T. Nailfold capillaroscopic changes in patients with chronic viral hepatitis. Microvasc Res. 2020;129:103970.
25. Mugii N, Hamaguchi Y, Horii M, Fushida N, Ikeda T, Oishi K, et al. Longitudinal changes in nailfold videocapillaroscopy findings differ by myositis-specific autoantibody in idiopathic inflammatory myopathy. Rheumatology (Oxford). 2023;62:1326-34.
26. Scheja A, Elborgh R, Wildt M. Decreased capillary density in juvenile dermatomyositis and in mixed connective tissue disease. J Rheumatol. 1999;26:1377-81.
27. Sanner H, Gran JT, Sjaastad I, Flatø B. Cumulative organ damage and prognostic factors in juvenile dermatomyositis: a cross-sectional study median 16.8 years after symptom onset. Rheumatology (Oxford). 2009;48:1541-7.
28. Liu Y, Zheng Y, Gang Q, Xie Z, Jin Y, Zhang X, et al. Perimysial microarteriopathy in dermatomyositis with anti-nuclear matrix protein-2 antibodies. Eur J Neurol. 2020;27:514-21.
29. Challa S, Hui M, Jakati S, Uppin MS, Rajasekhar L, Kannan MA, et al. Juvenile idiopathic inflammatory myopathies: a clinicopathological study with emphasis on muscle histology. Indian J Pathol Microbiol. 2019;62:61-6.
30. Mozaffar T, Pestronk A. Myopathy with anti-Jo-1 antibodies: pathology in perimysium and neighbouring muscle fibres. J Neurol Neurosurg Psychiatry. 2000;68:472-8.

Medical Journal of Bakırköy

Med J Bakirkoy 2025;21:48-54
DOI: 10.4274/BMJ.galenos.2025.2025.1-7

Research

Can Systemic Inflammation Response Index (SIRI) and Neutrophil-to-lymphocyte Ratio (NLR) Predict the Presence of Placenta Accreta Spectrum in Pregnant Women with Placenta Previa?

Sistemik Enflamasyon Yanıt İndeksi (SIRI) ve Nötrofil-lenfosit Oranı (NLR), Plasenta Previalı Gebe Kadınlarda Plasenta Akreta Spektrumunun Varlığını Öngörebilir mi?

Nihal Çallıoğlu[1,2], Emre Kar[3], İlke Özer Arslan[4], Selvi Aydın Şenel[1], İbrahim Polat[1], Işıl Turan Bakırcı[1], Tuğçe Tunç Arslanoğlu[1]

[1]University of Health Sciences Türkiye, Başakşehir Çam and Sakura City Hospital, Department of Perinatology, İstanbul, Türkiye

[2]University of Health Sciences Türkiye, Gaziosmanpaşa Training and Research Hospital, Department of Obstetrics and Gynecology, Division of Perinatology, İstanbul, Türkiye

[3]University of Health Sciences Türkiye, Başakşehir Çam and Sakura City Hospital, Department of Obstetrics and Gynecology, İstanbul, Türkiye

[4]Tekirdağ Namık Kemal University Faculty of Medicine, Department of Obstetrics and Gynecology, Tekirdağ, Türkiye

ABSTRACT

Objective: Can systemic inflammation response index (SIRI) and neutrophil-to-lymphocyte ratio (NLR) predict the presence of placenta accreta spectrum (PAS) in pregnant women with placenta previa (PP)?

Methods: This retrospective case-control study included 415 singleton pregnancies diagnosed with PP, of which 119 were in the study group with PAS, and 296 were with no evidence of placental invasion. Demographic characteristics, laboratory parameters, and SIRI values of the groups were compared. Cut-off values that could predict PAS were calculated.

Results: The mean gravidity, parity, abortion, and number of previous cesarean sections were higher in the PAS group compared to the control. Gestational age was lower in the PAS group. There was no significant difference between the groups regarding body mass index and maternal age. Mean lymphocyte and platelet counts were lower in the PAS group, while red cell distribution width (RDW) was higher than the control group. The cut-off value for RDW was 3.63 (66% sensitivity, 48% specificity) in the receiver operating characteristic (ROC) curve. The optimal sensitivity/specificity balance for NLR was 4.49, with 46% sensitivity and 69% specificity in the ROC curve.

Conclusion: RDW and NLR are useful auxiliary indicators for predicting PAS. The increases in SIRI values in the PAS group were not statistically significant. The relationship between inflammatory parameters and the histological subtypes of PAS should be investigated in larger case groups.

Keywords: Inflammatory biomarkers, placenta accreta spectrum, placenta previa, systemic inflammatory response index

ÖZ

Amaç: Sistemik enflamasyon yanıt indeksi (SIRI) ve nötrofil-lenfosit oranı (NLR) plasenta previalı (PP) hamile kadınlarda plasenta akreta spektrumunun (PAS) varlığını tahmin edebilir mi?

Gereç ve Yöntem: Bu retrospektif olgu-kontrol çalışmasına PP tanısı konulan 415 tekil gebelik dahil edildi, 119'u PAS çalışma grubundaydı ve 296'sında plasenta istilası kanıtı yoktu. Demografik verileri, laboratuvar sonuçları ve SIRI değerleri gruplar arasında karşılaştırıldı. PAS'yi öngören alıcı çalışma karakteristiği (ROC) eğrisi kesme değerleri hesaplandı.

Address for Correspondence: Nihal Çallıoğlu MD, University of Health Sciences Türkiye, Başakşehir Çam and Sakura City Hospital; Gaziosmanpaşa Training and Research Hospital, Department of Obstetrics and Gynecology, Division of Perinatology, İstanbul, Türkiye

E-mail: niyalcll@gmail.com **ORCID ID:** orcid.org/0000-0002-4324-692X

Cite as: Çallıoğlu N, Kar E, Özer Arslan İ, Aydın Şenel S, Polat İ, Turan Bakırcı I, et al. Can systemic inflammation response index (SIRI) and neutrophil-to-lymphocyte ratio (NLR) predict the presence of placenta accreta spectrum in pregnant women with placenta previa?. Med J Bakirkoy. 2025;21:48-54

Received: 15.01.2025
Accepted: 11.02.2025
Publication Date: 25.03.2025

ÖZ

Bulgular: Ortalama gravida, parite, düşük ve önceki sezaryen sayısı PAS grubunda kontrol grubuna göre daha yüksekti. PAS grubunda gebelik yaşı daha düşüktü. Gruplar arasında vücut kitle indeksi ve anne yaşı açısından önemli bir fark yoktu. PAS grubunda kontrol grubuna göre ortalama lenfosit ve trombosit sayıları daha düşük, kırmızı hücre dağılım genişliği (RDW) ise daha yüksekti. ROC eğrisinde RDW için kesme değeri 3,63 idi (%66 duyarlılık, %48 özgüllük). NLR için optimal duyarlılık/özgüllük dengesi 4,49 idi (%46 duyarlılık, %69 özgüllük).

Sonuç: RDW ve NLR, PAS'yi tahmin etmede faydalı yardımcı göstergelerdir. SIRI değerlerindeki artışlar PAS grubu için istatistiksel olarak anlamlı değildi. Enflamatuvar parametreler ve PAS'nin histolojik alt tipleri arasındaki ilişki daha büyük olgu gruplarında araştırılmalıdır.

Anahtar Kelimeler: Enflamatuvar biyobelirteçler, plasenta acreta spektrumu, plasenta previa, sistemik immün enflamatuvar indeks, sistemik enflamatuvar yanıt indeksi

INTRODUCTION

Placental invasion anomalies indicate abnormal trophoblast invasion into the myometrium, sometimes extending to the serosa or beyond, without decidua. The level of placenta intrusion might include placenta accreta, placenta increta, or placenta percreta (1,2). These histological subtypes often coexist and are generally called the placenta accreta spectrum (PAS).

Placenta previa (PP) is identified as one of the most important risk factors of PAS, defined by an internal cervical os with a placental edge distance of less than 20 mm. Another significant risk of PAS is prior cesarean section. In a prospective study evaluating the frequency of PAS in women with PP who underwent cesarean delivery, an increase in the number of cesarean deliveries corresponded to a higher frequency of PAS. While the coexistence of PAS was 3% after one cesarean delivery in a patient with PP, it rose to 67% after five or more cesarean deliveries (3). Other risk factors include maternal age, multiple pregnancies, multiparity, a history of prior uterine surgeries, pelvic radiation history, manual removal of the placenta, postpartum endometritis, infertility, and fertility treatments (4,5).

PAS is a significant cause of maternal morbidity because the placenta does not spontaneously separate during childbirth. Attempts to manually remove it can result in life-threatening bleeding, often necessitating a hysterectomy. Perinatal outcomes significantly improve when PAS is diagnosed before delivery. However, a large proportion of PAS cases cannot be diagnosed until childbirth (6). The first step is identifying risk factors in the mother. While PAS is often asymptomatic in the antenatal period, it is diagnosed through findings on obstetric ultrasound (USG) screenings. For women without clear risk factors for placental invasion anomalies, incidental findings can occur during routine USG examinations. Still, in most cases, the diagnosis is not made until after the placenta is delivered. Postpartum haemorrhage is a common indication for peripartum hysterectomy in PAS. Transfusion is the most frequently encountered complication, followed by other surgical complications, most commonly bladder injuries.

USG is the preferred choice for diagnosing PAS when performed by experienced professionals (7). Magnetic resonance imaging could be utilised if USG poses challenges, such as maternal obesity, a posteriorly located placenta, or laterally extending placental invasion. However, the success of imaging methods may vary depending on the experience of the specialist evaluating the method and the clinical characteristics of the patient. Considering the increasing prevalence of PAS and its adverse fetal and maternal outcomes, diagnostic tools that do not require clinical experience and are easy to apply have become the focus of attention. Inflammatory markers are widely utilised to predict overall morbidity and mortality in various cancer types. Numerous studies have suggested that the invasion of trophoblasts also shares many common features with the invasion of cancer cells (8). Based on this, markers such as mean platelet volume (MPV), platelet distribution width (PDW), red cell distribution width (RDW), neutrophil-to-lymphocyte ratio (NLR) and platelet-lymphocyte ratios (PLR) have been extensively investigated in diagnosing the presence of PAS (9-11).

Systemic immune-inflammation index (SII) and systemic immune response index (SIRI), are new indices that offer insights into the prognosis of certain cancer types, response to treatment, and risk assessment for cardiovascular diseases (12-14). Within the scope of this research, we aimed to elucidate the predictive value of SIRI and other inflammatory indices in PAS and diagnose its subtypes in PP.

METHODS

This case-control study included 415 singleton pregnancies diagnosed with PP, of which 119 were in the study group with PAS, and 296 were without evidence of placental invasion. Ethics committee approval has been granted by University of Health Sciences Türkiye, Başakşehir Çam and Sakura City Hospital, on 11/10/2023 with protocol number 2023-466.

Since the study was retrospective, informed consent was not obtained from the participants.

The location of placental implantation and the depth of myometrial invasion were determined by perinatology department physicians using transabdominal and transvaginal 2D grayscale and Doppler ultrasonography (Arietta 850, Hitachi, Tokyo, Japan) at the time of admission. The diagnosis of PAS was confirmed by macroscopic evaluation at the time of cesarean section and by histopathological evaluation postoperatively. The PAS group comprised pregnant women who underwent partial uterine resection or cesarean hysterectomy due to the detection of PAS during surgery; the diagnosis was histologically confirmed. The PP group included pregnant women confirmed to have PP during surgery but with no detected placental invasion.

Pregnant women with chronic systemic disorders such as hypertension and diabetes mellitus, those with ongoing infections, and smokers were excluded from the study. Additionally, for individuals with multiple pregnancies, complications such as preeclampsia, preterm premature rupture of the membranes (PPROM), intrauterine growth restriction, gestational diabetes mellitus, intrauterine fetal death, and pregnancy cholestasis were also excluded.

Patient data were sourced from our hospital management information system. Data reliability and validity were ensured by having one author enter the data, which another author then validated. Complete blood count components obtained from patients before medical or surgical intervention were used for analysis. Haematological analyses were performed in the same laboratory. NLR, PLR, monocyte-lymphocyte ratio (MLR), SII, and SIRI were calculated using neutrophil, platelet, monocyte, and lymphocyte values.

SIRI was calculated as the monocyte × neutrophil/lymphocyte; SII was calculated as the platelet × neutrophil/lymphocyte. Variables such as age, gravidity, parity, miscarriage history, previous cesarean count, gestational age at birth and body mass index at the time of delivery, along with the histological subtype of PAS, were evaluated in the patients. The predictive success of all variables in estimating PAS in pregnant women was calculated, and the cut-off values of significant variables were determined. The relationship between inflammatory indices of PAS histological subtypes was also investigated. Tubes containing K3EDTA were used for CBC analysis. CBC parameters were measured using an automated haematology analyser (XT2000i, Sysmex, Osaka, Japan).

Statistical Analysis

All statistical analyses were conducted using R software. Normality was assessed with the Shapiro-Wilk test. Continuous variables are expressed as means and standard deviations. The Mann-Whitney U test was employed to compare two groups for variables not normally distributed. For dependent variables with more than two categories, the Kruskal-Wallis test was used. Categorical data are presented as counts and percentages and analysed using chi-square and Fisher's exact tests as appropriate. The predictive ability of inflammatory parameters for PAS was assessed using receiver operating characteristic (ROC) curve analysis. A p-value of less than 0.05 was considered statistically significant.

RESULTS

In the study, 119 (26.7%) patients were in the PAS group, and 296 (73.3%) patients were in the PP group. The mean age of the patients in the PAS group was higher than the PP group, although the difference was not statistically significant (p=0.059). The patients' mean gravidity, parity, abortus, and number of previous c-sections were significantly higher in the PAS group than in the PP group (p-value <0.001 for all the variables). A significant difference was observed between the PAS and PP groups regarding gestational age (p<0.001). Additionally, the mean lymphocyte and platelet counts were significantly lower in the PAS group compared to the PP group (p=0.044 and p=0.018, respectively). Furthermore, the RDW and NLR were significantly higher in the PAS group than in the PP group (p=0.009 and p=0.011, respectively). The groups had no significant differences in MPV, PDW, PLR, MLR, SII, and SIRI. The demographic characteristics of the study population, haematological parameters, SII, SIRI, and other inflammatory indices are presented in Table 1.

The performance of inflammatory parameters in predicting PAS was analysed using the ROC curve. The Youden index was utilised to find the cut-off points for PAS diagnosis. The ROC curve cut-off value for RDW that yielded the best sensitivity/specificity balance was determined to be 3.63 (66% sensitivity, 48% specificity). The optimal sensitivity/specificity balance for NLR was achieved at a cut-off value of 4.49, resulting in 46% sensitivity and 69% specificity. The corresponding area under the curves and 95% confidence ıntervals can be found in Table 2 and Figure 1.

We compared the subtypes of PAS (accreta, increta, and percreta) based on the inflammatory parameters outlined in Table 3. Although there was a lower mean for both SII and SIRI in the increta subtype, no significant differences were observed across the various PAS subtypes.

Table 1. Comparison of demographic features. Laboratory test results and inflammatory parameters between healthy pregnant women and pregnant women with PAS

Parameters	PP (n=296)	PAS (n=119)	p-value
	Mean ± SD	Mean ± SD	
Maternal age (tear)	31.6±5.4	32.7±0.5	0.059[t]
Gravidity (n)	3.1±0.1	4.5±0.2	**<0.001**[*m]
Parity (n)	1.6±0.1	2.6±0.1	**<0.001**[*m]
Abortus (n)	0.5±0.1	0.9±0.1	**<0.001**[*m]
Number of previous cesarean section (n)	0.8±0.1	2.2±0.1	**<0.001**[*m]
Gestational ages at birth (week)	35.7±0.2	34.3±0.2	**<0.001**[*m]
BMI	28.0±5.1	28.5±5.2	0.444[m]
Neutrophil count (µL)	8.3±6.0	8.4±3.4	0.092[m]
Lymphocyte count (µL)	2.2±0.1	1.9±0.1	**0.044**[*m]
Monocyte count (µL)	0.7±0.02	0.7±0.03	0.359[m]
Platelet count (10^3/µL)	237.6±4.1	220.7±6.1	**0.018**[*m]
Mean platelet volume (fL)	10.9±0.1	10.7±0.1	0.087[m]
Platelet distribution width	13.2±0.2	12.9±0.2	0.231[m]
Red cell distribution width	14.9±0.2	15.3±0.2	**0.009**[*m]
Neutrophil-to-lymphocyte ratio	4.3±2.6	5.3±4.0	**0.011**[*m]
Monocyte-to-lymphocyte ratio	0.4±0.2	0.4±0.3	0.247[m]
Platelet-to-lymphocyte ratio	127.7±58.9	131.3±59.3	0.570[m]
Systemic immune-inflammation index (10^9/L)	1033.2±42.6	1149.7±86.5	0.281[m]
System inflammation response index	3.0±2.2	3.7±3.3	0.087[m]

PP: Placenta previa, PAS: Placenta accreta spectrum, BMI: Body mass index, [t]: Independent t-test, [m]: Mann-Whitney U test, SD: Standard deviation, [*]: A significant p-value is <0.05

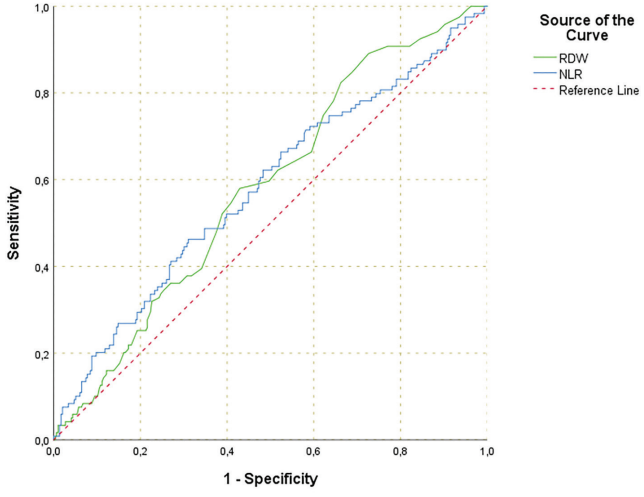

Figure 1. Receiver operating characteristic curve for the placental invasion anomalies in pregnant women with placenta previa

NLR: neutrophil-to-lymphocyte ratio, RDW: Red cell distribution width

DISCUSSION

In the presence of PP, high sensitivity is required for PAS because when PAS is diagnosed prenatally, maternal and perinatal outcomes significantly improve. Imaging techniques can help predict the extent of placental invasion (15). However, the diagnosis is not established in most PAS cases until delivery. The need for an accurate, easily detectable, and cost-effective diagnosis of PAS has led to the investigation of alternative diagnostic biomarkers. For this purpose, the effectiveness of serum biomarkers used in the screening for growth factors, cell-free DNA, fetal aneuploidy, and cardiac function disorders was investigated (16,17).

In this study, pregnant women with PP and PAS, were retrospectively examined regarding routinely measured hemogram parameters, and newly identified inflammatory markers. We found that some serum inflammatory markers

Table 2. ROC curve analysis to assess the performance of inflammatory parameters in predicting placenta accreata spectrum

Parameters	Cut-off value	Sensitivity (%)	Specificity (%)	AUC	p-value	95% confidence interval
RDW	3.6	66	48	0.582	**0.006***	0.523-0.640
NLR	4.5	46	69	0.580	**0.011***	0.518-0.642
SIRI				0.554	0.087	0.492-0.615
MLR				0.536	0.247	0.472-0.601
SII				0.534	0.283	0.472-0.596
PLR				0.518	0.565	0.457-0.579
PDW				0.462	0.234	0.401-0.524
MPV				0.446	0.087	0.384-0.508

RDW: Red cell distribution width, NLR: Neutrophile to lymphocyte ratio, SIRI: Systematic inflammation response index (calculated as monocyte*neutrophile/lymphocyte), MLR: Monocyte to lymphocyte ratio, SII: Systemic immune-inflammation index, PLR: Platelet count to lymphocyte ratio, PDW; Platelet distribution width, MPV: Mean platelet volume, ROC: Receiver operating characteristic, AUC: Area under the curve. *: A significant p-value is <0.05

Table 3. Inflammatory parameters according to histological subtypes of PAS

Parameters	Accreta (n=29)	Increta (n=22)	Percreta (n=35)	p-value
	Mean ± SD	Mean ± SD	Mean ± SD	
SII	1171.2±881.4	978.2±561.7	1401.3±1355.4	0.203[k]
NLR	5.0±3.7	4.8±2.8	6.3±5.5	0.345[k]
PLR	128.3±50.1	123.6±42.9	145.9±83.1	0.396[k]
MPV	12.6±0.9	10.8±1.6	10.5±1.0	0.391[k]
PDW	17.6±2.2	13.4±2.8	12.2±2.5	0.077[k]
SIRI	4.2±24.9	3.3±2.0	4.1±3.3	0.100[k]
MLR	0.4±0.3	0.4±0.2	0.4±0.3	0.123[k]
RDW	19.9±1.9	15.1±2.4	16.1±3.2	0.141[k]

SII: Systemic immune-inflammation index, NLR: Neutrophile to lymphocyte ratio, PLR: Platelet count to lymphocyte ratio, MPV: Mean platelet volume, PDW: Platelet distribution width, SIRI: System inflammation response index, MLR: Monocyte to lymphocyte rate, RDW: Red cell distribution width, SD: Standard deviation, [k]: Kruskal-Wallis test, *: A significant p-value is <0.05

could predict PAS in women with PP. Our study determined that RDW could predict PAS in PP, while no significant relationship was found between SII and SIRI. Additionally, no significant relationship was found between the histological subtypes of PAS and inflammatory markers.

The previous literature shows conflicting results regarding the relationship between PP and PAS, and inflammatory markers obtained from complete blood count. Ersoy et al. (10) found that the MPV and platelet large cell ratio values were reduced in patients diagnosed with placenta percreta in the third trimester compared to PP patients. In another study, it was reported that the NLR and PLR values in PP cases were significantly higher than in non-PP pregnant women (11). Abide Yayla et al. (9) demonstrated that NLR and MPV increased in PAS patients compared to those without placental invasion, while RDW decreased Karakoç et al. (18) stated that no significant difference was found in NLR and PLR values, but the delta neutrophil index was significantly higher in PP and PAS cases. According to Keles et al. (19), there was no difference in RDW between PAS and PP cases; however, PDW was lower, and MPV, NLR, and PLR were higher in PAS cases compared to PP cases. In our study, RDW and NLR were significantly higher in PAS than in PP cases. This result is consistent with a study suggesting that elevated RDW values indicate increased inflammation and oxidative stress (20).

Peripheral blood cells include pro-inflammatory cells, such as neutrophils, platelets, and monocytes; and anti-tumour immune cells, such as lymphocytes, that can indirectly reflect the tumour microenvironment (21). Keles et al. (19) found that the platelet and neutrophil counts were high, while the lymphocyte count was low in PAS cases compared to PP cases. Ersoy et al. (10) demonstrated a significant increase in the neutrophil count in PP patients compared to healthy controls. In our study, although there was no significant difference in the monocyte count between PAS and PP cases, compared to PP cases, the neutrophil count was higher, and the lymphocyte and platelet counts were lower in PAS cases.

SIRI is a new prognostic marker reflecting the inflammatory response. Elevated SIRI has been associated with poor prognosis in various cancers and inflammatory diseases (22,23). Wang et al. (24) associated high SIRI levels with reduced survival time, accelerated tumour progression, and increased rates of recurrence or metastasis in cancer patients. A higher SIRI level correlates with a stronger systemic immune-inflammatory response (25). In the obstetric field, SIRI has been utilised in several studies. In a recent study, SIRI was reported to have the highest diagnostic power among inflammatory parameters in determining the diagnosis of early pregnancy loss (26). Fang et al. (27), in their study comparing cervical cerclage with non-invasive procedures, found that initial SII and SIRI values were important biochemical markers in predicting maternal and neonatal outcomes. The relationship between SIRI levels and PAS has not been published yet. In our study, although we found higher SIRI values in PAS cases compared to PP cases, we could not establish a significant relationship between them.

SII is an objective marker reflecting systemic inflammation. Recently, SII has been associated with the diagnosis, prognosis, and response to treatment in various malignant tumours (13). Tanacan et al. (28) identified a relationship between elevated SII values in pregnant women with PPROM and negative neonatal outcomes. Keles et al. (19) found a significant increase in SII in pregnant women with PAS. In our study, although we observed higher SII values in PAS patients than in PP patients, we could not establish a significant relationship between the higher SII values and PAS patients.

In the literature, only a few studies have investigated the relationship between inflammatory parameters and the histological subtypes of PAS. Our study could not find a significant relationship between the histological subtypes of PAS and SII, SIRI, and inflammatory markers. Thus, we concluded that in addition to the depth of invasion, the extent of invasion could also influence inflammatory parameters in PAS patients. Our findings are consistent with the study that did not find a relationship between SII and other inflammatory markers and PAS (19).

The basic limitations of this study are that the data were obtained from a single clinical research centre, along with its retrospective design. The study cohort size was reduced due to patients not being included, adversely affecting the study's power. However, its strengths include a greater number of cases compared to previous studies and the evaluation of numerous haematological inflammatory parameters. The relationship between SIRI and the presence of PAS, and the histological subtypes of PAS, has been investigated for the first time.

Conclusion

As a result, PAS leads to changes in inflammatory parameters due to its invasive nature. In cases suspected to have placental invasion anomalies, parameters from complete blood count can also be utilised, in addition to imaging methods. RDW and NLR can be used to predict PAS in pregnancies with PP. However, the strength of this proposition should be supported by more comprehensive studies. Furthermore, the relationship between inflammatory parameters at different trimesters and maternal-fetal morbidity and mortality should be investigated. The association between inflammatory parameters and the histological subtypes of PAS should be explored in larger case groups.

ETHICS

Ethics Committee Approval: Ethics committee approval has been granted by University of Health Sciences Türkiye, Başakşehir Çam and Sakura City Hospital, on 11/10/2023 with protocol number 2023-466.

Informed Consent: Since the study was retrospective, informed consent was not obtained from the participants.

FOOTNOTES

Authorship Contributions

Concept: N.Ç., Design: N.Ç., E.K., İ.Ö.A., S.A.Ş., İ.P., I.T.B., T.T.A., Data Collection or Processing: E.K., İ.Ö.A., S.A.Ş., İ.P., I.T.B., T.T.A., Analysis or Interpretation: E.K., İ.Ö.A., S.A.Ş., İ.P., I.T.B., T.T.A., Writing: N.Ç.

Conflict of Interest: No conflict of interest was declared by the authors.

Financial Disclosure: The authors declared that this study received no financial support.

REFERENCES

1. Jauniaux E, Ayres-de-Campos D, Langhoff-Roos J, Fox KA, Collins S; FIGO Placenta Accreta Diagnosis and Management Expert Consensus Panel. FIGO classification for the clinical diagnosis of placenta accreta spectrum disorders. Int J Gynaecol Obstet. 2019;146:20-4.
2. Hu C, Zhang W, Pu H, Fei K, Li Q, Huang J. Quality evaluation of clinical practice guidelines for placenta accreta spectrum disorders. Heliyon. 2024;10(7):e28390.
3. Kadish E, Peled T, Sela HY, Weiss A, Shmaya S, Grisaru-Granovsky S, et al. Maternal morbidity following trial of labor after cesarean in women experiencing antepartum fetal death. Reprod Sci. 2024;31:3183-90.
4. Overton E, Wen T, Friedman AM, Azad H, Nhan-Chang CL, Booker WA, et al. Outcomes associated with peripartum hysterectomy in the setting of placenta accreta spectrum disorder. Am J Obstet Gynecol MFM. 2023;5:101174.
5. Conrad KP, von Versen-Höynck F, Baker VL. Pathologic maternal and neonatal outcomes associated with programmed embryo transfer. J Assist Reprod Genet. 2024;41:821-42.

6. Carusi DA, Fox KA, Lyell DJ, Perlman NC, Aalipour S, Einerson BD, et al. Placenta accreta spectrum without placenta previa. Obstet Gynecol. 2020;136:458-65.
7. Saxena U, Rana M, Tripathi S, Misra RN, Khambra P. Prediction of placenta accreta spectrum by prenatal ultrasound staging system in women with placenta previa with scarred uterus. J Obstet Gynaecol India. 2023;73(Suppl 2):191-8.
8. Yokouchi-Konishi T, Liu Y, Feng L. Progesterone receptor membrane component 2 is critical for human placental extravillous trophoblast invasion. Biol Reprod. 2023;109:759-71.
9. Abide Yayla C, Ozkaya E, Tayyar A, Senol T, Senturk MB, Karateke A. Predictive value of complete blood count parameters for placental invasion anomalies. J Matern Fetal Neonatal Med. 2017;30:2324-8.
10. Ersoy AO, Ozler S, Oztas E, Ersoy E, Kirbas A, Danisman N. The association between placenta previa and leukocyte and platelet indices - a case control study. Ginekol Pol. 2016;87:367-71.
11. Lei B, Guo M, Deng X, He S, Lu X, Wang Y, et al. Intraoperative cell salvage as an effective intervention for postpartum hemorrhage-Evidence from a prospective randomized controlled trial. Front Immunol. 2022;13:953334.
12. Dziedzic EA, Gąsior JS, Tuzimek A, Paleczny J, Junka A, Dąbrowski M, et al. Investigation of the associations of novel inflammatory biomarkers-systemic inflammatory index (SII) and systemic inflammatory response index (SIRI)-with the severity of coronary artery disease and acute coronary syndrome occurrence. Int J Mol Sci. 2022;23:9553.
13. Huang H, Liu Q, Zhu L, Zhang Y, Lu X, Wu Y, et al. Prognostic value of preoperative systemic immune-inflammation index in patients with cervical cancer. Scientific Reports. 2019;9:3284.
14. Zhao M, Duan X, Mi L, Shi J, Li N, Yin X, et al. Prognosis of hepatocellular carcinoma and its association with immune cells using systemic inflammatory response index. Future Oncol. 2022;18:2269-88.
15. Hussein AM, Elbarmelgy RA, Elbarmelgy RM, Thabet MM, Jauniaux E. Prospective evaluation of impact of post-Cesarean section uterine scarring in perinatal diagnosis of placenta accreta spectrum disorder. Ultrasound Obstet Gynecol. 2022;59:474-82.
16. Faraji A, Akbarzadeh-Jahromi M, Bahrami S, Gharamani S, Raeisi Shahraki H, Kasraeian M, et al. Predictive value of vascular endothelial growth factor and placenta growth factor for placenta accreta spectrum. J Obstet Gynaecol. 2022;42:900-5.
17. Zhang B, Han X, Long W, Xi S, Yu B, Yuan X. Association between red blood cell distribution width in late pregnancy and the incidence of adverse perinatal outcomes: a retrospective cohort study. Arch Med Res. 2024;55:103057.
18. Karakoç G, Yalcin SE, Yavuz A, Sarsmaz K, Şengül M, Yucel A. Delta neutrophil index as a promising biomarker for placental implantation disorders. Z Geburtshilfe Neonatol. 2021;225:412-7.
19. Keles A, Dagdeviren G, Yucel Celik O, Karatas Sahin E, Obut M, Cayonu Kahraman N, et al. Systemic immune-inflammation index to predict placenta accreta spectrum and its histological subtypes. J Obstet Gynaecol Res. 2022;48:1675-82.
20. Bahrami A, Nikoomanesh F, Khorasanchi Z, Mohamadian M, Ferns GA. The relationship between food quality score with inflammatory biomarkers, and antioxidant capacity in young women. Physiol Rep. 2023;11:e15590.
21. Bruand M, Barras D, Mina M, Ghisoni E, Morotti M, Lanitis E, et al. Cell-autonomous inflammation of BRCA1-deficient ovarian cancers drives both tumor-intrinsic immunoreactivity and immune resistance via STING. Cell Reports. 2021;36:109412.
22. Biyik M, Biyik Z, Asil M, Keskin M. Systemic inflammation response index and systemic immune inflammation index are associated with clinical outcomes in patients with acute pancreatitis? J Invest Surg. 2022;35:1613-20.
23. Wang TC, An TZ, Li JX, Pang PF. Systemic inflammation response index is a prognostic risk factor in patients with hepatocellular carcinoma undergoing TACE. Risk Manag Healthc Policy. 2021;14:2589-600.
24. Wang L, Zhou Y, Xia S, Lu L, Dai T, Li A, et al. Prognostic value of the systemic inflammation response index (SIRI) before and after surgery in operable breast cancer patients. Cancer Biomark. 2020;28(4):537-47.
25. Min L, Ziyu D, Xiaofei Z, Shunhe X, Bolin W. Analysis of levels and clinical value of CA19-9, NLR and SIRI in patients with pancreatic cancer with different clinical features. Cell Mol Biol (Noisy-le-grand). 2022;67:302-8.
26. Çallıoğlu N, Gül DK, Arslan İÖ, Geyikoğlu İ, Demirçivi E. Inflammatory markers in systemic immune-inflammatory index and inflammatory response index to predict early pregnancy loss. Saudi Med J. 2024;45:808-13.
27. Fang J, Lin Y, Chen Z, Lin Y, Pan M. The association of inflammatory markers with maternal-neonatal outcome after cervical cerclage. J Inflamm Res. 2023;16:245-55.
28. Tanacan A, Uyanik E, Unal C, Beksac MS. A cut-off value for systemic immune-inflammation index in the prediction of adverse neonatal outcomes in preterm premature rupture of the membranes. J Obstet Gynaecol Res. 2020;46:1333-41.

Medical Journal of Bakırköy

Med J Bakirkoy 2025;21:55-61
DOI: 10.4274/BMJ.galenos.2025.2024.12-6

Research

Comparison of Post-Operative Long-Term Surgical Fibrosis in the Multifidus Muscle Between Microdiscectomy and Microendoscopic Discectomy

Mikrodiskektomi ve Mikroendoskopik Diskektomi Sonrası Multifidus Kasındaki Uzun Dönem Cerrahi Fibrozisin Karşılaştırılması

Bülent Bozyiğit[1], Hakan Kına[2]

[1]Gözde International Hospitals, Clinic of Neurosurgery, İzmir, Türkiye

[2]İstinye University Faculty of Medicine, Department of Neurosurgery, İstanbul, Türkiye

ABSTRACT

Objective: The aim of this study is to compare long-term post-operative surgical fibrosis in the multifidus muscle between microdiscectomy (MD) and microendoscopic discectomy (MED) procedures.

Methods: The study included 70 patients with post-operative surgical fibrosis in the multifidus muscle. Various types of MED were analyzed, including percutaneous endoscopic lumbar discectomy (PELD), percutaneous endoscopic interlaminar discectomy (PEID), and unilateral biportal endoscopic discectomy (UBED). Creatine phosphokinase (CPK) and C-reactive protein (CRP) levels were measured pre-and post-operatively. Hospital stay duration and operative time were also recorded.

Results: The MD group demonstrated significantly higher post-operative CPK levels compared to the other groups ($p<0.05$). Similarly, CRP levels were highest in the MD group ($p<0.01$), while lower levels were observed in the PEID and PELD groups. The UBED group exhibited a larger cross-sectional area compared to each of the PEID and PELD groups ($p<0.01$). Additionally, the PELD group had the shortest hospital stay and operative time ($p<0.01$).

Conclusion: This study underscores significant variations in outcomes based on surgical approaches used for spinal conditions, particularly regarding post-operative fibrosis in the multifidus muscle. MD was associated with higher CPK and CRP levels, suggesting increased muscle injury and inflammatory response compared to PELD and PEID techniques.

Keywords: Surgical fibrosis, multifidus muscle, microdiscectomy, microendoscopic discectomy, creatine phosphokinase

ÖZ

Amaç: Bu çalışmanın amacı, mikrodiskektomi (MD) ve mikroendoskopik diskektomi (MED) işlemleri sonrası multifidus kasında oluşan uzun dönem cerrahi fibrozisi karşılaştırmaktır.

Gereç ve Yöntem: Çalışmaya, multifidus kasında cerrahi fibrozis gelişen 70 hasta dahil edilmiştir. MED'in farklı türleri incelenmiştir: Perkütan endoskopik lomber diskektomi (PELD), perkütan endoskopik interlaminar diskektomi (PEID) ve tek taraflı biportal endoskopik diskektomi (UBED). Kreatin fosfokinaz (CPK) ve C-reaktif protein (CRP) seviyeleri, ameliyat öncesi ve sonrası ölçülmüştür. Ayrıca, hastanede kalış süresi ve ameliyat süresi kaydedilmiştir.

Bulgular: MD grubunda ameliyat sonrası CPK seviyeleri, diğer gruplarla karşılaştırıldığında, istatistiksel olarak anlamlı derecede daha yüksek bulundu ($p<0,05$). Aynı şekilde, CRP seviyeleri de MD grubunda en yüksek düzeydeydi ($p<0,01$). PEID ve PELD gruplarında ise CRP seviyeleri daha düşüktü. UBED grubunun kesitsel alanı, PEID ve PELD gruplarına göre daha genişti ($p<0,01$). PELD grubu, en kısa hastanede kalış süresi ve operasyon süresi ile öne çıktı ($p<0,01$).

Sonuç: MD, daha yüksek CPK ve CRP seviyeleriyle ilişkili olduğu ve bu durumun ameliyat sonrası kas hasarı ve enflamatvuar yanıtın daha fazla olduğunu gösterdiği saptanmıştır.

Anahtar Kelimeler: Cerrahi fibrozis, multifidus kası, mikrodiskektomi, mikroendoskopik diskektomi, kreatin fosfokinaz

Address for Correspondence: Bülent Bozyiğit, Gözde International Hospitals, Clinic of Neurosurgery, İzmir, Türkiye
E-mail: bulentbzt@yahoo.com **ORCID ID:** orcid.org/0000-0001-5038-2260

Cite as: Bozyiğit B, Kına H. Comparison of post-operative long-term surgical fibrosis in the multifidus muscle between microdiscectomy and microendoscopic discectomy. Med J Bakirkoy. 2025;21:55-61

Received: 03.01.2025
Accepted: 11.02.2025
Publication Date: 25.03.2025

INTRODUCTION

Chronic low back pain is a major cause of disability worldwide and remains the leading non-cancerous reason for opioid prescriptions. Biomechanically, the multifidus and surrounding paraspinal muscles are vital for stabilizing the spine, ensuring correct posture, and limiting excessive vertebral movement. Various spinal disorders, such as scoliosis, spinal stenosis, and disc herniation, have been linked to paraspinal muscle fibrosis, atrophy, and fatty infiltration in clinical practice (1). The development of surgical fibrosis in the multifidus muscle during postoperative recovery is a critical factor influencing spinal stability (2). Microdiscectomy (MD) and microendoscopic discectomy (MED) are two widely used techniques for treating lumbar disc herniation, both designed to minimize tissue trauma (3). As the multifidus muscle plays a vital role in maintaining spinal balance and controlling movement, its damage during surgery can lead to significant pain and functional impairments. Postoperative fibrosis refers to the formation of scar tissue following spinal surgeries, such as MD and MED. This fibrosis results from tissue stress induced by surgical techniques, the body's inflammatory response, or surgical trauma (4). Fibrosis in the multifidus muscle can contribute to chronic pain, impaired muscle function, and decreased spinal stability (5). Postoperative fibrosis in the multifidus muscle is a recognized complication, particularly following lumbar disc surgeries such as MD and MED. However, there is limited research on the long-term effects of this fibrosis and its impact on surgical outcomes, leaving questions about the influence of these procedures on muscle tissue unanswered. For the treatment of lumbar disc herniation, interlaminar endoscopic lumbar discectomy is regarded as a less invasive alternative to microscopic lumbar discectomy. Nevertheless, studies investigating radiologic changes in the multifidus muscle following these procedures remain limited. Enhancing the volume and function of the multifidus muscle may contribute to better long-term surgical outcomes (6). This study aims to compare the long-term effects of MD and MED on the multifidus muscle, with the goal of refining surgical techniques and improving patient outcomes.

METHODS

This study was planned as a retrospective comparative analysis, involving 70 patients who underwent one of four surgical methods for lumbar disc herniation. The surgeries were performed by two experienced spine surgeons, each with over seven years of expertise in both open and endoscopic procedures. Eligible patients had disc herniation causing nerve root compression, which manifested as leg symptoms consistent with sciatica and back pain, persisting for at least six weeks despite conservative treatment. All patients underwent lumbar spine radiography, magnetic resonance imaging (MRI), and computed tomography for diagnosis.

Exclusion criteria included patients with foraminal or extraforaminal disc herniation, multilayer disc herniation, spinal stenosis, spondylolisthesis, scoliosis, prior lumbar surgery, spinal infections, tumors, or hip or knee arthritis. Demographic data (age, gender), along with laboratory markers including creatine phosphokinase (CPK) and C-reactive protein (CRP), were recorded during the first seven days post-surgery. Pain levels were evaluated on postoperative days (POD) 1, 3, 5, and 30. Additionally, the presence of fibrosis in the multifidus muscle was assessed via MRI (Figure 1). The Oswestry disability index (ODI), length of hospital stay, and surgery duration were also documented.

Ethical approval was granted by the İstinye University Human Research Ethics Committee (date: 01.08.2024, protocol no: 24-154), and all participants provided written informed consent.

Statistical Analysis

Statistical analyses were performed using SPSS (Version 22.0, IBM Corp., Armonk, NY), with data distribution normality assessed using the Shapiro-Wilk test. Descriptive statistics are presented as mean ± standard deviation or median (range) depending on the data distribution. Intergroup differences were evaluated using the Kruskal-Wallis test, and a p-value of less than 0.05 was considered statistically significant.

Surgical Procedures

Microdiscectomy

The patient was positioned prone, and a 3-cm midline incision was made. The paravertebral muscles were dissected using monopolar cautery, and the ligamentum flavum was excised during partial laminectomy and medial facetectomy under microscopic observation. The fractured disc fragment, extruded disc material, intra-annular fragments, and partial nucleus pulposus were carefully removed, preserving the endplate.

Percutaneous Endoscopic Lumbar Discectomy

This procedure was performed under local anesthesia with the patient in the prone position. A skin entry point, 10-13 cm from the midline, was identified. An 18-gauge spinal needle was inserted under fluoroscopic guidance, and

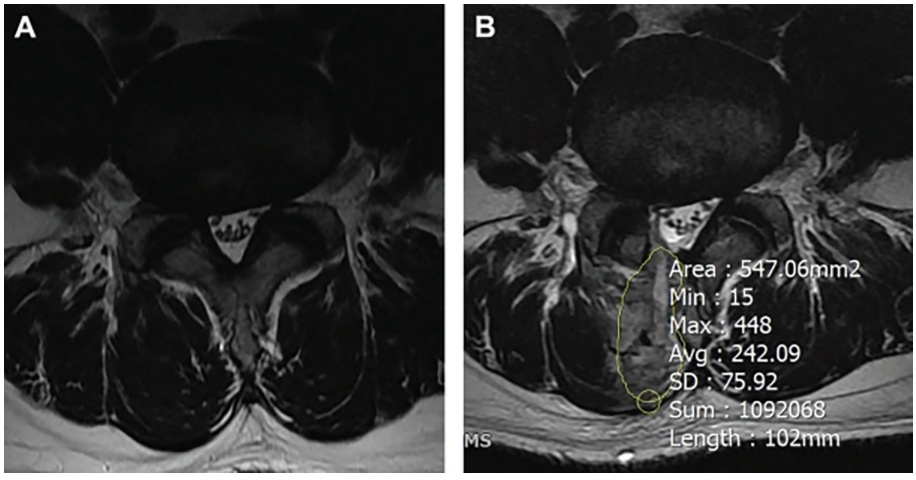

Figure 1. Comparison of the cross-sectional area (mm²) of high-intensity regions in the paraspinal muscle at the surgical site. Images from preoperative axial T2-weighted magnetic resonance imaging (MRI) (A) and postoperative MRI (B) are shown

after confirming the location of the nerve root, discography was performed using a contrast medium and indigo carmine. A guidewire was introduced, followed by a cannulated obturator, and a working cannula was inserted into the disc (7).

Percutaneous Endoscopic Interlaminar Discectomy

Under spinal anesthesia, the entry site was positioned at the lateral interlaminar space of the affected side. A small skin incision was made, and a dilator was placed into the interlaminar space. A working channel was inserted, with the final position confirmed by fluoroscopy. After the endoscope was introduced, soft tissue was cleared to expose the ligamentum flavum (8).

Unilateral Biportal Endoscopic Discectomy

Performed under epidural anesthesia, this technique involved cranial and caudal entry points placed 1 cm above and below the target lesion. The cranial site served as the primary endoscopic portal, while the caudal site was used as the functional portal. After fascia opening and muscle-splitting dissection, successive dilators were introduced, followed by insertion of an arthroscope into the endoscopic portal (9).

RESULTS

A total of 70 patients were included in the study to compare long-term post-operative surgical fibrosis in the multifidus muscle between the MD and MED techniques. Seventeen patients underwent percutaneous endoscopic interlaminar discectomy (PEID) and MD, while 18 patients underwent percutaneous endoscopic lumbar discectomy (PELD) and unilateral biportal endoscopic discectomy (UBED) (Table 1).

The mean age of the patients was 44.09 years in the MD group, compared to 42.91, 46.01, and 47.44 years in the PELD, PEID, and UBED groups, respectively. The average operation times were 56.44±15.75 minutes for PELD, 80.84±17.56 minutes for MD, 85.53±17.78 minutes for PEID, and 96.14±16.96 minutes for UBED. Hospital stays were 1.45±0.47 days for PELD, 2.87±0.66 days for PEID, 2.97±0.36 days for UBED, and 3.05±1.25 days for MD. Both operation time and hospital stay were shorter in the PELD group ($p<0.01$). In terms of high-intensity lesions (HIL), the cross-sectional area (CSA) was 97.64±109.83 mm² in the PELD group, 149.20±110.58 mm² in the PEID group, 481.16±233.39 mm² in the UBED group, and 629.94±208.67 mm² in the MD group ($p<0.01$) (Figure 1). The MD group showed the highest CSA, while the UBED group had a larger CSA than the PEID and PELD groups. ODI scores were 28.97±9.42 for MD, 30.47±9.24 for PELD, 28.57±11.66 for PEID, and 31.60±8.12 for UBED. ODI scores improved significantly by POD-30, with values of 13.95±7.05 for MD, 11.01±3.77 for PELD, 10.37±4.5 for PEID, and 10.33±5.4 for UBED, although the differences among groups were not statistically significant (Table 2).

The MD group had higher visual analog scale (VAS) scores for back pain on both POD-1 and POD-3. Specifically, VAS scores for leg pain and back pain were lowest in the PELD group at all time points ($p<0.05$) (Figure 2). CPK levels showed a pattern of increase and subsequent decrease. CPK levels peaked on POD-1 in 61 patients (88%), with the MD group showing the highest CPK-1 and CPK-3 levels ($p<0.05$). Significant differences were observed in CPK values at POD-5 and POD-7 across all groups (Figure 3). The CPK ratio was 1.67±0.55 in the MD group, compared to 1.21±0.48 in the

PELD group, 1.26±1.12 in the PEID group, and 1.34±0.55 in the UBED group (p=0.037). For CRP, significant outcomes were noted at POD-1, POD-3, POD-5, and POD-7 across all groups (Figure 4). CRP levels also peaked on POD-1 and POD-3, with the MD group exhibiting higher CRP-1, CRP-3, CRP-5, and CRP-57 levels compared to the other groups (p<0.05).

DISCUSSION

This study compared postoperative long-term surgical fibrosis in the multifidus muscle following MD and MED. A total of 70 patients with surgical fibrosis in the multifidus muscle were included, and levels of CPK and CRP were assessed both before and after surgery. The study also examined the length of hospital stays and the duration of the surgeries. The findings indicated that the MD group exhibited the highest CPK levels following surgery. MD surgery minimizes the size of skin incisions and improves visibility; however, muscle contraction and separation are still required. Minimally invasive spinal surgery procedures are becoming increasingly popular. Endoscopic surgeries provide several benefits, including minimal blood loss, reduced hospital stays, and faster recovery times (10). On the other hand, the MD group exhibited the highest CRP levels. CRP, an acute-phase protein produced by the liver, increases in response to inflammation, tissue damage, or infection. Post-surgery, CRP levels typically peak rapidly and normalize within five days. The extent of CRP elevation depends on the type and duration of the surgical procedure, with instrumented surgeries leading to higher peak levels compared to single-level decompression procedures. In the MD technique, the paraspinal muscle is detached from the lamina and facet joints using a muscle-stripping method. Excessive dissection, retraction, and muscle stripping during surgery may result in segmental instability, which contributes to severe low back pain (11).

Table 1. Operative levels

Level	MD	UBED	PELD	PEID
L1-L2	-	-	1	-
L2-L3	-	-	1	1
L3-L4	1	2	3	2
L4-L5	10	11	11	11
L5-S1	6	5	2	3
Total	17	18	18	17

MD: Microdiscectomy, UBED: Unilateral biportal endoscopic discectomy, PELD: Percutaneous endoscopic lumbar discectomy, PEID: Percutaneous endoscopic interlaminar discectomy

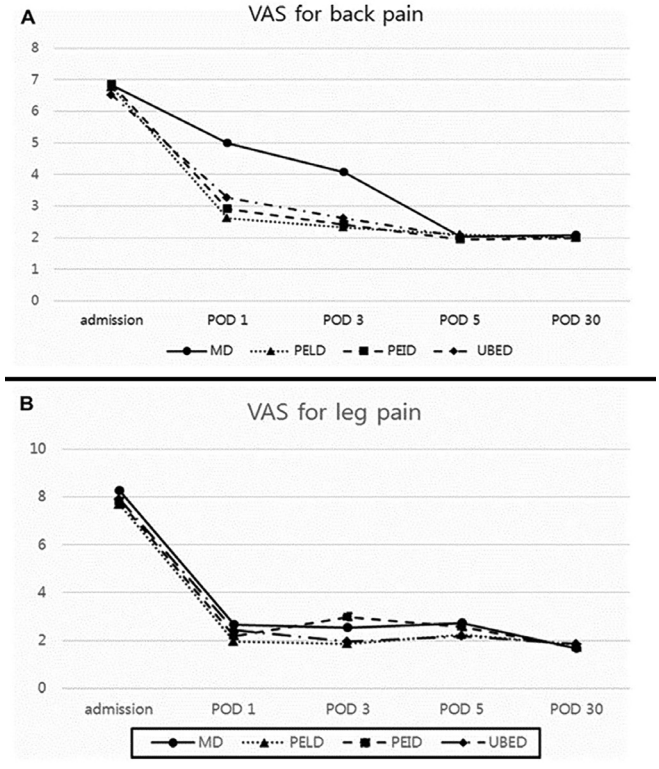

Figure 2. Variations in visual analog scale (VAS) scores among all groups: (A) for back pain and (B) for leg pain
MD: Microdiscectomy, UBED: Unilateral biportal endoscopic discectomy, PELD: Percutaneous endoscopic lumbar discectomy, PEID: Percutaneous endoscopic interlaminar discectomy

Table 2. Laboratory and clinical results of all techniques

	MD	PELD	PEID	UBED	p-value
Age	44.09 (11.34)	42.91 (6.52)	46.01 (8.92)	47.44 (12.22)	p>0.05
Sex (M:F)	6:11	11:7	6:11	8:10	p>0.05
OT, minutes	80.84 (17.56)	56.44 (15.75)	85.53 (17.78)	89.14 (18.98)	0.01
HS, days	9.05 (3.25)	4.15 (3.83)	6.47 (2.16)	6.53 (2.36)	0.02
CSA of HIL, mm^2	629.97 (208.67)	97.64 (109.83)	149.11 (110.58)	481.16 (233.37)	0.01
ODI, Adm	28.96 (9.43)	30.47 (9.24)	28.57 (11.66)	31.71 (8.14)	p>0.05
ODI, POD-30	13.95 (7.05)	11.01 (3.77)	10.37 (4.5)	10.33 (5.4)	p>0.05

MD: Microdiscectomy, PEID: Percutaneous endoscopic interlaminar discectomy, PELD: Percutaneous endoscopic lumbar discectomy, UBED: Unilateral biportal endoscopic discectomy, OT: Operation time, CSA: Cross sectional area, HIL: High intensity lesion, ODI: Oswestry disability index, POD: Postoperative days

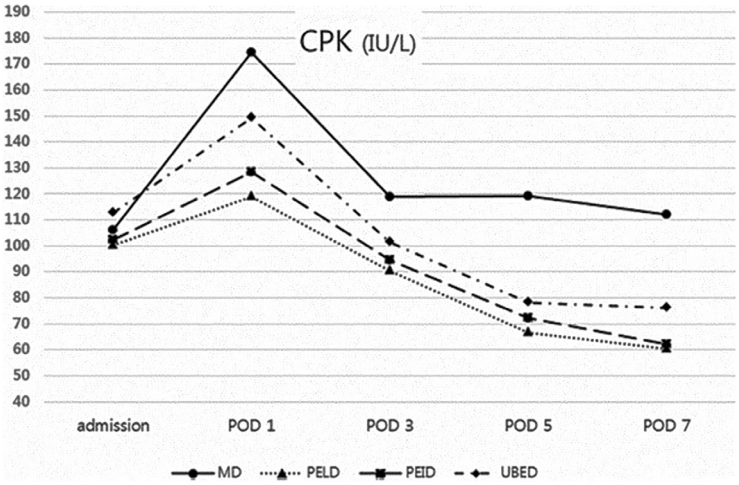

Figure 3. Fluctuations in creatine phosphokinase (CPK) levels across all study groups
MD: Microdiscectomy, UBED: Unilateral biportal endoscopic discectomy, PELD: Percutaneous endoscopic lumbar discectomy, PEID: Percutaneous endoscopic interlaminar discectomy

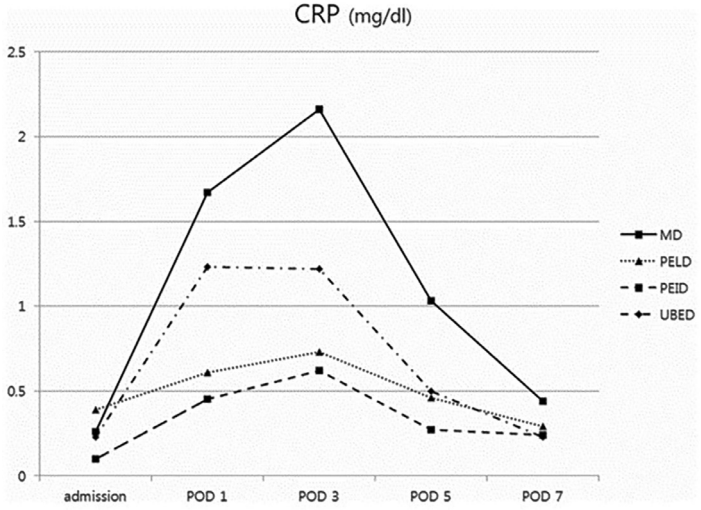

Figure 4. Alterations in C-reactive protein (CRP) levels observed in all groups
MD: Microdiscectomy, UBED: Unilateral biportal endoscopic discectomy, PELD: Percutaneous endoscopic lumbar discectomy, PEID: Percutaneous endoscopic interlaminar discectomy

In contrast, the PEID and PELD groups demonstrated significantly lower CRP levels. Among the groups, the PELD group showed the lowest CRP levels in the HIL of the paraspinal muscle, compared to UBED and MD. Full endoscopic procedures resulted in shorter hospital stays, fewer postoperative back pain, and fewer muscle injury. Similar results were observed for PEID and PELD. The UBED system, which uses two ports-one for the endoscope and one for surgical instruments-allows clear vision without the need for constant saline irrigation or muscle retraction. Surgical instruments can be used without restriction. According to our research, surgical invasiveness has an early effect on postoperative back discomfort and length of hospital stay (12). Furthermore, it was found that the UBED group had a larger CSA compared to the PEID and PELD groups. PEID and PELD employ muscle-splitting techniques using blunt obturators and successive dilators to preserve the paraspinal muscle. PEID requires partial facet joint and lamina removal, along with the cauterization of surrounding muscles and soft tissues to reach the epidural area, while PELD allows direct access to the disc fragment without the need for a barrier. The UBED technique integrates muscle-splitting and, to a lesser extent, muscle-stripping techniques (13). The comparison of postoperative long-term surgical fibrosis in the multifidus muscle following MD and MED offers significant

implications for clinical practice. The study's findings are crucial for clinical practitioners, particularly spine surgeons, as they provide valuable insights into how different surgical techniques impact the multifidus muscle. This knowledge can help guide decisions on whether to perform a MD or a MED, based on the potential effects on the multifidus muscle. These implications extend to surgical practice patterns, influencing how neurosurgeons and orthopedic surgeons approach spinal surgery. By understanding the long-term effects of these procedures on the multifidus muscle, surgeons may adjust their strategies to optimize patient outcomes. Such findings could also inform medical education programs, ensuring that practitioners are aware of the postoperative consequences of various procedures. The study also highlights the importance of patient education and informed decision-making. A thorough understanding of the long-term consequences of MD and MED on the multifidus muscle allows patients to make more informed choices regarding their treatment options. This patient-centered approach encourages active patient involvement in decision-making, helping them understand the potential risks and benefits of each surgical option.

Study Limitations

The study has two main limitations: the small sample size and the focus on long-term outcomes. Additionally, the level of CPK-MM in skeletal muscle was not measured, so it remains unclear whether the HIL observed in the paraspinal muscles reflect actual muscle damage. Follow-up MRI scans would be helpful to determine if these lesions are associated with muscle atrophy. Since the study is based on data from a specific cohort, the findings may not be applicable to other healthcare settings or populations. Further research should involve diverse cohorts to improve the generalizability of the results. The focus on fibrosis and its long-term effects on outcomes is also limited, leaving gaps in understanding how surgical procedures impact muscle tissue. Several factors may significantly influence these outcomes, but it is not feasible to address all variables within a single study.

CONCLUSION

The study found that the MD group exhibited the highest levels of CPK and CRP following surgery. These results suggest that MD surgery may have a more significant impact on muscle stress, as reflected by these biomarkers. In contrast, the PEID and PELD groups displayed lower CRP levels, indicating less inflammation. Additionally, the UBED group had a significantly larger CSA compared to the PEID and PELD groups. The PELD group also had shorter hospital stays and shorter operating times, suggesting a more efficient recovery process. While MD showed more substantial biomarker responses, PELD demonstrated the most favorable outcomes in terms of recovery time and hospital stay. Additional studies are required to validate these results and investigate the prolonged impacts of these surgical methods on muscle structure and the overall healing process.

ETHICS

Ethics Committee Approval: Ethical approval was granted by the İstinye University Human Research Ethics Committee (date: 01.08.2024, protocol no: 24-154).

Informed Consent: All participants provided written informed consent.

FOOTNOTES

Authorship Contributions

Surgical and Medical Practices: B.B., H.K., Concept: B.B., H.K., Design: B.B., H.K., Data Collection or Processing: B.B., H.K., Analysis or Interpretation: B.B., H.K., Literature Search: B.B., H.K., Writing: B.B., H.K.

Conflict of Interest: No conflict of interest was declared by the authors.

Financial Disclosure: The authors declare that this study received no financial support.

REFERENCES

1. Agha O, Mueller-Immergluck A, Liu M, Zhang H, Theologis AA, Clark A, et al. Intervertebral disc herniation effects on multifidus muscle composition and resident stem cell populations. JOR Spine. 2020;3:1091.
2. Zhang B, Liu S, Liu J, Yu B, Guo W, Li Y, et al. Transforaminal endoscopic discectomy versus conventional microdiscectomy for lumbar discherniation: a systematic review and meta-analysis. J Orthop Surg Res. 2018;13:1-9.
3. Kim S, Park GJ, Lee JU, Kim KH, Kim DH. Comparative study of the outcomes of unilateral biportal endoscopic discectomy and tubular microdiscectomy based on the visual analogue scale, Oswestry Disability Index, and Short-form 36. Journal of Minimally Invasive Spine Surgery and Technique. 2022;7:243-50.
4. Passavanti Z, Leschka S, Wildermuth S, Forster T, Dietrich TJ. Differentiating epidural fibrosis from disc herniation on contrast-enhanced and unenhanced MRI in the postoperative lumbar spine. Skeletal Radiol. 2020;49:1819-27.
5. Zhivotenko AP, Koshkareva ZV, Sorokovikov VA. Prevention of postoperative epidural fibrosis: current status of the issue. Хирургия позвоночника. 2019;16:74-81.
6. Lee C, Lee M, Lim W, Liu Y, Pakdeenit B, Kim J. Comparision study of multifidus muscle changes between microdiscectomy and full endoscopic interlaminar discectomy. Bone & Joint. 2021;103:29.
7. Fei-Long W, Cheng-Pei Z, Kai-Long Z, Du M-R, Liu Y, Heng W, et al. Comparison of different operative approaches for lumbar disc herniation: a network meta-analysis and systematic review. Pain Physician. 2021;24:381-92.

8. Qu N, Gong L, Yang X, Fu J, Zhang B, Qi Q. Cost and effectiveness of percutaneous endoscopic interlaminar discectomy versus microscope-assisted tubular discectomy for L5-S1 lumbar disc herniation. World Neurosurg. 2023;178:e712-9.
9. Jiang HW, Chen CD, Zhan BS, Wang YL, Tang P, Jiang XS. Unilateral biportal endoscopic discectomy versus percutaneous endoscopic lumbar discectomy in the treatment of lumbar disc herniation: a retrospective study. J Orthop Surg Res. 2022;17:30.
10. Gadjradj PS, Harhangi BS, Amelink J, van Susante J, Kamper S, van Tulder M, et al. Percutaneous transforaminal endoscopic discectomy versus open microdiscectomy for lumbar disc herniation: a systematic review and meta-analysis. Spine. 2021;46:538-49.
11. Ali N. Elevated level of C-reactive protein may be an early marker to predict risk for severity of COVID-19. J Med Virol. 2020;92:2409-11.
12. Ma X, Li W, Gao S, Cao C, Li C, He L, et al. Comparison of unilateral biportal endoscopic discectomy versus percutaneous endoscopic lumbar discectomy for the treatment of lumbar disc herniation: a systematic review and meta-analysis. Medicine. 2022;101:30412.
13. Wang L, Li C, Han K, Chen Y, Qi L, Liu X. Comparison of clinical outcomes and muscle invasiveness between unilateral biportal endoscopic discectomy and percutaneous endoscopic interlaminar discectomy for lumbar disc herniation at l5/s1 level. Orthopaedic Surgery. 2023;15:695-703.

Medical Journal of Bakırköy

Med J Bakirkoy 2025;21:62-69
DOI: 10.4274/BMJ.galenos.2024.2024.8-13

Research

The Impact of TRIMANO Adjustable Arm Holder on Proximal Humerus Fracture Management: Enhancing Surgery Duration, Surgical Efficiency, and Patient Outcomes

TRIMANO Ayarlanabilir Kol Tutucusunun Proksimal Humerus Kırığı Yönetimindeki Etkisi: Cerrahi Süre, Cerrahi Verimlilik ve Hasta Sonuçlarının İyileştirilmesi

Cumhur Deniz Davulcu[1], Muhammed Yusuf Afacan[1,2]

[1]İstanbul University-Cerrahpaşa, Cerrahpaşa Faculty of Medicine, Department of Orthopaedics and Traumatology, İstanbul, Türkiye
[2]İstanbul University-Cerrahpaşa, Cerrahpaşa, Institue of Graduate Studies, Department of Anatomy, İstanbul, Türkiye

ABSTRACT

Objective: This study investigates the impact of adjustable arm holders on ensuring stable fixation in the appropriate position and rotation during surgery, as well as on surgery duration and early postoperative functional outcomes in patients with proximal humerus fractures.

Methods: A retrospective evaluation was conducted on 34 patients with Neer 3-part or 4-part proximal humerus fractures. They were divided into two groups: eighteen patients without an adjustable arm holder and 16 patients with an adjustable arm holder TRIMANO FORTIS® (Arthrex, Maquet GmbH) during surgery. Surgery times were obtained from patient files, and functional outcomes were assessed postoperatively using joint range of motion and Constant-Murley scores.

Results: No significant difference in surgery duration was found based on the number of fracture parts (p=0.741). However, a significant difference was observed in postoperative Constant-Murley scores relative to the number of fracture parts (p=0.047), with 3-part fractures showing better functional recovery. The use of adjustable arm holders significantly reduced surgery time (p=0.003) and improved postoperative Constant-Murley scores (p=0.008). Increased surgery duration negatively impacted postoperative Constant-Murley scores (p=0.001). Regression analysis identified age, use of adjustable arm holders, and number of fracture parts as significant factors influencing postoperative Constant-Murley scores (p<0.0001), with age and number of fracture parts negatively affecting recovery, and the use of adjustable arm holders having a positive effect.

Conclusion: Adjustable arm holders significantly reduce surgery duration and improve postoperative functional outcomes in patients with Neer 3-part and 4-part proximal humerus fractures. Superior functional recovery was noted in patients with 3-part fractures compared to those with 4-part fractures.

Keywords: Arm, orthopedic equipment, patient positioning, humeral fractures, equipment design, operative time, outcome assessment, shoulder joint

ÖZ

Amaç: Bu çalışmada, ayarlanabilir kol tutucularının ameliyat sırasında uygun pozisyon ve rotasyonda stabil fiksasyon sağlamadaki etkisi, ameliyat süresi ve proksimal humerus kırığı olan hastalarda erken postoperatif fonksiyonel sonuçlar araştırılmıştır.

Gereç ve Yöntem: Neer 3 parçalı veya 4 parçalı proksimal humerus kırığı bulunan 34 hastanın retrospektif değerlendirmesi yapıldı. Hastalar, ameliyat sırasında ayarlanabilir kol tutucu TRIMANO FORTIS® (Arthrex, Maquet GmbH) kullanılmayan 18 hasta ve kullanılan 16 hasta olmak üzere iki gruba ayrıldı. Ameliyat süreleri hasta dosyalarından elde edildi ve fonksiyonel sonuçlar, postoperatif eklem hareket açıklığı ve Constant-Murley skorları ile değerlendirildi.

Bulgular: İki grup arasında yaş, cinsiyet dağılımı, takip süresi ve Neer kırık parçalarının sayısı açısından karşılaştırılabilir bir fark bulunmadı. Kırık parçalarının sayısına göre ameliyat süresinde anlamlı bir fark bulunmadı (p=0,741). Ancak, postoperatif Constant-Murley skorlarında kırık

Address for Correspondence: Cumhur Deniz Davulcu, İstanbul University-Cerrahpaşa, Cerrahpaşa Faculty of Medicine, Department of Orthopaedics and Traumatology, İstanbul, Türkiye
E-mail: cumhurdeniz.davulcu@iuc.edu.tr **ORCID ID:** orcid.org/0000-0002-6444-5047

Cite as: Davulcu CD, Afacan MY. The impact of TRIMANO adjustable arm holder on proximal humerus fracture management: enhancing surgery duration, surgical efficiency, and patient outcomes. Med J Bakirkoy. 2025;21:62-69

Received: 26.08.2024
Accepted: 30.10.2024
Publication Date: 25.03.2025

parçalarının sayısına göre anlamlı bir fark gözlendi (p=0,047); 3 parçalı kırıklar daha iyi fonksiyonel iyileşme gösterdi. Ayarlanabilir kol tutucularının kullanımı ameliyat süresini anlamlı derecede azalttı (p=0,003) ve postoperatif Constant-Murley skorlarını iyileştirdi (p=0,008). Artan ameliyat süresi, postoperatif Constant-Murley skorlarını olumsuz yönde etkiledi (p=0,001). Regresyon analizi, yaş, ayarlanabilir kol tutucu kullanımı ve kırık parçalarının sayısının postoperatif Constant-Murley skorlarını etkileyen önemli faktörler olduğunu gösterdi (p<0,0001); yaş ve kırık parçalarının sayısı iyileşmeyi olumsuz etkilerken, ayarlanabilir kol tutucu kullanımı olumlu bir etkiye sahipti.

Sonuç: Ayarlanabilir kol tutucularının kullanımı, Neer 3 parçalı ve 4 parçalı proksimal humerus kırığı olan hastalarda ameliyat süresini anlamlı ölçüde kısaltmakta ve postoperatif fonksiyonel sonuçları iyileştirmektedir. Üç parçalı kırıklarda, 4 parçalı kırıklara kıyasla üstün fonksiyonel iyileşme gözlemlenmiştir. Proksimal humerus kırıklarında ayarlanabilir kol tutucularının cerrahi protokollere entegrasyonu, cerrahi verimliliği ve hasta sonuçlarını iyileştirerek hasta bakımına katkı sağlayabilir.

Anahtar Kelimeler: Kol, ortopedik ekipman, hasta pozisyonlama, humerus kırıkları, ekipman tasarımı, ameliyat süresi, sonuç değerlendirme, omuz eklemi

INTRODUCTION

Proximal humerus fractures, constituting approximately 5-6% of adult fractures (1,2), were first classified by Neer in 1970. This is the most commonly used classification in such fractures, constituting four parts: articular surface of the humeral head, greater tuberosity, lesser tuberosity, and shaft (3-5). While humeral shaft fractures typically undergo conservative treatment, surgery becomes a crucial consideration in cases of displaced fractures to decrease the risk of non-union (6). Plate osteosynthesis emerges as the preferred surgical method over intramedullary nailing for humeral shaft fractures extending proximally, since intramedullary nailing heightens the risk of shoulder impingement, limits shoulder mobility, and often necessitates the removal of metal implants (7,8).

In proximal humerus fracture surgery, ensuring the patient's optimal positioning is imperative to facilitate the most effective surgical approach. Nonetheless, this necessitates assistant surgeons to maintain the patient's arm in the desired position throughout the entirety of the procedure, which may oblige them to be positioned further from the surgical area (9). Ensuring stable fixation in the correct position and rotation is paramount in proximal humerus fracture surgery. Without the utilization of an adjustable arm holder, achieving fixation in the desired position poses considerable challenges. These devices keep the limb in the right position, with or without traction, freeing up the surgical assistant to focus on other tasks during the procedure (9). TRIMANO FORTIS® (Arthrex, Maquet GmbH) serves as an adjustable arm holder attached to any operative table, aiding in upper limb surgeries. It can be maneuvered using an accessible handle to position the patient's arm optimally for the procedure. With its three-joint mechanism, the TRIMANO enables easy adjustments of the limb across various positions, accommodating a wide range of surgical procedures (10). The arm holder ensures the surgical position remains steady, allowing the surgeon to position the limb optimally for the most effective approach to the surgical site.

We hypothesize that employing adjustable arm holders will streamline surgical procedures, yielding improved outcomes. In this way, we assume that the patients' postoperative clinical results will be better that the surgery time will be significantly shorter. Consequently, our objective is to assess the impact of adjustable arm holders on surgical duration and early postoperative functional outcomes in patients undergoing proximal humerus fracture surgery.

METHODS

This study was approved by the İstanbul University-Cerrahpaşa Clinical Research Ethics Committee (number: E-83045809-604.01-1004836, date: 07.06.2024). Informed consent was obtained from all individual participants included in the study. The study encompassed patients treated at our clinic for proximal humerus fractures with plate osteosynthesis between 2020 and 2022 who consented to participate in the research. Exclusions comprised patients who were unreachable, those who missing regular follow-up appointments, individuals with follow-up periods less than one year post-operation, those who refused to participate, those who underwent prior surgical procedures on the same upper extremity, and individuals with documented rotator cuff tears or other shoulder pathologies.

In this study, two groups were established based on the utilization of the adjustable arm holder TRIMANO FORTIS® (Arthrex, Maquet GmbH) during proximal humerus surgery. Figure 1 shows the components of the TRIMANO and Figure 2 demonstrates set-up and usage. Patients were evaluated retrospectively. A total of 34 patients meeting the inclusion criteria were included in our study. The group in which adjustable arm holders were used consisted of 16 people, while the group in which they were not used consisted of 18 people. The groups were determined randomly. We evaluated patients' gender, age, operation year, number of fracture parts according to Neer classification, operation duration, follow-up time, and postoperative Constant-Murley scores (11,12).

Arm holders were randomly used during operations, without specific patient selection criteria. Patients were

Figure 1. TRIMANO adjustable arm holder components. The TRIMANO adjustable arm holder is shown in its storage case. The image on the right displays the arm holder fully extended

Figure 2. TRIMANO adjustable arm holder setup and usage. The left image shows the TRIMANO adjustable arm holder attached to an operating table, ready for use. The middle and right images illustrate the arm holder in action, securing a patient's arm during surgery to provide stable positioning and facilitate surgical procedures

operated on without arm holders due to the limited availability of arm holders and the potential occurrence of simultaneous shoulder arthroscopic procedures in our hospital. All surgeries were conducted by the same surgeon. Fractures were classified using the Neer classification system, and the number of fracture parts was recorded independently by two different surgeons. This process was repeated twice, yielding consistent results. The same surgeons performed operations in both groups, employing the (anterior) deltopectoral approach for all patients. The operation durations were extracted from the patients' medical records. The patients' pain status, activity level, arm positioning, abduction strength, and shoulder range of motion were evaluated individually. Constant-Murley scores were recorded at a minimum of one year post-operation.

Statistical Analysis

Within the scope of the study, the number of samples was calculated using power analysis. As a result of the power analysis performed with G*Power (version 3.1.9.6) in the 2-group study, the reliability was 95%, the effect size was 1.25, and the power value was 0.90. In this context, the minimum number of samples was calculated as 32. Accordingly, since it was deemed appropriate to conduct the study by taking at least 16 samples from each group, a minimum of 16 patients for each group was included in the study. In this study, a series of statistical analyses were performed to determine the factors affecting the results of surgical interventions performed with or without adjustable arm holders. Data analysis was performed using international business machines corporation Statistical Package for the Social Sciences statistics 24 software. Data analysis: the dataset consists of a total of 34 patients, including various demographic and clinical characteristics. These data include patients' surgery times, follow-up periods, fracture classifications according to Neer, use of adjustable arm holders, and postoperative Constant-Murley scores. Descriptive statistics: first, descriptive statistics (mean, standard deviation, minimum, maximum and median values) were calculated for variables such as the patients' surgery year, age, gender, fracture classification and use of adjustable arm holders. Correlation analysis: the relationships between the patient's surgery time, follow-up time, and postoperative Constant-Murley score were evaluated using the Pearson correlation coefficient (r). Statistical significance levels (p-values) and r are reported. The effect of categorical variables such as gender, number of fracture parts, and use of adjustable arm holder on patients' outcomes and surgery duration was analyzed with the Mann-Whitney U test. Chi-square test: the effect of the use of adjustable arm holders on the distribution of the number of fracture parts was examined with the chi-square test. Regression analysis: multiple linear regression analysis was performed for factors thought to be effective on the postoperative Constant-Murley score (age, use of adjustable arm holders, and number of fracture parts). In the analysis, the effects of independent variables on the dependent variable are reported along with unstandardized and standardized coefficients, t-statistics and p-values.

RESULTS

Considering the surgery year of the 34 patients participating in the study, the p-value obtained as a result of the chi-square test, was calculated as 0.278. This result shows that there is no statistically significant difference between the use of adjustable arm holders based on the year of surgery

(detailed in Table 1). There was no statistically significant difference in age between the groups (p>0.05). The p-value of the chi-square test for gender distribution is 0.968, indicating that there is no statistically significant difference between the groups in terms of gender. The p-value obtained as a result of the chi-square test for this variable is 1.000, which indicates that 3-and 4-part fractures, have a similar distribution in the groups with and without adjustable arm holders. The age, gender distribution, follow-up period, and the number of Neer fracture fragments of the patients are similar in both groups (detailed in Table 1 and Table 2). Operation duration in minutes, follow-up times in years, and postoperative Constant-Murley scores are detailed in Table 1. The average surgery time is 105.29 minutes, and the standard deviation is 15.02 minutes. The average follow-up period was 1.82 years. Constant-Murley scores obtained after surgery vary between 70 and 100. The mean score was calculated as 86.26. These results show that postoperative patients generally achieved high functional gains and had a good recovery process (Table 1).

There is no statistically significant difference in surgery times and postoperative Constant-Murley scores between male and female patients. There is no statistically significant difference in surgery time according to the number of fracture parts (detailed in Table 3). There is a statistically significant difference between postoperative Constant-Murley scores according to the number of fracture parts (p=0.047). It indicates that patients with 3-part fractures show higher functional recovery than those with 4-part fractures. The average surgery duration of patients without an adjustable arm holder was determined as 112.22 minutes, and the duration for patients with an adjustable arm holder was determined as 97.50 minutes. The use of adjustable arm holders significantly reduces the surgery time (p=0.003). The postoperative mean Constant-Murley score, of patients without an adjustable arm holder, was determined as 82.89, with a standard deviation of 7.35 and a median of 82. For the patients studied, the mean is 90.06, the standard deviation is 6.86, and the median is 91. The use of adjustable arm holders significantly improves

Table 1. The demographic, clinical, and surgical characteristics of the patients included in the study

		n	%	T-	%	T+	%	Min	Max	X	SD	M
OY 2020	*p=0.278	2	5.9	2	11.1	0	0.0					
OY 2021		24	70.6	11	61.1	13	81.3					
OY 2022		8	23.5	5	27.8	3	18.8					
Age Total Group		34						31	70	50.68	10.44	50
Age T-	**p=0.769	18	52.9					31	69	50.11	10.31	49
Age T+		16	47.1					32	70	51.31	10.88	51
Male	*p=0.968	19	55.9	10	55.6	9	56.3					
Female		15	44.1	8	44.4	7	43.8					
Neer 3-part	*p=1,000	17	50.0	9	50.0	8	50.0					
Neer 4-part		17	50.0	9	50.0	8	50.0					
TRIMANO	-	18	52.9									
	+	16	47.1									
Operation duration in minutes								85	145	105.29	15.02	100
Follow-up time in years								1	3	1.82	0.52	2
Postoperative Constant-Murley score								70	100	86.26	7.90	86

*Chi-square test, **Mann-Whitney U test, OY: Operation year, T-: Trimano not used, T+: Trimano used, n: Total number, Min: Minimum, Max: Maximum, X: Mean, SD: Standard deviation, M: Median

Table 2. Distribution of Neer classification types with and without adjustable arm holder

		Adjustable arm holder				Chi-square test
		TRIMANO -		TRIMANO +		
		n	%	n	%	p-value
Neer classification	**Neer 3-part**	9	52.9	8	47.1	1.000
	Neer 4-part	9	52.9	8	47.1	

-: Not used, +: Used, n: Total number

Table 3: Comparison of operation duration, follow-up times, and postoperative constant scores by gender, Neer classification, and use of adjustable arm holder

	Gender						Mann-W-hitney U test	NEER classification						Mann-W-hitney U test	Adjustable arm holder						Mann-W-hitney U test
	Male			Female				NEER 3-part			NEER 4-part				TRIMANO -			TRIMANO +			
	X	SD	M	X	SD	M	p-value	X	SD	M	X	SD	M	p-value	X	SD	M	X	SD	M	p-value
Operation duration in minutes	104.74	14.95	100	106.00	15.61	105	0.726	104.41	14.88	100	106.18	15.57	100	0.741	112.22	15.92	108	97.50	9.31	95	0.003
Follow-up times in year	1.84	0.50	2	1.80	0.56	2	0.794	1.88	0.49	2	1.76	0.56	2	0.489	1.83	0.62	2	1.81	0.40	2	1.000
Postoperative constant scores	86.37	7.58	86	86.13	8.55	84	0.972	89.24	8.07	92	83.29	6.70	84	0.047	82.89	7.35	82	90.06	6.86	91	0.008

SD: Standard deviation, X: Mean, M: Median

postoperative Constant-Murley scores (p=0.008) (detailed in Table 3).

A moderate negative correlation with r=-0.532 was determined between the patient's surgery time and the postoperative Constant-Murley score. This relationship is statistically significant with a value of p=0.001. This result shows that as the surgery duration increases, the postoperative Constant-Murley score decreases, meaning that prolonging the surgery duration may negatively affect functional results (Table 4).

The constant value in the regression analysis model was calculated as 119,456, and this value is statistically significant (t=23,436, p<0.0001). This is the mean value of the postoperative Constant-Murley score expected when each of the independent variables is zero. The effect of the age variable on the postoperative Constant-Murley score is negative (-0.516). The standardized coefficient (-0.682) shows that age reduces the postoperative Constant-Murley score, meaning that as age increases, the level of postoperative functional recovery decreases. This coefficient is statistically significant (t=-7,779, p<0.0001). The use of an adjustable arm holder has a positive effect on the postoperative Constant-Murley score (7,794). The standardized coefficient (0.500) indicates that this variable has a significantly positive effect on the score. The contribution of this variable is also statistically significant (t=5,923, p<0.0001). The effect of the number of fracture parts variable on the postoperative Constant-Murley score is negative (-3.056). The standardized coefficient (-0.196) indicates that more fracture fragments reduce the postoperative functional recovery score. This effect is statistically significant (t=-2,243, p=0.032). The R^2 value of the model was calculated as 0.787. This indicates that the model explains 78.7% of the variance in the dependent variable, meaning the model is highly effective. The f-statistic testing the overall significance of the model is 36,961, and this value is statistically significant (p<0.0001). This regression model clearly reveals that the factors affecting the postoperative Constant-Murley score are age, use of adjustable arm holders, and the number of fracture parts. While age and the number of fracture parts have a negative effect on postoperative recovery, the use of an adjustable arm holder has a positive effect (Table 5).

DISCUSSION

In our investigation, we examined the impact of the TRIMANO adjustable arm holder on managing proximal humerus fractures, with a focus on surgical duration, efficiency, and patient outcomes. Our results revealed a notable reduction in surgery time in the group utilizing

Table 4. Correlation analysis of operation duration, follow-up times, and postoperative constant scores

Correlation analysis		Operation duration in minutes	Follow-up times in year	Postoperative Constant-Murley scores
Operation duration in minutes	**r**	1.000	0.239	**-0.532**
	p-value		0.173	**0.001**
Follow-up times in year	**r**		1.000	0.041
	p-value			0.817
Postoperative constant scores	**r**			1.000
	p-value			

r: Pearson correlation coefficient

Table 5. Regression analysis for predicting postoperative constant scores

Regression analysis	Unstandardized coefficients		Standardized coefficients	t	p-value	R^2	F
	B	SE	Beta				
Constant-Murley*	119.456	5.097		23.436	**<0.0001**	0.787	36.961
Age	-0.516	0.066	-0.682	-7.779	**<0.0001**		
Adjustable arm holder	7.794	1.316	0.500	5.923	**<0.0001**		
Neer classification number of fracture parts	-3.056	1.363	-0.196	-2.243	**0.032**		

Dependent variable=Postoperative constant score, Method=Stepwise
*The constant value in the model is calculated as 119,456, which is statistically significant (t=23,436, p<0.0001). This value represents the expected mean postoperative Constant-Murley score when all independent variables are zero

adjustable arm holders, coupled with an improvement in postoperative Constant-Murley scores, indicating the potential benefits of employing this device in enhancing both surgical efficiency and patient recovery. Moreover, our findings underscore the adverse effect of prolonged surgery time on functional outcomes, while also demonstrating superior functional recovery in patients with 3-part fractures compared to those with 4-part fractures.

Adjustable extremity holders play a crucial role in orthopedic surgery by providing enhanced stability and facilitating improved surgical access. In the absence of such holders, assistant surgeons are tasked with positioning and maintaining stability throughout the procedure. However, utilizing adjustable holders eliminates the need for constant manual adjustment, resulting in reduced vibration and allowing surgeons to approach the surgical site with greater precision and ease. Numerous authors have demonstrated the impact of adjustable extremity holders on surgery duration, consistently noting a decrease in operating theater time with their utilization (9,10,13,14). Kim et al. (15) conducted a study examining the effect of intraoperative limb positioning on both-column acetabular fractures, yielding satisfactory radiological and clinical outcomes following the implementation of intraoperative traction with a limb positioner. Washburn et al. (16) detailed a technique for managing acute ankle traumas using a combination of a previously placed calcaneus external fixation pin and the TRIMANO (Arthrex, Naples, FL,) external positioning arm to apply skeletal traction during both arthroscopic and open definitive fixation procedures. Schulz-Drost et al. (17) reported that in the stabilization of flail chest injuries employing minimally invasive techniques aimed at addressing the core instability, if posterior and lateral approaches were deemed necessary, patients were positioned in a lateral decubitus posture. During this positioning, the ipsilateral arm was kept mobile using a TRIMANO three-dimensional (3D) Support Arm® (MAQUET Holding B.V. and Co. KG, Rastatt, Germany). In Böhringer et al. (18) study on intraoperative 3D imaging in plate osteosynthesis of proximal humerus fractures, the patient's arm was positioned freely with the assistance of a support arm (Arthrex TRIMANO®). Alkhani et al. (13) examined the transaxillary approach in the treatment of thoracic outlet syndrome by using the TRIMANO Arthrex arm as an assistive device. Their findings suggest that employing the TRIMANO Arthrex arm is both safe and beneficial in positioning and managing patients undergoing transaxillary first rib resection. Notably, its use reduces the requirement for surgical assistants and enhances surgeon comfort by ensuring stable exposure throughout the procedure. Ashour et al. (10) presented a case of elbow trauma requiring orthopedic and vascular repair, highlighting the TRIMANO device's usefulness in upper limb

plastic surgery. They recommend its adoption to streamline procedures, reduce staffing needs, and enhance training opportunities. Herzberg and Field (19) studied the use of a mechanical forearm holder during elbow arthroscopy in the lateral decubitus position. They discovered that this technique offers a simple and reproducible method to maintain elbow joint position without requiring an assistant, facilitating effective elbow arthroscopy. Gentile et al. (14) recommended utilizing the TRIMANO FortisTM arm in ankle arthroscopy. Their findings indicate that the TRIMANO arm enables rapid, one-handed manipulation of distraction during the procedure, streamlining ankle arthroscopy. Assiotis et al. (9) outlined a surgical technique that adapts the use of the TRIMANO FORTIS® dynamic pneumatic limb positioner (Arthrex, Maquet GmbH) for open and arthroscopic procedures involving the elbow, proximal forearm, midshaft, and distal humerus, and they reported that this approach provided simplicity, reproducibility, and improved surgical efficiency. Dongqiang et al. (20) proved that the TRIMANO universal robotic arm, when used with contact shoulder arthroscopy, significantly aids surgical procedures and clinical teaching. They also showed that its potential for integration with remote medicine and other disciplines (21) streamlines shoulder arthroscopy practices and enhance teaching platforms (20).

In our literature review, we did not come across any previous studies comparing patients who had arm holders during surgery with those who did not. This makes our study unique, as we analyzed surgery duration and functional outcomes in both groups for the first time in the literature.

Study Limitations

One limitation of our study may lie in the follow-up time, as we had recently introduced this device. Consequently, we focused on analyzing short-term outcomes. However, in the future, we plan to conduct a follow-up study to evaluate the long-term outcomes of the same patient groups.

CONCLUSION

In conclusion, our investigation into the impact of the TRIMANO adjustable arm holder on managing proximal humerus fractures reveals significant contributions to surgical efficiency, patient outcomes, and overall clinical practice. Consistent with the literature, our study confirms the efficacy of adjustable extremity holders in reducing surgery time, enhancing postoperative functional scores, and improving patient recovery. Importantly, our findings emphasize the detrimental effects of prolonged surgery time on functional outcomes, underscoring the importance of efficient surgical techniques. Furthermore, our study contributes to the existing body of knowledge by highlighting the superior functional recovery observed in patients with 3-part fractures compared to those with 4-part fractures. This evidence also underscores the power of the Neer classification system in predicting functional outcomes and guiding clinical decision-making in the management of proximal humerus fractures. Overall, our results support the widespread adoption of adjustable extremity holders, such as the TRIMANO device, as valuable tools in orthopedic surgery, offering tangible benefits in terms of surgical efficiency, patient recovery, and ultimately, improved clinical outcomes.

ETHICS

Ethics Committee Approval: This study was approved by the İstanbul University-Cerrahpaşa Clinical Research Ethics Committee (number: E-83045809-604.01-1004836, date: 07.06.2024).

Informed Consent: Informed consent was obtained from all individual participants included in the study.

FOOTNOTES

Authorship Contributions

Surgical and Medical Practices: C.D.D., M.Y.A., Concept: C.D.D., M.Y.A., Design: C.D.D., M.Y.A., Data Collection or Processing: C.D.D., M.Y.A., Analysis or Interpretation: C.D.D., M.Y.A., Literature Search: C.D.D., M.Y.A., Writing: C.D.D., M.Y.A.

Conflict of Interest: No conflict of interest was declared by the authors.

Financial Disclosure: The authors declared that this study received no financial support.

REFERENCES

1. Pencle F, Varacallo MA. Proximal humerus fracture. [Updated 2023 Aug 4]. In: StatPearls [Internet]. Treasure Island (FL): StatPearls Publishing; 2025 Jan-. Available from: https://www.ncbi.nlm.nih.gov/books/NBK470346/
2. Court-Brown CM, Caesar B. Epidemiology of adult fractures: a review. Injury. 2006;37:691-7.
3. Neer CS 2nd. Displaced proximal humeral fractures. I. Classification and evaluation. J Bone Joint Surg Am. 1970;52:1077-89.
4. Carofino BC, Leopold SS. Classifications in brief: the Neer classification for proximal humerus fractures. Clin Orthop Relat Res. 2013;471:39-43.
5. Marmor MT, Agel J, Dumpe J, Kellam JF, Marecek GS, Meinberg E, et al. Erratum: comparison of the Neer classification to the 2018 update of the orthopedic trauma association/AO fracture classification for classifying proximal humerus fractures: erratum. OTA Int. 2025;8:e379.

6. van de Wall BJM, Ochen Y, Beeres FJP, Babst R, Link BC, Heng M, et al. Conservative vs. operative treatment for humeral shaft fractures: a meta-analysis and systematic review of randomized clinical trials and observational studies. J shoulder Elb Surg. 2020;29:1493-504.
7. Maes V, Putzeys G. One-year follow-up after treatment of proximal and/or middle one-third humeral shaft fractures with a helical plate: healing rates, complications and functional outcome measures. BMC Musculoskelet Disord. 2021;22:890.
8. Kurup H, Hossain M, Andrew JG. Dynamic compression plating versus locked intramedullary nailing for humeral shaft fractures in adults. Cochrane Database Syst Rev. 2011:CD005959.
9. Assiotis A, Rumian A, Yeoh C, Uppal HS. Approaching the humerus, elbow, and proximal forearm using the trimano arm holder. Cureus. 2024;16:e58833.
10. Ashour T, Chadwick S, Wong J, Choukairi F. TRIMANO-A helping hand for upper limb surgery. JPRAS Open. 2023.
11. Constant CR, Murley AH. A clinical method of functional assessment of the shoulder. Clin Orthop Relat Res. 1987;214:160-4.
12. Constant CR, Gerber C, Emery RJH, Søjbjerg JO, Gohlke F, Boileau P. A review of the Constant score: modifications and guidelines for its use. J shoulder Elb Surg. 2008;17:355-61.
13. Alkhani M, Arsicot M, Oliny A, Millon A, Della Schiava N, Bordet M. Thoracic outlet syndrome: single-center experience on the transaxillary approach with the aid of the TRIMANO arthrex arm. J Vasc Surg Cases Innov Tech. 2024;10:101400.
14. Gentile M, Blickenstaff B, Peluso R, Lamba C, Fravel W. One-step distraction technique using Trimano FortisTM arm in ankle arthroscopy. Foot and Ankle Surg Tech Reports Cases. 2022;2:100111.
15. Kim JW, Oh CW, Park KH, Hong WK, Yoon SH, Lee GS, et al. Application of an intraoperative limb positioner for adjustable traction in both-column fractures of the acetabulum: a technical note with clinical outcome. J Clin Med. 2023;12:1682.
16. Washburn FJ, Umbel BD, Martin KD. Use of the external fixator calcaneus pin: using the TRIMANO to its full potential. Arthrosc Tech. 2022;11:e669-73.
17. Schulz-Drost S, Grupp S, Pachowsky M, Oppel P, Krinner S, Mauerer A, et al. Stabilization of flail chest injuries: minimized approach techniques to treat the core of instability. Eur J Trauma Emerg Surg. 2017;43:169-78.
18. Böhringer A, Cintean R, Eickhoff A, Gebhard F, Schütze K. Intraoperative 3D imaging in plate osteosynthesis of proximal humerus fractures. Arch Orthop Trauma Surg. 2023;143:4993-5000.
19. Herzberg G, Field LD. Use of a mechanical forearm holder during elbow arthroscopy in lateral decubitus position. Arthrosc Tech. 2024;102991.
20. Dongqiang G, Haoran G, Lei C, Wei L. Application of trimano universal manipulator in clinical and teaching of shoulder arthroscopy. J Musculoskelet Disord Treat. 2023;9.
21. He J, Baxter SL, Xu J, Xu J, Zhou X, Zhang K. The practical implementation of artificial intelligence technologies in medicine. Nat Med. 2019;25:30-6.

Medical Journal of Bakırköy

Med J Bakirkoy 2025;21:70-75
DOI: 10.4274/BMJ.galenos.2024.2024.3-12

Research

Comprehensive Analysis of Factors Affecting Surgical Outcomes in Intracranial Aneurysm Patients with Poor Prognosis

Kötü Prognozlu İntrakraniyal Anevrizma Hastalarında Cerrahi Sonuçları Etkileyen Faktörlerin Kapsamlı Analizi

Murat Baloğlu, Hakan Millet, Serdar Ercan

University of Health Sciences Türkiye, Eskişehir City Hospital, Clinic of Neurosurgery, Eskişehir, Türkiye

ABSTRACT

Objective: This research study examines the surgical outcomes of patients with severe aneurysmal subarachnoid hemorrhage (aSAH) based on data from a single center. The traditional conservative management approach has shown poor outcomes, leading to the consideration of surgical interventions. This study aims to assess the importance of surgical clipping in improving functional outcomes and identify factors influencing prognosis.

Methods: The study included 27 patients with poor-grade aSAH who underwent surgical interventions within 72 hours of the event. Data collected included patient demographics, clinical presentation, imaging findings, surgical details, complications, length of hospital stay, and functional outcomes at follow-up.

Results: The findings indicate that surgical interventions, including aneurysm clipping and decompressive craniectomy, were performed in selected cases. However, overall functional outcomes were limited, with a small number of patients showing favorable recovery. The six-month mortality rate was high, with infection and massive brain edema as leading causes of death. Advanced age was associated with increased mortality risk. Factors such as gender, clinical status upon admission, imaging findings, aneurysm location, and timing of surgery did not significantly impact the risk of death or length of survival.

Conclusion: This study contributes to understanding surgical management strategies for poor-grade aSAH. Further research and advancements are needed to improve outcomes. Identifying predictive factors for prognosis can aid in treatment decision-making and provide realistic expectations for recovery. The study underscores the complexity of poor-grade aSAH and the ongoing debate regarding optimal surgical interventions in these cases.

Keywords: Intracranial aneurysms, poor-grade, surgical outcomes, prognosis, timing of surgery

ÖZ

Amaç: Bu araştırma, kötü dereceli anevrizmal subaraknoid kanamalı (aSAH) hastaların cerrahi sonuçlarını tek merkezden elde edilen verilere dayanarak incelemektedir. Kötü dereceli aSAH olguları daha yüksek klinik şiddet ve daha kötü prognozlarla ilişkilidir. Geleneksel konservatif tedavi yaklaşımının kötü sonuçlar vermesi, anevrizmanın erken kliplenmesi gibi cerrahi müdahalelerin potansiyel tedavi stratejileri olarak değerlendirilmesine yol açmıştır. Bu çalışma, fonksiyonel sonuçların iyileştirilmesinde cerrahi kliplemenin önemini değerlendirmeyi ve prognozu etkileyen faktörleri belirlemeyi amaçlamaktadır.

Gereç ve Yöntem: Çalışmaya, olaydan sonraki 72 saat içinde cerrahi müdahale uygulanan kötü dereceli aSAH'li 27 hasta dahil edildi. Toplanan veriler arasında hasta demografik özellikleri, klinik görünüm, görüntüleme bulguları, cerrahi ayrıntılar, komplikasyonlar, hastanede kalış süresi ve takipteki fonksiyonel sonuçlar yer alıyordu.

Bulgular: Bulgular, seçilmiş olgularda anevrizma kliplemesi ve dekompresif kranyektomiyi içeren cerrahi müdahalelerin uygulandığını göstermektedir. Bununla birlikte, genel fonksiyonel sonuçlar sınırlıydı ve az sayıda hasta olumlu iyileşme gösterdi. Altı aylık ölüm oranı yüksekti;

Address for Correspondence: Serdar Ercan, University of Health Sciences Türkiye, Eskişehir City Hospital, Clinic of Neurosurgery, Eskişehir, Türkiye
E-mail: srdrercn@gmail.com **ORCID ID:** orcid.org/0000-0002-8299-1789

Cite as: Baloğlu M, Millet H, Ercan S. Comprehensive analysis of factors affecting surgical outcomes in intracranial aneurysm patients with poor prognosis. Med J Bakirkoy. 2025;21:70-75

Received: 01.05.2024
Accepted: 31.10.2024
Publication Date: 25.03.2025

enfeksiyon ve ağır beyin ödemi başlıca ölüm nedenleriydi. İleri yaş, artan ölüm riskiyle ilişkilendirildi. Cinsiyet, başvuru sırasındaki klinik durum, görüntüleme bulguları, anevrizmanın yeri ve ameliyatın zamanlaması gibi faktörler, ölüm riskini veya hayatta kalma süresini önemli ölçüde etkilemedi.

Sonuç: Bu çalışma, kötü dereceli aSAH için cerrahi tedavi stratejilerinin anlaşılmasına katkıda bulunmaktadır. Sonuçların iyileştirilmesi için daha fazla araştırma ve ilerlemeye ihtiyaç vardır. Prognoz için öngörücü faktörlerin belirlenmesi, tedaviye karar verilmesine yardımcı olabilir ve iyileşme için gerçekçi beklentiler sağlayabilir. Çalışma, düşük dereceli aSAH'ın karmaşıklığının ve bu olgularda optimal cerrahi müdahalelerle ilgili devam eden tartışmanın altını çiziyor.

Anahtar Kelimeler: İntrakraniyal anevrizmalar, kötü-dereceli, cerrahi sonuçlar, prognoz, ameliyatın zamanlaması

INTRODUCTION

Aneurysmal subarachnoid hemorrhage (aSAH) is a severe state characterized by hemorrhaging into the subarachnoid area due to the rupture of an intracranial aneurysm (1,2). Poor-grade aSAH refers to cases with a higher clinical severity, typically classified as Hunt and Hess grades IV and V. These patients face markedly poorer outcomes and numerous challenges in their management (3,4). Surgical intervention, particularly aneurysm clipping, has been increasingly considered as a potential treatment strategy in poor-grade aSAH cases (3,5,6). This research paper aims to provide insights into the surgical results of individuals with low-grade aSAH.

The traditional approach to the management of aSAH involved conservative measures as the primary therapy, with surgery postponed for individuals who have survived the initial critical period (5,7). However, this approach was associated with high mortality rates and poor functional outcomes in a substantial proportion of patients. Recent evidence suggests that aggressive surgical intervention, such as early aneurysm clipping, may yield improved functional outcomes (3,5-7). Ultra-early surgery has also been explored as a potential strategy to enhance overall survival rates. Consequently, the role of surgical intervention in poor-grade aSAH cases has become a topic of increasing interest and debate.

In this research study, we present the outcomes of surgical interventions performed on patients with poor-grade aSAH, based on data collected from a single tertiary neurosurgery facility. Our objective is to evaluate the significance of surgical clipping in enhancing functional results in these patients and identify factors that may influence the overall prognosis. By analyzing the specific roles of patient characteristics such as age, gender, and imaging findings, we intend to offer significant insights on how these characteristics predict the functional outcomes of patients with poor-grade aSAH. This study contributes to the existing body of knowledge regarding surgical management strategies for poor-grade aSAH and seeks to enhance our understanding of the potential benefits and limitations of surgical interventions in this challenging patient population.

METHODS

The study complied to the ethical principles of the Declaration of Helsinki and was authorized by the University of Health Sciences Türkiye, Eskişehir City Hospital Non-Interventional Clinical Research Ethics Committee (decision no: ESH/GOEK-2023/45, date: 17.08.2023). All people who participated in this study have provided informed consent. Patient data were de-identified and handled in strict confidentiality to ensure privacy and compliance with data protection regulations. This study utilized a retrospective single-center analysis to comprehensively evaluate surgical outcomes in poor-grade intracranial aneurysm patients. The study aimed to navigate the challenges associated with the management of this patient population and provide insights into their surgical outcomes.

The study involved adult participants aged 18 years or older who met specific criteria: (1) confirmation of at least one intracranial aneurysm using cerebral computed tomography angiography (CTA) and/or digital subtraction angiography (DSA); (2) Initial clinical assessment upon admission classified as Hunt and Hess grades IV or V; and (3) Surgical intervention within 72 hours after the onset of coma.

Participants who met any of these criteria were excluded from the study: (1) non-aneurysmal subarachnoid hemorrhage (sSAH) or sSAH of unknown etiology, (2) patients with aneurysms in the posterior circulation, (3) patients categorized as Hunt and Hess grades I, II, or III at arrival, (4) patients who ultimately received endovascular treatment instead of surgical intervention, (5) patients who suffered rebleeding from a remaining aneurysm after prior surgery, (6) patient with severe comorbid disease that affects consciousness.

Patient data were collected retrospectively from electronic medical records, radiological reports, and surgical databases. The collected information included demographic characteristics, clinical presentation, imaging

findings, surgical details, postoperative problems, duration of hospitalization, and functional status at the following evaluations.

The primary outcome measures assessed in this study were functional outcomes, including neurological status and quality of life, evaluated at follow-up. Secondary outcome measures included perioperative complications, length of hospital stay, and mortality rates.

Statistical Analysis

We utilized statistical methods such as the t-test and chi-square test, when needed, to present a clear summary of the main characteristics of our study sample. To identify characteristics associated with the risk of mortality and duration of life, we utilized Cox proportional hazard analysis, univariate and multivariate logistic regression analysis, to identify characteristics associated with the risk of mortality and duration of life. All statistical analyses were conducted, and the results were found to be significant at a significance level of less than 0.05. SPSS was used for all statistical analyses.

RESULTS

The study comprised 102 individuals with spontaneous SAH, 73 of whom had aneurysmal SAH. Twenty-seven patients had a poor-grade clinical condition upon admission, comprising 14 males and 13 females (Table 1).

Regarding the severity of SAH, 27 patients had Hunt and Hess scores of grades 4 or 5, indicating a more severe clinical presentation. Additionally, 21 patients had Fisher grade 4, suggesting a higher degree of subarachnoid blood on imaging.

Table 1. A compilation of data on each patient's clinical condition, Fisher grade, specific type and timing of surgery and the subsequent outcomes after 6 months

Patient	H-H grade	Fisher grade	Location	Surgery	Time of surgery (hours)	Outcome (GOS)
1	4	4	MCA	Clipping	48	1
2	5	4	MCA	Clipping	<24 h	1
3	5	4	ICA	Wrapping	72	1
4	4	4	aCom	Clipping	<24 h	3
5	4	3	aCom	Clipping	48	4
6	5	4	MCA	Clipping	48	1
7	5	4	MCA	Clipping	<24 h	1
8	5	4	aCom	Clipping	<24 h	3
9	4	3	MCA	Clipping	48	5
10	5	4	MCA	Clipping	48	1
11	5	4	aCom	Clipping	<24 h	4
12	4	4	MCA	Clipping	<24 h	3
13	4	3	MCA	Clipping	<24 h	1
14	5	4	MCA	Clipping	<24 h	1
15	5	4	aCom	Clipping	72	1
16	4	3	aCom	Clipping	<24 h	2
17	4	3	MCA	Clipping	48	5
18	5	4	aCom	Clipping	<24 h	4
19	4	4	pCom	Clipping	<24 h	3
20	5	4	aCom	Clipping	72	5
21	5	4	MCA	Wrapping	<24 h	1
22	5	4	MCA	Clipping	48	1
23	4	3	pCom	Clipping	48	2
24	4	4	MCA	Clipping	<24 h	3
25	5	4	MCA	Clipping	<24 h	1
26	5	4	aCom	Clipping	<24 h	1
27	5	4	aCom	Clipping	<24 h	1

H-H: Hunt-Hess, GOS: Glasgow Outcome Scale, aCom: Anterior communicating artery, MCA: Middle cerebral artery, pCom: Posterior communicating artery, ICA: Internal carotid artery

Imaging techniques played a crucial role in the diagnosis and evaluation of aneurysms. Of the patients, 24 had their aneurysms detected by CTA, while 3 cases required DSA for detection, as CTA failed to identify these aneurysms. Importantly, all aneurysms detected by CTA were confirmed by subsequent DSA. The majority of aneurysms (14) were located in the middle cerebral circulation, followed by 10 in the anterior cerebral circulation and 3 in the ophthalmic artery.

Complications associated with the ruptured aneurysm included intraparenchymal hematoma in 9 patients and intraventricular hematoma in 7 patients.

Treatment strategies varied among the patients. Sixteen patients underwent surgical clipping within 24 hours of admission, while 21 patients required the insertion of an external ventricular drain (EVD). Among the surgical approaches, eight patients underwent a standard pterional craniotomy, and 19 patients underwent an extensive unilateral decompressive craniectomy. Aneurysm clipping was performed in 25 cases, while 2 patients underwent aneurysm wrapping.

Post-surgical complications included hydrocephalus, requiring ventriculoperitoneal shunt surgery in 7 patients, and the development of massive brain edema in 4 patients (Table 2).

Table 2. Basic characteristics of participants

Factors		Mean
Age		56
Follow-up		14
Gender	Male	14
	Female	13
Hunt-Hess	Grade 4	11
	Grade 5	16
Fisher	Grade 3	6
	Grade 4	21
Side	Left	9
	Right	5
	Midline	10
Vessels	ICA	1
	MCA	14
	aCom	10
	pCom	2
ICH		9
IVH		7
Craniectomy	Pterional	8
	Decompressive	19
Surgery	Clipping	25
	Wrapping	2
VPS		7
Timing of surgery	<24 h	16
	48	8
	72	3
Status	Alive	12
	Death	15

MCA: Middle cerebral artery, aCom: Anterior communicating artery, ICA: Internal carotid artery, pCom: Posterior communicating artery, ICH: Intracerebral hematoma, IVH: Intraventricula hematoma, VPS: Ventriculo-peritoneal shunt

The average duration of follow-up in this study was 14 months. Only a small number of patients, (4) exhibited a favorable functional outcome, indicating a low rate of recovery. Notably, the mortality rate at the six-month mark was substantial, with 51% of patients succumbing to their condition. Infection and massive brain edema were identified as the leading causes of death. Univariate regression analysis showed that older age was linked to an increased risk of mortality, with an odds ratio of 1.027 per year and a 94% confidence interval (CI). Conversely, factors such as gender, clinical status upon admission, Fisher grade, aneurysm location, parent vessel size, cerebral edema development, the existence of cerebral hemorrhage, and performing ultra-early surgical intervention did not have a significant impact on the likelihood of mortality.

Individuals with poor-grade acute SAH have an average survival length of 4.2 months with a standard deviation of 0.5 months. The survival rates at various times during the study were as follows: 0.783 (95% CI 0.731-0.971) at one month, 0.696 (95% CI 0.531-0.912) at two months, and 0.522 (95% CI 0.353-0.772) at six months of follow-up. These figures indicate a gradual decrease in survival rates over time, underscoring the challenging nature of this condition and the limited long-term prognosis for patients with poor-grade acute SAH.

Further analysis using univariate Cox regression showed that variables like patient age, gender, clinical condition at admission, Fisher scale score, parent vessel size, aneurysm location, severe edema occurrence, cerebral hemorrhage existence, and operation timing did not significantly impact patient survival time.

DISCUSSION

Severe clinical grades of aSAH are associated with significantly worse prognoses compared to milder clinical grades. The debate regarding the optimal timing and extent of surgical intervention in these patients has persisted for a long time.

Conservative therapy was preferred for severe aSAH before large intracerebral hematomas occurred (8). Studies have shown that performing rapid surgical removal of a blood clot and clipping of an aneurysm at the same session can lead to improved outcomes. Recent studies indicate that intensive surgical treatment is beneficial for those with severe cases of aSAH. Early surgery during the first three days after the seizure may improve functional outcomes. Some studies even suggest a technique for improving treatment outcomes called ultra-early surgery (done within 24 hours) (7,9,10). Nevertheless, death and morbidity rates continue to be high despite these encouraging findings. Advanced age and surgical scheduling (ultra-early vs. early) do not appear to have a substantial impact on the risk of death or the duration of survival (11-13). Different surgical approaches were employed, including standard pterional craniotomy and extensive unilateral decompressive craniectomy. The choice of the specific approach depended on the characteristics and needs of each patient (2,8). Aneurysm clipping was the primary surgical intervention in 25 cases, with aneurysm wrapping performed in 2 patients. These findings are consistent with the prevailing treatment options for intracranial aneurysms, which involve a combination of surgical techniques tailored to the individual patient's condition.

High intracranial pressure (ICP) often occurs in patients with severe aSAH and can be caused by various pathogenic mechanisms. Inserting an EVD is a routine procedure to manage elevated ICP and drain fluid from the ventricular system. EVD implantation is generally effective but poses risks like rebleeding and infection. It is crucial to carefully analyze the association between EVD insertion and the greater likelihood of aneurysm re-bleeding (14-16).

The initial clinical grade upon admission plays a crucial role in predicting overall outcomes in aSAH patients. While some studies argue against the predictive value of the initial clinical grade, others highlight its significant correlation with final outcomes. The widely used Hunt-Hess grading scale, based on the patient's clinical status, aids in evaluating aSAH patients. Incorporating clinical grading into outcome prognosis assists in treatment decision-making and realistic expectations for recovery.

The exceedingly complex pathological process that is aSAH is generally acknowledged. Its development is regulated by a number of pathophysiological pathways, and its clinical effects are highly variable, and subject to a variety of outside influences. The prognosis is still poor despite recent improvements, especially for patients with severe aSAH. Poor-grade aSAH patients who go untreated have an almost 100% mortality rate (6,17). However, some people can have positive functional outcomes with the right therapy. Such favorable outcomes were seen in 22% of the patients in our series. Lashkarivand et al. (2) reported that 21.9% of their patients were independent, which aligns with the current study's results. Regrettably, there is no universally accepted method to determine whether patients with low scores are expected to have a favorable result (18). Our analysis indicates that a prediction model may precisely evaluate the mortality risk for patients with aSAH by taking into account a number of features identified in our research. Wilby et al. (19) demonstrated that aggressive treatment for severe aSAH is both clinically essential and cost-effective. Considering that the management of a low-grade aSAH patient incurs double the cost of managing a good-grade aSAH patient, it is important to take into account the entire ongoing medical cost (20).

Age is often considered a significant factor in the prognosis of many diseases, including aSAH. As people age, they may have a higher risk of complications and slower recovery due to decreased physiological reserve and the presence of comorbidities. However, in our study, advanced age did not appear to have a substantial impact on the risk of death or the duration of survival. Some studies have suggested that women may have worse outcomes than men, possibly due to hormonal differences or differences in vascular anatomy (3,8,17). In our study, gender did not significantly impact patient survival time. This could be due to the relatively small sample size or the specific characteristics of the patient population.

CONCLUSION

This thorough assessment of surgical results in intracranial aneurysm patients provides insight into the intricate nature of this ailment and the related challenges. The study findings indicate a limited rate of positive recovery, substantial mortality at six months, and a gradual decrease in survival rates over time. Advanced age emerged as a significant risk factor for increased mortality, while other factors investigated did not exhibit substantial influences on patient outcomes. These results contribute to the existing literature on poor-grade SAH and emphasize the need for further research and advancements in the management of this challenging condition.

ETHICS

Ethics Committee Approval: The study complied to the ethical principles of the Declaration of Helsinki and was authorized by the University of Health Sciences Türkiye, Eskişehir City Hospital Non-Interventional Clinical Research

Ethics Committee (decision no: ESH/GOEK -2023/45, date: 17.08.2023).

Informed Consent: All people who participated in this study have provided informed consent.

FOOTNOTES

Authorship Contributions

Surgical and Medical Practices: M.B., H.M., S.E., Concept: M.B., H.M., S.E., Design: M.B., H.M., S.E., Data Collection or Processing: M.B., H.M., S.E., Analysis or Interpretation: M.B., H.M., S.E., Literature Search: M.B., H.M., S.E., Writing: M.B., H.M., S.E.

Conflict of Interest: No conflict of interest was declared by the authors.

Financial Disclosure: The authors declare that this study received no financial support.

REFERENCES

1. Hijdra A, Braakman R, Van Gijn J, Vermeulen M, Van Crevel H. Aneurysmal subarachnoid hemorrhage. Complications and outcome in a hospital population. Stroke. 1987;18:1061-7.
2. Lashkarivand A, Sorteberg W, Rosseland LA, Sorteberg A. Survival and outcome in patients with aneurysmal subarachnoid hemorrhage in Glasgow coma score 3-5. Acta Neurochir. 2020;162:533-44.
3. Hutchinson PJ, Power DM, Tripathi P, Kirkpatrick PJ. Outcome from poor grade aneurysmal subarachnoid haemorrhage which poor grade subarachnoid haemorrhage patients benefit from aneurysm clipping? Br J Neurosurg. 2000;14:105-9.
4. Shirao S, Yoneda H, Kunitsugu I, Ishihara H, Koizumi H, Suehiro E, et al. Preoperative prediction of outcome in 283 poor-grade patients with subarachnoid hemorrhage: a project of the Chugoku-Shikoku Division of the Japan Neurosurgical Society. Cerebrovasc Dis. 2010;30:105-13.
5. de Gans K, Nieuwkamp DJ, Rinkel GJ, Algra A. Timing of aneurysm surgery in subarachnoid hemorrhage: a systematic review of the literature. Neurosurgery. 2002;50:336-40.
6. Laidlaw JD, Siu KH. Ultra-early surgery for aneurysmal subarachnoid hemorrhage: outcomes for a consecutive series of 391 patients not selected by grade or age. J Neurosurg. 2002;97:250-8.
7. Roos Y, Beenen L, Groen R, Albrecht K, Vermeulen M. Timing of surgery in patients with aneurysmal subarachnoid haemorrhage: rebleeding is still the major cause of poor outcome in neurosurgical units that aim at early surgery. J Neurol Neurosurg Psychiatry. 1997;63:490-3.
8. Zubkov Y. Treatment of patients with intracranial arterial aneurysms in the haemorrhagic period. Neurol Res. 1994;16:6-8.
9. Nowak G, Schwachenwald R, Arnold H. Early management in poor grade aneurysm patients. Acta Neurochir. 1994;126:33-7.
10. Oda S, Shimoda M, Sato O. Early aneurysm surgery and dehydration therapy in patients with severe subarachnoid haemorrhage without ICH. Acta Neurochir. 1996;138:1050-6.
11. Pan J-W, Zhan R-Y, Wen L, Tong Y, Wan S, Zhou Y-Y. Ultra-early surgery for poor-grade intracranial aneurysmal subarachnoid hemorrhage: a preliminary study. Yonsei Med J. 2009;50:521-4.
12. Phillips TJ, Dowling RJ, Yan B, Laidlaw JD, Mitchell PJ. Does treatment of ruptured intracranial aneurysms within 24 hours improve clinical outcome? Stroke. 2011;42:1936-45.
13. Wong GKC, Boet R, Ng SCP, Chan M, Gin T, Zee B, et al. Ultra-early (within 24 hours) aneurysm treatment after subarachnoid hemorrhage. World Neurosurg. 2012;77:311-5.
14. Cha KC, Kim JH, Kang HI, Moon BG, Lee SJ, Kim JS. Aneurysmal rebleeding: factors associated with clinical outcome in the rebleeding patients. J Korean Neurosurg Soc. 2010;47:119-23.
15. Inagawa T. Ultra-early rebleeding within six hours after aneurysmal rupture. Surgical Neurol. 1994;42:130-4.
16. Rajshekhar V, Harbaugh R. Results of routine ventriculostomy with external ventricular drainage for acute hydrocephalus following subarachnoid haemorrhage. Acta Neurochir. 1992;115:8-14.
17. Bailes JE, Spetzler RF, Hadley MN, Baldwin HZ. Management morbidity and mortality of poor-grade aneurysm patients. J Neurosurg. 1990;72:559-66.
18. Le Roux PD, Elliott JP, Newell DW, Grady MS, Winn HR. The incidence of surgical complications is similar in good and poor grade patients undergoing repair of ruptured anterior circulation aneurysms: a retrospective review of 355 patients. Neurosurgery. 1996;38:887-93.
19. Wilby MJ, Sharp M, Whitfield PC, Hutchinson PJ, Menon DK, Kirkpatrick PJ. Cost-effective outcome for treating poor-grade subarachnoid hemorrhage. Stroke. 2003;34:2508-11.
20. Dodel R, Winter Y, Ringel F, Spottke A, Gharevi N, Müller I, et al. Cost of illness in subarachnoid hemorrhage: a German longitudinal study. Stroke. 2010;41:2918-23.

Medical Journal of Bakırköy

Med J Bakirkoy 2025;21:76-82
DOI: 10.4274/BMJ.galenos.2025.2024.11-7

Research

Effects of Scalp Block on Postoperative Analgesia in Craniotomy Surgery: A Prospective, Randomized Controlled, Double-Blind Study

Kraniyotomi Cerrahisinde Scalp Bloğunun Postoperatif Analjezi Üzerindeki Etkileri: Prospektif, Randomize Kontrollü, Çift Kör Bir Çalışma

Muhammed Halit Satıcı[1], Mahmut Sami Tutar[1], Betül Kozanhan[1], Yasin Tire[1], İlker Çöven[2], Nuray Altay[3]

[1]University of Health Sciences Türkiye, Konya City Hospital, Clinic of Anesthesiology and Reanimation, Konya, Türkiye

[2]University of Health Sciences Türkiye, Konya City Hospital, Clinic of Neurosurgery, Konya, Türkiye

[3]Harran University Faculty of Medicine, Department of Anesthesiology and Reanimation, Şanlıurfa, Türkiye

ABSTRACT

Objective: Postoperative pain following craniotomy is a significant concern, primarily resulting from surgical incisions and fixation devices. Effective pain management involves various strategies, including systemic analgesics, patient-controlled analgesia, and regional anesthesia techniques. Among regional anesthesia methods, the scalp block provides effective pain control by blocking the nerves innervating the scalp with local anesthetics. This study aimed to evaluate the effectiveness of the scalp block in reducing postoperative pain in craniotomy patients, assessed using the numerical rating scale (NRS).

Methods: Patients were divided into two groups: Group S, receiving the SCALP block, and group C, serving as the control group. Pain scores were recorded at 0, 2, 4, 6, 8, 12, and 24 hours postoperatively. Secondary outcomes included total amount of tramadol administered for rescue analgesia, time to first analgesia, postoperative nausea and vomiting (PONV) incidence, and patient satisfaction.

Results: Group S demonstrated significantly lower NRS scores than Group C at all measured time points ($p<0.001$). The median time to first rescue analgesia was 12 (8-12) hours in group S, while it was 0 (0-1) hours in group C ($p<0.001$). Tramadol consumption was significantly reduced in group S [75 (60-123) mg] compared to Group C [280 (220-280) mg; $p<0.001$].

Conclusion: The scalp block effectively manages postoperative pain, reduces analgesic requirements, and improves patient comfort. It also minimizes complications such as PONV, making it a valuable option for postoperative care following craniotomy.

Keywords: Craniotomy, numerical rating scale scores, rescue analgesia, scalp block

ÖZ

Amaç: Kraniyotomi sonrası postoperatif ağrı, öncelikli olarak cerrahi kesiler ve fiksasyon cihazlarından kaynaklanan önemli bir endişedir. Etkili ağrı yönetimi, sistemik analjezikler, hasta kontrollü analjezi ve bölgesel anestezi teknikleri dahil olmak üzere çeşitli stratejileri içerir. Bölgesel anestezi yöntemleri arasında scalp bloğu, kafa derisini innerve eden sinirleri lokal anesteziklerle bloke ederek etkili ağrı kontrolü sağlar. Bu çalışmanın amacı, kraniyotomi hastalarında postoperatif ağrıyı azaltmada scalp bloğunun etkinliğini, sayısal derecelendirme ölçeği (NRS) kullanılarak değerlendirmektir.

Gereç ve Yöntem: Hastalar iki gruba ayrıldı: Scalp bloğu alan grup S ve kontrol grubu olarak görev yapan grup C. Ağrı skorları postoperatif 0, 2, 4, 6, 8, 12 ve 24. saatlerde kaydedildi. İkincil sonuçlar kurtarma analjezik kullanımı olarak uygulanan toplam tramadol miktarı, ilk analjeziye kadar geçen süre, ameliyat sonrası bulantı ve kusma (PONV) insidansı ve hasta memnuniyeti yer almaktadır.

Bulgular: Grup S, ölçülen tüm zaman noktalarında grup C'den önemli ölçüde daha düşük NRS skorları gösterdi ($p<0,001$). İlk kurtarma analjezisine kadar geçen medyan süre grup S'de 12 (8-12) saat iken, grup C'de 0 (0-1) saatti ($p<0,001$). Tramadol tüketimi grup S'de [75 (60-123) mg] grup C'ye [280 (220-280) mg; $p<0,001$] kıyasla önemli ölçüde azaldı.

Sonuç: Scalp bloğu ameliyat sonrası ağrıyı etkili bir şekilde yönetir, analjezik gereksinimlerini azaltır ve hasta konforunu artırır. Ayrıca PONV gibi komplikasyonları da en aza indirir ve bu da onu kraniyotomi sonrası ameliyat sonrası bakım için değerli bir seçenek haline getirir.

Anahtar Kelimeler: Kraniyotomi, sayısal derecelendirme skalası, kurtarma analjezisi, scalp blok

Address for Correspondence: Muhammed Halit Satıcı, University of Health Sciences Türkiye, Konya City Hospital, Clinic of Anesthesiology and Reanimation, Konya, Türkiye

E-mail: halit_satici@hotmail.com **ORCID ID:** orcid.org/0009-0005-0652-3624

Cite as: Satıcı MH, Tutar MS, Kozanhan B, Tire Y, Çöven I, Altay N. Effects of SCALP block on postoperative analgesia in craniotomy surgery: a prospective, randomized controlled, double-blind study. Med J Bakirkoy. 2025;21:76-82

Received: 28.12.2024
Accepted: 14.01.2025
Publication Date: 25.03.2025

INTRODUCTION

Craniotomy procedures are frequently associated with considerable postoperative pain that may result in hemodynamic disturbances, impaired sleep quality, and prolonged hospital stays (1,2). Pain-induced physiological responses include elevated blood pressure, intracranial pressure, heart rate, and increased morbidity and mortality risks (3,4). While opioids are commonly employed for managing such pain, their use is associated with various adverse effects, such as delayed recovery, sedation, nausea, vomiting, and difficulties in conducting accurate neurological assessments (5). The scalp block, a regional analgesia technique, has gained prominence for its effectiveness in reducing postoperative pain and maintaining hemodynamic stability during neurosurgical interventions (6,7). This method has been recognized as a critical component of multimodal analgesia strategies aimed at controlling pain and mitigating physiological stress responses triggered by surgical trauma (1,3,8-10). Given these challenges and the potential advantages of the scalp block, further investigation is needed into its efficacy in optimizing postoperative pain management and reducing associated complications in craniotomy patients.

This study hypothesizes that implementing the scalp block can significantly lower numerical rating scale (NRS) scores and decrease postoperative analgesic consumption. The primary focus is to evaluate its influence on NRS scores, with secondary objectives including the time to first rescue analgesic administration, total rescue analgesia required, patient satisfaction levels, and the incidence of nausea and vomiting.

METHODS

Ethics Approval and Registration

Ethical approval for the study was obtained from the Clinical Research Ethics Committee of the Harran University (decision no: HRÜ/24.13.01, date: 09.09.2024). It was registered on ClinicalTrials.gov (Identifier: NCT06588751) and conducted in accordance with the 2013 revision of the Declaration of Helsinki and the Consolidated Standards of Reporting Trials guidelines (11). Prior to randomization, all participants provided both written and verbal informed consent. Participants were subsequently allocated randomly into one of two groups: Group S, which received the scalp block, or group C, which was managed with multimodal analgesia.

Patient Population and Inclusion/Exclusion Criteria

The study population consisted of patients aged 18 to 65 years who underwent craniotomy under general anesthesia, and were categorized with an American Society of Anesthesiologists (ASA) physical status classification of I-III. Criteria for exclusion included individuals with contraindications to regional anesthesia, altered consciousness levels, coagulation abnormalities, anti-coagulant therapy, known hypersensitivity to local anesthetics, active infections at the injection site, chronic pain syndromes, or pregnancy.

Randomization

This study was a prospective, randomized, controlled, double-blind, multicenter trial. Patients were allocated to two primary groups using a randomization process managed by an anesthesiologist at each clinic, who utilized these opaque, sealed envelopes to ensure allocation concealment. Group S consisted of patients who received the scalp block, while Group C included those managed with multimodal analgesia alone. To uphold blinding and reduce bias, the anesthesiologists managing the randomization process were excluded from involvement in other parts of the study, and the clinicians performing the scalp block were similarly not involved in data collection or analysis. Additionally, the participants, the interventionist, and the data analyst remained blinded to group assignments. Two anesthesia specialists independently recorded primary and secondary postoperative outcomes.

Standard Anesthesia, and Multimodal Analgesia Protocol

Pulse oximetry, electrocardiography, non-invasive blood pressure, and end-tidal carbon dioxide measurements, were used for monitoring all patients, and standard anesthesia protocols were followed. A 20-gauge intravenous (IV) cannula was inserted, and isotonic fluid therapy was initiated. General anesthesia was initiated using IV midazolam (1 mg), propofol (2 mg/kg), fentanyl (1.5 mcg/kg), and rocuronium (0.6 mg/kg). Maintenance of anesthesia was achieved with remifentanil (0.05-0.1 mcg/kg/min) and propofol (4-12 mg/kg/h), adjusted to maintain hemodynamic stability. All patients underwent the same surgical procedure. All patients were extubated upon completion of the surgical procedure.

Postoperatively, IV morphine (3 mg) was administered, along with 1 g of paracetamol and 8 mg of dexamethasone, prior to the patient's transfer to the intensive care unit (ICU). In the ICU, paracetamol (1 g IV every 8 hours) and tenoxicam (20 mg IV every 12 hours) were given, with tramadol (1 mg/kg IV), provided for NRS scores ≥4. Ondansetron (4 mg IV) was used as needed for nausea and vomiting.

Scalp Block Procedure

After the surgical procedure, patients in group S were placed in a partially seated position. The skin was cleansed

using 5% povidone-iodine for antisepsis and covered with a sterile drape. Each target nerve, including the supraorbital, supratrochlear, zygomaticotemporal, auriculotemporal, greater auricular, greater occipital, and lesser occipital nerves, was injected with 2 mL of 0.25% bupivacaine. These nerves provide sensory innervation to the forehead and scalp. The circumferential scalp block was performed bilaterally with a cumulative dose of 28 mL of 0.25% bupivacaine.

The supratrochlear and supraorbital nerves were anesthetized near the brow, specifically at the superior medial orbital margin and over the palpable supraorbital notch. The zygomaticotemporal nerve was targeted at the posterior edge of the zygomatic arch. The auriculotemporal and greater auricular nerves were blocked at the tragus, adjacent to the pulsating superficial temporal artery, and at the mastoid process. Lastly, the greater and lesser occipital nerves were anesthetized at the medial and lateral portions of the superior nuchal line.

Outcome Measures

The primary outcome was the evaluation of postoperative pain levels, assessed using the NRS, where 0 represents no pain and 10 indicates the worst imaginable pain. Pain scores were documented at 0, 2, 4, 6, 8, 12, and 24 hours post-surgery.

Secondary outcomes included the total amount of tramadol administered as rescue analgesia, the time elapsed before the first dose of rescue analgesics, the requirement for antiemetic medication, the incidence of postoperative nausea and vomiting (PONV), and patient satisfaction levels.

Demographic and clinical characteristics, including age, sex, weight, height, duration of surgery, and ASA classification, were recorded for both groups. Patient satisfaction was evaluated using a 5-point Likert scale, with 1 signifying "completely dissatisfied" and 5 indicating "completely satisfied".

Statistical Analysis

The main objective of this study was to evaluate and compare the NRS scores of the two groups 4 hours after surgery. Based on previous research, a reduction of 2 points in NRS scores between groups was deemed clinically significant for determining the required sample size (12). Preliminary data from a study involving 10 patients undergoing craniotomy who received multimodal analgesia as part of the control group indicated a mean NRS score of 5.5±1.7 at 4 hours postoperatively. Using these findings, an Independent Samples t-test model was applied with a Cohen's D effect size of 1.176. This analysis determined that a minimum of 17 patients per group would be required to achieve 95% statistical power, with an alpha error threshold of 5%. To account for potential dropouts, the final sample size was increased to 20 patients per group, resulting in 40 participants.

The data in this study were analyzed using IBM SPSS Statistics software, version 26.0. The Shapiro-Wilk test was applied to evaluate the normality of the data distribution. Continuous variables were expressed as mean ± standard deviation or as median with interquartile ranges (25^{th}-75^{th} percentiles) based on their distribution. Categorical variables were summarized as frequencies and percentages. For the analysis of continuous variables, the Independent Samples Student's t-test was employed when parametric assumptions were satisfied. When these assumptions were not satisfied, the Mann-Whitney U test was applied. Categorical data were analyzed using Fisher's exact test or the chi-square test. Analysis of Variance was applied to repeat measurements across different time points. Statistical significance was defined as $p<0.05$ for all analyses.

RESULTS

At the outset of the study, 45 patients were screened for eligibility. Five patients opted not to participate and were subsequently excluded. The remaining 40 participants were randomized and managed according to the established study protocol, with equal allocation to the two groups (group C: n=20; group S: n=20) (Figure 1).

The baseline characteristics, such as patient demographics and the duration of surgery, showed no significant differences between the two groups (Table 1).

Primary Outcome

Throughout the first 24 hours after surgery, group C exhibited higher NRS scores than group S at all time points. This difference was statistically significant at the 0, 2, 4, 6, 8, 12, and 24 hours ($p<0.001$) (Figure 2).

Rescue Analgesia Requirement

All patients in group C required rescue analgesia, while four patients in group S did not need it ($p<0.001$). Group C had significantly higher total tramadol consumption within 24 hours [280 (220–280) mg vs. 75 (60–123) mg, $p<0.001$] and a shorter time to the first use of rescue analgesics [0 (0-1) hours vs. 12 (8-12) hours, $p<0.001$]. Significant differences in rescue analgesia were also observed across the time intervals "0-6", "12–24", and "0-24" ($p<0.001$ for all, Table 2).

Adverse Events, Analgesic Characteristics, and the Likert Scale

Throughout the first 24 hours after surgery, PONV occurred in 17 patients (85%) in group C and 4 patients (20%) in group S, with this difference reaching statistical significance (p<0.001). The need for anti-emetic treatment was also notably lower in group S compared to group C (4 patients vs. 17 patients, p<0.001). Additionally, patient satisfaction scores, measured using the Likert scale, were significantly higher in group S, with a median score of 5 (4-5) compared to 2 (2-2) in group C (p<0.001) (Table 3).

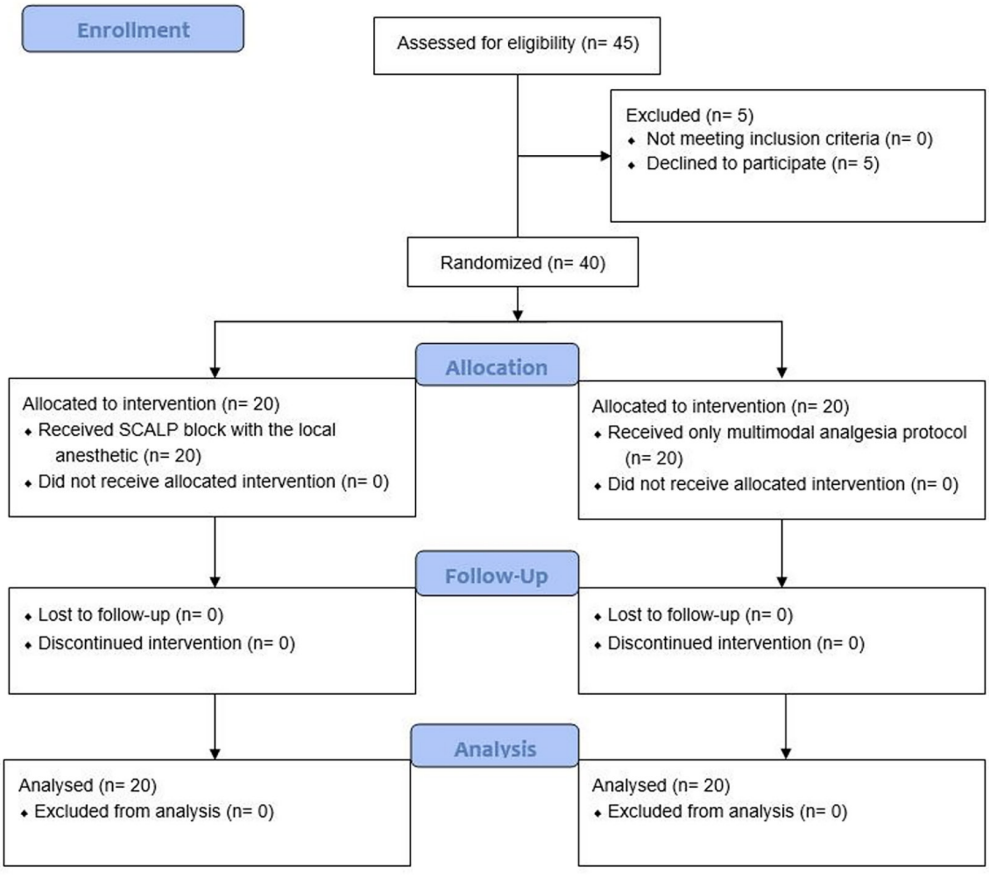

Figure 1. Consolidated standards of reporting trials flow study diagram describing patients' progress through the study

Table 1. Baseline characteristics by groups

Factors	Group C (n=20)	Group S (n=20)	p-value
Age (yr)	51±16	48±17	0.656
Female	9 (45%)	10 (50%)	1
Smoking	4 (20%)	8 (40%)	0.300
Coronary artery disease	2 (10%)	3 (15%)	1
Hypertension	6 (30%)	9 (45%)	0.513
Lung disase	3 (15%)	2 (10%)	1
Height (cm)	168.7±7.2	168.5±8.6	0.921
Weight (kg)	69±6.5	71±12.5	0.540
Surgery time (min)	170±48.1	159.8±30.9	0.428

Data presented as mean ± standard deviation, median (Q1-Q3), or n (%)
yr: year, cm: Centimeter, kg: Kilogram, min: Minutes

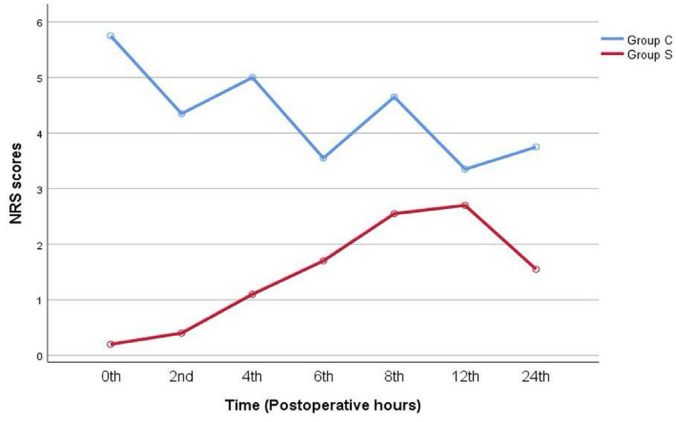

Figure 2. Postoperative numerical rating scores
NRS: Numerical rating scale

Table 2. Postoperative rescue analgesic characteristics among groups

Factors	Group C (n=20)	Group S (n=20)	p-value
First rescue analgesic time (h)	0 (0-1)	12 (8-12)	<0.001
Tramadol consumption (mg)	280 (220-280)	75 (60-123)	<0.001
Rescue analgesic usage, time frame (h)			
0-6	20 (100%)	2 (10%)	<0.001
6-12	20 (100%)	16 (80%)	0.122
12-24	15 (75%)	4 (20%)	<0.001
0-24	20 (100%)	16 (80%)	<0.001

Data are presented as median (Q1-Q3), n (%)
h: Hour, mg: Milligram

Table 3. Comparison of incidence of adverse effects, anti-emetic drug usage, and the likert scale

Factors	Group C (n=20)	Group S (n=20)	p-value
PONV	17 (85%)	4 (20%)	<0.001
The need for antiemetic drug	17 (85%)	4 (20%)	<0.001
Likert scale	2 (2-2)	5 (4-5)	<0.001

Data presented as median (Q1-Q3) or n (%)
PONV: Postoperative nausea and vomiting

DISCUSSION

In this study, patients who underwent a scalp block demonstrated significantly lower postoperative pain scores, reduced rescue analgesic requirements, a decreased incidence of PONV, and a diminished need for antiemetic medications. Additionally, the time to the first analgesic administration was significantly extended, and patient satisfaction levels were higher in this group.

Approximately 80% of patients undergoing craniotomy are believed to endure moderate to severe pain following the procedure (13). Unmanaged acute postoperative pain can trigger physiological responses such as increased heart rate, which may exacerbate myocardial ischemia and hypoxia, thereby elevating the risk of cardiovascular complications (14). Moreover, poorly managed pain during the early postoperative phase increases the likelihood of chronic pain development. Despite advancements in anesthesia and pain management, postoperative analgesia in craniotomy patients remains suboptimal. This is partly attributed to the side effects of frequently used analgesics, such as opioids, which may cause excessive sedation, respiratory depression, and prolonged recovery times. These limitations highlight the challenges of achieving effective pain control in neurosurgical patients (1). Additionally, postoperative pain management in this patient group is particularly challenging due to various neurosurgical complications; such as intracranial bleeding, increased intracranial pressure, cerebral ischemia, seizures, hypertension, air embolisms, cranial nerve injuries, and brain tissue swelling (15).

Earlier research has shown that regional scalp nerve blocks are effective in alleviating postoperative pain and decreasing opioid use in patients undergoing craniotomy. Notably, the preoperative administration of regional scalp nerve blocks has been shown to lower pain scores for up to 16 hours postoperatively (16). These blocks function by inhibiting sodium channels in nerve cell membranes, thereby reducing nerve excitability and conductivity. This mechanism not only mitigates stress responses triggered by surgical trauma but also decreases the need for anesthetic agents. By reducing pain and improving surgical outcomes, scalp nerve blocks enhance rehabilitation and decrease the likelihood of adverse effects (17).

In this study, patients administered a scalp block consistently reported lower pain scores during the first 24 hours after surgery. Additionally, these patients consumed less rescue analgesia and experienced a prolonged time to the first analgesic requirement, often ranging from 8 to 12 hours. These findings suggest that the scalp block is effective for early and late postoperative pain management.

Studies evaluating scalp block recipients have reported significant reductions in anesthetic agent dosages, decreased adverse reactions and complications, and consistently lower pain scores during various postoperative stages (17-19). Furthermore, the reduction in opioid consumption observed in this study not only decreases the risk of dependence but also minimizes opioid-related side effects, such as nausea, sedation, and respiratory depression. The absence of these adverse effects underscores the safety and clinical benefits of the scalp block. Consistent with prior research, patients in this study who received a scalp block exhibited lower maximum NRS scores and required fewer anti-emetics during the first 12 hours postoperatively. However, the total rescue analgesic dosage administered within 24 hours did not differ significantly in certain studies (20).

In the present study, tramadol consumption was significantly lower in the scalp block group compared to the control group. Moreover, nausea or vomiting was reported in only four patients in this group, a finding likely attributable to the reduced opioid usage. The low incidence of PONV further contributed to higher satisfaction scores. Combining a scalp block with systemic analgesics like paracetamol, nonsteroidal anti-inflammatory drugs, and adjunctive

therapies like dexmedetomidine infusion; along with opioids reserved for rescue analgesia, appears to optimize pain control while minimizing side effects in craniotomy patients (21).

One study noted that patients receiving a scalp block without incorporating a multimodal analgesia protocol did not achieve expected outcomes such as reduced pain scores, lower rescue analgesia use, or decreased PONV incidence (22). In this study, the combination of a scalp block with paracetamol and nonsteroidal anti-inflammatory drugs, while reserving tramadol for rescue analgesia, proved to be a practical multimodal approach for postoperative pain control.

Study Limitations

The study only investigated the effects of the scalp block within the initial 24-hour postoperative period. Previous research indicates that postoperative pain is most severe within the first 24 hours following surgery, and effective pain management during this critical window significantly impacts patient recovery, satisfaction, and overall clinical outcomes (1,23). For this reason, our analysis focused exclusively on the first 24 hours. Moreover, the inclusion of various indications for craniotomy, such as cranial masses and intracranial hematomas, may have introduced heterogeneity in the patient population. Future research should explore the influence of the scalp block on long-term recovery outcomes and its impact on patients' overall quality of recovery.

CONCLUSION

The scalp nerve block has demonstrated significant effectiveness in enhancing patient comfort and improving pain management in the postoperative period. Moreover, its ability to reduce undesirable side effects (e.g., nausea and vomiting), lowers the need for analgesic consumption, and enhance patient satisfaction underscores its clinical efficacy and positive contribution to patient-centered care. Based on these findings, the scalp nerve block is recommended as a preferred analgesic approach, particularly for procedures associated with significant postoperative pain, such as craniotomy.

ETHICS

Ethics Committee Approval: Ethical approval for the study was obtained from the Clinical Research Ethics Committee of the Harran University (decision no: HRÜ/24.13.01, date: 09.09.2024).

Informed Consent: Prior to randomization, all participants provided both written and verbal informed consent.

FOOTNOTES

Authorship Contributions

Surgical and Medical Practices: M.H.S., M.S.T., Concept: M.H.S., B.K., Design: M.H.S., Y.T., Data Collection or Processing: M.H.S., İ.Ç., N.A., Analysis or Interpretation: M.H.S., M.S.T., Literature Search: M.H.S., B.K., Writing: M.H.S., N.A.

Conflict of Interest: We declare that no conflict of interest exists for any of the authors.

Financial Disclosure: The authors declared that this study received no financial support.

REFERENCES

1. Guilfoyle MR, Helmy A, Duane D, Hutchinson PJA. Regional scalp block for postcraniotomy analgesia: a systematic review and meta-analysis. Anesth Analg. 2013;116:1093-102.
2. Hansen MS, Brennum J, Moltke FB, Dahl JB. Pain treatment after craniotomy: where is the (procedure-specific) evidence? A qualitative systematic review. Eur J Anaesthesiol. 2011;28:821-9.
3. Tuchinda L, Somboonviboon W, Supbornsug K, Worathongchai S, Limutaitip S. Bupivacaine scalp nerve block: hemodynamic response during craniotomy, intraoperative and post-operative analgesia. Asian Biomedicine. 2010;4:243-51.
4. Saha P, Chattopadhyay S, Rudra A, Roy S. Pain after craniotomy: A time for reappraisal? Indian Journal of Pain. 2013;27:7-11.
5. Nguyen A, Girard F, Boudreault D, Fugère F, Ruel M, Moumdjian R, et al. Scalp nerve blocks decrease the severity of pain after craniotomy. Anesth Analg. 2001;93:1272-6.
6. Papangelou A, Radzik BR, Smith T, Gottschalk A. A review of scalp blockade for cranial surgery. J Clin Anesth. 2013;25:150-9.
7. Kim HS, Lee SJ, Kim CS, Kim JT. Effect of triamcinolone added to scalp nerve block for postoperative pain management of Moyamoya disease. Korean J Anesthesiol. 2011;61:173-4.
8. Ayoub C, Girard F, Boudreault D, Chouinard P, Ruel M, Moumdjian R. A comparison between scalp nerve block and morphine for transitional analgesia after remifentanil-based anesthesia in neurosurgery. Anesth Analg. 2006;103:1237-40.
9. Pinosky ML, Fishman RL, Reeves ST, Harvey SC, Patel S, Palesch Y, et al. The effect of bupivacaine skull block on the hemodynamic response to craniotomy. Anesth Analg. 1996;83:1256-61.
10. Chaki T, Sugino S, Janicki PK, Ishioka Y, Hatakeyama Y, Hayase T, et al. Efficacy and safety of a lidocaine and ropivacaine mixture for scalp nerve block and local infiltration anesthesia in patients undergoing awake craniotomy. J Neurosurg Anesthesiol. 2016;28:1-5.
11. Moher D, Hopewell S, Schulz KF, Montori V, Gøtzsche PC, et al. CONSORT 2010 explanation and elaboration: updated guidelines for reporting parallel group randomised trials. BMJ. 2010;340:869.
12. Salaffi F, Stancati A, Silvestri CA, Ciapetti A, Grassi W. Minimal clinically important changes in chronic musculoskeletal pain intensity measured on a numerical rating scale. Eur J Pain. 2004;8:283-91.
13. Moharari RS, Emami P, Neishaboury M, Sharifnia SH, Kianpour P, Hatam M, et al. Scalp nerve block for enhanced pain control and analgesic optimization in elective craniotomy: a randomized controlled trial with analgesia nociception index monitoring. World Neurosurg. 2024;189:e55-e60.

14. Haldar R, Kaushal A, Gupta D, Srivastava S, Singh PK. Pain following craniotomy: reassessment of the available options. Biomed Res Int. 2015;2015:509164.
15. Hwang JY, Bang JS, Oh CW, Joo JD, Park SJ, Do SH, et al. Effect of scalp blocks with levobupivacaine on recovery profiles after craniotomy for aneurysm clipping: a randomized, double-blind, and controlled study. World Neurosurg. 2015;83:108-13.
16. Stieger A, Romero CS, Andereggen L, Heisenberg D, Urman RD, Luedi MM. Nerve blocks for craniotomy. Curr Pain Headache Rep. 2024;28:307-13.
17. Zhang Y, He K, Chen L, Ji K, Zhang Z, Wang W. Role of scalp nerve block in improving the quality of rehabilitation in patients after meningioma resection: A randomized controlled clinical trial. Medicine (Baltimore). 2024;103:38324.
18. Altaf I, Banday J, Naaz S, Ozair E, Punetha P, Challam KS. A randomized control trial on comparative effect of scalp nerve block using levobupivacaine versus fentanyl on the attenuation of pain and hemodynamic response to pin fixation. Bali J Anaesthesio. 2021;5:66-71.
19. Moharari RS, Emami P, Neishaboury M, Sharifnia SH, Kianpour P, Hatam M, et al. Scalp nerve block for enhanced pain control and analgesic optimization in elective craniotomy: a randomized controlled trial with analgesia nociception index monitoring. World Neurosurg. 2024;189:55-60.
20. Lee EK, Lee S, Kwon JH, Lee SH, Park SJ, Kim Y, et al. The efficacy of scalp nerve block in postoperative pain management after microvascular decompression: a randomized clinical trial. J Clin Med. 2023;12:4242.
21. Mestdagh FP, Lavand'homme PM, Pirard G, Joshi GP, Sauter AR, Van de Velde M. PROSPECT working group* of the european society of regional anaesthesia and pain therapy (ESRA). Pain management after elective craniotomy: A systematic review with procedure-specific postoperative pain management (PROSPECT) recommendations. Eur J Anaesthesiol. 2023;40:747-57.
22. Kitsiripant C, Boonyamarn A, Oofuvong M, Prathep S, Kaewborisutsakul A. Cost-effectiveness and efficacy of scalp block for elective supratentorial craniotomy in resource-limited settings: A randomized controlled trial. Surg Neurol Int. 2024;15:191.
23. Song J, Li L, Yu P, Gao T, Liu K. Preemptive scalp infiltration with 0.5% ropivacaine and 1% lidocaine reduces postoperative pain after craniotomy. Acta Neurochir (Wien). 2015;157:993-8.

Medical Journal of Bakırköy

Med J Bakirkoy 2025;21:83-89
DOI: 10.4274/BMJ.galenos.2024.2024.8-3

Research

Anatomical Study of Bile Ducts by Magnetic Resonance Cholangiopancreatography

Safra Kanallarının Manyetik Rezonans Kolanjiyopankreatografi ile Anatomik Değerlendirmesi

Tahir Fatih Dikici[1], Zeliha Fazlıoğulları[2], Ayşe Gamze Özcan[2], Mustafa Koplay[3], Ahmet Kağan Karabulut[2], İsmihan İlknur Uysal[4], Nadire Ünver Doğan[2]

[1]Alanya Alaaddin Keykubat University, Vocational School of Health Services, Department of Therapy and Rehabilitation, Antalya, Türkiye
[2]Selçuk University Faculty of Medicine, Department of Anatomy, Konya, Türkiye
[3]Selçuk University Faculty of Medicine, Department of Radiology, Konya, Türkiye
[4]Necmettin Erbakan University Meram Faculty of Medicine, Department of Anatomy, Konya, Türkiye

ABSTRACT

Objective: A variety of anatomical variations in the intrahepatic and extrahepatic bile ducts (BD) may cause different problems during surgical intervention. Therefore, the objective of this study was to investigate the prevalence and types of anatomical variations in BD in normal patients.

Methods: The present study evaluated magnetic resonance cholangiopancreatography (MRCP) images of 303 patients (146 men, 157 women). The objective of this study was to evaluate variations in the intrahepatic and extrahepatic BD and anatomical variations in the gallbladder. The biliary confluence angle, diameter of the common BD prior to its union with the pancreatic duct, diameter of the duct formed by their junction, and length of the short cystic duct (CD) were also evaluated.

Results: In this study, anomaly of the right posterior duct opening to the left hepatic duct (HD) was found in 12 cases (4%), trifurcation variation in 26 cases (8.6%), and abnormal variation of the aberrant right HD opening to the common HD in 15 cases (5%). Corresponding to the CD, a long CD variation was found in 20 cases (6.6%) and a short cystic channel variation in 7 cases (2.3%). In addition, a negative correlation was found between age and angle of confluence. A significant correlation was found between long CD variation and stone formation.

Conclusion: Anatomic investigation of the BD using the non-invasive MRCP technique and the definition of variations are of great importance in terms of assisting surgical planning, minimizing the likelihood of complications during operations, and facilitating transplantation surgery.

Keywords: Bile ducts, cholangiopancreatography, variation

ÖZ

Amaç: İntrahepatik ve ekstrahepatik safra kanallarında (BD) görülebilen çeşitli anatomik varyasyonlar, cerrahi girişimlerde değişik problemlere yol açabilmektedir. Bu nedenle çalışmamızda normal olgularda BD'nin anatomik varyasyonlarının görülme sıklığını ve tiplerini araştırmayı amaçladık.

Gereç ve Yöntem: Çalışmada manyetik rezonans kolanjiyopankreatografi (MRCP) çekilen 303 olgunun (146 erkek, 157 kadın) görüntüleri değerlendirmiştir. Bu olgularda intrahepatik ve ekstrahepatik BD'nin varyasyonları ile safra kesesinin anatomik varyasyonları belirlenmiştir. Ayrıca biliyer konfluens açısı, ductus choledochus'un ductus pancreaticus ile birleşmeden önceki çapı ve birleşimi ile oluşan kanalın çapı ve kısa sistik kanal uzunluğu ölçülmüştür.

Bulgular: Çalışmada 12 olguda (%4) ductus hepaticus sinister'e açılan ductus segmentalis posterior dexter anomalisi, 26 olguda (%8,6) trifurkasyon varyasyonu, 15 olguda (%5) ductus hepaticus communis'e açılan aberran sağ hepatik kanal varyasyonu belirlendi. Yirmi olguda (%6,6) uzun sistik kanal varyasyonu, 7 olguda (%2,3) kısa sistik kanal varyasyonu tespit edildi. Ayrıca yaş ile konfluens açısı arasında negatif yönde bir ilişki, uzun sistik kanal varyasyonu ile taş oluşumu arasında anlamlı ilişki olduğu bulunmuştur.

Sonuç: Günümüzde kullanılan MRCP tekniği ile non-invaziv olarak BD'nin anatomik değerlendirmesi ve varyasyonlarının belirlenmesi; cerrahi planlamaya yardımcı olması, operasyonlar sırasında oluşabilecek komplikasyonların en aza indirilmesi ve transplantasyon cerrahisinde yardımcı olması yönünden önemlidir.

Anahtar Kelimeler: Safra yolları, kolanjiopankreatografi, varyasyon

Address for Correspondence: Zeliha Fazlıoğulları, Selçuk University Faculty of Medicine, Department of Anatomy, Konya, Türkiye
E-mail: z_topal@yahoo.com; ztopal@selcuk.edu.tr **ORCID ID:** orcid.org/0000-0002-5103-090X

Cite as: Dikici TF, Fazlıoğulları Z, Özcan AG, Koplay M, Karabulut AK, Uysal İİ, et al. Anatomical study of bile ducts by magnetic resonance cholangiopancreatography. Med J Bakirkoy. 2025;21:83-89

Received: 13.09.2024
Accepted: 21.10.2024
Publication Date: 25.03.2025

INTRODUCTION

Bile is produced in the liver and transported to the duodenum via the bile ducts (BD). The ducts are divided into two categories: Intrahepatic and extrahepatic BD. The BD up to the porta hepatis is designated as intrahepatic BD, whereas the BD after the porta hepatis is classified as extrahepatic BD (1). The anatomy of the intrahepatic BD was consistent with the segmental anatomy of the liver, as defined by the Couniaud classification. The two channels are formed by the union of the segmental ducts. Of these channels, the right hepatic duct (HD) drains the right lobe of the liver and the right half of the caudate lobe, while the left HD drains the left lobe of the liver, the quadrate lobe, and the left half of the caudate lobe. The fusion of these two channels forms the common HD. In addition, the angle formed at the junction of these two channels is referred to as the biliary confluency angle (2). The common BD is formed by the opening of the cystic duct (CD) into the common HD, occurring approximately in the middle portion of the porta hepatis and the ampulla of Vater. The common BD joins with the pancreatic duct (PD) and opens into the second duodenum section. The incidence of normal anatomy of the biliary system is 58% (3). The gallbladder and BD are formations that exhibit considerable variations and anomalies and have close connections in their vicinity. These situations may present challenges for surgeons. The variation in the branching of BD ranges from 24% to 37%. BD variations can be grouped according to their location, including those found at the hepatic bifurcation, CD, and pancreatobiliary junction, as well as other less common variations (4-6). Therefore, surgeons who will be working in the region should be well-versed in the anatomy and variations of this region and exercise caution in the presence of potential discrepancies (7). Magnetic resonance cholangiopancreatography (MRCP) is a magnetic resonance imaging (MRI) technique using the T2 sequence to permit the non-invasive evaluation of the anatomy and pathologies of the pancreaticobiliary system. This method enables rapid, accurate, and non-complication evaluation of the BD without the use of contrast material (8). Anatomical variations in intra-or extrahepatic BD can cause various problems during surgical procedures. It is important to know the formation patterns and anatomical variations of BD to minimize complications that may occur during surgery and to prevent possible errors that may occur during radiological evaluation. In this study, we aimed to investigate the frequency and types of anatomical variations in BD in normal patients.

METHODS

The study included images from 615 patients who underwent MRCP at the Department of Radiology between 2014 and 2016. Ethical approval for the study was obtained from the Local Ethics Committee of the Selçuk University Faculty of Medicine (approval no: 2015/312, date: 08.12.2015). MRCP examinations were performed using standard body perception with a 1.5 Tesla power MRI unit (Magnetom Aera, Siemens, Erlangen, Germany). These examinations were performed with patients fasting for at least 5-6 hours to ensure gallbladder filling and gastrointestinal emptying. T2-weighted images were acquired as a sequence using the 2-dimensional single-shot fast spin echo technique. Evaluation was performed using maximum intensity projection images in the coronal and axial planes. Of the 615 retrospectively reviewed images, 312 patients were excluded from the study if they had undergone surgery to the liver, pancreas, gallbladder, or duodenum, if the anatomic reference points could not be followed due to tumor, or if optimal imaging was not possible. The MRCP images of the remaining 303 patients were analyzed. In these examinations, age, sex, presence or absence of stones in the biliary system, presence of variation at various levels, dilatation, and diameter of the common BD were examined. The following criteria were used to evaluate the identified variations: Variations defined at the level of bifurcation: An anomalous aberrant right HD variation in which the right posterior duct opens directly to common HD or CD; trifurcation variation formed by the right posterior duct at the junction level of the right anterior duct and left HD and the right posterior duct. This is an anomaly of the right posterior duct draining into the left HD.

The opening of the CD into the extrahepatic BD from the left side was defined as medial insertion, the opening of the extrahepatic BD from the distal 1/3 was defined as long CD or distal insertion, and the length of the CD 5 mm was defined as short CD variation. The length of the CD was measured, and short CD variations were found and recorded. The upper localization variation of the gallbladder was defined as when the conditions of at least 1/2 of the gallbladder above the level of the portal hilus, the fundus directed upward, and the CD directed cranially along its course were met. The localization of the transfer was defined by the long axis of the gallbladder perpendicular to the long axis of the common BD and the fundus being in the same plane as the infundibulum in the axial sections. In addition, the appearance of the fundus on the left side of the common BD was also reported as a left

localization variation of the fundus. The separate opening of common BD and PD into the duodenum is a reported variation. When the minor duodenal papilla, proximal to the PD, opened into the duodenum, it was termed pancreatic divisum. The angle formed at the junction of the right and left HDs is defined as the biliary confluence angle. In our study, cases with trifurcation variations were not included in the measurement of confluence angle. Additionally, in cases with aberrant right hepatic variation and drainage anomaly of the right posterior duct to the left HD, the angle formed by the right anterior duct and the left HD was measured and evaluated as the confluence angle. Angle measurements were performed on the MRCP image taken in the coronal view and by measuring the angle at its widest level. The diameter of the common BD before its union with the PD and the diameter of the duct formed by its union were measured. Forty-five cases with dilatation of the common BD due to various reasons and 42 cases in which the MRCP image was not optimized in this region were not included in the diameter measurement. In 7 cases with variations in which the common BD and PD entered the duodenum separately, the diameter of the common BD immediately before entering the duodenum was measured.

Statistical Analysis

Comparisons between two groups were performed using the Mann-Whitney U test when parametric assumptions were not met, and the Student's t-test (Independent Samples t-test) when they were met. Data were summarized as mean, standard deviation, and percentage, and the chi-square test was used to compare categorical variables. A p-value of <0.05 was considered significant. The data were analyzed using IBM SPSS Statistics 21 software.

RESULTS

Of the 303 cases reviewed in our study, 146 (48.2%) were male and 157 (51.8%) were female. The age of the patients ranged from 18 to 92 years (mean 54.49±18.83). The mean age of the male and female patients was 56.12 and 52.97 years, respectively. In 204 of the 303 reviewed cases (67.3%), stones were found at different levels of the gallbladder and BD, and stones were more common in women (35%) than in men (32.3%).

One or more variations were found at different levels of the biliary system in 93 (30.7%) of the 303 cases included in this study. More than one variation was found in 12 (12.9%) cases in which variations were detected. It was determined that 4% of the total 303 cases had multiple variations. In 4 of the 12 cases in which more than one variation was found, long CD and medial insertion variation (mediodistal insertion) were found together.

The most common variation was trifurcation (8.6%). An anomalous right posterior duct draining into the left HD was observed in 12 patients (4%), and aberrant right HD variation was observed in 15 patients (5%) (Figure 1, Table 1).

When CD was evaluated according to its opening into the common HD, the longest CD (6.6%) was the most common. In 5 of these cases (17.8%), both variations occurred together, and the percentage of mesiodistal insertion variation in the total number of cases was 1.7% (Figure 2, Table 1). The mean CD length in cases with short CD variation was measured as 3.63±0.8 mm. When evaluating the location of the gallbladder, we found that it was the most common site of transfer. At the pancreaticobiliary level, in 7 cases (2.3%), the PD and common BD opened into the first part of the small intestine through separate channels. Among these variations, the ratio of pancreas divisum, which was detected in 2 cases (28.5%) patients, to the total number of patients was 0.7% (Figure 3, Table 1). In our study, the biliary confluence angle was measured in 277 cases, excluding 26 cases with trifurcation variations, and the mean value was 77.32°±23.39°. In 216 patients, the diameter of the common BD before it opens into the duodenum and joins the PD (diameter 1) and the diameter of the duct formed after the junction (diameter 2) were measured. In 7 cases where common BD and PD entered the duodenum separately, the diameter of the common BD immediately before entering the duodenum (diameter 3) was calculated (Table 2).

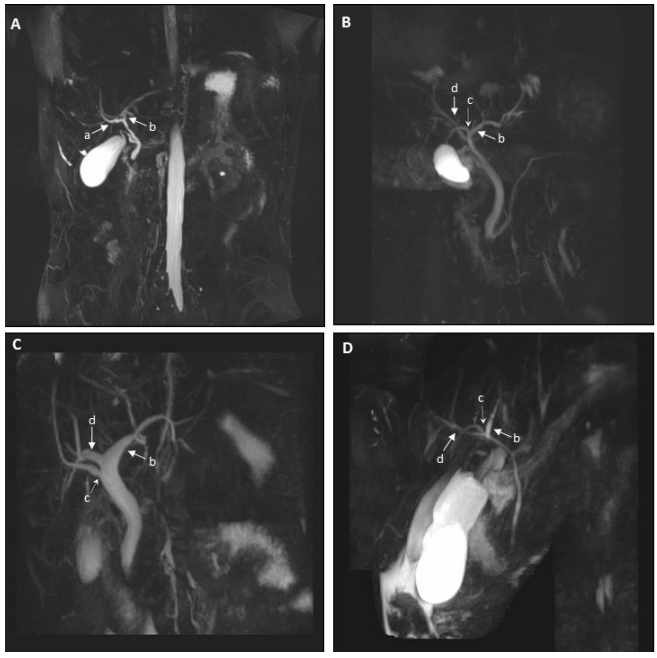

Figure 1. A) Normal bile ducts, **B)** Anomaly of the right posterior duct draining into left hepatic duct, **C)** Aberrant right hepatic duct variation, **D)** Trifurcation variation (**a:** Right hepatic duct, **b:** Left hepatic duct, **c:** Right posterior duct, d: Right anterior duct)

Table 1. Number and percentage of identified variations

Variations	Number of variations	Percentage (%)
Anomaly of the right posterior duct opening to the left hepatic duct	12	4
Aberrant right hepatic duct	15	5
Trifurcation	26	8.6
Long cystic duct	20	6.6
Medial insertion	8	2.6
Mediodistal insertion	5	1.7
Short cystic duct	7	2.3
Transferred location of gallbladder	7	2.3
Variation in the gallbladder fundus located on the left side	1	0.3
Superior localization of the gallbladder	4	1.3
The common bile duct and pancreatic duct were opened separately into the duodenum	7	2.3
Pancreas divisum	2	0.7
Multiple variation	12	4
Total	**93**	**30.7**

Table 2. Mean, minimum, and maximum values

	N	Min.	Max.	Mean ± SD
Age	303	18	92	54.49±18.83
Confluence angle	277	21.4°	152.7°	77.33°±23.39°
Diameter 1 (mm)	216	1.56	8.64	3.80±1.33
Diameter 2 (mm)	216	2.81	13.05	5.75±1.47
Diameter 3 (mm)	7	2.7	4.55	3.64±0.74
Short cystic duct (mm)	7	2.34	4.94	3.64±0.82

Min.: Minimum, Max.: Maximum, SD: Standard deviation, mm: Millimeter

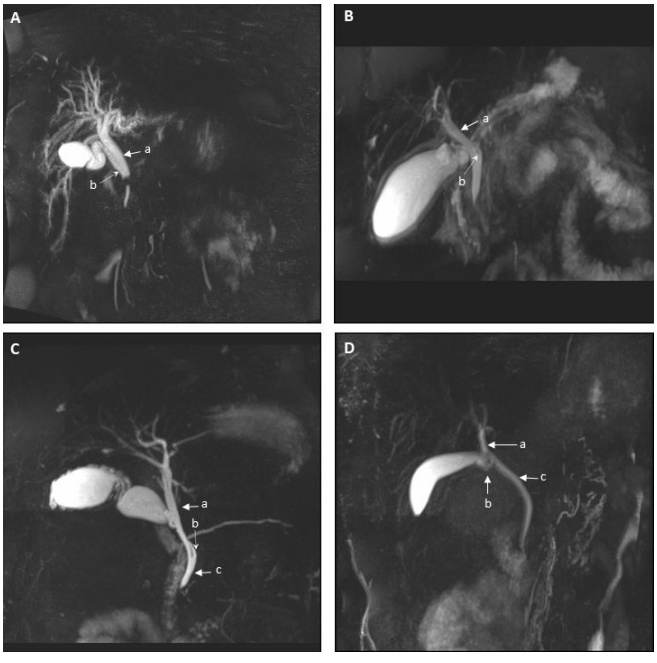

Figure 2. A) Long cystic duct variation, **B)** Medial insertion variation, **C)** Mediodistal insertion variation, **D)** Short cystic duct variation (**a:** Common hepatic duct, **b:** Cystic duct, **c:** Common bile duct)

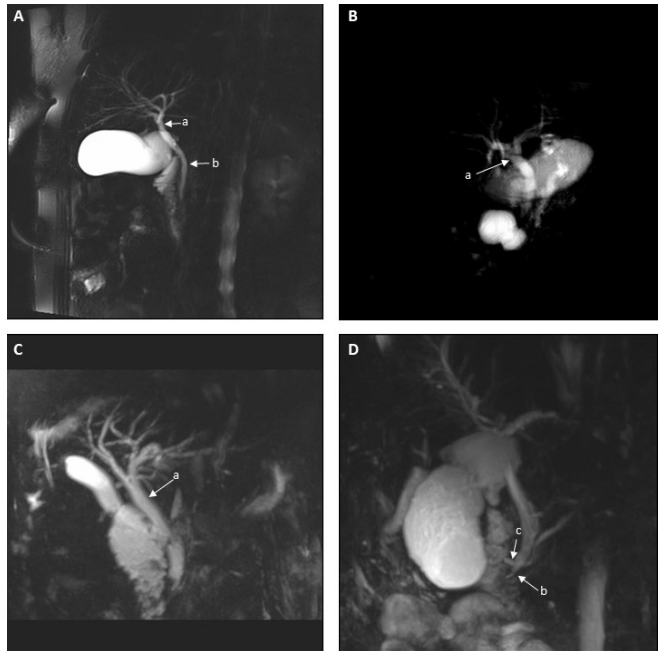

Figure 3. A) Transferred localization of the gallbladder, **B)** Variation in the gallbladder fundus located on the left, **C)** Superior localization of the gallbladder, **D)** Pancreatic divisum variation (**a:** Common hepatic duct, **b:** Common bile duct, **c:** Pancreatic duct)

Table 3. Studies in the literature

	Method	N	Number of Variations	Percentage variation (%)
Cabada Giadás et al. (15)	CT Cholangiography	101	23	22.7
Düşünceli et al. (5)	MRCP	475	115	24.2
Lee et al. (16)	MRCP	170	130	76.4
De Filippo et al. (17)	MRCP	350	148	42.3
Deka et al. (18)	MRCP	299	126	42.2
Renzulli et al. (19)	MRCP	1004	369	36.7
The present study	MRCP	303	93	30.7

CT: Computed tomography, MRCP: Magnetic resonance cholangiopancreatography

In 7 cases with variations in which the common BD and PD entered the duodenum separately, the mean diameter of the common BD just before entering the duodenum (diameter 3) was 3.63 mm.

Correlations between the detected variations, presence of stones, age, sex, confluence angle, diameter 1, diameter 2, diameter 3, and short CD length were studied separately. A statistically significant negative correlation was found between confluence angle and age ($p<0.05$). In other words, as age increases, the confluence angle decreases. Considering the previously defined correlation between diameter 1 and diameter 2 and age, a significant positive correlation was found ($p<0.05$). A significant correlation was found between long CD variation and stone formation and between long CD variation and diameters 1 and 2. In other words, people with long CD variations are more likely to have stones in their BD. The incidence of both right posterior anomaly opening into the left HD and mesiodistal insertion variation was higher in men than in women.

DISCUSSION

Anatomical variations of the gallbladder and BD are major risk factors for surgery in this region. In addition, these variations, other than just the risk of damage, may be risk factors for many biliary tract and pancreatic diseases, such as common BD stones, recurrent pancreatitis, and cholangitis (9,10). Damage to the varicose BD during surgical intervention may result in postoperative bile leakage or infection, and atrophic or hypertrophic changes may be observed as a result of obstruction due to improper connection of this variegated duct (11,12). Ignoring the variable structures within Calot's triangle, which are at the highest risk of damage during cholecystectomy, especially the aberrant right HD variation, by the surgeon may result in ligation or dissection of the wrong duct (3,13). Various imaging studies have been conducted showing anatomical variations of the BD, and the incidence rate is 24%-37% (4,5). Among the methods used to visualize BD, US and conventional single-slice computed tomography are of limited use and inadequate for the study of non-dilated BD. Another method, intravenous cholangiography, cannot provide detailed anatomical imaging. Among the contrast methods, percutaneous transhepatic cholangiography and Endoscopic Retrograde Cholangiopancreatography (ERCP) are considered the gold standards. However, they are invasive, operator dependent, expensive, and associated with significant complications (4,13,14). In the study conducted by Cabada Giadás et al. (15) using three-dimensional helical CT, another imaging modality, anatomical variation at different levels of the biliary system was found in 22.7% of 101 cases. With this method, anatomical structures in the BD can be evaluated with high success rates, but the disadvantages of this method are the high side effects of the contrast agent and the use of ionizing radiation (15-19) (Table 3).

MRCP is preferred over other methods because it has a 90% accuracy rate compared with ERCP, is non-invasive, does not use contrast media, is independent of the practitioner, is inexpensive, does not involve ionizing radiation, and does not carry the risk of complications (8,20). Vitellas et al. (21) reported that MRCP had an accuracy of 98% for aberrant HD and 95% for CD variations. Taourel et al. (4) found that MRCP and ERCP were highly sensitive and specific for BD variations. We included patients who underwent MRCP because it is non-invasive and does not expose patients to ionizing radiation.

Many studies in the literature have examined the anatomical variations of the BD. The rates of variation in these studies vary. In their study using MRCP images from 350 patients, De Filippo et al. (17) found that the BD variation rate was 42.3%. In our study, the rate was 30.7%. In the meta-analysis study conducted by Cucchetti et al. (22), the anatomical variations of intrahepatic BD in the literature of cases undergoing liver transplantation in Europe between 1980 and 2010 were reviewed. According to this study, a normal anatomical biliary system was found in 64.5% (22).

In our study, a similar result was obtained, as a normal biliary system was found in 69.3%.

In the study that reviewed 6 different studies conducted by Deka et al. (18), it was found that 57.8% of the 299 cases whose MRCP images were examined had a normal anatomical BD. Additionally, this study concluded that there was no association between gender and variations. We found a significant relationship between sex and right posterior duct anomaly opening to the left HD and mesiodistal insertion variation.

Mariolis-Sapsakos et al. (23) conducted a study examining only the anatomical variations of the right HD on 73 cadavers, and it was reported that the right HD had normal anatomy in 65.75% of the cases. In our study, normal right HD anatomy was observed in 82.5% of the patients. We believe that this difference between studies is due to ethnic origin.

Uysal et al. (24) examined only intrahepatic ductal variation using MRCP images of 1011 cases and detected intrahepatic ductal variation at a rate of 24.3%. Among these variations, right posterior duct anomaly opening into the left HD was recorded at a rate of 4.15%, aberrant right HD at a rate of 7.2%, and trifurcation at a rate of 8%. In our study, similar to the study of Uysal et al. (24), trifurcation variation was found in 8.6% of cases and right posterior duct anomaly opening to the left HD was 4%.

In a study of 1041 patients, Renzulli et al. (19) investigated the anatomical variations of the BD using the MRCP method. In this study, variations at different levels of BD were detected in 635 cases (36.7%). The most common variation was the right posterior duct anomaly, with approximately 16.2% opening into the left HD.The most common BD anomaly in most studies is the right posterior duct anomaly draining into the left HD (4,23). However, in some studies, including our study, trifurcation variation was the most common BD anomaly (24).

Although there are different results when evaluating the opening of the CD into the extrahepatic BD, in most studies, the CD was longer than the short CD. In our study, the long CD was larger than the short CD. There are only few studies on the location of the gallbladder, and similar to our study, the transfer location and upper location of the gallbladder are in close proportion (4). In our study, unlike the literature, the variation in which the fundus of the gallbladder is on the left and the variation in which the common BD and PD open separately to the duodenum were evaluated for the first time. Haliloglu et al. (25) investigated the relationship between biliary confluence angle and age, sex, and body mass index in 40 patients and found that the confluence angle was independent of these parameters. Similar to this study, we did not find a statistically significant difference between the confluence angle and sex.

Study Limitations

Our study has several limitations. First, because our study was retrospective, we only included patients who underwent MRCP for various reasons in the study group. Therefore, our study population does not fully reflect the community. Second, the MRCP method was not compared with more invasive methods, such as intraoperative cholangiography and surgery.

CONCLUSION

Gallbladder and BD show 24%-37% variation. Knowledge regarding these variations is extremely important for surgical interventions in this region. In our study, the trifurcation variation was the most common. However, aberrant right HD variation carries the greatest risk of damage because it lies in Calot triangle. In addition, the risk of stone formation is high in patients with long CD variations. In long-term CD variations, the increase in the diameter of the common BD before and after its union with the PD should be considered in the treatment of such diseases. We believe that our findings will guide surgeons in surgical interventions in this region and help in planning the treatment of patients, as it is a risk factor for many biliary tract and pancreatic diseases, such as common BD stones, recurrent pancreatitis, and cholangitis.

ETHICS

Ethics Committee Approval: The study Ethical approval for the study was obtained from the Local Ethics Committee of the Selçuk University Faculty of Medicine (approval no: 2015/312, date: 08.12.2015).

Informed Consent: Since this study was retrospective, patient consent was not required.

FOOTNOTES

Authorship Contributions

Concept: T.F.D., Z.F., A.K.K., İ.İ.U, N.Ü.D., Design: T.F.D., Z.F., M.K., A.K.K., İ.İ.U, N.Ü.D., Data Collection or Processing: T.F.D., Z.F., M.K., Analysis or Interpretation: T.F.D., Z.F., A.G.Ö., Literature Search: T.F.D., Z.F., Writing: T.F.D., A.G.Ö.

Conflict of Interest: No conflict of interest was declared by the authors.

Financial Disclosure: The authors declared that this study received no financial support.

REFERENCES

1. Standring S. Gray's anatomy e-book: the anatomical basis of clinical practice: Elsevier Health Sciences; 2016. p: 1173-7.
2. Moore KL, Dalley AF, Agur AMR. Clinically oriented anatomy. 6th ed. Wolters Kluwer: Lippincott Williams & Wilkins; 2014. p: 277-80.
3. Mortelé KJ, Ros PR. Anatomic variants of the biliary tree: MR cholangiographic findings and clinical applications. AJR Am J Roentgenol. 2001;177:389-94.
4. Taourel P, Bret PM, Reinhold C, Barkun AN, Atri M. Anatomic variants of the biliary tree: diagnosis with MR cholangiopancreatography. Radiology. 1996;199:521-7.
5. Düşünceli E, Erden A, Erden İ. Biliyer sistemin anatomik varyasyonları: MRKP bulguları. Tanısal ve Girişimsel Radyoloji. 2004;10:296-303.
6. Janssen BV, van Laarhoven S, Elshaer M, Cai H, Praseedom R, Wang T, et al. Comprehensive classification of anatomical variants of the main biliary ducts. Br J Surg. 2021;108:458-62.
7. Songur A, Çağlar V, Gönül Y, Özen OA. Gallbladder and biliary tract anatomy. Journal of Surgical Arts. 2009;2:12-9. Turkish.
8. Arda K, Aktaş E, Çiledağ N. Manyetik rezonans kolanjiyopankreatografi. Güncel Gastroenteroloji. 2010:39-5.
9. Dähnert W. Radiology review manual. Lippincott: Williams & Wilkins; 2010.
10. Naeem MQ, Ahmed MS, Hamid K, Shazlee MK, Qureshi F, Asad Ullah M. Prevalence of different hepatobiliary tree variants on magnetic resonance cholangiopancreatography in patients visiting a tertiary care teaching hospital in Karachi. Cureus. 2020;12:e12329.
11. Sutton D. Textbook of radiology and imaging. Churchill Livingston: China; 2000.
12. Sarin YK. Biliary ductal and vascular anomalies associated with choledochal cyst. Journal of Indian Association of pediatric Surgeons. 2005;10:86-8.
13. Turner MA, Fulcher AS. Chapter 75- Gallbladder and biliary tract: normal anatomy and examination techniques. In: Textbook of gastrointestinal radiology, Gore RM, Levine MS, editors. Philadelphia: WB Saunders; 2000.
14. Caoili EM, Paulson EK, Heyneman LE, Branch MS, Eubanks WS, Nelson RC. Helical CT cholangiography with three-dimensional volume rendering using an oral biliary contrast agent: feasibility of a novel technique. AJR Am J Roentgenol. 2000;174:487-92.
15. Cabada Giadás T, Sarría Octavio de Toledo L, Martínez-Berganza Asensio MT, Cozcolluela Cabrejas R, Alberdi Ibáñez I, Alvarez López A, et al. Helical CT cholangiography in the evaluation of the biliary tract: application to the diagnosis of choledocholithiasis. Abdom Imaging. 2002;27:61-70.
16. Lee CM, Chen HC, Leung TK, Chen YY. Magnetic resonance cholangiopancreatography of anatomic variants of the biliary tree in Taiwanese. J Formos Med Assoc. 2004;103:155-9.
17. De Filippo M, Calabrese M, Quinto S, Rastelli A, Bertellini A, Martora R, et al. Congenital anomalies and variations of the bile and pancreatic ducts: magnetic resonance cholangiopancreatography findings, epidemiology and clinical significance. Radiol Med. 2008;113:841-59. English, Italian.
18. Deka P, Islam M, Jindal D, Kumar N, Arora A, Negi SS. Analysis of biliary anatomy according to different classification systems. Indian J Gastroenterol. 2014;33:23-30.
19. Renzulli M, Brandi N, Brocchi S, Balacchi C, Lanza C, Pettinari I, et al. Association between anatomic variations of extrahepatic and intrahepatic bile ducts: do look up! J Anat. 2023;242:683-69.
20. Tuncel E. Klinik Radyoloji. 1. Baskı. İstanbul: Nobel&Güneş Tıp Kitabevi; 2008.
21. Vitellas KM, Keogan MT, Spritzer CE, Nelson RC. MR cholangiopancreatography of bile and pancreatic duct abnormalities with emphasis on the single-shot fast spin-echo technique. Radiographics. 2000;20:939-57; quiz 1107-8, 1112. Erratum in: Radiographics 2000;20:1494.
22. Cucchetti A, Peri E, Cescon M, Zanello M, Ercolani G, Zanfi C, et al. Anatomic variations of intrahepatic bile ducts in a European series and meta-analysis of the literature. J Gastrointest Surg. 2011;15:623-30.
23. Mariolis-Sapsakos T, Kalles V, Papatheodorou K, Goutas N, Papapanagiotou I, Flessas I, et al. Anatomic variations of the right hepatic duct: results and surgical implications from a cadaveric study. Anat Res Int. 2012;2012:838179.
24. Uysal F, Obuz F, Uçar A, Seçil M, Igci E, Dicle O. Anatomic variations of the intrahepatic bile ducts: analysis of magnetic resonance cholangiopancreatography in 1011 consecutive patients. Digestion. 2014;89:194-200.
25. Haliloglu N, Erden A, Erden İ. Normal biliary confluence angle in classical junction type: assessment with MR cholangiopancreatography. Ankara Üniversitesi Tıp Fakültesi Mecmuası. 2009;62:163-5.

Medical Journal of Bakırköy

Med J Bakirkoy 2025;21:90-96
DOI: 10.4274/BMJ.galenos.2024.2024.12-4

Research

Beyond Motor Symptoms: A Comprehensive Analysis of Sexual Dysfunction in Cervical Dystonia

Servikal Distonide Cinsel İşlev Bozukluğu Üzerine Kapsamlı Bir Değerlendirme

Özge Gönül Öner[1], Gözde Baran[2]

[1]Göztepe Prof. Dr. Süleyman Yalçın City Hospital, Clinic of Neurology, İstanbul, Türkiye

[2]University of Health Sciences Türkiye, Sancaktepe Şehit Prof. Dr. İlhan Varank Training and Research Hospital, Clinic of Neurology, İstanbul, Türkiye

ABSTRACT

Objective: Dystonia is a neurological disorder marked by involuntary muscle contractions, leading to repetitive movements or abnormal postures. While non-motor symptoms like anxiety, depression are well-documented, the prevalence and impact of sexual dysfunction in cervical dystonia remain understudied. This study explores the prevalence of sexual dysfunction and its relationship with other factors in cervical dystonia patients.

Methods: This prospective study included 28 patients with cervical dystonia. Data were collected using the Beck Depression Inventory (BDI), Tsui Rating Scale for cervical dystonia (Tsui), visual analog scale (VAS), and Arizona Sexual Experiences Scale (ASLS). Analyses included descriptive statistics, correlation, multiple regression, and subgroup analyses.

Results: 71.4% of patients reported sexual dysfunction. No significant correlations were found between ASLS scores and age, disease duration, BDI, or Tsui scores. A moderate, non-significant correlation existed between ASLS and VAS scores (r=0.331, p=0.082). Subgroup analysis showed the highest ASLS scores in patients aged 50-60 and those with 5-10 years of disease duration. A significant difference in ASLS scores was observed between males and females (p=0.05), with females having higher scores. Additionally, comparisons between patients with and without sexual dysfunction showed no significant association with comorbidities.

Conclusion: Sexual dysfunction is prevalent in cervical dystonia, notably in older females with higher depression and pain levels. Comprehensive care addressing both motor and non-motor symptoms is crucial. Future research should focus on longitudinal studies and therapeutic interventions.

Keywords: Dystonia, non-motor symptoms, sexual dysfunction

ÖZ

Amaç: Distoni, istemsiz kas kasılmalarıyla karakterize, tekrarlayıcı hareketlere veya anormal püstüre yol açan nörolojik bir bozukluktur. Anksiyete ve depresyon gibi motor dışı semptomlar iyi belgelenmiş olmasına rağmen, servikal distonide cinsel işlev bozukluğunun yaygınlığı ve etkisi yeterince araştırılmamıştır. Bu çalışma, servikal distoni hastalarında cinsel işlev bozukluğunun yaygınlığını ve diğer faktörlerle ilişkisini incelemektedir.

Gereç ve Yöntem: Bu prospektif çalışmaya servikal distonili 28 hasta dahil edilmiştir. Veriler Beck Depresyon Ölçeği (BDÖ), servikal distoni için Tsui Derecelendirme Ölçeği (Tsui), görsel analog skala (VAS) ve Arizona Cinsel Deneyimler Ölçeği (ASLS) kullanılarak toplanmıştır. Analizler, tanımlayıcı istatistikler, korelasyon, çoklu regresyon ve alt grup analizlerini içermektedir

Bulgular: Hastaların %71,4'ü cinsel işlev bozukluğu bildirmiştir. ASLS skorları ile yaş, hastalık süresi, BDÖ veya Tsui skorları arasında anlamlı bir korelasyon bulunmamıştır. ASLS ve VAS skorları arasında orta düzeyde, anlamlı olmayan bir korelasyon saptanmıştır (r=0.331, p=0.082). Alt grup analizi, 50-60 yaş aralığındaki hastalarda ve 5-10 yıllık hastalık süresine sahip olanlarda en yüksek ASLS skorlarının olduğunu göstermiştir. ASLS skorları açısından kadınlar ve erkekler arasında anlamlı bir fark bulunmuştur (p=0.05), kadınların daha yüksek skorlara sahip olduğu görülmüştür. Ayrıca, cinsel işlev bozukluğu olan ve olmayan hastalar arasındaki karşılaştırmalarda eşlik eden hastalıklarla anlamlı bir ilişki saptanmamıştır.

Sonuç: Cinsel işlev bozukluğu, özellikle depresyon ve ağrı düzeyleri daha yüksek olan yaşlı kadınlarda servikal distonide yaygındır. Hem motor hem de motor dışı semptomları ele alan kapsamlı bir bakım yaklaşımı kritik öneme sahiptir. Gelecekteki araştırmalar, uzunlamasına çalışmalar ve terapötik müdahalelere odaklanmalıdır.

Anahtar Kelimeler: Distoni, non-motor semptomlar, cinsel işlev bozukluğu

Address for Correspondence: Özge Gönül Öner, Göztepe Prof. Dr. Süleyman Yalçın City Hospital, Clinic of Neurology, İstanbul, Türkiye

E-mail: ozgegonl@gmail.com **ORCID ID:** orcid.org/0000-0003-4199-442X

Cite as: Öner ÖG, Baran G. Beyond motor symptoms: a comprehensive analysis of sexual dysfunction in cervical dystonia. Med J Bakirkoy. 2025;21:90-96

Received: 10.12.2024
Accepted: 20.12.2024
Publication Date: 25.03.2025

INTRODUCTION

Dystonia is a neurological disorder characterized by repetitive movements and unusual postures caused by persistent or intermittent muscle contractions. It is believed to arise from the pathology of physiological neuronal pathways among the basal ganglia (1). Dystonia is categorized as focal, segmental, or generalized based on the body regions involved. Focal dystonia impacts a single body area, whereas segmental dystonia involves two or more interconnected regions. The most common examples of focal dystonia are blepharospasm and cervical dystonia, whereas segmental dystonia includes cranio-cervical dystonia and Meige syndrome (2) today, focal dystonia is considered an isolated movement disorder with many non-motor symptoms. Anxiety, depression, and social phobia are the most well-documented mental health conditions (3,4). It is also known that cognitive and emotional disorders or sleep disorders, are observed in the cervical dystonia (5). Studies examining non-motor symptoms in dystonia patients have frequently investigated mood, cognition, sleep, quality of life, apathy, and anxiety, but sexual dysfunction has not been included in these studies (6). Sexual health is an important aspect of mental health and is often researched in Parkinson's disease. The relationship between sexual dysfunction and dystonia, however, remains poorly understood and needs further investigation, as it negatively affects patients' psychological and physical health, quality of life, and treatment process (7). To date, sexual dysfunction in dystonia patients has only been examined in two case-control studies (4,7). Additionally, no studies on this topic have been conducted in Turkey. This study aims to investigate sexual dysfunction in cervical dystonia and contribute to the limited literature and clinical perspective on this subject.

METHODS

This study is a prospective, descriptive survey conducted with 28 cervical dystonia patients who were followed at the botulinum toxin applications and movement disorders outpatient clinic.

Selection and Identification of Cases

Inclusion criteria included individuals aged 18-65 years, identifying as heterosexual, and diagnosed with focal cervical dystonia. Patients were excluded if they had a more extensive form of dystonia (e.g., hemidystonia, multifocal dystonia, or generalized dystonia), acquired dystonia, or a history of dementia, brain trauma, stroke, neurodegenerative disease, or psychosis. Those with blepharospasm were also not included. These exclusions were necessary to ensure the accuracy and reliability of assessments, as such conditions could interfere with the comprehension and completion of sexual dysfunction tests, or be associated with additional comorbidities that might influence sexual dysfunction.

All assessments were obtained at least 12 weeks after the last botulinum toxin application during the dose-end period.

The study was approved on 26.06.2024 by the Ethics Committee of University of Health Sciences Türkiye, Sancaktepe Şehit Prof. Dr. İlhan Varank Training and Research Hospital (decision no: 200, date: 26.06.2024). This study informed consent was obtained from all patients.

Data Collection Tools

Data on patients' age, gender, type, and localization of dystonia were obtained from their files filled out during regular end-of-dose evaluations at the botulinum toxin applications clinic, to monitor both the severity of dystonia and non-motor symptoms. Mood assessment was done using the Beck Depression Inventory (BDI-II), pain assessment using the visual analog scale (VAS), dystonia severity assessment using the Tsui Rating Scale for cervical dystonia (Tsui), and sexual function assessment using the Arizona Sexual Experiences Scale (ASLS).

The BDI-II is a self-report scale consisting of 21 questions scored between 0-63, used to assess depression. The cutoff values for mild/moderate/severe depression are 13/19/28, respectively (8).

The VAS is a one-dimensional scale commonly used to measure pain, consisting of a 100 mm line drawn vertically or horizontally. The two ends of this line contain two descriptive words for pain intensity (0= "no pain", 100= "worst/unbearable pain"). The patient is instructed to indicate a point on the line that reflects the severity of their pain. The portion from 0 to the mark is measured. Pain is classified as no pain (0-4 mm), mild pain (4-44 mm), moderate pain (45-74 mm), and severe pain (75-100 mm). In our study, pain was classified into the categories of no pain/mild pain and moderate/severe pain for analysis purposes.

Tsui, ranging between 0-25 (most disabling), grades the dystonic head, neck, and shoulder movements and postures (9).

The ASLS is a self-report scale that assesses sexual dysfunction, with separate forms for men and women, each containing five questions. It examines sexual desire, mental and physiological arousal, and orgasm. The total scores range between 5 and 30. Higher scores indicate increased levels of sexual dysfunction. Total scores of 19 and above indicate sexual dysfunction.

Statistical Analysis

Statistical analyses were conducted to assess variables using SPSS 15.0 (Statistical Package for the Social Sciences) (IBM SPSS Inc., Chicago, IL). Mean±standard deviation were used for variables in descriptive statistics. The Shapiro-Wilk test was used to evaluate whether the data followed a normal distribution. For variables following a normal distribution, Pearson correlation analysis was used. For variables not following a normal distribution, Spearman correlation analysis was employed. Pearson correlation analysis (parametric) was employed to examine the relationship between ASLS, Tsui, age, and disease duration, while Spearman correlation analysis (non-parametric) was utilized for the correlation between ASLS, BDI, and VAS scores. For assessment of the relationship between ASLS scores and gender, we used the Spearman correlation analysis (non-parametric) as gender is a categorical variable. Additionally, multiple regression analysis was performed to determine if age, disease duration, VPS score, and gender could predict ASLS scores. Subgroup analyses were conducted to compare mean ASLS scores across different age groups and disease durations. Lastly, the Mann-Whitney U test was utilized to compare ASLS scores between males and females.

RESULTS

A comprehensive overview of the patients, including the prevalence of depression, pain, sexual dysfunction, and comorbid conditions, is summarized in Table 1. The mean age of the patients was 48.1 years (median: 46, ranging from 35 to 66), and the average duration of the disease was 8.3 years (median: 8, ranging from 2 to 14). The majority of the patients were female (85.7%). Comorbid conditions were present in 42.9% of patients, with the most common comorbidities being hypertension (17.9%) and diabetes mellitus (14.3%). Other comorbidities included hyperlipidemia (7.1%), and systemic lupus erythematosus (3.6%). Levels of depression, pain, sexual dysfunction, and comorbid conditions are presented in Table 1.

Relationship Between Sexual Disfunction and Other Variables

Results indicated that ASLS and Tsui scores, age, and disease duration adhered to a normal distribution, whereas BDI and VAS scores did not. The conducted statistical tests were mentioned in the methods section.

Results of the correlation analyses between ASLS scores and other variables are summarized in Table 2.

There was a very weak correlation between ASLS and age, disease duration, and gender, Tsui, BDI ($p>0.05$) and between ASLS between ASLS and VAS score ($p>0.05$). These results indicate that there is no significant correlation between ASLS scores and Tsui scores, BDI scores, age, disease duration, VAS score, or gender.

Results of the Detailed Statistical Analysis

Multiple Regression Analysis is performed to determine whether a combination of variables (age, disease duration, VAS score, gender) can predict ASLS scores (Table 3). The regression model indicates that none of the independent

Table 1. Descriptive data regarding patients

Age; mean±SD (median, minimum-maximum)	48.1±8.9 (46, 35-66)
Disease duration (years) mean±SD (median, minimum-maximum)	8.3±3.7 (8, 2-14)
Female %	85.7%
Male %	14.3%
Comorbid conditions	
None	57.1% (n=16)
Diabetes mellitus	14.3% (n=4)
Hypertension	17.8% (n=5)
Hyperlipidemia	7.1% (n=2)
Systemic lupus erythematosus	3.6% (n=1)
Depression level distribution	
Minimum	60.7% (n=17)
Mild	17.9% (n=5)
Moderate	10.7% (n=3)
Severe	10.7% (n=3)
Visual pain score distribution	
No pain	57.1% (n=16)
Moderate	28.6% (n=8)
Mild	7.1% (n=2)
Severe	7.1% (n=2)
Sexual disfunction level distribution	
Yes	71.4% (n=20)
No	28.6% (n=8)

SD: Standard deviation

Table 2. Correlation between ASLS and other variables

Variables	Correlation coefficient	P-value
ASLS & Age	0.035	0.856
ASLS & Disease Duration	0.019	0.917
ASLS & Gender	-0.150	0.438
ASLS & Tsui	0.251	0.193
ASLS & BDI	0.186	0.339
ASLS & VAS Score	0.331	0.082

ASLS: Arizona Sexual Experiences Scale, BDI: Beck depression Inventory, Tsui: The Tsui Rating Scale for Cervical Dystonia, VAS: Visual analog scale

variables (age, disease duration, VAS score, gender) is statistically significant as predictors of ASLS scores (p-values >0.05). However, VAS score and gender are close to being significant predictors, with p-values of 0.077 and 0.084, respectively (Table 3).

Subgroup analysis is performed to assess ASLS scores within clinically meaningful subgroups, such as by age range and disease duration (Table 4). The mean ASLS score varies across different age groups. Patients aged 50-60 have the highest mean ASLS score, while those aged 30-40 have the lowest (Table 4). The mean ASLS score also varies across different disease durations. Patients with a disease duration of 5-10 years have the highest mean ASLS score, while those with a duration of 0-5 years have the lowest. These differences are not statistically analyzed for significance here (Table 4). Comparative Analysis of ASLS scores between different groups (male vs. female) was performed. A significant difference in ASLS scores between males and females (p=0.05) was detected. Females have a higher mean ASLS score compared to males (Table 4).

Table 3. Results of the multiple regression analyses

Variable	Coefficient	SE	T-value	P-value	95% confidence interval
Constant	9.7684	9.687	1.008	0.324	[-10.142, 29.679]
Age	-0.0410	0.174	-0.236	0.815	[-0.401, 0.319]
Disease duration	-0.0737	0.296	-0.249	0.805	[-0.689, 0.542]
VAS	2.6341	1.415	1.861	0.077	[-0.305, 5.573]
Gender	-6.2287	3.438	-1.811	0.084	[-13.297, 0.839]

SE: Standard error, VAS: Visual analog scale

Table 4. Subgroup analyses

Age group	Mean ASLS score
30-40	17
40-50	21
50-60	23
60-70	18
Disease duration	
0-5 years	15
5-10 years	22
10-15 years	20
Gender	
Male	13.0
Female	20.5

ASLS: Arizona Sexual Experiences Scale

Comparison of Patient Characteristics by Sexual Dysfunction Status

In this study, patients with cervical dystonia who had sexual dysfunction were compared to those without sexual dysfunction in terms of age, BDI score, and disease duration. Patients with sexual dysfunction (n=20) had an average age of 48.1 years, with a mean disease duration of 8.3 years. The mean depression level, as measured by the BDI score, was 16.7 in this group. In contrast, patients without sexual dysfunction (n=8) had an average age of 44.4 years and a mean disease duration of 8 years, with an average depression level (BDI score) of 10.9. In both groups, the majority was female, and the VAS scores were generally similar.

To determine whether there were significant differences between patients with and without sexual dysfunction in terms of age, depression level (BDI), pain score (VAS), and disease duration, an independent t-test was performed. The t-test results indicated no significant differences between the two groups in terms of age (t=1.546, p=0.134), BDI score (t=1.002, p=0.325), VAS score (t=0.893, p=0.380), and disease duration (t=0.069, p=0.946). Additionally, a chi-square test was conducted to examine if gender distribution differed between the groups. This analysis revealed a significant difference in gender between the groups (χ^2=37.7, p<0.001), suggesting that being female may be a determining factor for sexual dysfunction in this patient population. These analyses indicate that while clinical variables such as age, depression, pain level, and disease duration do not show significant effects on sexual dysfunction, gender appears to be a distinguishing factor (Table 5). Additionally, a chi-square test was performed to examine whether the presence of comorbid diseases differed between groups with and without sexual dysfunction. The analysis results indicated no significant difference in comorbidity presence between the groups (χ^2=0.648, p=0.723). This finding suggests that comorbid conditions, such as diabetes and hypertension, are not significantly associated with sexual dysfunction in this patient population (Table 5).

Table 5. Comparative analysis of demographic and clinical characteristics between patients with and without sexual dysfunction

Variable	Test statistic	P-value
Age	t=1.546	0.134
BDI	t=1.002	0.325
VAS score	t=0.893	0.380
Disease duration	t=0.069	0.946
Gender	χ^2=37.7	**<0.001**
Comorbidity presence	χ^2=0.648	0.723

ASLS: Arizona Sexual Experiences Scale, BDI: Beck depression inventory, VAS: Visual Analog Scale

DISCUSSION

Our study investigates the prevalence of sexual dysfunction in cervical dystonia and explores the relationships between sexual dysfunction and various factors such as age, depression, and pain. It contributes to the current literature on the non-motor symptoms of dystonia, particularly sexual dysfunction, and highlights the importance of comprehensive patient care.

When evaluating our study results alongside existing literature, several important insights emerge regarding the relationship between sexual dysfunction in dystonia and other factors such as age, depression, and pain. In the literature, the prevalence of sexual dysfunction among dystonia patients varies, but significant rates have been consistently reported. Sexual dysfunction has been identified in 45% of cervical dystonia patients. (7). Sexual dysfunction in these patients, is often linked with depressive symptoms and other non-motor issues (10). In our study, sexual dysfunction was identified in 71.4% of the patients. In subgroup analysis, the mean ASLS score varies across different age groups. Patients aged 50-60 have the highest mean ASLS score, while those aged 30-40 have the lowest. Patients with a disease duration of 5-10 years have the highest mean ASLS score. Comparative analysis found a significant difference in ASLS scores between males and females ($p=0.05$). Females have a higher mean ASLS score than males. Our finding of 71.4% in cervical dystonia patients significantly exceeds the 45% prevalence reported in the literature (7). This higher prevalence could be attributed to differences in sample characteristics. Our study sample consists of a predominantly female sample and shows a higher prevalence of depression. We did not find any significant correlation between sexual dysfunction and other factors in our study. Nevertheless, the weak correlation between ASLS scores and age may indicate that sexual dysfunction increases with age. This is consistent with numerous studies that have documented a decline in sexual function with age, due to both physiological and psychological changes (7). Even though there was a weak positive correlation between BDI scores and ASLS scores in our study, the evidence was insufficient to draw definitive conclusions. This aligns with previous literature indicating that depression may increase the risk of sexual dysfunction in dystonia patients (10). Depression can affect sexual health through multiple pathways, including reduced libido, impaired arousal, and decreased sexual satisfaction (10). Also, a weak positive correlation between VAS scores and ASLS scores may suggest that higher pain levels are associated with increased sexual dysfunction. This aligns with previous research highlighting the detrimental effects of pain on sexual function (7). The management of pain in dystonia patients may be crucial for enhancing their sexual health. These findings underscore the importance of incorporating sexual health assessments into routine clinical practice for dystonia patients. Utilizing validated tools such as the ASLS can help identify patients at risk of sexual dysfunction (10).

In our study, no significant difference was found in the presence of common comorbid conditions (such as diabetes, hypertension, hyperlipidemia, and systemic lupus erythematosus) between cervical dystonia patients with and without sexual dysfunction. This finding suggests that sexual dysfunction in dystonia may manifest as an inherent non-motor symptom rather than being secondary to systemic conditions. Although studies addressing sexual dysfunction specifically in dystonia patients are limited, existing research often links sexual dysfunction to non-motor symptoms such as depression, anxiety, and pain. For example, a study reported a 45% prevalence of sexual dysfunction in dystonia patients, highlighting its association with psychological factors such as depression and anxiety (7). However, this study did not examine the impact of physical comorbidities on sexual function in detail. Similarly, another study found that sexual dysfunction negatively impacts quality of life in dystonia patients, although comorbid conditions were not specifically evaluated in terms of their effect on sexual health (10). Given these findings, the lack of association between comorbid conditions and sexual dysfunction in our study may indicate that sexual dysfunction in dystonia is more closely linked to neurological and psychosocial factors rather than to systemic health conditions. The absence of studies directly examining the relationship between sexual dysfunction and comorbid conditions in dystonia patients underscores the need for further research with larger cohorts to explore this potential relationship in depth.

One study explored the neural circuits associated with dystonia and their dysfunctions. It focused on the psychiatric symptoms frequently seen in dystonia patients and their management (11). Cognitive behavioral therapy and mindfulness were suggested as psychotherapeutic approaches. Addressing depression and pain through appropriate interventions, including cognitive-behavioral therapy, mindfulness, and pharmacotherapy, can significantly improve sexual function (11). Future longitudinal studies should be conducted to better understand the relationships between sexual dysfunction, depression, pain, comorbidities, and other factors in patients with dystonia. Additionally, exploring the efficacy of various therapeutic interventions, such as deep brain stimulation

(DBS), physical therapy, and complementary therapies like manual therapy and massage, can provide insights into comprehensive treatment approaches (12,13). Further development and validation of dystonia-specific assessment tools are also needed to accurately evaluate and monitor sexual dysfunction and other non-motor symptoms in this population (10).

Study Limitations

There are several limitations. First comes the issue of a small patient number. A bigger cohort would provide more reliable results. Secondly, the cross-sectional design limits establishing causality from the findings. Third, the exclusion criteria, including non-heterosexual individuals and those with other forms of dystonia or significant comorbidities, may limit the applicability of the results to all dystonia patients. Future studies including a more diverse population would enhance the generalizability. Despite these limitations, our study provides valuable insights into the prevalence and factors associated with sexual dysfunction in cervical dystonia patients, highlighting the need for comprehensive patient care.

Conclusion

This study highlights the significant prevalence of sexual dysfunction among cervical dystonia patients and underscores its association with various demographic and clinical factors such as age, gender, depression, comorbidities, and pain. The findings reveal that sexual dysfunction is more commonly observed in older female patients who report higher levels of depression and pain. Despite the lack of statistically significant correlations between ASLS scores and variables such as age, disease duration, and depression levels, the trends observed suggest the need for further exploration. The study emphasizes the importance of adopting a comprehensive healthcare approach that addresses both motor and non-motor symptoms, including sexual health, to improve the overall quality of life for these patients. By integrating regular assessments of sexual function into clinical practice, healthcare providers can identify and manage sexual dysfunction more effectively. Future studies are needed to better understand the relationships between sexual dysfunction and other factors in dystonia patients. Additionally, investigating the efficacy of various therapeutic interventions, such as cognitive-behavioral therapy, mindfulness, and pharmacotherapy, can provide valuable insights into improving sexual health and overall well-being in this population. Overall, this study contributes to the limited literature on sexual dysfunction in dystonia and highlights the need for further research and comprehensive patient care strategies to address this critical aspect of non-motor symptoms.

ETHICS

Ethics Committee Approval: The study was approved on 26.06.2024 by the Ethics Committee of University of Health Sciences Türkiye, Sancaktepe Şehit Prof. Dr. İlhan Varank Training and Research Hospital (decision no: 200, date: 26.06.2024).

Informed Consent: This study informed consent was obtained from all patients.

FOOTNOTES

Authorship Contributions

Surgical and Medical Practices: Ö.G.Ö., G.B., Concept: Ö.G.Ö., Design: Ö.G.Ö., Data Collection or Processing: Ö.G.Ö., G.B., Analysis or Interpretation: Ö.G.Ö., G.B., Literature Search: G.B., Writing: Ö.G.Ö.

Conflict of Interest: No conflict of interest was declared by the authors.

Financial Disclosure: The authors declare that this study received no financial support.

REFERENCES

1. Albanese A, Bhatia K, Bressman SB, Delong MR, Fahn S, Fung VS, Hallett M, et al. Phenomenology and classification of dystonia: a consensus update. Mov Disord. 2013;28:863-73.
2. Balint B, Mencacci NE, Valente EM, Pisani A, Rothwell J, Jankovic J, et al. Dystonia. Nat Rev Dis Primers. 2018;4:25. Erratum in: Nat Rev Dis Primers. 2018;4:37.
3. Gündel H, Wolf A, Xidara V, Busch R, Ceballos-Baumann AO. Social phobia in spasmodic torticollis. J Neurol Neurosurg Psychiatry. 2001;71:499-504.
4. Perozzo P, Salatino A, Cerrato P, Ricci R. Sexual well-being in patients with blepharospasm, spasmodic torticollis, and hemifacial spasm: a pilot study. Front Psychol. 2016;7:1492.
5. Jahanshahi M, Sartory G, Marsden CD. EMG biofeedback treatment of torticollis: a controlled outcome study. Biofeedback Self Regul. 1991;16:413-48.
6. Maione R, Formica C, Quartarone A, Lo Buono V. The impact of non-motor symptoms on quality of life in cervical dystonia. J Clin Med. 2023;12:4663.
7. Marek M, Grobe-Einsler M, Bedarf JR, Wabbels B, Paus S. Sexual dysfunction in cervical dystonia and blepharospasm. Neuropsychiatr Dis Treat. 2018;14:2847-2852.
8. Arkar H, Şafak C.Klinik bir örneklemde Beck Depresyon Envanterinin boyutlarının araştırılması. Türk Psikoloji Dergisi. 2004;19:117-23.
9. Tsui JK, Eisen A, Stoessl AJ, Calne S, Calne DB. Double-blind study of botulinum toxin in spasmodic torticollis. Lancet. 1986;2:245-7.
10. Peall KJ, Berman BD, Bruggemann N, Defazio G, Gimeno H, Jinnah HA, et al. Non-motor symptoms in dystonia: from diagnosis to treatment. Dystonia. 2023:11860.

11. Gill JS, Nguyen MX, Hull M, van der Heijden ME, Nguyen K, Thomas SP, et al. Function and dysfunction of the dystonia network: an exploration of neural circuits that underlie the acquired and isolated dystonias. Dystonia. 2023;2:11805.

12. Farzal Z, Lamotte G, Mundel E, Bahroo LB, Pagan FL. Movement disorders moment: treatment approaches to cervical dystonia. Practical Neurology. Last Accessed Date: 03.06.2024. Available from: https://practicalneurology.com

Medical Journal of Bakırköy

Med J Bakirkoy 2025;21:97-103
DOI: 10.4274/BMJ.galenos.2024.2023.10-7

Research

Etiological and Clinical Characteristics of Cases with Pancreatitis

Pankreatit Tanılı Olguların Etiyolojik ve Klinik Özellikleri

Pınar Bilen[1], Nafiye Urgancı[2], Merve Usta[2], Dilek Güller[2]

[1]University of Health Sciences Türkiye, Şişli Hamidiye Etfal Training and Research Hospital, Clinic of Pediatrics, İstanbul, Türkiye

[2]University of Health Sciences Türkiye, Şişli Hamidiye Etfal Training and Research Hospital, Clinic of Pediatric Gastroenterology, İstanbul, Türkiye

ABSTRACT

Objective: This study aimed to evaluate the clinical, laboratory, and etiological features of children with pancreatitis.

Methods: Sixty-three patients who were followed up between 2005 and 2019 and diagnosed with pancreatitis were enrolled in the study. The patients were classified into groups 1 and 2, with acute and chronic pancreatitis, respectively. The demographic, etiological, clinical features, and laboratory parameters were evaluated retrospectively.

Results: The mean age was 11.1±2.3 (range 3.9-16.7 years) and M/F was 1.6. The most common causes were biliary sludge, gallstones (14.2%), and familial Mediterranean fever (FMF) (11%). Group 1 included 46 patients (73.1%) and group 2 included 17 patients with acute recurrent pancreatitis and 7 patients with chronic pancreatitis. The most common causes were idiopathic (50%), biliary sludge and stones (15.3%), and infections (13%) in group 1 and idiopathic (17.7%), FMF (17.7%), cystic fibrosis (17.7%), and genetics (17.7%) in group 2. There were no statistically significant differences in laboratory parameters between the groups (p>0.05).

Conclusion: In developing countries where consanguineous marriage is common, genetic diseases, especially FMF, should be considered in patients presenting with abdominal pain, amylase, and lipase elevation and diagnosed with pancreatitis.

Keywords: Acute pancreatitis, etiology, treatment, children

ÖZ

Amaç: Çalışmanın amacı pankreatit tanılı çocukların klinik, laboratuvar ve etiyolojik özelliklerini değerlendirmektir.

Gereç ve Yöntem: Çalışmaya 2005-2019 yılları arasında pankreatit tanısıyla takip edilen 63 hasta dahil edildi. Hastalar grup 1, akut pankreatitli hastalar ve grup 2, akut tekrarlayan pankreatitli veya kronik pankreatitli hastalar olarak sınıflandırıldı. Demografik, etiyolojik, klinik özellikler ve laboratuvar parametreleri retrospektif olarak değerlendirildi.

Bulgular: Ortalama yaş 11,1±2,3 (dağılım 3,9-16,7 yıl) ve E/K 1,6 idi. En sık görülen nedenler safra çamuru, safra taşları (%14,2) ve ailevi Akdeniz ateşi (FMF) (%11) idi. Grup 1'de 46 (%73,1) hasta, grup 2'de ise 17 akut tekrarlayan pankreatit ve 7 kronik pankreatit hastası yer aldı. Grup 1'de en sık görülen nedenler idiyopatik (%50), safra çamuru ve taşları (%15,3) ve enfeksiyonlar (%13), idiyopatik (%17,7), FMF (%17,7), kistik fibrozis (%17,7) ve idiyopatik (%17,7) idi. Grup 2'de genetik (%17,7). Gruplar arasında laboratuvar parametreleri açısından istatistiksel olarak anlamlı fark yoktu (p>0,05).

Sonuç: Akraba evliliğinin yaygın olduğu gelişmekte olan ülkelerde karın ağrısı, amilaz ve lipaz yüksekliği ile başvuran ve pankreatit tanısı alan hastalarda başta FMF olmak üzere genetik hastalıklar da düşünülmelidir.

Anahtar Kelimeler: Akut pankreatit, etiyoloji, tedavi, çocuklar

Address for Correspondence: Prof. MD, Nafiye Ugancı, University of Health Sciences Türkiye, Şişli Hamidiye Etfal Training and Research Hospital, Clinic of Pediatric Gastroenterology, İstanbul, Türkiye
E-mail: nafiyeurganci@yahoo.com **ORCID ID:** orcid.org/0000-0003-4854-507X

Cite as: Bilen P, Ugancı N, Usta M, Güller D. Etiological and clinical characteristics of cases with pancreatitis. Med J Bakirkoy. 2025;21:97-103

Received: 02.11.2023
Accepted: 02.05.2024
Publication Date: 25.03.2025

INTRODUCTION

The incidence of acute pancreatitis (AP) in childhood tends to increase gradually. The annual incidence of this condition is approximately 1/10,000 in children (1). The increase in frequency may be related to the actual increase in the prevalence of the disease among children and the increase in awareness (2).

Pancreatitis is inflammation of the pancreas, which is usually a self-limiting disease with a mild course in children (3,4). It is characterized by clinical symptoms such as abdominal pain, nausea, and vomiting, and increased digestive enzyme levels (3,4). Pancreatitis was classified by the International Study group of Pediatric Pancreatitis: In search for a cuRE group; as acute, acute recurrent, or chronic (5,6). The incidence of acute recurrent pancreatitis (ARP) after the first AP attack is 20%, and that of chronic pancreatitis (CP) is 35% (7). In children, these rates are 21.5% and 22%, respectively (8). The incidence of ARP among children within the first 5 months after the first AP attack was 70% (9).

There are significant differences in etiology, incidence, clinical manifestations, complications and prognosis when compared with adults (9-11). While the most common causes in adults are alcohol and gallstones (10), the causes vary according to age in children, including obstructive/biliary, infections, metabolic trauma, toxins, systemic illness, inborn errors of metabolism, and genetic predispositions (4,11-13).

The etiological and clinical features, laboratory findings, and imaging findings of pediatric patients with pancreatitis were examined.

METHODS

Sixty-three patients with pancreatitis who were followed up in the pediatric gastroenterology department between 2005 and January 2019 were included in the study. The medical records of the patients were analyzed retrospectively.

The diagnosis of AP was based on the presence of at least two of three criteria, including clinical symptoms such as abdominal pain, nausea, and vomiting; increased serum amylase levels (>3 times upper limit of normal); and/or increased serum lipase levels (>3 times upper limit of normal), and radiological findings consistent with pancreatitis (5,6). Two or more than 2 attacks of AP at different periods when pancreatic enzymes return to normal is considered ARP. CP is considered if one of the three criteria, including typical abdominal pain, exocrine pancreatic insufficiency, or endocrine pancreatic insufficiency, exists in addition to characteristic imaging findings (5,6). The patients were classified as group 1, patients with AP, and as group 2, patients with ARP or CP. Non-pancreatic amylase/lipase elevations, such as parotitis, mumps, appendicitis, macroamylasemia and peritonitis were excluded.

Biochemical and hematological examinations were performed in all patients. Amylase clearance (amylase clearance =100 x (Urine amylase (U/L Ux Serum creatinine) / (Serum amylase x Urine creatinine) was calculated (14). Amylase clearance >5 was considered AP. Ultrasonography (US) and magnetic resonance imaging (MRI) examinations, which are among the imaging methods that help diagnose pancreatitis, were evaluated in the department of radiology.

The study was approved by the Ethics Committee of University of Health Sciences Türkiye, Şişli Hamidiye Etfal Training and Research Hospital (no: 1355, date: 10/01/2019). Informed consent was obtained from the patient' parents.

Statistical Analysis

Statistical analysis was performed using the Statistical Package for the Social Sciences (SPSS) 22.0 package program (SPSS Inc, Chicago, Illinois, U.S.A.). The Shapiro-Wilk test was applied to all variables to determine whether there was a normal or abnormal distribution. Frequency distributions were expressed as numbers and percentages, variables with normal distribution were expressed as mean ± standard deviation, and variables without normal distribution were expressed as median (minimum-maximum). In the comparison of paired groups, the Independent Samples t-test for numerical variables with normal distribution and Mann-Whitney U test for variables with abnormal distribution were used. Chi-square analysis was used in the analysis of categorical data. $P<0.05$ was considered significant for all results.

RESULTS

Sixty-three patients (mean age: 11.1±2.3, range 3.9-16.7 years, M/F: 1.6) were included in the study. In total, 11.2% of the patients were under 5 years old, 26.9% were 6-10 years old, and 61.9% were 11-17 years old. Abdominal pain was found in 95.2% of the patients, nausea and vomiting in 57.1%, fever in 14.2%, and jaundice in 3.1% at admission. The most common causes were bile sludge and stones (14.2%), familial Mediterranean fever (FMF) (11%), and infections (9.6%) (Table 1).

None of the patients had anemia, leukocytosis, hyper- or hypocalcemia, hyper/hypoglycemia, or serology for hepatitis A, B, and C. Serum immunoglobulin G, A, and M levels and lactate dehydrogenase values were found to be within age-appropriate limits, with average levels

of 1002, 231, 218, and 254.2 U/L, respectively. Laboratory parameters at admission are presented in Table 2. Direct bilirubinemia was detected in only one patient. While this case was followed up with the diagnosis of hereditary spherocytosis and gallstones, endoscopic retrograde cholangiopancreatography (ERCP) was performed because of the sudden onset of abdominal pain, high liver enzyme levels, amylase, lipase, and direct bilirubin. Clinical and laboratory improvements were observed after the removal of choledochal stones. Cholecystectomy was performed during follow-up. Abnormal ultrasonographic findings among imaging methods were observed in only 22 (35.5%) patients (Table 2).

No significant differences were observed in terms of age, gender, and laboratory parameters between the two groups. The most common causes were idiopathic (50%), biliary sludge and stones (15.3%), and infections (13%) in group 1 and idiopathic (17.7%), FMF (17.7%), cystic fibrosis (17.7%), and genetics (17.7%) in group 2 (Table 3). There were no statistically significant differences between the findings observed by US and MRI in the cases in Groups 1 and 2 ($p>0.05$) (Table 4).

All cases were closely followed for the first 48 hours. Oral feeding of 8 (12.6%) patients with moderate or severe clinical status was stopped for 48 h by intravenous fluid administration and then slowly reopened. Oral feeding was not interrupted in any of the other patients. Prophylactic antibiotics and proton pump inhibitors were initiated. Creon was initiated in six patients with CP. No attack has been observed for 6 months.

During follow-up, patients with pancreatitis were also examined for accompanying diseases and complications. A 5.5-year-old male patient with AP secondary to type 1 hyperlipidemia and 9.5, 15.5, and 8.5-year-old girls without any additional disease, but due to pleural effusion and respiratory distress, were followed up in the intensive care unit. Plasmapheresis was applied to patients with hyperlipidemia type 1, and a decrease in triglyceride levels and improvement in the AP clinic were observed. Because the serum liver enzyme levels of 6 patients who had an AP attack due to gallstones increased 4 times the average and total bilirubin levels increased 5 times the normal, ERCP and elective cholecystectomy were performed in these patients.

Table 1. Distribution of patients with pancreatitis according to etiology

Idiopathic	26	(41.2%)
Gall sludge and stones	9	(14.2%)
FMF	7	(11%)
Infections		
Cytomegalovirus IgM	1	(1.6%)
Parvovirus B19 IgM	2	(3.2%)
M. pneumoniae	3	(4.8%)
Obesity	3	(4.8%)
Cystic fibrosis	3	(4.8%)
Trauma	2	(3.2%)
Hereditary		
SPINK mutation	2	(3.2%)
PRSS1 mutation	1	(1.6%)
Drugs	1	(1.6%)
Hemolytic uremic syndrome	1	(1.6%)
Anatomical malformation		
Duplication cyst of the duodenum	1	(1.6%)
Hyperlipidemia	1	(1.6%)

Ig: Immunoglobulin, FMF: Familial Mediterranean fever

Table 2. Laboratory parameters and ultrasonographic findings upon admission

Laboratory findings	
Hemoglobin (10-13.5 g/dL)	13.2 (9.6-16.4)
Hematocrit (31-41%)	38.8 (27.3-47.4)
Amylase (28-100 U/L)	630.9 (53-2134)
Lipase (7-39 U/L)	915.2 (44-4947.6)
Amylase clearance	5.56 (5.1-7.35)
Glucose (74-106 mg/dL)	103.3 (67-167)
Calcium (8.8-10.8 mg/dL)	8.67 (8.1-10.53)
Total protein (5.7-8 g/dL)	6.73 (4.17-7.85)
Albumin (3.5-5.2 g/dL)	4.13 (2.6-5.05)
AST (0-40 U/L)	35.6 (9-408)
ALT (0-41 U/L)	32.8 (5-221)
GGT (0-17 U/L)	41.7 (7-234.3)
ALP (<300 U/L)	197.9 (63-613)
LDH (120-300 U/L)	254.2 (34-624)
Total bilirubin (0.3-1.2 mg/dL)	0.8 (0.13-5.74)
Direct bilirubin (0-0.2 mg/dL)	0.34 (0.07-4.3)
IgG (mg/dL)	1040 (830-1320)
IgA (mg/dL)	176 (62-352)
IgM (mg/dL)	142 (39.1-299)
Ultrasonographic findings	
Gall sludge and stones	9 (14.2%)
Increase in pancreatic size	5 (7.9%)
Pancreatic edema	4 (6.3%)
Dilatation in bile ducts	2 (3.1%)
Hemorrhagic pancreatitis	1 (1.5%)
Necrotizing pancreatitis	1 (1.5%)

AST: Aspartate aminotransferase, ALT: Alanine aminotransferase, GGT: Gamaglutamyl transpeptidase, ALP: Alkaline phosphatase, LDH: Lactate dehidrogenase, Ig: Immunoglobulin

Table 3. Comparison of patients in groups 1 and 2

	Group 1	Group 2	p-value
	(n=46)	(n=17)	
Age (mean, ± SD, years)	11.2±3.1	12.1±2.4	1.00
Gender (M/F)	1.5 (28/18)	1.8 (11/6)	0.28
Etiology			
Idiopathic	23 (50%)	3 (17.7%)	0.023
Gall stone and sludge	7 (15.3%)	2 (11.7%)	1.00
Infection	6 (13%)	-	0.17
FMF	4 (8.6%)	3 (17.7%)	0.37
Trauma	2 (4.3%)	-	1.00
Hyperlipidemia	1 (2.2%)	-	1.00
Drug	1 (2.2%)	-	1.00
HUS	1 (2.2%)	-	1.00
Obesity	1 (2.2%)	2 (11.7%)	0.17
CF	-	3 (17.7%)	0.017
Anatomic malformation	-	1 (5.8%)	0.269
Genetic	-	3 (17.7%)	0.017
Laboratory parameters			
Hemoglobin (10.5-13.5 g/dL)	13.8 (9.6-16.4)	13.4 (13.3-14.1)	0.89
Hematocrit (31-41%)	37.4 (36-45.2)	37.3 (27.3-47.4)	0.85
Glucose (74-106 mg/dL)	111 (81-167)	91 (67-101)	0.52
Calcium (8.8-10.8 mg/dL)	9.78 (8.1-10.35)	10.4 (10.2-10.53)	0.41
Phosphorus (2.5-4.5 mg/dL)	3.11 (2.9-4.5)	3.98 (3.94-4.95)	0.21
Chloride (97-107 mg/dL)	101 (95-103.4)	97.2 (94-102)	0.96
Creatinine (0.6-1.2 mg/dL)	0.61 (0.46-0.93)	0.57 (0.37-0.63)	0.82
Amylase (28-100 U/L)	746 (53-2134)	841 (758-1074)	0.63
Lipase (7-39 U/L)	1027 (237-4947.6)	1058 (44-1506)	0.70
Amylase clearance	4.8 (3.1-7.35)	5.3 (3.5-5.8)	0.74
AST (0-40 U/L)	49 (9-58.8)	23 (17-408)	0.67
ALT (0-41 U/L)	15.8 (5-58.1)	90 (9-221)	0.54
GGT (0-17 U/L)	105 (11-234.3)	11 (7-168)	0.76
LDH (110-295 U/L)	183 (34-321)	219 (204-624)	0.21
ALP (0-300 U/L)	154 (63-2804)	204 (203-613)	0.53
Total bilirubin (0.3-1.2 mg/dL)	0.43 (0.19-5.74)	0.4 (0.13-0.77)	0.11
Direct bilirubin (0-0.02 mg/dL)	0.27 (0.11-4.3)	0.35 (0.1-0.7)	0.21
Total protein (5.7-8 g/dL)	5.58 (4.17-7.58)	7.9 (6.5-7.85)	0.69
Albumin (3.5-5.2 g/dL)	4.7 (2.6-4.54)	4.9 (4.1-5.05)	0.40

p<0.05 is statistically significant. AST: Aspartate aminotransferase, ALT: Alanine aminotransferase, GGT: Gamaglutamyl transpeptidase, ALP: Alkaline phosphatase, LDH: Lactate dehidrogenase, FMF: Familial Mediterranean fever, HUS: Hemolyticuremic syndrome, CF: Cystic fibrosis, SD: Standard deviation

Seven patients with abdominal pain, fever, and joint pain had homozygous R202Q FMF mutations. Colchicine treatment was initiated in 3 patients who experienced recurrent pancreatitis attacks. Patients whose complaints decreased after treatment were still followed up without any problems. In one of the cases, a pseudopancreatic cyst developed in the early period. However, regression was observed during follow-up. Mortality was not observed in any of the patients.

DISCUSSION

Any stimulus that disrupts the mechanisms that protect the acinar cells of the pancreas against autodigestion (such

Table 4. Radiological findings of patients in groups 1 and 2

	Group 1 (n=46)	Group 2 (n=17)	p-value
Ultrasonographic findings			
Normal	29 (64.4%)	12 (68%)	0.76
Gall sludge and stones	8 (18%)	1 (6%)	0.42
Increase in pancreatic size	3 (7%)	2 (11%)	0.60
Pancreatic edema	2 (4.4%)	2 (11%)	0.29
Dilatation in bile ducts	2 (4.4%)	0	1.00
Hemorrhagic pancreatitis	1 (2.2%)	0	1.00
Necrotizing pancreatitis	0	1 (6%)	0.26
CT and/or MRI findings	12 (26%)	8 (47%)	
Pancreatic edema	9 (75%)	5 (62.5%)	0.64
Necrotizing pancreatitis	1 (8%)	0	1.00
Dilated duct of Wirsung	1 (8%)	3 (37.5%)	0.25
Hemorrhagic pancreatitis	1 (8%)	0	1.00
Peripancreatic fluid collection	5 (25.4%)	3 (27.3%)	1.00

p<0.05 is statistically significant. MRI: Magnetic resonance imaging, CT: Computed tomography

as reflux of bile to the pancreatic duct, drugs or trauma) activates digestive enzymes, causing inflammation, vascular damage, and necrosis in the pancreatic tissue, leading to the development of pancreatitis.

Pancreatitis is caused by various causes such as biliary diseases (gallstones, microlithiasis), infections, trauma, and metabolic causes in childhood (4,12,15). Sağ et al. (16) reported that 25% of their patients with AP had idiopathic pancreatitis, 14.3% had systemic diseases such as hemolytic uremic syndrome, Henoch-Schönlein purpura, and connective tissue diseases, 11.1% had trauma, and 9.5% had cholelithiasis. Park et al. (17) found that 36.2% of 215 AP cases were due to biliary causes and 25.6% to drugs. Pezzilli et al. (18) observed that biliary diseases were the most common cause of pancreatitis (20%), followed by viral infections (12%). CholedochaL cysts and hyperlipidemia were reported as the most common causes in Fayyaz et al. (19). While Kandula and Lowe (20) found multisystemic disease (33.3%) and systemic infections (18.4%) to be the most common causes in 87 cases, Lautz et al. (21) determined that most of the cases were idiopathic (31.3%) in their large-series. Majbar et al. (22) reported that the most common causes were drugs (19%) and cholelithiasis (13%) in 94 patients with AP. Consistent with the literature, 41.2% of our patients with AP were idiopathic, followed by biliary diseases, infections, FMF, CF, and trauma, in order of frequency. We believe that these differences in the causes of AP may be related to ethnic or geographic changes.

Al Hindi et al. (3) found that pediatric AP was more common in males and age between six years and 10 years. No significant difference was observed in this study.

An increase of more than 3 times in amylase and lipase levels is indicative of the diagnosis of AP (2,4,10). In our cases, amylase and lipase levels were detected approximately 10 times higher than the normal limits. Since amylase clearance in the first 24 h was calculated as >5, all cases were evaluated as AP. In our study, no significant differences were observed between the groups in terms of laboratory and imaging findings.

Although AP improved after the first attack, 10-30% of the cases developed ARP with an increase in the number of attacks. The causes of ARP differ from AP. The most common causes are biliopancreatic structural disorders and obstructions, such as gallstones (8). In studies conducted in adults, patients with idiopathic ARP and genetically induced ARP often progress to CP (23). Poddar et al. (8) reported that the most common causes of 320 cases of ARP and CP were idiopathic (70% and 88%, respectively), followed by biliary diseases, familial pancreatitis, and anatomical malformations. In our country, Ünlüsoy et al. (24) reported that 47% of patients with ARP and CP were idiopathic. We can explain the low rate of this rate in patients with ARP and CP can be explained by the small number of patients.

ARP has been reported in FMF, especially in adulthood, due to duodenal amyloid accumulation (25). In our study, the frequency of FMF was significantly higher in patients with AP, ARP, and CP than in the other studies. We can explain this with the high rate of consanguineous marriage in our country. In addition, it was claimed that the heterozygous R202Q mutation did not cause pancreatitis, whereas the detection of homozygous R202Q mutation in all cases with pancreatitis and the decrease in AP or ARP attacks after colchicine treatment were remarkable.

It is known that CTFR, PRSS1, SPINK and CTCR mutations are among the genetic causes of CP (26). *CTFR, PRSS1*, or *SPINK* gene mutations were detected in 79% of the cases and family history was found to be positive in 5% in a study conducted between 2000 and 2009 in children under the age of 18 who were diagnosed with ARP and CP in a single center (27). This rate was reported to be 17.6% in a study from our country (24). In our study, only two of our patients with ARP and CP had SPINK mutations and 1 had PRSS1 mutations. Our mutation rate was 4.8%, which can be explained by the fact that mutation examinations have been performed in our hospital in recent years.

Local complications, such as acute fluid collection and pseudocysts, can occur in the presence of acute severe

pancreatitis. Although studies have shown that acute fluid collection in adults mostly regresses spontaneously, half of pancreatic pseudocysts and most pancreatic acids require therapeutic intervention (8,28). Until now, data on complications secondary to pancreatitis in the pediatric population. Al Hindi et al. (3) reported three cases complicated by pseudocysts. In our study, a 3 cm cyst developed in the tail of the pancreas in one patient (1.6%) with ARP. The cyst was less than 6 cm in size, and it resolved spontaneously in 8 weeks without drainage.

Although the AP-related mortality rate varies in different studies, it was reported to be 0.4-6% and it is thought that mortality is mainly related to the underlying cause (20,29). Lautz et al. (21) observed a mortality rate of 2.4% in patients with AP and suggested that this was not directly related to the severity of AP but was related to the underlying comorbidity. Goday et al. (30) found a mortality rate of 0.3% and mortality rate due to secondary causes of 6.8% in patients with AP who needed pediatric intensive care. Mortality was not observed in any of our patients, but 3 cases (4.8%) who developed pleural effusion and respiratory distress were followed up without secondary complications in the intensive care unit.

As stated in the literature, the incidence of patients with pancreatitis has been increasing among pediatric patients in recent years. Although the causes of pancreatitis are variable, most cases are still idiopathic, as in our study, consistent with the literature.

CONCLUSION

In conclusion, contrary to countries where the etiology of pancreatitis is diverse, such as ours, where consanguineous marriage is common, genetic diseases, especially FMF, should be considered in patients presenting with abdominal pain, amylase, and lipase elevation and diagnosed with pancreatitis. Patients with pancreatitis should be closely monitored for supportive therapy, complications, and CP.

ETHICS

Ethics Committee Approval: The study was approved by the Ethics Committee of University of Health Sciences Türkiye, Şişli Hamidiye Etfal Training and Research Hospital (no: 1355, date: 10/01/2019).

Informed Consent: Informed consent was obtained from the patient' parents.

FOOTNOTES

Authorship Contributions

Surgical and Medical Practices: P.B., N.U., M.U., D.G., Concept: P.B., N.U., Design: P.B., N.U., Data Collection or Processing: P.B., M.U., D.G., Analysis or Interpretation: P.B., N.U., Literature Search: P.B., N.U., Writing: P.B., N.U.

Conflict of Interest: No conflict of interest was declared by the authors.

Financial Disclosure: The authors declared that this study received no financial support.

REFERENCES

1. Morinville VD, Barmada MM, Lowe ME. Increasing incidence of acute pancreatitis at an American pediatric tertiary care center: is greater awareness among physicians responsible? Pancreas. 2010;39:5-8.
2. Grzybowska-Chlebowczyk U, Jasielska M, Flak-Wancerz A, Więcek S, Gruszczyńska K, Chlebowczyk W, Woś H. Acute pancreatitis in children. Prz Gastroenterol. 2018;13:69-75.
3. Al Hindi S, Khalaf Z, Nazzal K, Nazzal O, Ahmed A, Alshaibani L. Acute pancreatitis in children: the clinical profile at a tertiary hospital. Cureus. 2021;13:e14871.
4. Abu-El-Haija M, Kumar S, Quiros JA, Balakrishnan K, Barth B, Bitton S, et al. Management of acute pancreatitis in the pediatric population: a clinical report from the North American Society for Pediatric Gastroenterology, Hepatology and Nutrition Pancreas Committee. J Pediatr Gastroenterol Nutr. 2018;66:159-76.
5. Morinville VD, Husain SZ, Bai H, Barth B, Alhosh R, Durie PR, et al. Definitions of pediatric pancreatitis and survey of present clinical practices. J Pediatr Gastroenterol Nutr. 2012;55:261-5.
6. Morinville VD, Lowe ME, Ahuja M, Barth B, Bellin MD, Davis H, et al. Design and implementation of INSPPIRE. J Pediatr Gastroenterol Nutr. 2014;59:360-4.
7. Petrov MS, Yadav D. Global epidemiology and holistic prevention of pancreatitis. Nat Rev Gastroenterol Hepatol. 2019;16:175-84.
8. Poddar U, Yachha SK, Borkar V, Srivastava A, Kumar S. A report of 320 cases of childhood pancreatitis: increasing incidence, etiologic categorization, dynamics, severity assessment, and outcome. Pancreas. 2017;46:110-5.
9. Sweeny KF, Lin TK, Nathan JD, Denson LA, Husain SZ, Hornung L, et al. Rapid progression of acute pancreatitis to acute recurrent pancreatitis in children. J Pediatr Gastroenterol Nutr. 2019;68:104-9.
10. Freeman AJ, Maqbool A, Bellin MD, Goldschneider KR, Grover AS, Hartzell C, et al. Medical management of chronic pancreatitis in children: a position paper by the North American Society for Pediatric Gastroenterology, Hepatology, and Nutrition Pancreas Committee. J Pediatr Gastroenterol Nutr. 2021;72:324-40.
11. Schwarzenberg SJ, Uc A, Zimmerman B, Wilschanski M, Wilcox CM, Whitcomb DC, et al. Chronic pancreatitis: pediatric and adult cohorts show similarities in disease progress despite different risk factors. J Pediatr Gastroenterol Nutr. 2019;68:566-73.

12. Karne S, Gorelick FS. Etiopathogenesis of acute pancreatitis. Surg Clin North Am. 1999;79:699-710.
13. Suzuki M, Minowa K, Isayama H, Shimizu T. Acute recurrent and chronic pancreatitis in children. Pediatr Int. 2021;63:137-49.
14. Warshaw AL, Fuller AF Jr. Specificity of increased renal clearance of amylase in diagnosis of acute pancreatitis. N Engl J Med. 1975;292:325-8.
15. Felderbauer P, Müller C, Bulut K, Belyaev O, Schmitz F, Uhl W, Schmidt WE. Pathophysiology and treatment of acute pancreatitis: new therapeutic targets--a ray of hope? Basic Clin Pharmacol Toxicol. 2005;97:342-50.
16. Sağ E, Kaya G, Bahat-Özdoğan E, Karahan SC, İmamoğlu M, Sarıhan H, et al. Acute pancreatitis in children: A single center experience over ten years. Turk J Pediatr. 2018;60:153-8.
17. Park A, Latif SU, Shah AU, Tian J, Werlin S, Hsiao A, et al. Changing referral trends of acute pancreatitis in children: A 12-year single-center analysis. J Pediatr Gastroenterol Nutr. 2009;49:316-22.
18. Pezzilli R, Morselli-Labate AM, Castellano E, Barbera C, Corrao S, Di Prima L, Lucidi V, Carroccio A. Acute pancreatitis in children. An Italian multicentre study. Dig Liver Dis. 2002;34:343-8.
19. Fayyaz Z, Cheema HA, Suleman H, Hashmi MA, Parkash A, Waheed N. Clinical presentation, aetiology and complications of pancreatitis in children. J Ayub Med Coll Abbottabad. 2015;27:628-32.
20. Kandula L, Lowe ME. Etiology and outcome of acute pancreatitis in infants and toddlers. J Pediatr. 2008;152:106-10.
21. Lautz TB, Chin AC, Radhakrishnan J. Acute pancreatitis in children: Spectrum of disease and predictors of severity. J Pediatr Surg. 2011;46:1144-9.
22. Majbar AA, Cusick E, Johnson P, Lynn RM, Hunt LP, Shield JP. Incidence and clinical associations of childhood acute pancreatitis. Pediatrics. 2016;138:e20161198.
23. Kumar S, Ooi CY, Werlin S, Abu-El-Haija M, Barth B, Bellin MD, et al. Risk factors associated with pediatric acute recurrent and chronic pancreatitis: lessons from INSPPIRE. Lessons From INSPPIRE. JAMA Pediatr. 2016;170:562-9.
24. Ünlüsoy Aksu A, Sarı S, Eğritaş Gürkan Ö, Dalgic B. Pancreatitis in Turkish children: a single center experience. Cukurova Med J 2019;44:991-8.
25. Sisk CM, Chamberlin W, Rholl VL, Rholl JC. Acute recurring pancreatitis: a manifestation of duodenal amyloid deposition. Case report and review. Gastrointest Endosc. 2001;53:656–7.
26. Taylor CJ, Chen K, Horvath K, Hughes D, Lowe ME, Mehta D, et al. ESPGHAN and NASPGHAN report on the assessment of exocrine pancreatic function and pancreatitis in children. J Pediatr Gastroenterol Nutr. 2015;61:144-53.
27. Sultan M, Werlin S, Venkatasubramani N. Genetic prevalence and characteristics in children with recurrent pancreatitis. J Pediatr Gastroenterol Nutr. 2012;54:645-50.
28. Cheruvu CV, Clarke MG, Prentice M, Eyre-Brook IA. Conservative treatment as an option in the management of pancreatic pseudocyst. Ann R Coll Surg Engl. 2003;85:313-6.
29. Pant C, Sferra TJ, Lee BR, Cocjin JT, Olyaee M. Acute recurrent pancreatitis in children: a study from the Pediatric Health Information System. J Pediatr Gastroenterol Nutr. 2016;62:450-2.
30. Goday PS, Wakeham M, Kuhn EM, Collins MM, Werlin SL. Acute pancreatitis in the pediatric intensive care unit. J Pediatr Gastroenterol Nutr. 2015;61:108-12.

Medical Journal of Bakırköy

Med J Bakirkoy 2025;21:104-111
DOI: 10.4274/BMJ.galenos.2024.2024.8-1

Research

Comparison of the Efficacy of Different Local Anesthetic Volumes on the Success of Combined Interscalene-Supraclavicular Nerve Block

Farklı Lokal Anestetik Hacimlerinin Kombine İnterskalen-Supraklavikular Sinir Bloğunun Başarısına Olan Etkinliklerinin Karşılaştırılması

Özlem Melike Ekşi[1], Gökhan Sertcakacılar[2,3], Yaser Pektaş[2], Güneş Özlem Yıldız[2], Zafer Çukurova[2], Gülsüm Oya Hergünsel[2]

[1]Marmara University Faculty of Medicine, Department of Physical Medicine and Rehabilitation, Division of Pain Medicine, İstanbul, Türkiye
[2]University of Health Sciences Türkiye, Bakırköy Dr. Sadi Konuk Training and Research Hospital, Clinic of Anesthesiology and Intensive Care, İstanbul, Türkiye
[3]Outcomes Research Consortium, Texas, USA

ABSTRACT

Objective: Brachial plexus blocks are used as an alternative to general anesthesia for most procedures performed in the upper extremity. This study aimed to compare the perioperative anesthetic and analgesic efficacy of combined interscalene block-supraclavicular brachial plexus block (ISB+SCB), with different volumes of local anesthetic (LA) under ultrasound guidance.

Methods: Data from 85 patients who underwent ISB+SCB for anesthesia in proximal upper extremity surgery including unilateral humerus and shoulder procedures between March 2021 and September 2023 were retrospectively reviewed. According to the local anaesthetic volume of bupivacaine administered, the patients were divided into two groups: the high volume group (Group H), with 18 mL or more, and the low volume group (Group L), with less than 18 mL. Patients were evaluated in terms of anesthetic and analgesic effects in the perioperative period.

Results: Postoperative pain scores and additional analgesic requirements were not significantly different between the two groups during the follow-up period. Motor block was terminated in all patients (100%) at the 8th postoperative hour in Group L, whereas the rate was 89.4% in Group H. A statistically significant difference was found between the two groups (p=0.047). In Group H, the resolution of motor block in all patients was determined at the 12th postoperative hour. The volume of LA given in both groups was sufficient for surgical anesthesia.

Conclusion: Ultrasound-guided ISB+SCB with lower LA volume may provide effective surgical anesthesia and analgesia with similar efficacy and shorter duration of motor block in shoulder and humerus surgery.

Keywords: Upper extremity, interscalene block, supraclavicular block, low volume local anesthetic

ÖZ

Amaç: Brakiyal pleksus blokları, üst ekstremitede gerçekleştirilen çoğu prosedür için genel anesteziye alternatif olarak kullanılmaktadır. Bu çalışmada, ultrason eşliğinde farklı volümlerde lokal anestezi (LA) ile yapılan kombine interskalen blok-supraklavikular brakiyal pleksus bloğunun (İSB+SCB), perioperatif anestezik ve analjezik etkinliğinin karşılaştırılması hedeflenmiştir.

Gereç ve Yöntem: Mart 2021 ile Eylül 2023 tarihleri arasında tek taraflı humerus ve omuz girişimlerini içeren proksimal üst ekstremite cerrahisinde anestezi amacıyla İSB+SCB uygulanan 85 hastanın verileri geriye dönük olarak tarandı. Uygulanan bupivakaine LA volümüne göre hastalar, 18 mL ve üstü uygulanan yüksek hacimli grup (Grup H) ve 18 mL'den daha düşük volüm uygulanan düşük hacimli grup (Grup L) olmak üzere iki gruba ayrıldı. Hastalar perioperatif dönemde anestezik ve analjezik etki açısından değerlendirildi.

Bulgular: Postoperatif ağrı skorları ve ek analjezik gereksinimi karşılaştırıldığında iki grup arasında takip süresince anlamlı fark saptanmadı. Motor blok ise Grup L'de postoperatif 8. saatte hastaların tamamında (%100) sonlanırken, Grup H'de bu oran %89,4 olarak saptandı ve iki grup arasında istatistiksel olarak anlamlı fark bulundu (p=0,047). Grup H'de motor bloğun tüm hastalarda geri dönüş zamanı postoperatif 12. saat olarak belirlendi. Her iki grupta da verilen LA hacmi cerrahi anestezi için yeterli idi.

Address for Correspondence: Özlem Melike Ekşi, Marmara University Faculty of Medicine, Department of Physical Medicine and Rehabilitation, Division of Pain Medicine, İstanbul, Türkiye
E-mail: ozlemeksi91@hotmail.com **ORCID ID:** orcid.org/0000-0002-9947-979X

Cite as: Ekşi ÖM, Sertcakacılar G, Pektaş Y, Yıldız GÖ, Çukurova Z, Hergünsel GO. Comparison of the efficacy of different local anesthetic volumes on the success of combined interscalene-supraclavicular nerve block. Med J Bakirkoy. 2025;21:104-111

Received: 06.08.2024
Accepted: 21.10.2024
Publication Date: 25.03.2025

ÖZ

Sonuç: Ultrason kılavuzluğunda daha düşük LA hacmi ile uygulanan İSB+SCB, omuz ve humerus cerrahisinde benzer etkinlik ve daha kısa motor blok süresi ile etkin cerrahi anestezi ve analjezi sağlayabilir.

Anahtar Kelimeler: Üst ekstremite, interskalen blok, supraklavikular blok, düşük hacim lokal anestezik

INTRODUCTION

Anesthesia for upper extremity and shoulder surgery can be provided by general anesthesia, regional anesthesia, or a combination of these. Although general anesthesia provides precise airway control, side effects related to general anesthesia and opioids may adversely affect patient comfort and prolong hospital stays with inadequate pain control in a fragile patient population (1). Regional anesthesia techniques maintain more stable hemodynamics compared to general anesthesia, prevent airway instrumentation, and provide adequate intraoperative and postoperative analgesia (2).

Peripheral nerve blocks used for anesthesia and analgesia in upper extremity and shoulder surgery vary according to the patient and the surgical procedure to be performed (1). The distribution, size, and innervation of the blocked surgical area may not be fully achieved with a single peripheral nerve block (3). For this reason, combined block applications are becoming increasingly popular. For example, interscalene block (ISB) and supraclavicular block (SCB) may be sufficient for the proximal arm, but if the surgical intervention involves the distal arm, the ulnar nerve must also be blocked (4).

The interscalene approach to the brachial plexus is the preferred technique for shoulder and proximal arm surgical procedures. However, there is a 100% incidence of ipsilateral phrenic nerve involvement and hemidiaphragm paralysis, resulting from blockade of the C3-5 cervical nerve roots at high volumes. There is also a risk of Horner's syndrome secondary to sympathetic blockade hoarseness and respiratory distress with recurrent laryngeal nerve blockade, and hypotensive-bradycardic events with the Bezold-Jarisch reflex (5). This limits the use of ISB, aimed at reducing the volume of LA used in ISB by increasing dual block applications (6). Infraclavicular-suprascapular block to prevent phrenic nerve paralysis in humeral head fracture repair; axillary-ISB in multiple fractures of the humerus, shoulder, and elbow, and supraclavicular-ISB used for multiple fractures of the humerus are some of the dual blocks in the literature (6-10). However, dual block application requires high doses of local anesthetic (LA) (6). Although the use of a lower volume of LA when performed under ultrasonography (USG) guidance has reduced complications, there are not enough studies on combined blocks, to reach the required area in the proximal upper extremity (11). In addition, there is no clear consensus on the appropriate dose of LA for surgical anesthesia (12).

The extent of blockage in peripheral nerve block applications depends on the neural structure, anatomy, volume, and concentration of the LA used (13). Although the amount of LA required can be reduced by closer perineural needle placement under USG guidance, especially in dual block applications, the minimum required LA dose in peripheral nerve blocks cannot be standardized because it also depends on the structure of the nerve (14).

The primary aim of this study was to compare the effect of different volumes of LAs on perioperative anesthetic and 24-hour pain scores in patients undergoing ISB+SCB for shoulder and humerus surgery. The secondary aim was to evaluate the need for additional postoperative analgesics, changes in vital parameters, and sensory and motor block return times between the two groups.

METHODS

Patient Selection

Our retrospective, single-center, observational study was performed after Clinical Research Ethics Committee of University of Health Sciences Türkiye, Bakırköy Dr. Sadi Konuk Training and Research Hospital (approval no.: 2023-22-10, date: 20.11.2023) was obtained. The data of patients who underwent shoulder arthroscopy operation for unilateral humeral fracture open reduction internal fixation, shoulder impingement syndrome, slap lesion surgery, and rotator cuff rupture, and who underwent ISB+SCB for anesthesia between 02.03.2021 and 18.09.2023 in the orthopedic clinic, were retrospectively reviewed. Eighty-five patients with American Society of Anesthesiologists (ASA) physical status I-III, aged 18-75 years, in whom the operation was completed uneventfully with regional anesthesia were included in the study. Patients excluded from the study included those with incomplete information in the pain and patient follow-up form, those younger than 18 years of age, those with a neurological deficit involving the upper extremity, those with a bleeding coagulation disorder, those with a history of alcohol-substance abuse, those with psychological illness, those with advanced chronic obstructive pulmonary disease, and those in whom the block was performed only for analgesia, were excluded from the study.

Preoperative Preparation & Block Technique

Peripheral vascular access was provided to all patients after preoperative monitoring in accordance with ASA guidelines. Intravenous (i.v.), midazolam 0.02 mg/kg was administered as premedication before the procedure.

SCB

The patient was placed in a supine position with the head rotated 45 degrees to the opposite side. After sterilization of the area to be blocked, the brachial plexus was identified around the subclavian artery in the supraclavicular fossa using a 5-13 MHz linear ultrasound probe (Esaote MyLabSeven/Esaote S-P.A, Genoa, Italy) for SCB. A 100 mm 22 gauge insulated needle (Stimuplex Insulated B Braun Medical, Germany) was used to target the deep brachial plexus above the first rib using the inplane technique. LA was injected after negative aspiration, from posterior to anterior and lateral to medial. After the corner pocket was formed, the remaining volume was injected just above and lateral to the subclavian artery.

ISB

For USG-guided ISB, the brachial plexus was re-imaged from the supraclavicular fossa. The probe was advanced cephalad along the level of the cricoid cartilage, and hypoechoic, oval C5 and C6 cervical nerve roots were visualized between the anterior and middle scalene muscles in the interscalene groove. The LA was injected after aspiration. Diffusion of LAs was visually confirmed by USG. All blocks were performed by an anesthetist with at least five years of experience.

When scanned retrospectively, standard 6 mL 2% prilocaine for rapid onset of action and 0.5% bupivacaine in different volumes for prolonged duration of action were used as LA agents in both blocks. According to the volume of bupivacaine LA administered, the patients were divided into two groups: high volume group (Group H), with 18 mL or more, and low volume group (Group L), with less than 18 mL.

Perioperative Evaluation

Patient and pain follow-up form, pinprick test, and modified Bromage scale were used as data collection tools. In addition to demographic data; ASA score; operation information; operation time and volume of LAs administered; numeric pain score (NRS) at 0-1-4-8-12-16-20 and 24 hours; additional rescue analgesic requirement; return time of sensory and motor block; and hemodynamic and vital parameters (systolic, diastolic, and mean blood pressure), which were evaluated by the routine pain team using the postoperative pain assessment form in our hospital, were documented on these forms. In the ward, 3 doses of 1 g paracetamol and 3 doses of 50 mg tramadol hydrochloride, were administered IV as routine analgesia protocol. In patients with an NRS score above 3 who needed additional analgesia, 50 mg dexketoprofen trometamol i.v. was administered as rescue analgesia. Our study was conducted in accordance with the 1995 Declaration of Helsinki (as revised in Brazil, 2013).

Statistical Analysis

In this study, the Number Cruncher Statistical System 2017 (Kaysville, Utah, USA) program will be used for statistical analyses. While evaluating the study data, the frequency and percentage values for categorical variables, as well as the mean and standard deviation values for continuous variables, will be given. Normal distribution tests of continuous variables will be conducted using the Kolmogorov-Smirnov test. Chi-square analysis will be used for the relationships between categorical variables. Where appropriate, categorical variables will also be evaluated with Fisher's exact, and Fisher's Freeman Halton test. Independent Samples t-tests will be used for two-group comparisons in continuous independent variables that exhibit a normal distribution. For variables that do not fulfill the assumption of normal distribution, the Mann-Whitney U test will be used for two independent group comparisons. $P<0.05$ will be considered statistically significant.

RESULTS

After the application of inclusion and exclusion criteria, a total of 85 patients, 38 (44.7%) in Group L and 47 (55.2%) in Group H, were included in the study. When demographic data were analyzed, the mean age of all patients was 57.8±15.9 years; 63.5% were male and 36.5% were female. ASA risk groups were similar between the two groups ($p>0.05$). 55.3% of the patients in Group L and 48.9% in Group H were in the ASA II risk group. Similar operations were performed between the two groups, with humeral surgery being the predominant operation in 68% of patients in Group L and 55% in Group H. Surgical time was 125.2±42.3 min in Group L and 122.3±37.2 min in Group H ($p=0.73$). Anesthesia times were similar between the two groups ($p=0.75$) (Table 1).

There was no significant difference between the two groups during the follow-up period when systolic-diastolic blood pressure and peak heart rate were compared (Table 2). There was also no significant difference between the two groups when postoperative pain scores and additional analgesic requirements were compared (Table 3).

When the duration of the motor-sensory block was analyzed, the sensory block was terminated at the 12th postoperative hour in both groups. The block efficiency

was similar between the two groups during the follow-up period. The motor block duration returned to function at the 8th hour postoperatively in all patients (100%) in Group L. In contrast, this rate was 89.4% in Group H, and a statistically significant difference was found between the two groups (p=0.047). The return of motor function in all patients in Group H was determined as the 12th hour postoperatively. During the follow-up period, the duration of sensory-motor block was similar between the two groups except for the 8th postoperative hour (Table 3).

Complications were observed in each of 3 patients in Groups 1 and 2 (7.9% and 6.4%, respectively), and no significant difference was observed between the two groups. Ptosis resolved at 4 hours with conservative treatment in 3 patients in Group L and 2 patients in Group H; while 1 patient in Group H had hoarseness that resolved spontaneously.

Table 1. Demographic data

Parameters (mean ± SD)	Total (n=85)	Grup L (n=38)	Grup H (n=47)	p
Age (year)	57.8±15.9	58.5±16.6	57.1±15.4	0.698
Gender (n; %)				0.821
1 (Male)	54 (63.5)	25 (65.8)	29 (61.7)	
2 (Female)	31 (36.5)	13 (34.2)	18 (38.3)	
ASA (n; %)				0.695
1	10 (11.8)	5 (13.2)	5 (10.6)	
2	44 (51.8)	21 (55.3)	23 (48.9)	
3	31 (36.5)	12 (31.6)	19 (40.4)	
Operation type (n; %)				0.155
1 (Arthroscopy)	22 (25.9)	6 (15.8)	16 (34)	
2 (ORİF)	52 (61.2)	26 (68.4)	26 (55.3)	
3 (Other)	11 (12.9)	6 (15.8)	5 (10.6)	
Duration of anesthesia (min)	158.8±36.2	160.2±38.4	157.7±34.7	0.754
Surgical time (min)	123.6±39.4	125.2±42.3	122.3±37.2	0.736

ASA: American Society of Anesthesiologists, SD: Standard deviation, ORIF: Open reduction internal fixation

Table 2. Vital parameters

HR (beats/min)				
0th hour	70.8±11.7	68.9±13.2	72.3±10.2	0.189
1st hour	73.1±14.6	70.2±11.3	75.9±16.9	0.102
4th hour	79.1±12	78.1±12.1	79.8±12.1	0.590
8th hour	80.8±13.4	79.5±13.2	82.2±13.8	0.443
12th hour	82.2±11.7	81.3±11.5	83.2±12.1	0.588
16th hour	80.5±9.8	79±11.4	81.7±8.2	0.350
20th hour	77.7±8.7	79.2±9.9	76.8±7.8	0.303
24th hour	80.8±11	79.4±10.9	82±11.2	0.484
SBP (mmHg)				
0th hour	118.5±20.8	117.2±19.6	119.4±21.9	0.639
1st hour	121.6±18.6	119.9±15.4	123.3±21.4	0.456
4th hour	122.9±16.9	125.1±18.5	121.4±15.6	0.373
8th hour	122.9±16.1	124.1±17.1	121.5±14.9	0.531
12th hour	128.6±14.2	131.6±14	125.4±14	0.140
16th hour	125.9±16.8	126.9±15.4	125.1±18.2	0.727
20th hour	124.7±13.3	125.6±13.6	124.1±13.3	0.689
24th hour	125.4±13.8	126.9±14.8	124.2±13.1	0.562
DBP (mmHg)				
0th hour	71.1±12.1	71.1±13.4	71.1±11.2	0.982
1st hour	72±9.9	71.1±8.4	72.8±11.3	0.494
4th hour	71.8±8	73.4±8.5	70.7±7.4	0.178
8th hour	71.3±7.8	71.2±7.7	71.6±8	0.842
12th hour	75±8.9	74.5±8.4	75.4±9.6	0.736
16th hour	71.6±8.6	72±6.2	71.3±10.3	0.768
20th hour	73.5±7.6	74.7±7.8	72.2±7.5	0.232
24th hour	73.1±8.2	73.6±7.7	72.7±8.8	0.743

HR: Heart rate, SBP: Systolic blood pressure, DBP: Diastolic blood pressure

DISCUSSION

In our study, combined ISB+SCB was performed under USG-guided guidance, and postoperative efficacy of high- and low-volume LAs (18 mL and above and less than 18 mL) was evaluated. Postoperative pain scores and additional analgesic requirements were similar between the two groups.

Blockade of the brachial plexus can provide effective anesthesia and analgesia in the entire upper extremity. However, the type of block applied differs according to the location of the operation (15). While distal extremity anesthesia can be achieved with infraclavicular and isolated nerve blocks, the ISB and SCB should be combined to ensure a high success rate in procedures requiring anesthesia of the proximal arm. This is because even if a sufficient volume of LA is injected into the SCB, it may fail to block the C5 and C6 nerve roots (16). However, dual block (ISB and SCB) requires a high dose of LA agent, which increases the risk of LA toxicity and side effects (3). Studies with ultrasound guidance and electrical nerve stimulation techniques have focused on block success rate, block initiation time, and LA dose (15). Although ultrasonographic visualization of the needle, the target nerve, and the injected LA have been associated with increased block success rates, decreased block initiation times, and decreased amount of LA required for successful nerve block, there is no clear consensus on the dose, and volume to be administered (17-19). In our study, we aimed to evaluate the effect of different volumes of ISB-SCB block on anesthetic success, postoperative pain

Table 3. Postoperative data

Additional analgesia (n; %)				
0th hour	2 (2.4)	1 (2.6)	1 (2.1)	0.697
1st hour	6 (7.1)	4 (10.5)	2 (4.3)	0.243
4th hour	7 (8.2)	2 (5.3)	5 (10.6)	0.314
8th hour	19 (22.4)	8 (21.1)	11 (23.4)	0.796
12th hour	22 (25.9)	12 (31.6)	10 (21.3)	0.281
16th hour	29 (34.1)	10 (26.3)	19 (40.4)	0.173
20th hour	31 (36.5)	13 (34.2)	18 (38.3)	0.697
24th hour	26 (30.6)	13 (34.2)	13 (27.7)	0.515
NRS (mean±SD)				
0th hour	0 (0)	0 (0)	0 (0)	0.249*
1st hour	0 (1)	0 (1)	0 (1)	0.861*
4th hour	0 (2)	1 (2)	0 (2)	0.365*
8th hour	2.5 (2)	2 (2)	3 (2)	0.576*
12th hour	3 (2)	3 (3)	2 (1)	0.853*
16th hour	3 (2)	2 (3)	3 (2)	0.122*
20th hour	3 (2)	3 (2)	3 (2)	0.541*
24th hour	3 (2)	3 (2)	3 (2)	0.671*
Sensory (n ; %)				
0th hour				0.842
Negative	53 (62.4)	24 (63.2)	29 (61.7)	
Partial	6 (7.1)	2 (5.3)	4 (8.5)	
Positive	26 (30.6)	12 (31.6)	14 (29.8)	
1st hour				0.529
Negative	27 (31.8)	14 (36.8)	13 (27.7)	
Partial	12 (14.1)	6 (15.8)	6 (12.8)	
Positive	46 (54.1)	18 (47.4)	28 (59.6)	
4th hour				0.768
Negative	17 (20)	7 (18.4)	10 (21.3)	
Partial	7 (8.2)	4 (10.5)	3 (6.4)	
Positive	61 (71.8)	27 (71.1)	34 (72.3)	
8th hour				0.467
Negative	3 (3.6)	1 (2.6)	2 (4.3)	
Partial	5 (6)	1 (2.6)	4 (8.5)	
Positive	77 (90.6)	36 (94.7)	41 (87.2)	
12th hour				n/a
Positive	85 (100)	38 (100)	47 (100)	
16th hour				n/a
Positive	85 (100)	38 (100)	47 (100)	
20th hour				n/a
Positive	85 (100)	38 (100)	47 (100)	
24th hour				n/a
Positive	85 (100)	38 (100)	47 (100)	

Table 3. Continued

Motor (n; %)				
0th hour				0.335
Negative	45 (52.9)	17 (44.7)	28 (59.6)	
Partial	15 (17.6)	7 (18.4)	8 (17)	
Positive	25 (29.4)	14 (36.8)	11 (23.4)	
1st hour				
Negative	24 (28.2)	10 (26.3)	14 (29.8)	0.590
Partial	14 (16.5)	8 (21.1)	6 (12.8)	
Positive	47 (55.3)	20 (52.6)	27 (57.4)	
4th hour				
Negative	11 (12.9)	2 (5.3)	9 (19.1)	0.165
Partial	8 (9.4)	4 (10.5)	4 (8.5)	
Positive	66 (77.6)	32 (84.2)	34 (72.3)	
8th hour				0.047
Partial	5 (5.9)	0 (0)	5 (10.6)	
Positive	80 (94.1)	38 (100)	42 (89.4)	
12th hour				
Positive	85 (100)	38 (100)	47 (100)	n/a
16th hour				
Positive	85 (100)	38 (100)	47 (100)	n/a
20th hour				
Positive	85 (100)	38 (100)	47 (100)	n/a
24th hour				
Positive	85 (100)	38 (100)	47 (100)	n/a
Complications (n; %)	6 (7.1)	3 (7.9)	3 (6.4)	0.787

*Values presented as median (interquartile range) and comparisons made using the Mann-Whitney U test
+presented as median (IQR)
NRS: Numeric rating scale, IQR: Interquartile range, SD: Standard deviation

scores, and the need for additional analgesia in shoulder and humerus surgical procedures.

The use of low-dose 0.5% ropivacaine in ultrasound-guided ISB was first reported by Riazi et al. (20). The study included patients who underwent open and arthroscopic shoulder surgery and ISB in 5 mL and 20 mL volumes for analgesia. In this prospective randomized controlled trial (RCT), no significant difference was found between the two groups in LA volume and pain scores, sleep quality, and total opioid consumption up to 24 hours postoperatively (20). In the present study, similar results were obtained in the groups. In another RCT, Abdelhaq et al. (3) divided 93 patients who underwent combined SCB+ISB for humeral fracture, into three groups according to the volume of LA administered. Standard 20 mL (10 mL 0.5% bupivacaine + 10 mL 2% lidocaine), and different volumes (20-15-10 mL) of LA were administered for SCB and ISB, respectively. It was emphasized that the amount of LA administered to the ISB could be reduced with dual block, but that the duration of analgesia was significantly reduced with the reduction of LA volume (3). In another RCT, 5 or 15 mL, 0.5% ropivacaine doses were compared for patients undergoing superior truncal block (STB) during shoulder arthroscopies. Postoperative pain score, additional analgesic use, duration of analgesia, side effects, and patient satisfaction were found to be similar between the two groups (21). This contrast in the literature may be explained by differences in the volume of LA administered, the use of blocks for postoperative analgesia, and the fact that the operation was performed under general anesthesia (20,21). In the present study, the median volume of bupivacaine administered was 18 mL because of applying a combined block (ISB-SCB) and the provision of surgical anesthesia with a regional block in all patients.

One of the factors affecting the duration of peripheral nerve block is the dose of LA, which is the product of volume and concentration. The effect of LA volume, concentration, and dose on the duration of the block varies in studies (22). In one study, it was shown that the duration of motor and sensory block was significantly shortened by decreasing 1.5% mepivacaine, from 40 mL to 15 mL in patients undergoing axillary brachial plexus block (23). In another study, no significant correlation was found between volume increase and onset of block, and motor block duration in patients undergoing humeral surgery. Sensory block duration was found to be prolonged with volume increase (3). In the present study, sensory block duration was similar between the two groups, whereas motor block duration was significantly prolonged in the high-volume group. Although there are many publications in the literature indicating a direct relationship between the amount of LA given and duration, it is not clear whether this effect depends on dose, volume, or their combination (22-25). In another study evaluating the effect of different volumes and concentrations

of ropivacaine on the duration of analgesia after ISB in shoulder surgery, it was concluded that both volume and concentration affected the duration independently (26). In another study conducted to evaluate whether the decrease in the duration of sensory and motor block was mainly related to the decrease in volume or the decrease in dose, patients who underwent axillary block were divided into three groups. Group 1 used 20 mL of 1.5% mepivacaine (300 mg), Group 2 used 30 mL of 1% mepivacaine (300 mg) and Group 3 used 30 mL of 1.5% mepivacaine (450 mg). When the groups with equal doses were compared, it was reported that sensory and motor block lasted longer in the group with higher concentration and smaller volume (Groups A and B), but this was not statistically significant. The use of diluted and low-dose LAs (Group B) was shown to significantly shorten the duration of motor and sensory blocks compared to high doses and high concentrations (Group C) (22). The difference may be related to variations in concentration and dose reported in the literature.

LA systemic toxicity and the development of complications are directly related to the dose, volume, concentration, and site of administration of LA (14). In a study investigating the relationship between the volume of LA administered (5 mL vs 20 mL) and complications in shoulder surgery, ultrasonographic measurements and respiratory function tests showed that the incidence of diaphragm paralysis was significantly reduced in the 5 mL group. Although Horner's syndrome, hoarseness, hiccough, and respiratory distress occurred in 8 patients (40%), no adverse outcome was reported in the low-volume group (20). Similarly, Kim et al. (21) evaluated the efficacy of STB with 5 mL and 15 mL of LA in shoulder surgery and showed that analgesic efficacy was similar, with less hemidiaphragm paralysis in the low-volume group. This is due to the spread of LA along the prevertebral fascia, resulting in phrenic nerve block and hemidiaphragm paralysis due to C3-C5 involvement. There is also a risk of Horner's syndrome secondary to sympathetic blockade, hoarseness with recurrent laryngeal nerve blockade, respiratory distress, and hypotensive-bradycardic events with the Bezold-Jarisch reflex (5). In addition, proximity to the epidural space may cause neuraxial spread and LA systemic toxicity (LAST) at high doses (27). Although phrenic nerve involvement was not evaluated in our study, respiratory distress was not observed in any patient. Horner's syndrome was seen in three patients in each group, with there being no statistically significant difference between them.

Study Limitations

The main limitations of our study are its retrospective nature, the small number of patients, and the fact that it was conducted at a single center. Sufficient data on volume and block onset time could not be obtained in the groups. In addition, phrenic nerve involvement was not evaluated in patients who underwent a block. However, providing surgical anesthesia as well as postoperative analgesia with regional block, and avoiding the possible effects of general anesthesia are the strengths of our study.

CONCLUSION

Effective anesthesia and optimal surgical conditions can be achieved by using low-volume ISB-SCB applied in shoulder and humerus surgery. In addition, the shortening of motor block return time and the ability to provide effective analgesia up to 24 hours postoperatively may encourage the use of low doses for peripheral nerve blocks in clinical practice, highlighting additional advantages of this application.

ETHICS

Ethics Committee Approval: Ethical approval was obtained from the Clinical Research Ethics Committee of University of Health Sciences Türkiye, Bakırköy Dr. Sadi Konuk Training and Research Hospital (approval no.: 2023-22-10, date: 20.11.2023).

Informed Consent: Retrospective, single-center, observational study.

FOOTNOTES

Authorship Contributions

Surgical and Medical Practices: Ö.M.E., Y.P., Z.Ç., Concept: Ö.M.E., G.S., Y.P., G.O.H., Design: Ö.M.E., G.S., G.Ö.Y., Data Collection or Processing: Ö.M.E., Y.P., Z.Ç., Analysis or Interpretation: Ö.M.E., G.Ö.Y., G.O.H., Literature Search: Ö.M.E., G.Ö.Y., G.O.H., Writing: Ö.M.E., G.S., Z.Ç.

Conflict of Interest: No conflict of interest was declared by the authors.

Financial Disclosure: The authors declare that this study received no financial support.

REFERENCES

1. Hadzic A, Williams BA, Karaca PE, Hobeika P, Unis G, Dermksian J, et al. For outpatient rotator cuff surgery, nerve block anesthesia provides superior same-day recovery over general anesthesia. Anesthesiology. 2005;102:1001-7.
2. Mirza F, Brown AR. Ultrasound-guided regional anesthesia for procedures of the upper extremity. Anesthesiol Res Pract. 2011;2011:e579824.
3. Abdelhaq MM, Kamal AM, Elramely MA. Different volumes of local anesthetics in ultrasound-guided combined interscalene-supraclavicular block for traumatic humeral fracture. OJAnes. 2016;6:55-62.

4. Nadeau MJ, Lévesque S, Dion N. Ultrasound-guided regional anesthesia for upper limb surgery. Can J Anaesth. 2013;60:304-20.
5. ASRA [Internet]. [cited: 2023 Dec 11]. How i do it: regional anesthesia for shoulder surgery. Available from: https://www.asra.com/news-publications/asra-newsletter/newsletter-item/asra-news/2020/11/01/how-i-do-it-regional-anesthesia-for-shoulder-surgery
6. Falyar CR, Grossman EC. Ultrasound-guided interscalene-supraclavicular block for intramedullary nailing of a pathologic humeral fracture: practical application of ultrasound-guided regional anesthesia. AANA J. 2014;82:219-22.
7. Brown AR, Parker GC. The use of a "reverse" axis (axillary-interscalene) block in a patient presenting with fractures of the left shoulder and elbow. Anesth Analg. 2001;93:1618-20.
8. Martínez J, Sala-Blanch X, Ramos I, Gomar C. Combined infraclavicular plexus block with suprascapular nerve block for humeral head surgery in a patient with respiratory failure: an alternative approach. Anesthesiology. 2003;98:784-5.
9. Urban MK, Urquhart B. Evaluation of brachial plexus anesthesia for upper extremity surgery. Reg Anesth. 1994;19:175-82.
10. Guttman OT, Soffer RJ, Rosenblatt MA. The ultrasound-guided supraclavicular-interscalene (UGSCIS) block: a case report. Pain Pract. 2008;8:62-4.
11. McNaught A, Shastri U, Carmichael N, Awad IT, Columb M, Cheung J, et al. Ultrasound reduces the minimum effective local anesthetic volume compared with peripheral nerve stimulation for interscalene block. Br J Anaesth. 2011;106:124-30.
12. Lim JA, Lim H, Lee JH, Kwak SG, Kim JH, Song SY, et al. Local anesthetic volume in ultrasound-guided interscalene block and opioid consumption during shoulder arthroscopic surgery. Medicine (Baltimore). 2021;100:e26527.
13. Raizada N, Chandralekha, Jain PC, Kumar A. Does compounding and increase in concentration of local anaesthetic agents increase the success rate of brachial plexus block ? Indian J Anaesth. 2002;46:193-6.
14. Mather LE, Copeland SE, Ladd LA. Acute toxicity of local anesthetics: underlying pharmacokinetic and pharmacodynamic concepts. Reg Anesth Pain Med. 2005;30:553-66.
15. O'Donnell BD, Iohom G. Local anesthetic dose and volume used in ultrasound-guided peripheral nerve blockade. Int Anesthesiol Clin. 2010;48:45-58.
16. Vermeylen K, Engelen S, Sermeus L, Soetens F, Van de Velde M. Supraclavicular brachial plexus blocks: review and current practice. Acta Anaesthesiol Belg. 2012;63:15-21.
17. Kapral S, Greher M, Huber G, Willschke H, Kettner S, Kdolsky R, et al. Ultrasonographic guidance improves the success rate of interscalene brachial plexus blockade. Reg Anesth Pain Med. 2008;33:253-8.
18. Casati A, Baciarello M, Di Cianni S, Danelli G, De Marco G, Leone S, et al. Effects of ultrasound guidance on the minimum effective anesthetic volume required to block the femoral nerve. Br J Anaesth. 2007;98:823-7.
19. Willschke H, Bösenberg A, Marhofer P, Johnston S, Kettner S, Eichenberger U, et al. Ultrasonographic-guided ilioinguinal/iliohypogastric nerve block in pediatric anesthesia: what is the optimal volume? Anesth Analg. 2006;102:1680-4.
20. Riazi S, Carmichael N, Awad I, Holtby RM, McCartney CJL. Effect of local anesthetic volume (20 vs 5 ml) on the efficacy and respiratory consequences of ultrasound-guided interscalene brachial plexus block. Br J Anaesth. 2008;101:549-56.
21. Kim H, Han JU, Lee W, Jeon YS, Jeong J, Yang C, et al. Effects of local anesthetic volume (standard versus low) on incidence of hemidiaphragmatic paralysis and analgesic quality for ultrasound-guided superior trunk block after arthroscopic shoulder surgery. Anesth Analg. 2021;133:1303-10.
22. Fenten MGE, Schoenmakers KPW, Heesterbeek PJC, Scheffer GJ, Stienstra R. Effect of local anesthetic concentration, dose and volume on the duration of single-injection ultrasound-guided axillary brachial plexus block with mepivacaine: a randomized controlled trial. BMC Anesthesiol. 2015;15:130.
23. Schoenmakers KPW, Wegener JT, Stienstra R. Effect of local anesthetic volume (15 vs 40 mL) on the duration of ultrasound-guided single shot axillary brachial plexus block: a prospective randomized, observer-blinded trial. Reg Anesth Pain Med. 2012;37:242-7.
24. Latzke D, Marhofer P, Zeitlinger M, Machata A, Neumann F, Lackner E, et al. Minimal local anesthetic volumes for sciatic nerve block: evaluation of ED 99 in volunteers. Br J Anaesth. 2010;104:239-44.
25. Ponrouch M, Bouic N, Bringuier S, Biboulet P, Choquet O, Kassim M, et al. Estimation and pharmacodynamic consequences of the minimum effective anesthetic volumes for median and ulnar nerve blocks: a randomized, double-blind, controlled comparison between ultrasound and nerve stimulation guidance. Anesth Analg. 2010;111:1059-64.
26. Fredrickson MJ, Abeysekera A, White R. Randomized study of the effect of local anesthetic volume and concentration on the duration of peripheral nerve blockade. Reg Anesth Pain Med. 2012;37:495-501.
27. Kessler J, Schafhalter-Zoppoth I, Gray AT. An ultrasound study of the phrenic nerve in the posterior cervical triangle: implications for the interscalene brachial plexus block. Reg Anesth Pain Med. 2008;33:545-50.

Medical Journal of Bakırköy

Med J Bakirkoy 2025;21:112-120
DOI: 10.4274/BMJ.galenos.2024.2024.5-13

Research

Association of Different Doses of Curcumin with Preadipocyte to Adipocyte Differentiation

Farklı Kurkumin Dozları ile Preadiposit-Adiposit Farklılaşması Arasındaki İlişki

Pınar Çetinalp[1], Sevgin Değirmencioğlu[2], Sevda Tanrıkulu Küçük[1], Muhammed Seyithanoğlu[3], Yıldız Öner İyidoğan[4], Hikmet Koçak[5]

[1]T.C. Demiroğlu Bilim University Faculty of Medicine, Department of Biochemistry, İstanbul, Türkiye
[2]Kırklareli University Faculty of Medicine, Department of Biochemistry, Kırklareli, Türkiye
[3]Kahramanmaraş Sütçü İmam University Faculty of Medicine, Department of Biochemistry, Kahramanmaraş, Türkiye
[4]İstinye University Faculty of Medicine, Department of Biochemistry, İstanbul, Türkiye
[5]İstinye University Faculty of Medicine, Department of Medical Education, İstanbul, Türkiye

ABSTRACT

Objective: Human adipose tissue participates in fat storage and immune response. Curcumin (CUR) decreases adipocyte differentiation by inhibiting inflammatory cytokines and by activating anti-inflammatory cytokines. In this study, we aimed to determine the suppressor effects of different doses of CUR (0.5 µM, 5 µM, 10 µM, 20 µM, 50 µM) on preadipocyte-adipocyte differentiation and its anti-inflammatory role in adipocytes.

Methods: Differentiation of cells was performed using Oil Red O. The mRNA expression levels of adiponectin, C/EBPα, COX-2, IL-6, leptin, NFκB1, PPARγ, SIRT-1, TNF-α, TRPV1, UCP2, VEGF-A, VEGF-RI, and VEGF-RII were evaluated in preadipocyte and adipocytes.

Results: CUR decreased the differentiation of preadipocytes-adipocytes and the release of proinflammatory cytokines by regulating the expression of *C/EBPα* and *PPARγ* gene expressions.

Conclusion: CUR inhibited adipogenic transcription factors and adipocyte differentiation at all concentrations. The anti-inflammatory effect was greatest at 50 µM.

Keywords: Curcumin, differentiation, adipocytes, anti-inflammatory

ÖZ

Amaç: İnsan yağ dokusu yağ depolanmasının yanısırada immun cevapda da rol oynar. Kurkuminin (CUR) enflamatuvar sitokinleri inhibe ederek ve anti-enflamatuvar sitokinlerin aktive ederek adiposit farklılaşmasını azalttığı gösterilmiştir. Bu çalışmada farklı dozlardaki CUR'un (0,5 µM, 5 µM, 10 µM, 20 µM, 50 µM) preadiposit-adiposit farklılaşmasındaki baskılayıcı etkisini ve adipositlerdeki anti-enflamatuvar rolünü ortaya çıkarmayı hedefledik.

Gereç ve Yöntem: Hücrelerin farklılaşması Oil Red O kullanılarak, adiponektin, C/EBPα, COX-2, IL-6, leptin, Nükleer NFκB1, PPARγ, SIRT-1, TNF-α, TRPV1, UCP2, VEGF-A, VEGF-RI ve VEGF-RII mRNA ekspresyon düzeyleri preadipositlerde ve adipositlerde saptandı.

Bulgular: CUR'un, preadipositlerin adipositlere farklılaşmasını ve proinflamatuar sitokinlerin salınımını azalttı. Bunu, *C/EBPα* ve *PPARγ* gen ekspresyonlarını düzenleyerek yaptı

Sonuç: Sonuç olarak, CUR, 0,5-50 µM arasındaki tüm dozlarda adipojenik transkripsiyon faktörlerini ve adiposit farklılaşmasını inhibe etti. Anti-enflamatuvar etkisini en fazla 50 µM'de gösterdi.

Anahtar Kelimeler: Kurkumin, farklılaşma, adipositler, anti-enflamatuvar

Address for Correspondence: Pınar Çetinalp, T.C. Demiroğlu Bilim University Faculty of Medicine, Department of Biochemistry, İstanbul, Türkiye
E-mail: pinarcetinalp@outlook.com **ORCID ID:** orcid.org/0000-0003-3194-9676

Cite as: Çetinalp P, Değirmencioğlu S, Tanrıkulu Küçük S, Seyithanoğlu M, Öner İyidoğan Y, Koçak H. Association of different doses of curcumin with preadipocyte to adipocyte differentiation. Med J Bakirkoy. 2025;21:112-120

Received: 05.04.2024
Accepted: 02.09.2024
Publication Date: 25.03.2025

INTRODUCTION

Human adipose tissue is involved in fat storage and also plays a role in immune response. Adipose tissue includes various cell types such as preadipocyte cells, adipocyte cells, endothelial cells, mast cells, fibroblasts, diverse immune cells, stem cells (1,2). It may also inhibit weight earning and metabolic diseases through the activation of specialized heat-productive adipocytes (3,4). The expression of transcriptional regulators such as peroxisome proliferator-activated receptor gamma (*PPAR-γ*) and CCAAT/enhancer binding protein α (C/EBPα), sirtuin (SIRT), and transient receptor potential vanilloid 1 (TRPV1) receptor and 2, receptors induce the differentiation of adipocytes and adipogenesis. Previous studies have revealed that TRPV1 channels participate in weight loss by enhancing intracellular Ca^{2+} levels (5-10).

Brown adipose tissue (BAT) comprises preadipocyte that express high levels of thermogenic genes. These preadipocyte are located in special stores and play a role in providing energy equality in all body parts by participating in thermogenesis, converting excess amounts of chemical/nutritional energy into heat energy. In contrast, brown-like adipocyte cells, also termed beige cells, grow in white adipocyte cells in response to various activators (5). The activities of beige and brown fat cells are important for reducing metabolic diseases, including obesity, in humans and mice (11). White adipose tissue (WAT) consists of adipocytes that store energy as triglycerides. However, BAT is functionally and physically different from WAT, and body mass index is adversely proportional to the amount of BAT suppression of adipocyte differentiation (from brown cells to white cells) and could be an effective strategy for preventing and treating obesity (12).

Activation and excessive expression of the SIRTs family are contained in the trans-differentiation or "browning" course of WAT to BAT (13). Beige adipocytes specialize in the dissipation of heat as energy. It does this by increasing their high mitochondrial content and the expression of mitochondria-related genes such as uncoupling proteins (UCPs). UCPs are a family of the mitochondrial anion carrier protein family that are targeted for weight loss therapy, with a role in controlling body temperature and energy balance (11).

White adipocytes produce and secrete a large number of adipokine, such as growth factors, cytokines, vasodilators, hormones, and others, including signal molecules (1,2). Adipokines have several functions. Regulation of appetite and energy, glucose and fat and metabolism, endothelial cell function, insulin function, inflammation, blood pressure, atherosclerosis, hemostasis, metabolic syndrome, and so on are some of these functions (14). Leptin, adiponectin (visfatin), inflammatory cytokines such as tumor necrosis factor-α (TNF-α), cyclooxygenase-2 (COX-2), iterleukin-6 (IL-6), interleukin-1 (IL-1), platelet activator inhibitor-1 (PAI-1), angiogenic proteins such as vascular endothelial growth factor (VEGF) and its receptor as VEGF-receptor (VEGF-R) are produced and secreted from white adipocytes. The molecular mechanisms of the effects of these adipokines are not fully understood, and research on this is still being conducted (9,15-17).

Various thermogenic dietary factors have been shown to prevent obesity and metabolic syndrome through antioxidant and anti-inflammatory mechanisms. Curcumin (CUR) is a polyphenolic compound derived from turmeric (Curcuma longa) plants belonging to the gingerol (Zingiberaceae) family. It has a wide variety of biological and pharmacological effects (18).

The thermogenic function of CUR was previously described as inhibiting the differentiation of adipocytes from preadipocyte (19). It has been reported that CUR inhibits adipocyte differentiation by affecting various regulators. CUR can lower the expression of PPARγ and C/EBPα leading to a decrease in lipid accumulation in adipocytes and ameliorating obesity and hyperlipidemia in patients with metabolic syndrome (20,21). CUR plays a potential role in reducing triglycerides. It does this by interacting with various targets, including cholesteryl ester transfer protein, peroxisome proliferator-activated receptor alpha, PPAR-γ and lipoprotein lipase (22). CUR, a natural polyphenol, is suggested to suppress adipocyte differentiation in the early stage by inhibiting the secretion of some regulators and inflammatory cytokines and by activating the secretion of anti-inflammatory cytokines (7,22,23). CUR is also reported to induce both the production and breakdown of triglyceride-rich lipoproteins to reduce plasma cholesterol and triglyceride concentrations by attenuating the expression of lipogenic genes (22). It can affect TRPV receptor 1 and TRPV2 receptor located in the intestinal jejunum and thus may have effects on both WAT and BAT (24,25).

The current study aimed to explore the molecular mechanisms of the inhibitory effects of different CUR doses on human preadipocyte-adipocyte (HPAd) cell differentiation. We also examined an adequate dose of CUR supplements to prevent adipocyte-related oxidative and inflammatory status. This study is the first to examine the effect of CUR on the HPAd cell differentiation.

In our study, we used the following methods with all CUR doses we prepared, and CUR doses were studied in triplicate in all methods.

METHODS

Procedures

Thawing, Detection, and Culturing Human Preadipocyte Cells

A vial containing $5x10^5$ human preadipocyte cells (HPAd from heart tissue, Catalog no: 802h-05a, cell Applications, San Diego CA, mycoplasma testing has been carried out for the cell line) seeded in preadipocyte growth medium (Cell Applications, San Diego CA) in 25 cm^2 (Corning, NY) tissue culture flasks under standard conditions and 25 cm^2 flask (Corning, NY) with preadipocyte growth medium in a 37 °C incubator containing 5% CO_2 (Sanyo MCO-20AIC, Moriguchi, Osaka, Japan) was incubated for 24 h. Microscopic examination showed that the cells were attached to the flask the next day and multiplied in the following days. When the flask surface contained 70-80% cells (confluen), the other passages were made with a Subculture Reagent Kit (cell applications, San Diego CA) according to the manufacturing protocol until the cells reached a sufficient number, and then the preadipocyte differentiation step was initiated.

Differentiation of Preadipocytes into Adipocytes

In order to differentiate $16x10^6$ cells into adipocyte cells, $2x10^5$ cells/2 mL preadipocyte cells were seeded into 5 of 6-well plates with growth medium. The next day, it was observed that the cells were attached to the wells, and the growth medium was changed. Adipocyte differentiation medium (cell applications, San Diego CA) was added to the cells into each well. During the addition of the adipocyte differentiation medium, different concentrations of CUR were also pipetted into the respective wells. In the first plates 3 wells formed the control cells, and in the other plates, different doses of CUR were added to 3 wells and plates were incubated in a 37 °C incubator containing 5% CO_2. Preadipocyte cells were followed for 15 days until they differentiated into adipocyte cells, and their medium was changed every 3 days. At the end of the 15^{th} day, when the cells were examined under a microscope (Leica Wetzlar, Germany), granulated oil drops were observed in the cells, which differentiated into adipocyte cells. The different doses of CUR were diluted with dimethyl sulfoxide and prepared. The applied CUR (Sigma, Germany) doses were 0.5 µM, 5 µM, 10 µM, 20 µM and 50 µM.

Staining of Differentiated Adipocyte Cells Using Oil Red O

Differentiation of cells was performed using the Oil Red O dye method. $15x10^3$ control cells/3 well stained with Oil Red O dye (Lipid Oil Red O Staining kit, Sigma-Aldrich, USA) according to kit procedure. Finally, ultrapure water was added to the cells and examined under a microscope. It was determined that they were painted with Oil Red O, and photographs were taken. Additionally, Oil Red O staining was quantified for all groups of adipocytes and preadipocyte in a 96-well plate reader (BioTek Instruments, USA) at 492 nm according to the kit procedure. For each group, experiments were repeated three times and measurements were performed in triplicate.

Quantifying mRNA Expression in Cells Using qRT-PCR

For mRNA expression quantification, total RNA was extracted from the cells using RNAzol RT solution (MRC, USA) according to the manufacturer's protocol. The concentration and purity of the RNA samples were then evaluated using a NanoDrop 2000 (Thermo Scientific, USA), where 1 µl of RNA was pipetted into the device. Prior to reverse transcription, RNA concentrations were standardized. Reverse transcription was performed using the Script cDNA Synthesis Kit (Jena Bioscience, Germany) following the kit protocol. The resulting cDNA was then amplified by qRT-PCR using the qPCR GreenMaster with the UNG Kit (Jena Bioscience, Germany). The remaining procedures followed the methodology outlined in the experiment by Değirmencioğlu et al. (17). Primers were sourced from LGC (Denmark), and all calculations were performed in triplicate. The primers used are detailed in Table 1.

Statistical Analysis

Results are presented as means±standard deviation of three experiments. Statistical analyses were performed using GraphPad Prism 5 software (San Diego, CA). One-way analysis of variance (ANOVA) was used to compare quantitative data among the groups. If the results of the ANOVA were significant, Tukey's multiple comparison test was used to compare groups' means ($p<0.05$).

RESULTS

The effects of different CUR doses on lipid accumulation during preadipocyte-adipocyte differentiation were determined using the Oil Red O dye method. Lipid accumulation was significantly increased during differentiation in control adipocytes ($p<0.001$). All different doses of CUR inhibited lipid accumulation, and the difference was statistically significant compared with the control adipocytes ($p<0.001$) (Figure 1).

Effects of CUR on *C/EBP-α* and *PPAR-γ* Gen Expresion

C/EBP-α expression levels were significantly increased in adipocytes during differentiation ($p<0.001$). Different doses

of CUR treatments (CUR 0.5-50 μM) during differentiation decreased C/EBP-α mRNA levels compared with adipocytes ($p<0.001$) (Figure 2).

Also *PPAR-γ* gen expression in adipocytes is enhanced significantly during differentiation compared with that in preadipocyte. CUR treatment during differentiation showed different effects on *PPAR-γ* gen expressions. In comparison to adipoyctes; Expression of *PPAR-γ* significantly decreased in CUR 0.5, CUR 10 ($p<0.01$) and CUR 50 ($p<0.05$) groups and significantly increased in the CUR 20 group ($p<0.001$) (Figure 2).

Effect of CUR on Adipokine Gene Expression

Adipokine mRNA expression was decreased in all CUR groups compared with adipocytes ($p<0.001$). The reduction in adipokine levels was not dose dependent (Figure 3). Leptin mRNA levels were significantly increased in all CUR-treated adipocytes except the CUR 50 group compared with the control adipocytes ($p<0.01$). In the CUR 50 group, leptin mRNA levels were significantly decreased ($p<0.01$) (Figure 3).

Effects of CUR on Proinflammatory Cytokines

COX-2 mRNA expression was significantly increased in all CUR-treated adipocytes compared with control adipocytes ($p<0.05$ for CUR 0.5, $p<0.001$ for CUR 5, CUR 10, CUR 20 and CUR 50). *IL-6* gene expression levels significantly changed during differentiation of CUR-added adipocytes. While a statistically significant increase was found in the CUR 0.5 and CUR 5 groups ($p<0.001$), IL-6 mRNA levels were significantly decreased in the CUR 10, CUR 20 and CUR 50 groups ($p<0.001$) in comparison with the control adipocytes. TNF-α mRNA levels were significantly increased in all CUR groups except the CUR 50 group in comparison with the control adipocytes ($p<0.05$ for CUR 0.5, $p<0.001$ for CUR 5, CUR 10 and CUR 20). In the CUR 50 group, mRNA levels of TNF-α significantly decreased ($p<0.001$) (Figure 4). The reduction of NFkB1 mRNA levels in the CUR 5 group and increase in the CUR 10 group were statistically significant compared with the control adipocytes ($p<0.001$ for both) (Figure 4).

Table 1. Primer list for RT-PCR

Gene name	Gene bank	Primer sequences	Product size (bp)
PPARG	NM_138712.5	Forward 5′-AGGATGCAAGGGTTTCTTCCG-3′ Reverse 5′-CCGCCAACAGCTTCTCCTTC-3′	200
CEBPA	NM_001285829.1	Forward 5′-CACCGCTCCAATGCCTACTG-3′ Reverse 5′-CTAAGGACAGGCGTGGAGGA-3′	200
NFKB1	NM_003998.4	Forward 5′-ACTGCTGGACCCAAGGACAT-3′ Reverse 5′-CGCCTCTGTCATTCGTGCTT-3′	105
TNF-α	NM_000594.4	Forward 5′-ACTGCTGGACCCAAGGACAT-3′ Reverse 5′-CGCCTCTGTCATTCGTGCTT-3′	81
UCP2	NM_001381944.1	Forward 5′-CTTCTGCACCACTGTCATCG-3′ Reverse 5′-GTGACGAACATCACCACGTT-3′	195
VEGFA	NM_001025366.3	Forward 5′-CCCACTGAGGAGTCCAACA -3′ Reverse 5′-CTCTCCTATGTGCTGGCCTT-3′	72
VEGFR1	NM_002019.4	Forward 5′-TTACCGAATGCCACCTCCAT-3′ Reverse 5′-CTTGGGTTTGCTGTCAGTCC-3′	105
VEGFR2	NM_002253.4	Forward 5′-CTCAGCAGGATGGCAAAGAC-3′ Reverse 5′-AGGTGAGGTAGGCAGAGAGA-3′	92
TRPV1	NM_080704.4	Forward 5′-ACCCTGTTTGTGGACAGCTA-3′ Reverse 5′-CAAGGCCAGGGAGAATACCA-3′	129
SIRT-1	NM_012238.5	Forward 5′-TATGCTCGCCTTGCTGTAGA-3′ Reverse 5′-TGGCTGGAATTGTCCAGGAT-3′	132
COX2	NM_000963.4	Forward 5′-GCTTCCATTGACCAGAGCAG-3′ Reverse 5′-CTCCACAGCATCGATGTCAC-3′	159
LEP	NM_000230.3	Forward 5′-TGGAGAAGCTGATGCTTTGC-3′ Reverse 5′-GGACCATTCAGAGGGTCACA-3′	196
ADIPOQ	NM_001177800.2	Forward 5′-GGATGTGAAGGTCAGCCTCT-3′ Reverse 5′-TACACCTGGAGCCAGACTTG-3′	141
GAPDH	NM_002046.7	Forward 5′-ACCCAGAAGACTGTGGATGG-3′ Reverse 5′-TCAGCTCAGGGATGACCTTG-3′	124
ACTB	NM_001101.5	Forward 5′-CCCTGGAGAAGAGCTACGAG-3′ Reverse 5′-GGAAGGAAGGCTGGAAGAGT-3′	96

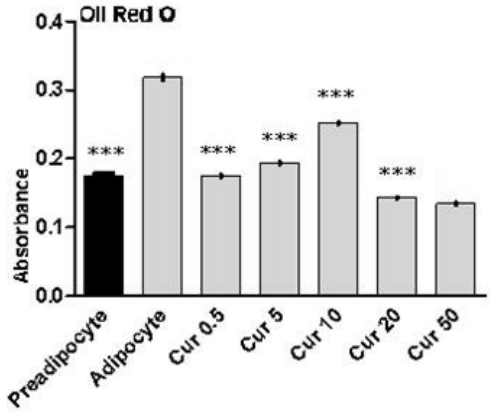

Figure 1. Comparison of the differentiation of absorbance values of different doses of CUR-added adipocytes, adipocytes, and preadipocyte stained with Oil Red O dye method

***p<0.001 in comparison to adipocytes. Data are expressed as mean±SD

Cur 0.5: Differentiated adipocytes in the presence of 0.5 µM Curcumin (CUR)

Cur 5: Differentiated adipocytes in the presence of 5 µM Curcumin (CUR)

Cur 10: Differentiated adipocytes in the presence of 10 µM Curcumin (CUR)

Cur 20: Differentiated adipocytes in the presence of 20 µM Curcumin (CUR)

Cur 50: Differentiated adipocytes in the presence of 50 µM Curcumin (CUR)

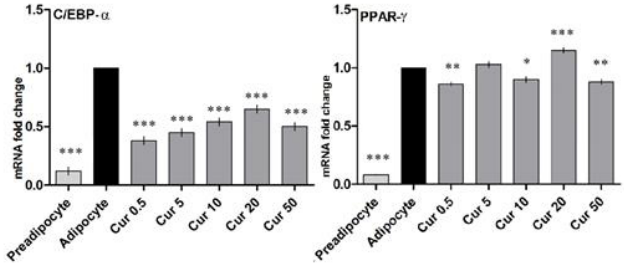

Figure 2. Effects of Curcumin on the expression of *C/EBP-α* and *PPAR-γ* genes during the differentiation of preadipocyte to adipocytes

*p<0.05, **p<0.01, ***p<0.001 in comparison to adipocytes. Data are expressed as mean±SD

Cur 0.5: Differentiated adipocytes in the presence of 0.5 µM Curcumin (CUR)

Cur 5: Differentiated adipocytes in the presence of 5 µM Curcumin (CUR)

Cur 10: Differentiated adipocytes in the presence of 10 µM Curcumin (CUR)

Cur 20: Differentiated adipocytes in the presence of 20 µM Curcumin (CUR)

Cur 50: Differentiated adipocytes in the presence of 50 µM Curcumin (CUR)

PPAR-γ; Peroxisome proliferator-activated receptor gamma

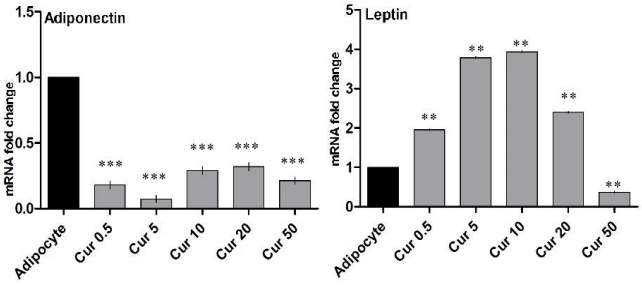

Figure 3. Adiponectin and Leptin mRNA levels in control adipocytes and different dose of Curcumin added adipocytes

**p<0.01, ***p<0.001 in comparison to adipocytes. Data are expressed as mean±SD.

Cur 0.5: Differentiated adipocytes in the presence of 0.5 µM Curcumin (CUR)

Cur 5: Differentiated adipocytes in the presence of 5 µM Curcumin (CUR)

Cur 10: Differentiated adipocytes in the presence of 10 µM Curcumin (CUR)

Cur 20: Differentiated adipocytes in the presence of 20 µM Curcumin (CUR)

Cur 50: Differentiated adipocytes in the presence of 50 µM Curcumin (CUR)

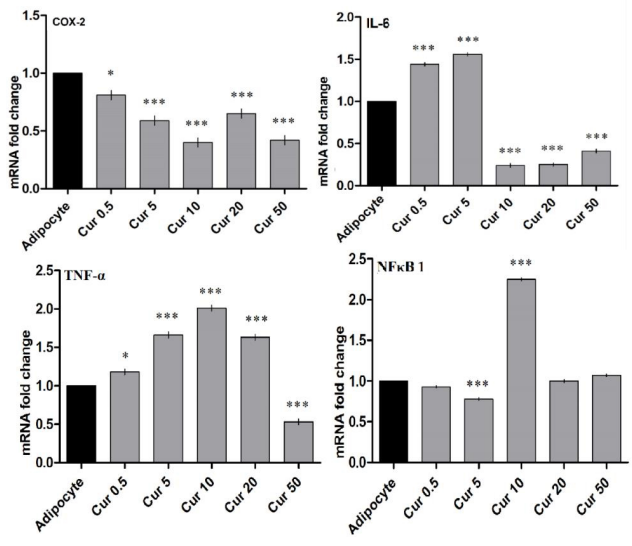

Figure 4. COX2, IL6, TNF-α and NFκB1 mRNA levels in control adipocytes and different dose of Curcumin added adipocytes

*p<0.05, ***p<0.001 in comparison to adipocytes. Data are expressed as mean±SD.

Cur 0.5: Differentiated adipocytes in the presence of 0.5 µM Curcumin (CUR)

Cur 5: Differentiated adipocytes in the presence of 5 µM Curcumin (CUR)

Cur 10: Differentiated adipocytes in the presence of 10 µM Curcumin (CUR)

Cur 20: Differentiated adipocytes in the presence of 20 µM Curcumin (CUR)

Cur 50: Differentiated adipocytes in the presence of 50 µM Curcumin (CUR)

Effects of CUR on Angiogenic Proteins

VEGF-A mRNA levels of CUR-added adipocytes significantly decreased during differentiation in CUR 0.5, CUR 20, and CUR 50 groups ($p<0.01$ for CUR 0.5, CUR 20, $p<0.001$ for CUR 50) and significantly increased in the CUR 10 group ($p<0.001$) in comparison to control adipocytes. VEGF-R1 mRNA levels were significantly increased in all CUR-treated adipocytes except CUR 50 compared with control adipocytes ($p<0.001$). In the CUR 50 group, VEGF-RI mRNA levels were significantly decreased ($p<0.001$) (Figure 5). Elevated VEGF-R2 mRNA levels were found in all CUR groups except for CUR 5. Statistically significant increase in gene expression in CUR 0.5 ($p<0.05$), CUR 10 ($p<0.001$), CUR 20 ($p<0.01$) and CUR 50 ($p<0.001$) adipocytes compared with control adipocytes (Figure 5).

Effects of CUR on TRPV-1, UCP-2, and SIRT-1 expression

TRPV-1 mRNA levels changed significantly in all CUR groups except for CUR 50 compared with control adipocytes ($p<0.001$). UCP-2 mRNA levels were significantly decreased in all CUR groups ($p<0.001$). SIRT-1 mRNA levels reduction was only statistically significant in the CUR 0.5 ($p<0.01$) and CUR 5 ($p<0.05$) groups CUR 50 compared with control adipocytes (Figure 6).

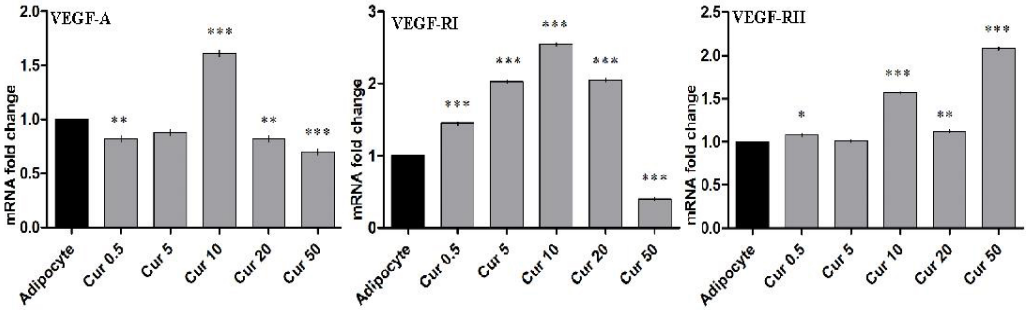

Figure 5 VEGF-A, VEGF-RI, and VEGF-RII mRNA levels of control adipocytes and different dose of Curcumin added adipocytes
*p<0.05, **p<0.01, ***p<0.001 in comparison to adipocytes. Data are expressed as mean±SD
Cur 0.5: Differentiated adipocytes in the presence of 0.5 μM Curcumin (CUR)
Cur 5: Differentiated adipocytes in the presence of 5 μM Curcumin (CUR)
Cur 10: Differentiated adipocytes in the presence of 10 μM Curcumin (CUR)
Cur 20: Differentiated adipocytes in the presence of 20 μM Curcumin (CUR)
Cur 50: Differentiated adipocytes in the presence of 50 μM Curcumin (CUR)

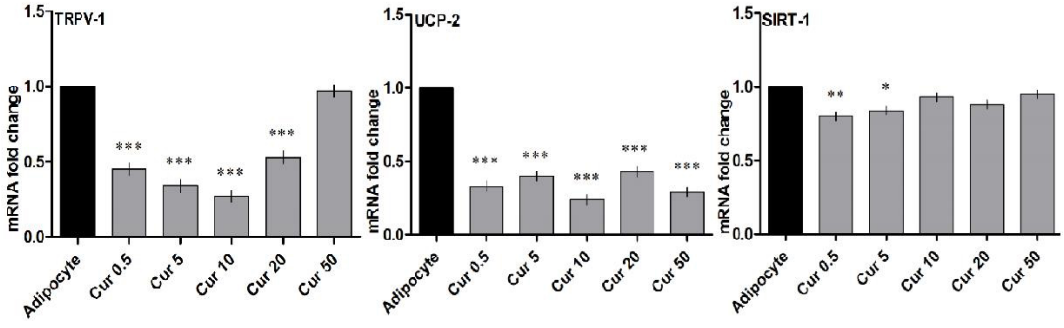

Figure 6. TRPV-1, UCP-2, and SIRT-1 mRNA levels of control adipocytes and different dose of Curcumin added adipocytes
p<0.05, ***p<0.01, ***p<0.001 in comparison to adipocytes. Data are expressed as mean±SD.
Cur 0.5: Differentiated adipocytes in the presence of 0.5 μM Curcumin (CUR)
Cur 5: Differentiated adipocytes in the presence of 5 μM Curcumin (CUR)
Cur 10: Differentiated adipocytes in the presence of 10 μM Curcumin (CUR)
Cur 20: Differentiated adipocytes in the presence of 20 μM Curcumin (CUR)
Cur 50: Differentiated adipocytes in the presence of 50 μM Curcumin (CUR)

DISCUSSION

Adipocyte differentiation is an important process in the identification of adipocytes during the development of adipogenesis and obesity. Augmented adiposity is a risk factor for chronic inflammation and related metabolic disorders. CUR, a natural polyphenol obtained from the rhizomes of the CUR longa plant, exhibits antioxidant and anti-inflammatory properties (26,27). CUR also plays a role as a thermogenic and anti-adipogenesis factor and suppresses adipocyte differentiation by inhibiting some regulators in the early stages of adipocyte differentiation pathways (18,19,24). Therefore, it is important to clarify the mechanism by which CUR regulates adipose differentiation. Clarifying the molecular and cellular mechanisms that regulate adipogenesis and inflammatory factor expression will help prevent and treat inflammatory diseases, obesity, insulin resistance, and metabolic syndrome.

In the present study, human adipocytes incubated with CUR significantly decreased C/EBPα mRNA expression in a dose-independent manner. Zhao et al. (20) also found lipid accumulation in doses independent of CUR in 3T3-L1 cells. This result is consistent with the results of our study. However especially 50 μM CUR treatment lowered PPARγ mRNA expression levels. CUR has been shown to decrease the expression of C/EBPα and PPARγ leading to reduced lipid accumulation in adipocytes and improved obesity and hyperlipidemia in patients with metabolic syndrome (20,21). Additionally, one of the pathways that suppresses adipocyte differentiation is the inhibition of mRNA levels of adipogenic transcription factors such as C/EBPa and PPARγ (22,28). CUR inhibits the adipogenic differentiation of human bone marrow mesenchymal stem cells. This effect ocCURs by inhibiting C/EBPa and PPARγ (29). Our results are similar to those of recent studies. On the other hand, PPARγ is also associated with SIRT-1 protein expression. It has been reported that PPARγ transactivation activity is inhibited by the direct or indirect effects of SIRT-1 protein (30). However, SIRT mRNA levels were not affected by CUR treatment. This suggests that the effect of PPARγ on adipogenesis differentiation with CUR treatment may be via a non-transcriptional mechanism, and this result also indicates that the anti-adipogenic effect of CUR is due to transition cellular events that CUR in the early stage of adipocyte differentiation.

CUR was informed to be affected by TRPV1 located in the intestinal jejunum and in this wise has affected both WAT and BAT differentiations (25). UCP-2 has now been identified as an important molecule in metabolic thermogenesis, such as diet-induced and cold heat production, which is an important component of energy expenditure, and it was also found that its dysfunction contributes to the development of obesity (11). *UCP-2* gene expression is upregulated by through a prostaglandin/PPARg-mediated pathway (11). In our study, UCP-2 and TRPV1 mRNA levels were significantly reduced in adipocytes following incubation with different concentrations of CUR. This reduction may be related to cellular lipid accumulation. According to our CUR knowledge, there are not enough studies showing the effects of CUR on UCP2 and TRPV1 levels. We demonstrated for the first time that CUR has no effect on UCP2 expression during adipocyte differentiation. Mahadik et al. (11) found that obese subjects showed decreased *UCP2* gene expression in adipose tissue. CUR applied during adipocyte differentiation does not seem to be effective on TRPV1 levels. This suggests that the pathways of metabolic thermogenesis and adipogenesis are not related. The lack of correlation between C/EBPα and thermogenesis parameters strengthens our hypothesis. The specific role of adipokine and related pathways in the inflammatory state is not understood. The inflammation may be the cause or the inductive effect of adipokine secretion. It has been reported that CUR has beneficial effects against obesity-related inflammation (12). Therefore, it is important to underly the relationship between CUR and inflamed adipocyte differentiation. CUR prevents inflammation by modulating proinflammatory cytokines, such as COX-2, IL-6, and -α and also related pathways, such as NF-κB and PPARγ (9,15,16). A recent study showed that CUR downregulates the expression of COX-2 and NF-κB and suppresses inflammation in colistin-induced toxic neuroblastoma-2a cells (15,16). In our study, NF-κB did not change during adipocyte differentiation, but CUR decreased the expression of the proinflammatory markers COX-2, TNF-α and IL-6 mRNA in adipocytes. 50 μM treatment of CUR seem to be more effective in suppressing inflammation. This finding suggests that the anti-inflammatory effect of CUR may be associated with a decrease in PPARγ mRNA levels and that CUR plays no role in suppressing NF-κB. Leptin and adiponectin are important adipokines for energy balance and metabolism. There are many confusing results regarding the levels of leptin and adiponectin in adipocytes (17). In our study, leptin mRNA levels in adipocytes decreased with 50 μM CUR administration, whereas adiponectin mRNA levels decreased significantly with dose-independent CUR administration. Because both adipokine are secreted from adipose tissue, their low levels may be associated with decreased fat accumulation resulting from CUR in adipocytes. Our results are consistent with those by Kim et al. (24).

In this study, it was first concluded that CUR suppresses the differentiation of human preadipocyte to adipocytes and decreases the release of proinflammatory cytokines such as COX-2, TNF-α and IL-6, but it does so by regulating *C/EBPα* and *PPARγ* gene expressions outside the NF-κB pathway. One of our important findings was that CUR effectively suppressed adipogenic transcription factors and adipocyte differentiation at all doses between 0.5-50 μM, but showed its anti-inflammatory effect especially in the application of CUR of 50 μM, the highest dose in our study.

Study Limitations

We would like to define that this study also has some limitations. We couldn't determine the protein expression levels. Also, we could not measure another indicator of lipid levels as triglyceride levels which is, along with Oil Red O staining. However, this study is important because it is the first to investigate that CUR suppresses the differentiation of human preadipocyte to adipocytes and decreases the release of proinflammatory cytokines.

CONCLUSION

In conclusion, the inhibitory effect of CUR on adipocyte differentiation is associated with its anti-inflammatory effect, and this beneficial effect is more pronounced, especially at high concentrations.

ETHICS

Ethics Committee Approval: Since this study was on genes, no ethics committee was required.

Informed Consent: Since this study was about genes, patient consent was not required.

Authorship Contributions

Surgical and Medical Practices: P.Ç., S.D., S.T.K., Concept: P.Ç., S.D., S.T.K., M.S., Y.Ö.İ., H.K., Design: P.Ç., S.D., S.T.K., M.S., Y.Ö.İ., H.K., Data Collection or Processing: P.Ç., S.D., S.T.K., M.S., Y.Ö.İ., H.K., Analysis or Interpretation: P.Ç., S.D., S.T.K., M.S., Y.Ö.İ., H.K., Literature Search: P.Ç., S.D., S.T.K., Writing: P.Ç., Y.Ö.İ.

Conflict of Interest: No conflict of interest was declared by the authors.

Financial Disclosure: The authors declare that this study received no financial support.

REFERENCES

1. Recinella L, Orlando G, Ferrante C, Chiavaroli A, Brunetti L, Leone S. Adipokines: new potential therapeutic target for obesity and metabolic, rheumatic, and cardiovascular diseases. Front Physiol. 2020;11:578966.
2. Weschenfelder C, Schaan de Quadros A, Lorenzon Dos Santos J, Bueno Garofallo S, Marcadenti A. Adipokines and adipose tissue-related metabolites, nuts and cardiovascular disease. Metabolites. 2020;10:32.
3. Choe SS, Huh JY, Hwang IJ, Kim JI, Kim JB. Adipose tissue remodeling: its role in energy metabolism and metabolic disorders. Front Endocrinol (Lausanne). 2016;7:30.
4. Leiherer A, Mündlein A, Drexel H. Phytochemicals and their impact on adipose tissue inflammation and diabetes. Vascul Pharmacol. 2013;58:3-20.
5. Azhar Y, Parmar A, Miller CN, Samuels JS, Rayalam S. Phytochemicals as novel agents for the induction of browning in white adipose tissue. Nutr Metab (Lond). 2016;13:89.
6. Rosen ED, Hsu CH, Wang X, Sakai S, Freeman MW, Gonzalez FJ, et al. *C/EBPalpha* induces adipogenesis through PPARgamma: a unified pathway. Genes Dev. 2002;16:22-6.
7. Aggarwal BB. Targeting inflammation-induced obesity and metabolic diseases by curcumin and other nutraceuticals. Annu Rev Nutr. 2010;30:173-99.
8. Villarroya F, Iglesias R, Giralt M. PPARs in the Control of Uncoupling Proteins Gene Expression. PPAR Res. 2007;2007:74364.
9. Chan MM. Inhibition of tumor necrosis factor by curcumin, a phytochemical. Biochem Pharmacol. 1995;49:1551-6.
10. Milne JC, Lambert PD, Schenk S, Carney DP, Smith JJ, Gagne DJ, et al. Small molecule activators of SIRT1 as therapeutics for the treatment of type 2 diabetes. Nature. 2007;450:712-6.
11. Mahadik SR, Lele RD, Saranath D, Seth A, Parikh V. *Uncoupling protein-2 (UCP2)* gene expression in subcutaneous and omental adipose tissue of Asian Indians: relationship to adiponectin and parameters of metabolic syndrome. Adipocyte. 2012;1:101-7.
12. Poher AL, Altirriba J, Veyrat-Durebex C, Rohner-Jeanrenaud F. Brown adipose tissue activity as a target for the treatment of obesity/insulin resistance. Front Physiol. 2015;6:4.
13. Wang S, Liang X, Yang Q, Fu X, Rogers CJ, Zhu M, et al. Resveratrol induces brown-like adipocyte formation in white fat through activation of AMP-activated protein kinase (AMPK) α1. Int J Obes (Lond). 2015;39:967-76.
14. Zorena K, Jachimowicz-Duda O, Ślęzak D, Robakowska M, Mrugacz M. Adipokines and obesity. potential link to metabolic disorders and chronic complications. Int J Mol Sci. 2020;21:3570.
15. Fain JN. Release of interleukins and other inflammatory cytokines by human adipose tissue is enhanced in obesity and primarily due to the nonfat cells. Vitam Horm. 2006;74:443-77.
16. Wang SL, Li Y, Wen Y, Chen YF, Na LX, Li ST, et al. Curcumin, a potential inhibitor of up-regulation of TNF-alpha and IL-6 induced by palmitate in 3T3-L1 adipocytes through NF-kappaB and JNK pathway. Biomed Environ Sci. 2009;22:32-9.
17. Değirmencioğlu S, Çetinalp P, Seyithanoğlu M, Tanrıkulu Küçük S, Koçak H, Öner İyidoğan Y. Capsaicin modulates adipocyte cell differentiation and inflammatory gene expression. Experimed. 2024;14:116-25.
18. Sharma RA, Gescher AJ, Steward WP. Curcumin: the story so far. Eur J Cancer. 2005;41:1955-68.
19. Manjunatha H, Srinivasan K. Hypolipidemic and antioxidant effects of dietary curcumin and capsaicin in induced hypercholesterolemic rats. Lipids. 2007;42:1133-42.
20. Zhao D, Pan Y, Yu N, Bai Y, Ma R, Mo F, et al. Curcumin improves adipocytes browning and mitochondrial function in 3T3-L1 cells and obese rodent model. R Soc Open Sci. 2021;8:200974.
21. Ganjali S, Sahebkar A, Mahdipour E, Jamialahmadi K, Torabi S, Akhlaghi S, et al. Investigation of the effects of curcumin on serum

cytokines in obese individuals: a randomized controlled trial. ScientificWorldJournal. 2014;2014:898361.

22. Sahebkar A. Low-density lipoprotein is a potential target for curcumin: novel mechanistic insights. Basic Clin Pharmacol Toxicol. 2014;114:437-8.
23. Tanrıkulu-Küçük S, Başaran-Küçükgergin C, Seyithanoğlu M, Doğru-Abbasoğlu S, Koçak H, Beyhan-Özdaş Ş, et al. Effect of dietary curcumin and capsaicin on testicular and hepatic oxidant-antioxidant status in rats fed a high-fat diet. Appl Physiol Nutr Metab. 2019;44:774-82.
24. Kim CY, Le TT, Chen C, Cheng JX, Kim KH. Curcumin inhibits adipocyte differentiation through modulation of mitotic clonal expansion. J Nutr Biochem. 2011;22:910-20.
25. Nalli M, Ortar G, Schiano Moriello A, Di Marzo V, De Petrocellis L. Effects of curcumin and curcumin analogues on TRP channels. Fitoterapia. 2017;122:126-31.
26. Hatcher H, Planalp R, Cho J, Torti FM, Torti SV. Curcumin: from ancient medicine to current clinical trials. Cell Mol Life Sci. 2008;65:1631-52.
27. Pulido-Moran M, Moreno-Fernandez J, Ramirez-Tortosa C, Ramirez-Tortosa M. Curcumin and health. Molecules. 2016;21:264.
28. Moseti D, Regassa A, Kim WK. molecular regulation of adipogenesis and potential anti-adipogenic bioactive molecules. Int J Mol Sci. 2016;17:124.
29. Wang T, Yan R, Xu X, Li X, Cao L, Gao L, et al. Curcumin represses adipogenic differentiation of human bone marrow mesenchymal stem cells via inhibiting kruppel-like factor 15 expression. Acta Histochem. 2019;121:253-9.
30. Picard F, Kurtev M, Chung N, Topark-Ngarm A, Senawong T, Machado De Oliveira R, et al. SIRT1 promotes fat mobilization in white adipocytes by repressing PPAR-gamma. Nature. 2004;429:771-6. Erratum in: Nature. 2004;430:921.

Medical Journal of Bakırköy

Med J Bakirkoy 2025;21:121-126
DOI: 10.4274/BMJ.galenos.2024.2024.8-7

Case Report

A Novel Approach in Cerebellar Cystic Pilocytic Astrocytoma Surgery: Spherical Coordinate System

Serebellar Kistik Pilositik Astrositom Cerrahisinde Yeni Bir Yaklaşım: Küresel Koordinat Sistemi

Abdullah Emre Taçyıldız[1,2], Özden Erhan Sofuoğlu[3], Rabia Burçin Girgin[4]

[1]Malatya Turgut Özal University Faculty of Medicine, Department of Neurosurgery, Malatya, Türkiye

[2]Karabük University Faculty of Medicine, Department of Neurosurgery, Karabük, Türkiye

[3]Republic of Türkiye Ministry of Health, İstanbul Bakırköy Prof. Dr. Mazhar Osman Mental Health and Neurological Diseases Training and Research Hospital, Clinic of Neurosurgery, İstanbul, Türkiye

[4]İnonü University Faculty of Medicine, Department of Pathology, Malatya, Türkiye

ABSTRACT

Achieving gross total resection is the primary prognostic factor in pilocytic astrocytomas. The spherical coordinate system (SCS) is an alternative to the Cartesian system for defining a point's location in space. While the Cartesian system uses X, Y, and Z axes, the SCS utilizes ρ (distance from the origin), θ (the angle with the positive X-axis, 0 to 360 degrees), and ϕ (the angle with the positive Z-axis, 0 to 180 degrees). A 73-year-old female patient presented with headaches, dizziness, and gait disturbance over the past month, along with nausea and vomiting. She had previously undergone cerebellar tumor surgery in February 2020, and two years later, similar solid and cystic structures reappeared, suggesting a residual tumor. In such cases, using the SCS may help reduce remnant tumor rates and minimize the need for secondary operations.

Keywords: Cystic pilocytic astrocytoma, spherical coordinate system

ÖZ

Küresel koordinat sistemi (KKS), uzayda bir noktanın yerini tanımlamak için kullanılan alternatif bir yöntemdir. Kartezyen koordinat sisteminde X, Y ve Z yönleri kullanılırken, KKS'de kullanılan bileşenler ρ (orijinden olan uzaklık, her zaman sıfırdan büyük), θ (ρ'nin pozitif X ekseni ile yaptığı açı, 0 ile 360 derece arasında değişebilir) ve ϕ (ρ'nin pozitif Z ekseni ile yaptığı açı, 0 ile 180 derece arasında değişebilir) olarak tanımlanır. Yetmiş üç yaşındaki kadın hasta, son bir aydır baş ağrısı, baş dönmesi ve yürüme bozukluğu şikayetleriyle başvurdu. Başvuru sırasında ayrıca mide bulantısı ve kusma şikayetleri de mevcuttu. Hasta, Şubat 2020'de serebellar tümör ameliyatı geçirmişti. İki yıl sonra, aynı solid kitle ve kistik yapılar tekrar gözlemlendi. Bu durumda, başlangıçta tümör kalıntısı olabileceği düşünüldü. KKS, Kartezyen koordinat sistemi gibi vaka yönetiminde potansiyel bir alternatif olarak kullanılabilir. Bu yaklaşım, tümör kalıntısı oranlarını ve ikinci operasyon gereksinimini azaltabilir.

Anahtar Kelimeler: Kistik pilositik astrositom, küresel koordinat sistemi

INTRODUCTION

Thomas Stromer, quote "measure what can be measured, and make measurable what cannot be measured" attributed to Galileo; He simplifies it by saying "measure what needs to be measured" (1). (In the same article, it is stated that this statement attributed to Galileo is not precise) Advanced mathematical calculations have been used in medicine for over a hundred years. Horsley and Clarke introduced the stereotaxy apparatus, which is a device that combined coordinate systems and anatomy, in 1908 (2). Since many revolutionary advances such as stereotactic functional surgery, stereotactic radiosurgery, and associated biopsy have developed to the present day, these technologies have significantly improved patient outcomes. It has provided significant contributions to human life (2-4).

Address for Correspondence: Abdullah Emre Taçyıldız, Malatya Turgut Özal University Faculty of Medicine, Department of Neurosurgery, Malatya, Türkiye; Karabük University Faculty of Medicine, Department of Neurosurgery, Karabük, Türkiye

E-mail: abdullahemretacyildiz@gmail.com **ORCID ID:** orcid.org/0000-0001-5806-243X

Cite as: Taçyıldız AE, Erhan Sofuoğlu Ö, Girgin RB. A novel approach in cerebellar cystic pilocytic astrocytoma surgery: spherical coordinate system. Med J Bakirkoy. 2025;21:121-126

Received: 30.08.2024
Accepted: 20.12.2024
Publication Date: 25.03.2025

The dominant prognostic factor in pilocytic astrocytomas is the performance of gross total resection (5). Mair et al. (6) showed that the localization of the lesion is critical for effective tumor resectability.

The spherical coordinate system (SCS) is one of the alternative methods used to define the location of a point in space (7). The X, Y, Z directions are used in the Cartesian coordinate system. In the SCS, ρ, θ, and ϕ are defined as follows: ρ (radial distance) the from the origin , to be calculated, always greater than zero; θ (azimuth angle), the angle of ρ with the positive X-axis, which can take a value between 0 and 360 degrees; ϕ (elevation angle or polar angle), the angle that ρ makes with the positive Z-axis, which can take a value between 0 and 180 degrees 7. Our aim in presenting the case is to calculate the location of the preoperative solid mass with mathematical accuracy using a SCS. Our other aim is to present an alternative coordinate system to the Cartesian system used in stereotaxy.

CASE REPORT

A 73 year-old female patient with headache, dizziness, and gait disturbance in the last month. At the time of presentation, there was nausea and vomiting. On physical examination, she had dysmetria, dysdiadochokinesia and ataxia. The examination showed an arterial blood pressure of 120/75 mmHg, a pulse rate of 80/minute, a respiratory rate of 20 breaths/min, and an axillary temperature of 36.2 °C. She had a Glasgow Coma Scale (GCS) of 15. The patient was cooperative, with clear consciousness and oriented to time, place, and person. She did not have any weakness or neurological deficits. Also, coronary artery disease and diabetes mellitus were detected in anamnesis. The patient was comprehensively informed about the surgical procedure and its associated risks, and informed consent was obtained from the patient.

Surgical History

The patient had surgery for a cerebellar tumor in the second month of 2020 (Figure 1A,B). The previous pathology report indicated that there was no tumor tissue. The same solid mass and cystic structures were observed after two years. In this case, firstly, the total impression of the remnant tumor was considered (Figure 1C,D).

Preoperative Calculations with Imaging and Spherical Coordinate System

The patient's cerebellar cystic space-occupying lesion resembles a sphere. The cerebellar cystic lesion was considered to be spherical, and an attempt was made to reach the solid lesion. With the help of the SCS, the coordinates of the solid lesion were calculated according to the point designated as the center of the sphere. The distance of the solid lesion to the center of the cyst; That is, the "ρ" value, was approximately 12 mm (Figure 2A). The angle of the solid lesion with the x-axis of the cyst, that is, the θ value, was calculated between 300° and 346° (Figure 2B). The angle of the solid lesion with the z-axis of the cyst, that is, the ϕ value was calculated between 97° and 144° (Figure 2C). The coordinates of the patient's solid lesion were calculated as r, θ1- θ2, ϕ1- ϕ2 values according to the accepted center of the cyst: 12 mm, 300°-346°, 97°-144°.

Surgical Technique

The surgery was started with precise calculations in the pre-operative stage. The tumor was completely resected in approximately 70 minutes. The patient was taken to the intensive care unit in the early post-operative stage. However, the patient's GCS decreased to 12 after 2 hours. Control brain tomography shows cerebellar edema and mild brainstem compression. The patient was started on 600 mg mannitol. After medical treatment, the patient's GCS rose again to 15 on the postoperative second day. Mannitol treatment was terminated after gradually reducing the dose. The patient was taken to the service on the 5th postoperative day. On the 15th postoperative day, the patient was discharged with full recovery. The reason the patient is monitored for such a long time is the imbalance in blood pressure and glucose levels. In this process, necessary branch consultations were conducted.

Postoperative control brain magnetic resonance imaging (MRI) examinations of the patient showed that the total tumor resection was successful and the cyst had disappeared (Figure 3A). Pilocytic astrocytoma, WHO grade 1 was detected in histopathological examination (Figure 3B).

A neoplastic proliferation with a rich capillary vascular network within the cerebellum was remarkable in hematoxylin-eosin sections. This lesion had no distinctive capsule structure but was well demarcated. Neoplastic cells were clear, polygonal or rounded, with abundant cytoplasm and revealed no prominent nucleoli (Figure 3 B1,B2). These neoplastic cells were positive for glial fibrillary acidic protein (Figure 3 B3), S100, and ATRX and negative for OLIG-2 and Neu-N. The proliferation index was about 1-2% as determined with the marker Ki67 (not shown). When clinical, radiological, and histopathological findings were evaluated together, the case was diagnosed as pilocytic astrocytoma/ WHO grade 1.

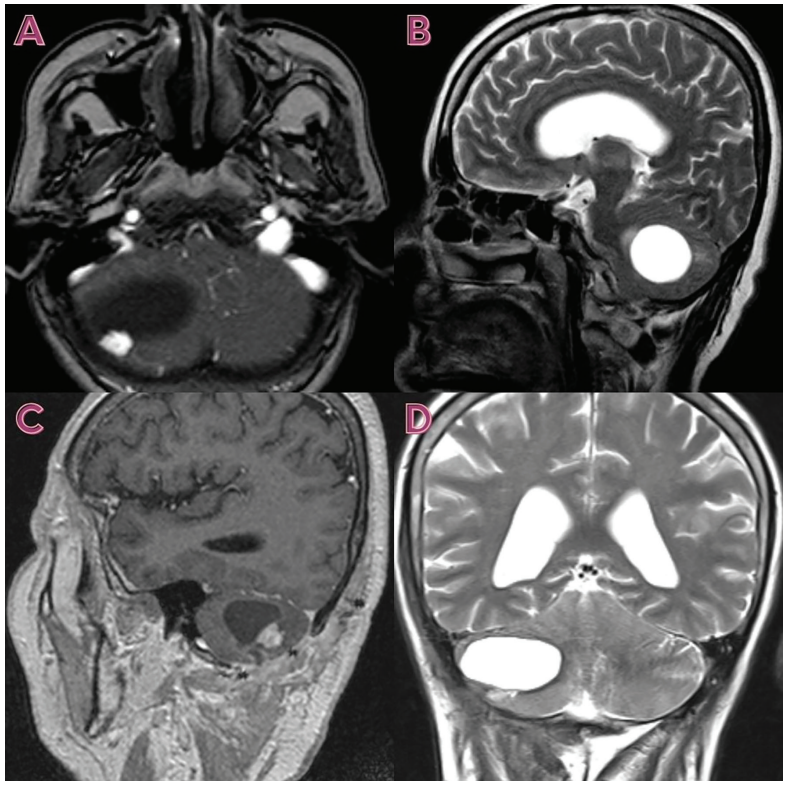

Figure 1. (A) Preoperative magnetic resonance imaging (MRI) images of the case are viewed in the 2nd month of 2020. (B) two months post operative MRI images showed the solid mass and cyst of the lesion after the first surgery

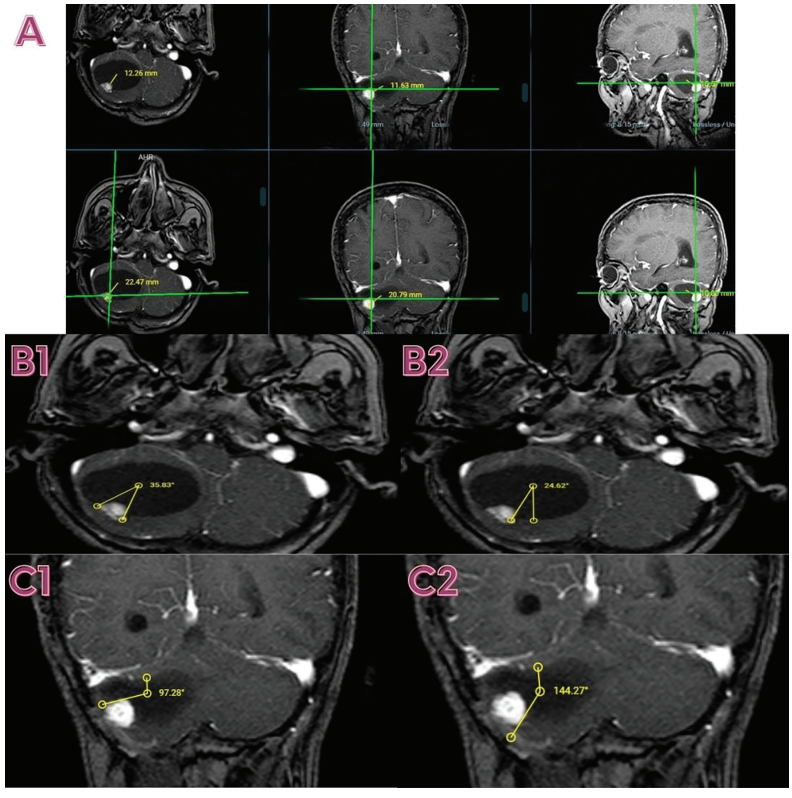

Figure 2. A: The distance of the solid lesion to the tumor center was calculated in contrast-enhanced MRI. B2: in contrast-enhanced axial sections, "θ" values of solid tumor were calculated according to the accepted center of the cyst. C2: in contrast-enhanced coronal sections, ϕ values of solid tumor were calculated relative to the accepted center of the cyst

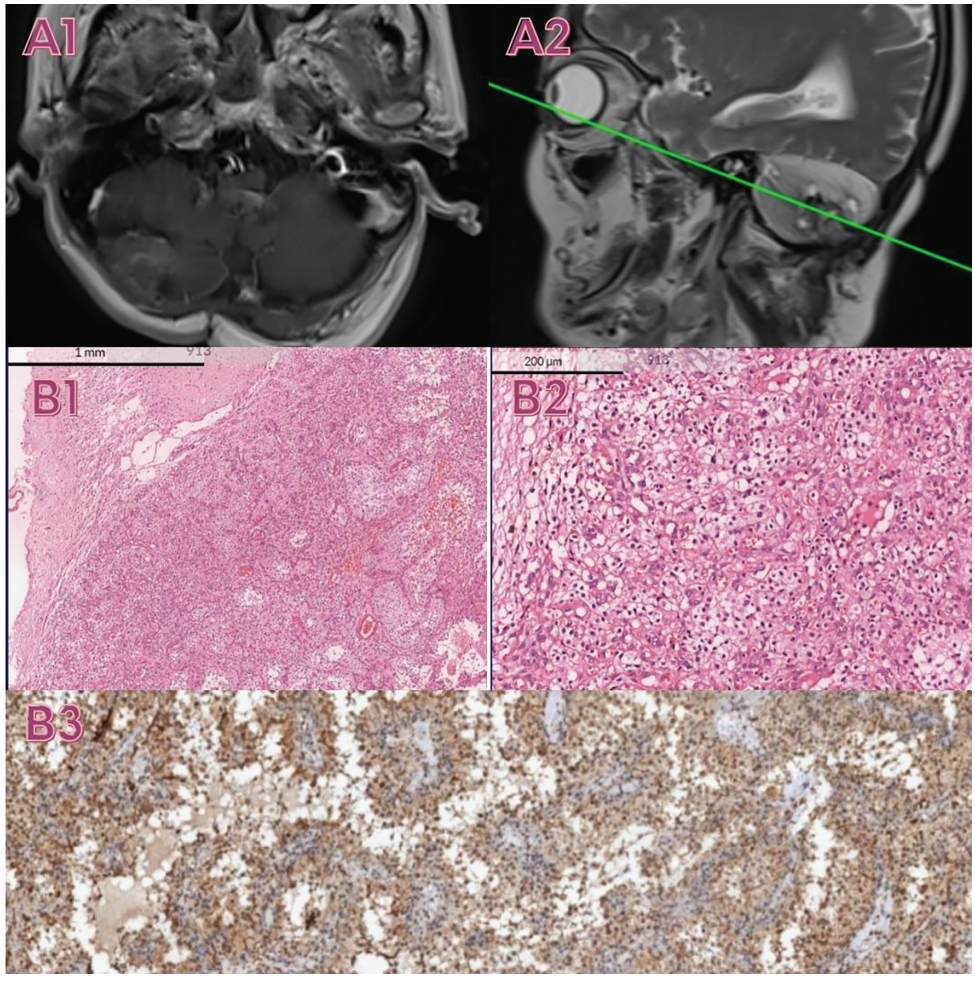

Figure 3. (A1-A2) In contrast-enhanced (A1) and sagittal sections (A2) taken postoperatively, it is observed that the tumor and cyst have completely disappeared. (B1-B2) well circumscribed neoplastic lesion with polygonal-rounded cells with abundant cytoplasm and a rich capillary vascular network (H&E, digitally scanned) (B3) neoplastic cells were positive for GFAP (digitally scanned)
GFAP; Glial fibrillary acidic protein

DISCUSSION

As far as we could detect, the finding of tumor localization using the SCS was reported in the literature for the first time. The SCS can also be used as an alternative in case management, just like the Cartesian coordinate system. This may reduce the rates of remnant tumors and secondary operations. This case report provides a foundation for a more in-depth study of SCS and its clinical outcomes.

However, a study in the engineering literature shows Cheng joint rotations with an SCS (8).

Techniques such as intraoperative MRI are available to guide surgeons during surgery (9). Several techniques are beneficial during surgery, depending on the pathology of the tumor, such as intraoperative ultrasound navigation, 5-aminolevulinic acid, and Fluorescein Na, and intraoperative computed tomography (10). The mathematical calculations that we used to find the tumor's address can potentially be used alone or in combination with the techniques we mentioned above (Figure 2).

After reaching the cyst, we were able to immediately locate the solid tumor, whose spherical coordinates we calculated. We completely removed the solid lesion by circumferential excision. It can be simplified in an illustration to make the mathematical calculations easier (Figure 4). A cystic sphere can be divided into 8 chambers. The locations of these chambers can be evaluated with MRI. Sphere-like cyst: 8 chambers as superior-lateral-posterior, superior-lateral-anterior, inferior-lateral-posterior, inferior-lateral-anterior, superior-medial-posterior, superior-medial-anterior, inferior-medial-posterior, inferior-medial-anterior are separable. Solid mass was calculated in the inferior, lateral, and posterior chambers of the cyst (Figures 2A, 4A). Cystic cerebellar hemangioblastomas that may

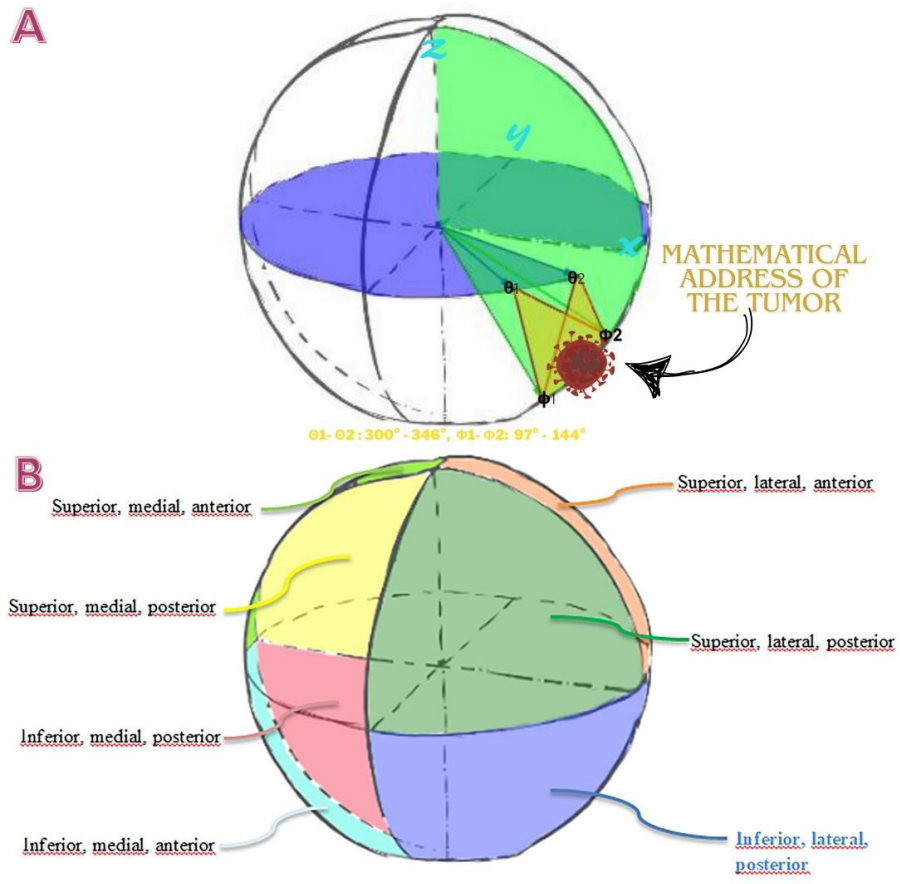

Figure 4. (A) Posterior view of the spherical coordinate system. (B) The division of a sphere into 8 chambers is shown to simplify the spherical coordinate system. In our opinion, the solid mass was inferior, lateral and posterior to the globe. (Figure 2A) (Since the mass is in the right cerebellum, the drawing was drawn in the prone position with posterior view, and in the natural anatomical position for the right side cerebellum)

have similar radiological characteristics due to remnant tumors have been reported in literature (11). The mathematical system we used could be useful in locating tumors. It can reduce the amount of residual and remnant tissue.

Study Limitations

Our study has some limitations, and it progresses by initially accepting the cyst as a sphere. We are aware that the cyst is not a complete sphere. Since the cyst was not a complete sphere, the coordinates of the solid mass were calculated approximately. However, even this calculation was sufficient to locate the tumor. The presented study is based on a single case, limiting the generalizability of findings. A broader patient cohort would be necessary to validate the consistency and efficacy of the SCS approach across different anatomical variations.

CONCLUSION

The article lacks a comparative analysis with traditional stereotactic methods. A comparative study would provide a clearer understanding of the advantages and disadvantages of the SCS in contrast to existing techniques.

ETHICS

Informed Consent: The patient was comprehensively informed about the surgical procedure and its associated risks, and informed consent was obtained from the patient.

FOOTNOTES

Authorship Contributions

Surgical and Medical Practices: A.E.T., Ö.E.S., Concept: A.E.T., Design: A.E.T., Data Collection or Processing: R.B.G., Analysis or Interpretation: A.E.T., Ö.E.S., Literature Search: A.E.T., Writing: A.E.T., R.B.G.

Conflict of Interest: No conflict of interest was declared by the authors.

Financial Disclosure: The authors declare that this study received no financial support.

REFERENCES

1. T. Strohmer. "Measure what should be measured: progress and challenges in compressive sensing," in IEEE Signal Processing Letters, 2012;19:887-93.
2. Yang I, Udawatta M, Prashant GN, Lagman C, Bloch O, Jensen R, et al. Stereotactic radiosurgery for neurosurgical patients: a historical review and current perspectives. World Neurosurg. 2019;122:522-31.
3. Ostertag CB, Mennel HD, Kiessling M. Stereotactic biopsy of brain tumors. Surg Neurol. 1980;14:275-83.
4. Spiegel EA, Wycis HT, Marks M, Lee AJ. Stereotaxic apparatus for operations on the human brain. Science. 1947;106:349-50.
5. Villanueva KG, Rea ND, Krieger MD. Novel surgical and radiologic risk factors for progression or recurrence of pediatric pilocytic astrocytoma. Pediatr Neurosurg. 2019;54:375-85
6. Mair MJ, Wöhrer A, Furtner J, Simonovska A, Kiesel B, Oberndorfer S, Ungersböck K, Marosi C, Sahm F, Hainfellner JA, Rössler K, Preusser M, Widhalm G, Berghoff AS. Clinical characteristics and prognostic factors of adult patients with pilocytic astrocytoma. J Neurooncol. 2020;148:187-98.
7. Reed BC, editor. Keplerian Ellipses: The Physics of the Gravitational Two-body Problem. 1st ed. Morgan & Claypool Publishers; 2019.
8. Cheng PL. A spherical rotation coordinate system for the description of three-dimensional joint rotations. Ann Biomed Eng. 2000;28:1381-92.
9. Choudhri AF, Siddiqui A, Klimo P Jr, Boop FA. Intraoperative MRI in pediatric brain tumors. Pediatr Radiol. 2015;45 Suppl 3:S397-405.
10. Tejada Solís S, de Quintana Schmidt C, Gonzalez Sánchez J, Fernández Portales I, Del Álamo de Pedro M, Rodríguez Berrocal V, et al. Intraoperative imaging in the neurosurgery operating theatre: a review of the most commonly used techniques for brain tumour surgery. Neurocirugia (Astur : Engl Ed). 2020;31:184-94.
11. Cervio A, Villalonga JF, Mormandi R, Alcorta SC, Sevlever G, Salvat J. Surgical treatment of cerebellar hemangioblastomas. Surg Neurol Int. 2017;8:163.